Multistage Corona Formation in Algonquin Metagabbro, Southwestern Grenville Province, Ontario

Jillian L. Kendrick

Submitted in partial fulfillment of the requirements

for the degree of Bachelor of Science, Honours

Department of Earth Sciences, Dalhousie University

Halifax, Nova Scotia

March 2015

Distribution License

DalSpace requires agreement to this non-exclusive distribution license before your item can appear on DalSpace.

NON-EXCLUSIVE DISTRIBUTION LICENSE

You (the author(s) or copyright owner) grant to Dalhousie University the non-exclusive right to reproduce and distribute your submission worldwide in any medium.

You agree that Dalhousie University may, without changing the content, reformat the submission for the purpose of preservation.

You also agree that Dalhousie University may keep more than one copy of this submission for purposes of security, back-up and preservation.

You agree that the submission is your original work, and that you have the right to grant the rights contained in this license. You also agree that your submission does not, to the best of your knowledge, infringe upon anyone's copyright.

If the submission contains material for which you do not hold copyright, you agree that you have obtained the unrestricted permission of the copyright owner to grant Dalhousie University the rights required by this license, and that such third-party owned material is clearly identified and acknowledged within the text or content of the submission.

If the submission is based upon work that has been sponsored or supported by an agency or organization other than Dalhousie University, you assert that you have fulfilled any right of review or other obligations required by such contract or agreement.

Dalhousie University will clearly identify your name(s) as the author(s) or owner(s) of the submission, and will not make any alteration to the content of the files that you have submitted.

If you have questions regarding this license please contact the repository manager at dalspace@dal.ca.

Grant the distribution license by signing and dating below.

_____ _____

Name of signatory Date

Abstract

The petrology, chemistry, and time of intrusion of alkaline mafic bodies in the southwest Grenville Province have been used to differentiate between autochthonous and allochthonous domains in this region. In the allochthons, the characteristic mafic suite is a group of coronitic metagabbros, the Algonquin metagabbros, which intruded at approximately 1152 Ma. Metamorphism at ca. 1050 Ma produced spectacular coronitic textures between igneous olivine and plagioclase and between igneous Fe-Ti oxides and plagioclase. This study examines in detail one metagabbro body exposed as a continuous 150 m wide outcrop in a roadcut near Emsdale, Ontario. Corona structures are used to estimate the P-T conditions experienced by this coherent body during metamorphism, test hypotheses of corona formation from previous work, and deduce its textural history.

Samples are divided into three types differentiated by their mineral assemblages and textures. In Type 1 samples, which have the best preserved igneous texture, opx + Fe-Ti oxide symplectite pseudomorphs after primary olivine are separated from plagioclase by coronas of opx, ± cpx, amph ± bt, grt + amph ± cpx ± opx ± plag symplectite. Coronas surrounding Fe-Ti oxides include amph + bt and grt + amph ± cpx ± opx ± plag symplectite. Type 2 samples represent the next developmental stage; relict igneous plagioclase and clinopyroxene are progressively recrystallized and a sodic plagioclase moat appears between amphibole and garnet. Type 3 samples, the latest stage, retain little to no igneous texture, with coronas largely obscured by late amph + plag + cpx + opx.

P-T estimates indicate that coronas in the metagabbro preserve the products of three stages of metamorphism. Type 1 preserves a prograde assemblage at ca. 800 ± 70°C and 11.0 ± 0.5 kb, Type 2 represents peak metamorphism at ca. 880 ± 70 °C and 13.0 ± 1.0 kb, and Type 3 phases overprinting coronas are retrograde at ca. 750 ± 70 °C and 9.5 ± 0.5 kb. The types define a “hairpin” shaped P-T path of metamorphism for the metagabbro body with a small temperature range. Corona formation was a prograde metamorphic process driven by diffusion until metamorphic fluids were intruded into the metagabbro around peak metamorphism, causing textural reworking of igneous phases and coronas in rock near veins. The opx + Fe-Ti oxide symplectite pseudomorphs after olivine are proposed to have formed by transfer of ilmenite from magmatic Fe-Ti oxides in response to an increase in fO_2 of the system.

Keywords: Grenville Province, Algonquin metagabbro, granulite facies metamorphism, coronitic metagabbro, multistage coronas, olivine corona, Fe-Ti oxide corona, olivine pseudomorph

Table of Contents

Table of Figures

Table of Tables

Acknowledgments

I am indebted to my honours supervisor Rebecca Jamieson, for providing me with this both challenging and exciting project. Its completion would not have been possible without her guidance, support, and invaluable revisions along the way. I also thank Glenn Chapman for his indispensable assistance in the field with sample collection and photography, as well as his advice during the writing of this thesis. Dan MacDonald is acknowledged for his tutelage in the electron microprobe lab and I am grateful to Gordon Brown for the superb quality of thin sections used for analysis. I have also benefitted from the encouragement of Martin Gibling and my friends in the honours class of 2015. Finally, I thank the friendly and supportive community of faculty and students in the Department of Earth Sciences for making my last year at Dalhousie one I will not forget.

Chapter 1: Introduction

1.1 Purpose of Study

A coronitic metagabbro or "coronite" refers to a gabbro displaying a coronitic texture, a reaction texture that develops at the contact between two minerals and is characterized by one mineral becoming enveloped in one or more concentric shells of the reaction products (Bruno et al., 2004). The rock hosting the texture need not necessarily be gabbroic, but "coronite" is considered by some to refer exclusively to olivine gabbros exhibiting this texture (Davidson, 1991). Here, the coronites under consideration are in fact derived from olivine gabbros; therefore the second usage will be employed.

In coronites, coronas form by a series of reactions between minerals in disequilibrium, commonly olivine and plagioclase or Fe-Ti oxides and plagioclase. Product minerals typically include orthopyroxene, clinopyroxene, amphibole, spinel, and garnet, and symplectic intergrowths are common (e.g. Murthy, 1958; Frodesen, 1968; Joesten, 1986; Johnson and Carlson, 1990). The corona typically surrounds the mafic phase and may be preserved at various stages of development. Coronites therefore often record information about a multi-stage metamorphic process, providing an excellent opportunity to study the metamorphic history of the rock. Understanding the reaction history allows a pressure-temperature (P-T) path of metamorphism for the coronite body to be deciphered. On a larger scale, distinct suites of metagabbro have been used to differentiate tectonic domains in complex orogens such as the Grenville Province and to shed light on their evolution. This study focuses on a coronite body belonging to the

Algonquin metagabbro suite, located in the poorly exposed and largely unmapped Novar subdomain of the Grenville Province.

1.2 The Grenville Province

The Mesoproterozoic Grenville Province comprises the youngest rocks of the Canadian Shield and extends as a continuous belt from southern Ontario to the eastern coast of Labrador (Rivers et al., 1989). These rocks represent the roots of a Himalayan-scale collisional orogen, hereafter the Grenville Orogen, which formed between approximately 1200 Ma and 1000 Ma on the southeastern margin of the Laurentian continent (Wynne-Edwards 1972; Rivers et al 1989, 2012). Episodic accretion of magmatic arcs and/or micro-continental terranes to Laurentia resulted in a series of tectonic events that affected both Laurentian rocks and the accreted material (Culshaw et al., 1997). Subsequent exhumation and erosion over the last ca. 1000 My have exposed high-grade metamorphic rocks that were deformed at depths of 20-30 km below the surface, revealing a window into deep crustal processes like those that may be active beneath large modern mountain belts (Culshaw et al., 1997).

The eastern shoreline of Georgian Bay on Lake Huron marks the southwestern exposed limit of the Grenville Province in Canada. The nearly continuous bedrock exposure along the bay as well as inland outcrop have allowed for the interpretation of large scale structures and the definition of discrete lithotectonic domains (Culshaw et al., 1997), described in this work using the terminology of Wynne-Edwards (1972) and Carr et al. (2000) (Figure 1.1). At the northern flank of the orogen, the Grenville Front Tectonic Zone (GFTZ) is a northeast-striking thrust zone that intersects the northeastern

shoreline of Georgian Bay. To the southeast, the high-grade Central Gneiss Belt (CGB) is overlain by the younger Composite Arc Belt (CAB) across a major northeast-striking tectonic boundary referred to as the Composite Arc Belt Boundary Zone (CABBZ). Within the CGB, the Allochthon Boundary Thrust (ABT) separates parautochthonous Laurentian continental material below from farther-travelled allochthonous Laurentian and accreted domains above (Rivers et al., 1989; Ketchum & Davidson 2000).

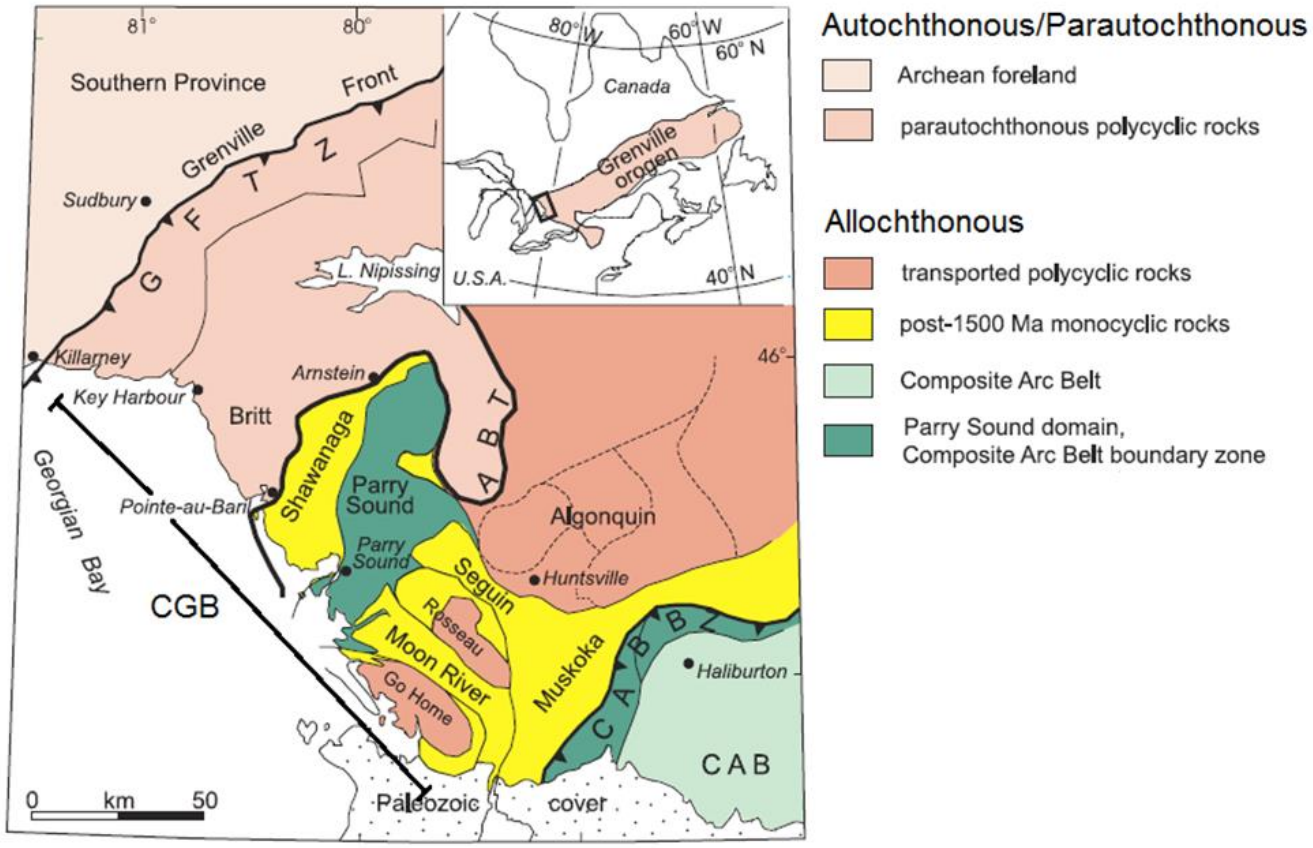

Figure 1.1: Map of the southwestern Grenville Province showing the major domains and structural features (modified after Jamieson et al., 2007, who modified it after Culshaw et al. 1997 and Ketchum and Davidson, 2000). GFTZ = Grenville Front Tectonic Zone, CGB = Central Gneiss Belt, ABT = Allochthon Boundary Thrust, CABBZ = Composite Arc Belt Boundary Zone, CAB = Composite Arc Belt.

The Algonquin metagabbros were intruded into the deep levels of the Laurentian margin ca. 1150 Ma, and were metamorphosed and deformed during their transport over the Laurentian margin during the Ottawan Orogeny ca. 1050 Ma (Heaman and

LeCheminant, 1993); earlier estimates from Davidson and van Breemen (1988) were ca. 1170 Ma for intrusion and 1045 Ma for metamorphism. A more detailed account of the geological setting of these bodies is provided in chapter 2. The present study focuses on a recently exposed example of a coronitic metagabbro in the southwestern part of the CGB.

1.3 Coronitic Metagabbros of the Western Central Gneiss Belt

In the western Grenville Province, a distinctive suite of coronitic metagabbros, formally termed the Algonquin metagabbros (Rivers, 1997) but widely referred to simply as "coronites", is restricted to the allochthonous domains of the CGB, excluding the Parry Sound Domain (Figure 1.2). The Algonquin metagabbro suite was examined in-depth by Grant (1987, 1988) in the most comprehensive study of the group to date. She studied metagabbro bodies throughout the western Central Gneiss Belt from the Go Home, Opeongo, Huntsville, Seguin, Rosseau, Kawagama, and Kiosk subdomains (Figures 1.1 and 2.1) and summarized their protolith features and the spectrum of corona development they represented. Algonquin metagabbros originated from olivine gabbro protoliths with an igneous assemblage of olivine-plagioclase-augite-Fe-Ti oxide and accessory apatite, biotite, and baddeleyite (Grant, 1987). The rocks have a bulk composition transitional between tholeiitic and alkaline with a signature similar to that of continental flood basalts and their feeders. Coronas around olivine and Fe-Ti oxide are present throughout the entire suite, with variable preservation of the originally coarse- to very coarse-grained igneous phases. Grant identified three broad stages of corona development within the suite, from texturally unevolved coronite to increasing levels of textural reworking; these stages are described in more detail in chapter 5. Early stages with well-preserved coronas

were thought to have formed during slow cooling of the gabbro bodies at depth after crystallization, whereas later stages were interpreted to represent metamorphic reworking during Grenvillian metamorphism (Grant 1987). Grant's extensive work on the suite supplies the standard of Algonquin metagabbro characteristics to which the results of the present study are compared, and her hypotheses regarding their development are tested.

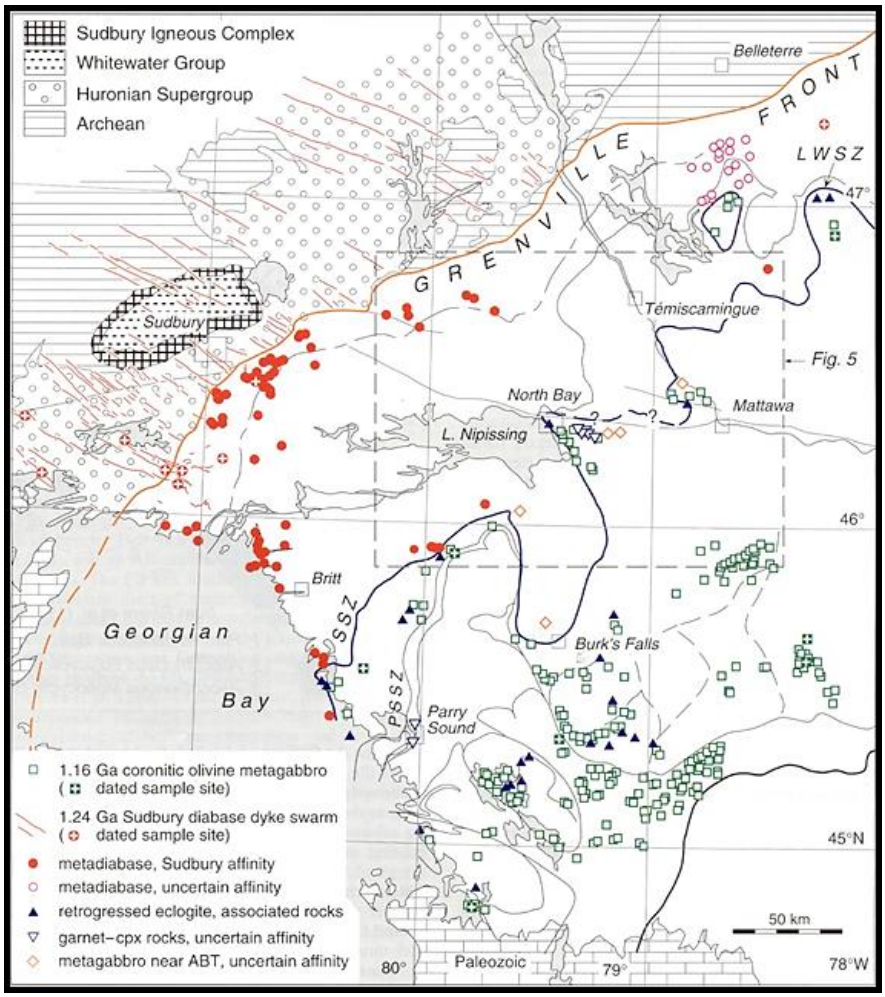

Figure 1.2: Distribution of metagabbro bodies in the southwestern Grenville Province. Algonquin metagabbro is referred to as "coronitic olivine metagabbro" (after Ketchum and Davidson, 2000). Algonquin metagabbros (green squares) were used to constrain the position of the ABT (blue line).

Further work on Algonquin metagabbros has included U-Pb isotopic dating of igneous baddeleyite and metamorphic zircon initially by Davidson and van Breemen (1988), who interpreted corona development to be coeval with the formation of

"raspberry-textured" zircon. Their work on four metagabbro samples revealed ages of 1170 ± 30 Ma and ca. 1045 Ma for igneous crystallization and metamorphism respectively; a later study by Heaman and LeCheminant (1993) found a crystallization age of 1152 ± 2 Ma and a metamorphic age of ca. 1050 Ma for a single sample. Work by Ketchum and Davidson (2000) aimed to distinguish Algonquin metagabbros from other mafic bodies in the CGB, such as the Sudbury metadiabase dykes located north of the ABT (Figure 1.2). The two have similar primary and metamorphic mineral assemblages and corona textures, but differing whole-rock chemistry and ages. Algonquin metagabbros have relatively higher Ca, Al, Cr, and Ni contents than the metadiabase and a slightly more primitive character overall (Ketchum and Davidson, 2000). Ba and light rare earth element (LREE) enrichment is characteristic of the more alkaline Sudbury dykes. In addition, the dykes were intruded at ca. 1235 Ma, approximately 65 My prior to the emplacement of the coronitic metagabbros (Dudàs et al., 1994).

1.4 Previous Work on Coronites

Coronites are distributed throughout the world, commonly in terranes affected by regional metamorphism. Early work on these bodies focused on whether the coronitic texture was a result of residual melt reacting with olivine and Fe-Ti oxides during late stages of crystallization (particularly advocated by Joesten, 1986), or by subsequent regional metamorphism. More recently, the latter explanation has come to be widely accepted (e.g. Ashworth, 1986; Bruno et al., 2004), and was applied to Grenvillian coronites by Davidson and van Breeman (1988), Grant (1988), Johnson and Carlson (1990), and Bethune and Davidson (1997). Others have proposed a multi-step process, in

which the initial stages of the corona are formed through magmatic processes, with later metamorphism forming the outer shells (Frodesen, 1968, Gallien et al., 2012).

Two main hypotheses have been proposed for corona development: a single-stage process in which all product shells grow simultaneously (e.g. Grant, 1988), and a multi-stage process in which each product shell grows sequentially (e.g. Joesten, 1986). Although a single-stage model can explain the mineral assemblages, workers such as Johnson and Carlson (1990) and Gallien et al. (2012) noted that detailed textural observations indicate more complexity and point to progressive evolution of each product shell under disequilibrium conditions.

The role of fluid in corona-forming reactions is also poorly understood. Sapountzis (1975) recognized from previous studies that corona assemblages may be hydrous, anhydrous, or both, and Gallien et al. (2012) identified examples of each in one genetically related group of coronites. Claeson (1998) proposed that fluid interaction with the reactant phases is essential for corona formation, based on the observation that plagioclase included in olivine only reacted near fractures.

In some coronites, relict olivine at the centre of coronas is replaced by an orthopyroxene + magnetite/ilmenite/spinel symplectite pseudomorph (e.g. Frodesen, 1968; Zeck et al., 1982; Claeson, 1998; Gallien et al., 2012). Fluid interaction with olivine and nearby Fe-Ti oxides is commonly interpreted to be the cause of the reaction, whereas Gallien et al. (2012) proposed that the olivine was oxidized to produce magnetite and orthopyroxene. However, these hypotheses have yet to undergo rigorous testing and the timing of the pseudomorph reaction with respect to corona formation is uncertain (Zeck et al., 1982). Both Zeck et al. (1982) and Claeson (1998) reported a consistent

juxtaposition of the symplectites and magmatic Fe-Ti oxides, but the role of the oxides in the reaction remains unknown.

1.5 Contribution of this Study

This study is designed as a detailed examination of a single, well-exposed example of Algonquin coronitic metagabbro. A large metagabbro body, recently exposed by highway construction, was selected for sampling and petrographic and microprobe analysis. The objectives of this study are:

- To determine the metamorphic pressure-temperature (P-T) conditions experienced by this coronite body during Grenvillian metamorphism.
- To investigate the various styles and stages of corona formation preserved within this body, building on the previous work of Grant (1987) and others;

The results of the study have applications in the broader context of both the Grenville Province and the general petrology of coronites. Anticipated outcomes relevant to the Grenville Province include:

- A detailed description of a widespread lithology that is characteristic of specific structural levels in the western Grenville orogen;
- Estimates of the temperatures and pressures of formation of well-preserved mineral assemblages formed at different stages of metamorphism; and from these a well-constrained P-T-t path;
- A P-T history of a single, coherent body affected by Grenvillian metamorphism.

Anticipated results applicable to the investigation of coronites include:

- Testing the applicability of different corona formation hypotheses to a coronite body in a region where similar work has been done;
- Documenting the sequence of mineral assemblages and associated reactions leading to the development of coronitic texture;
- Testing a range of hypotheses for the formation of orthopyroxene pseudomorphs after olivine in some coronites.

Chapter 2: Geological Setting and Field Relations

2.1 Geological Context and Outcrop Location

Algonquin metagabbros, typically concentrated in clusters, appear in the allochthonous belt of CGB, which is separated from the underlying parautochthonous belt by the ABT. This allochthonous belt is divided into three main domains (Culshaw et al., 1997; Jamieson et al., 2007 and references therein): Shawanaga, Algonquin, and Muskoka (Figure 1.1). The coronite examined in this study is in the Algonquin Domain, a polycyclic allochthonous unit (Rivers et al. 1989) where Algonquin metagabbros are especially abundant. The term polycyclic refers to rocks showing evidence of having experienced one or more major tectonic events prior to the Grenville Orogeny; in contrast, the monocyclic units record only the Grenville Orogeny (Rivers et al. 1989). Unlike the monocyclic units, polycyclic units contain abundant granulite-facies rocks and are sparsely migmatitic (Ketchum and Davidson, 2000), with evidence of eclogite-facies metamorphism in the form of isolated retrogressed eclogite pods (Ketchum and Davidson, 2000; Rivers et al. 2002; Marsh and Culshaw, 2014).

The Algonquin Domain is characterized by granulite-facies gneisses derived from a variety of protoliths, including both plutonic and sedimentary rock (Culshaw et al., 1983). Several subdomains within the domain (Figure 2.1), separated by discrete zones of highly strained ‘straight’ gneiss, are dominated by different types of gneiss (Culshaw et al., 1983). In highly deformed gneisses, relict textures and structures have been destroyed and igneous and sedimentary protoliths of similar composition formed gneisses with very similar characteristics after metamorphism (Davidson and Grant, 1986). In the Algonquin

Domain, metaplutonic gneisses are identified by distinct relict igneous texture and metasedimentary paragneisses by the presence of aluminum-silicate phases (Culshaw et al., 1983; Davidson and Grant, 1986).

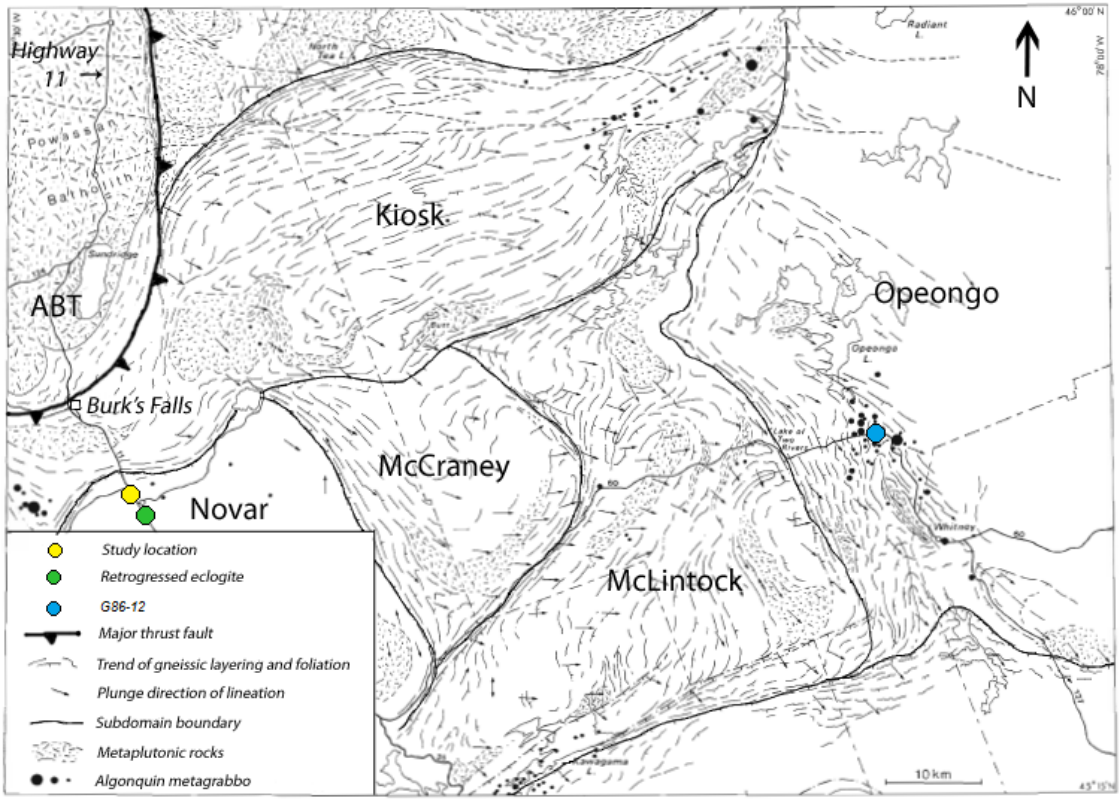

Figure 2.1: Map of the Algonquin Domain, modified after Davidson and Grant (1986). Novar, McCraney, McLintock, and Opeongo are subdomains of the Algonquin Domain. Not shown is the Huntsville subdomain, located south of the Novar subdomain. Sample G86-12 from the Opeongo subdomain was not collected as part of this study and is discussed in chapter 5.

The coronite examined here is in the Novar subdomain of the Algonquin Domain (Figure 2.1). This region is not well mapped, but it can be distinguished from nearby domains on the basis of rock type. The Novar subdomain is dominated by coarse-grained orthogneiss with distinct igneous texture and some metasedimentary rocks (Nadeau, 1990), in contrast to the migmatitic meta-monzonites characteristic of the Kiosk Domain (Foster, 2012) and the granulites and mylonites of the Huntsville subdomain (Nadeau, 1990) to the north and south, respectively (Figure 2.1). Common protolith types in the

Novar subdomain are megacrystic granite and charnockite as well as quartz diorite in the northwest with thin, local layers of sediment-derived aluminous paragneiss (Culshaw et al., 1983). Also present are well-preserved Algonquin metagabbro intrusions and more recently discovered retrogressed eclogite pods (Davidson, 1991; see Figures 1.2 and 2.1). Algonquin metagabbros typically range from 5 to 800 m in diameter and now have tectonic contacts with their host gneisses, though rare examples of possible chilled margins exist (Grant, 1987).

The study location lies only a few kilometers south of the proposed northern boundary of the Novar subdomain and approximately 12 km south of Burk's Falls, where highly strained and complexly folded straight gneisses indicate the presence of a large-scale structure, possibly the ABT. Roughly 2 km south of the coronite body is an exposure of retrogressed eclogite; based on preliminary field and petrographic data (Jamieson, pers. comm. 2014), textures and mineral assemblages indicate that the rock attained HP metamorphic conditions. The proximity of this coronite to these features raises interesting questions about the nature of tectonic boundaries in this area, as evidence of HP metamorphism has not been reported in the Algonquin metagabbro suite (Grant, 1987; Davidson, 1991).

2.2 Outcrop Description

Highway 11 construction in 2005 near Emsdale, Ontario revealed a coronite body at least 150 m wide, hereafter informally termed the Emsdale coronite or metagabbro (Figure 2.2, 2.3). The small knoll it creates in the topography indicates its resistance to weathering and erosion relative to the host rocks. Along the highway, the nearest exposed

host rock, a migmatitic grey orthogneiss, is found in contact with the retrogressed eclogite. Although the Emsdale coronite does not appear to be located within a genetically related coronite cluster, this could reflect poor bedrock exposure in the region. The highly retrogressed and deformed amphibolites normally found at coronite margins in contact with the host (Grant, 1987) are found only near shear zones, pegmatite, and veins in this outcrop. The northernmost end of the outcrop is relatively less resistant to weathering, as it has crumbled while the rest of the exposure maintained a clean, higher cliff face.

The coarse-grained relict igneous assemblage is visible to the naked eye in outcrop with a sub-ophitic to ophitic texture (Figure. 2.4). Well-formed, clouded plagioclase laths range from 1 to 3 cm long, and interstitial black clinopyroxene is typically similar in size or slightly larger. Also visible in outcrop are the remnants of olivine as well as Fe-Ti oxides, both of which never exceed 1 cm and have visible coronas against plagioclase. Accessory apatite crystals are commonly large enough to be identified by the unaided eye, with lengths up to 0.5 cm. These areas of typical gabbroic texture are cut seemingly at random by patches of exceptionally coarse plagioclase and clinopyroxene, which may reach up to 10 cm in size (Figure 2.4b). Other irregular patches enriched in mafic phases or plagioclase are locally associated with abundant garnet (Figure 2.4c). No evidence of internal contacts was found, and variation in primary texture is random along the outcrop. Mineral textures in the northernmost 20 m of the outcrop are obscured by weathering and required thin section examination to identify the cumulate of mafic phases (most < 1 cm).

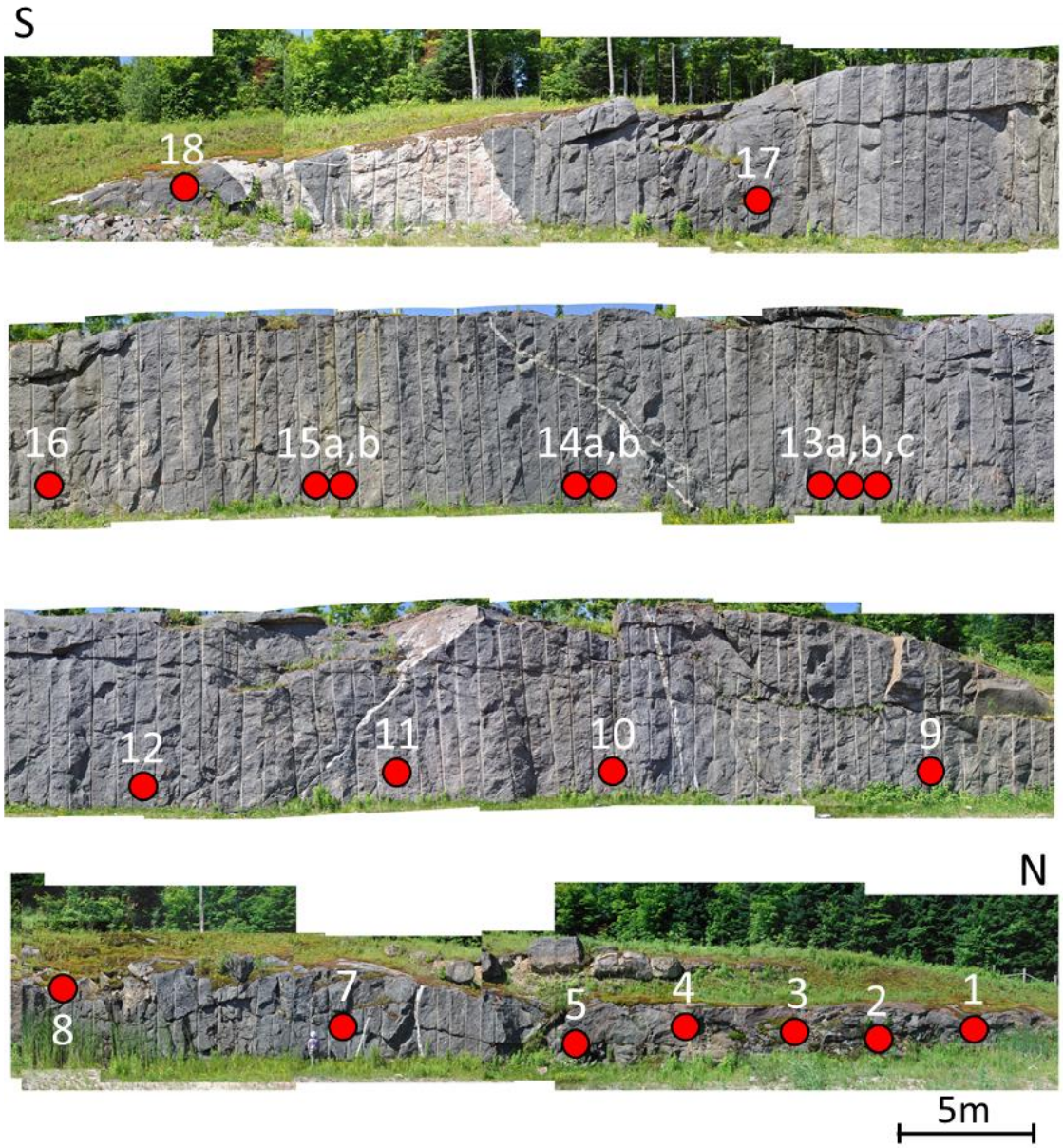

Figure 2.2: Panorama of the Emsdale coronite, beginning at the southernmost point. Red circles show sample locations. The outcrop is approximately 150 m wide.

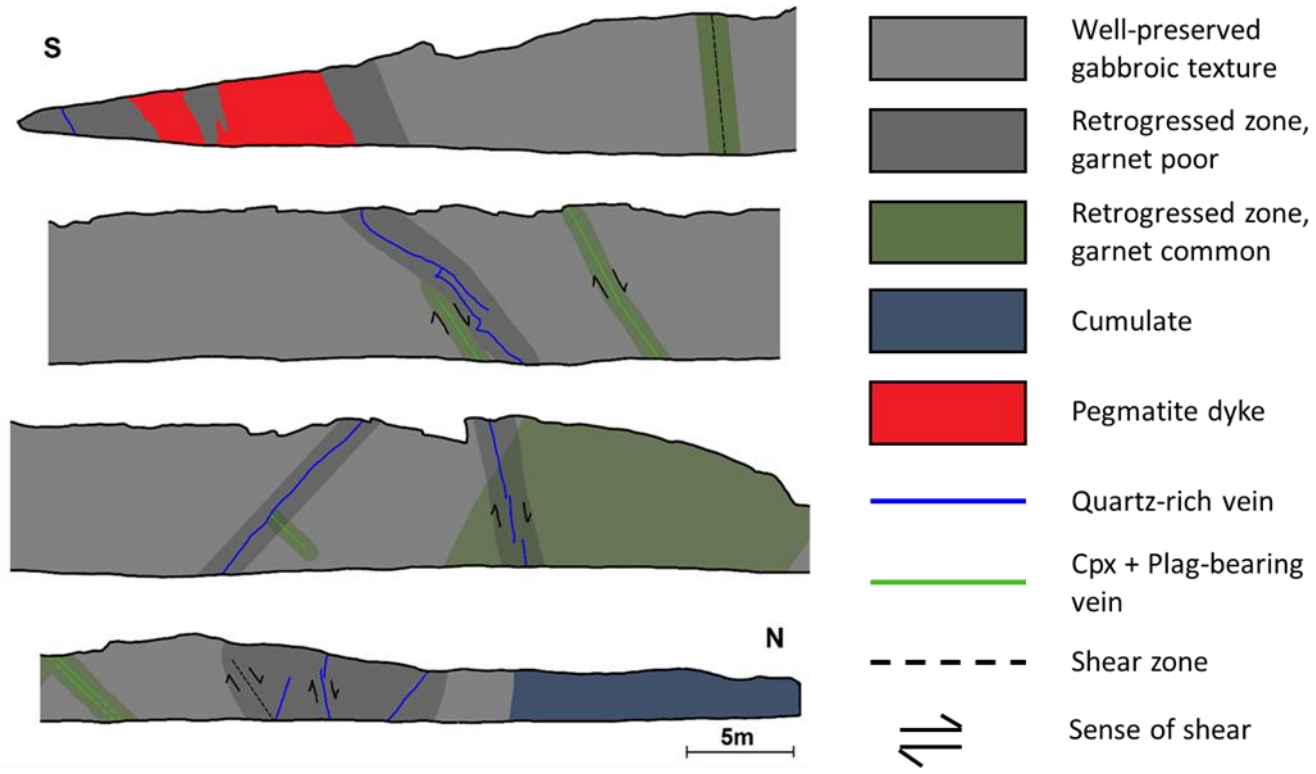

Figure 2.3: Schematic representation of the outcrop. Major cross-cutting veins and shear zones have been emphasized and associated zones of retrogression have been estimated.

The coronite roadcut hosts several veins, a pegmatite dyke, and shear zones (Figure 2.3). The largest of these features is a pegmatite dyke at the southern end of the outcrop with a minimum width of approximately 5 m; this is associated with a zone of retrogression to amphibolite 1.5 m wide. Several quartz-rich veins 10 to 15 cm thick also cut the outcrop, dipping approximately 80° either to the north or south. Two of the largest veins are conjugate, each dipping nearly 45° toward the north and south; the south-dipping vein strikes approximately northeast (central part of Figure 2.3). Zones of amphibolite 1 m wide surround these veins on both sides. A second set of ca. 3 cm-thick

veins in the coronite body are all north-dipping at approximately 40-50°. Clinopyroxene forms the core of the vein, with a rim of a plagioclase (Figure 2.5a). Garnet is abundant in the surrounding 5 cm, and the igneous texture is partially overprinted by metamorphic phases within 1 m of the vein. Shear zones in the body all have dextral shear sense (top down to the north) with a dip of approximately 70-80° to the north (Figure 2.5b) and are typically associated with veins.

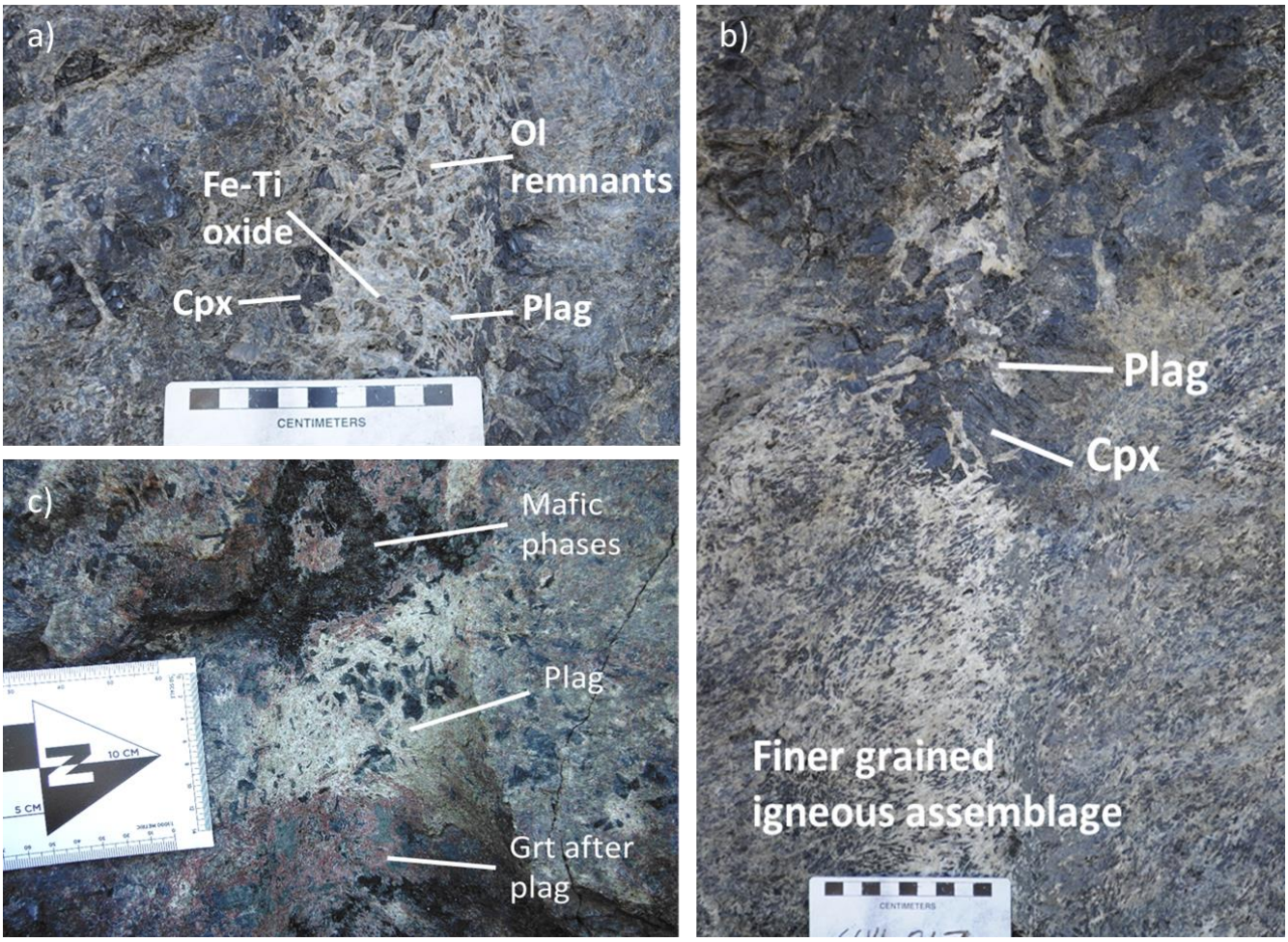

Figure 2.4: Primary textures preserved in outcrop. A) Well-preserved igneous texture, coarse-grained and sub-ophitic to ophitic. B) Coarse-grained patch cross-cutting typical texture. C) Coexisting patches enriched in mafic phases and plagioclase, both associated with abundant garnet.

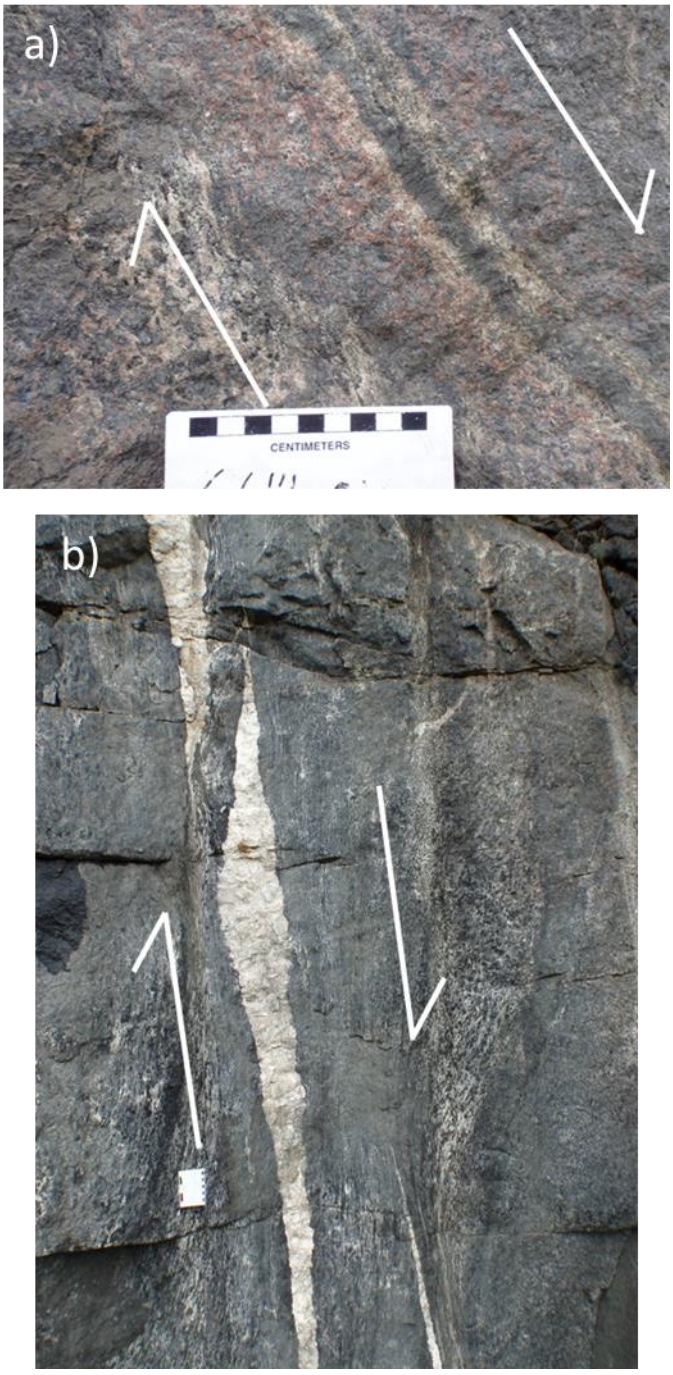

Figure 2.5: Examples of veins in outcrop. A) Clinopyroxene + plagioclase vein with abundant garnet. Note the weak foliation of nearby rock. B) Sheared quartz-rich vein. Arrows indicate shear sense determined by deflections of the fabric into the shear zone.

2.3 Data Collection

Hand samples were collected using a sledgehammer at stations positioned 5 or 10 m apart along the outcrop from north to south (Figure 2.2). The smooth face of the roadcut imposed limitations on sampling, and drilling was not possible. Twenty-one samples were chosen to represent the range of compositions and textures seen in outcrop. At stations near veins, samples both unaffected and affected by retrogression were taken, as well as a sample of the vein itself.

Chapter 3: Petrography and Mineral Chemistry

3.1 Introduction

In this chapter, the results of petrographic analyses from 39 normal thin sections and 10 polished sections, 8 of which were used for EMP analysis, are presented. Characteristics of the protolith were deduced from samples with the best preserved igneous texture (3.2 below). On the basis of corona textures and assemblages, Emsdale coronite samples are classified into several types (3.3 below). Mineral compositions and textural data are presented together below for each corona type.

3.2 Protolith

The Algonquin metagabbro suite is interpreted to be derived from olivine gabbro protoliths (Grant, 1987). For the Emsdale coronite and others in the suite (Grant, 1987), the main igneous rock-forming phases were plagioclase, olivine, clinopyroxene, and Fe-Ti oxides; the former two as early phases and the latter two crystallizing later interstitially. Accessory apatite was an early phase, whereas accessory biotite was likely late. Emsdale coronite samples with well-preserved igneous textures and olivine pseudomorphs showed the following modal abundance, estimated by thin section examination: 45-60% plagioclase, 10-25% clinopyroxene, 8-12% olivine, 8-12% Fe-Ti oxides, 1-2% apatite, 1-2% biotite, <1% baddeleyite, and <1% sulphides. These proportions generally agree with those reported by Grant (1987) from Fe-rich bodies to the east of the study area.

3.3 Corona Types and Assemblages

The three main textural types of the Emsdale coronite are described below, along with their corresponding mineral chemistries. These types represent three general stages of corona development: early (Type 1a, b), late (Type 2), and loss of corona texture (Type 3a, b). Distribution of the types in outcrop is correlated with the distribution of veins and pegmatite (Figure 3.1).

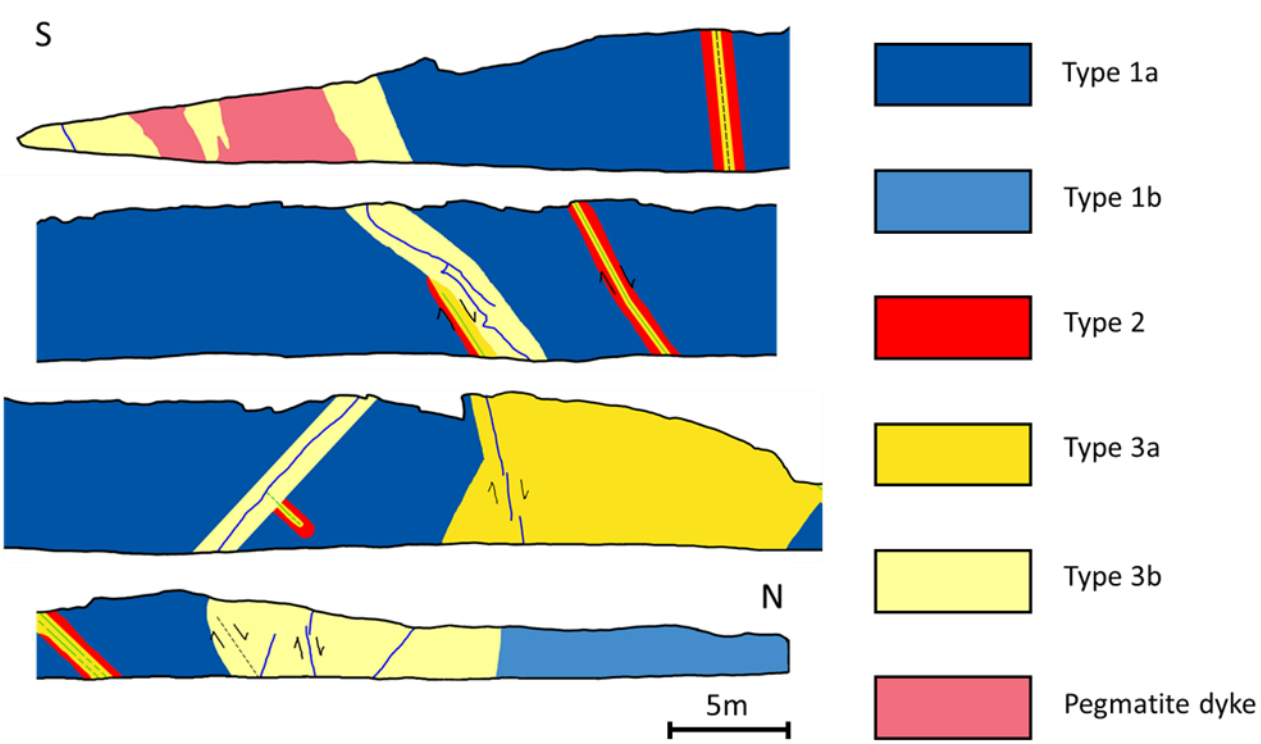

Figure 3.1: Simplified distribution of Types 1, 2, and 3 in outcrop. Type 2 and 3a are commonly associated with clinopyroxene + plagioclase-bearing veins (see Figure 2.3) and Type 3b is found near pegmatite and quartz-bearing veins. Type 1b is restricted to the northern cumulate zone. Type 1a is metagabbro least affected by veins, and has been inferred where veins are not observed. In reality, Type 1a is likely less abundant due to other homogeneities in outcrop outlined in chapter 2.

3.4 Type 1

3.4.1 Textural Features

Type 1 samples are interpreted to represent the early stages of corona development in the Emsdale metagabbro. These samples are from parts of the outcrop least affected by intrusion of veins or pegmatite, and are divided into two varieties. Type 1a preserves a typical relict gabbroic texture, whereas Type 1b developed in the plagioclase-poor cumulate rocks at the north end of the outcrop (Figure 3.2).

Relict phases in Types 1a and 1b show similar textures. Relict plagioclase (≤ 2 cm long in 1a, < 1 cm in 1b) retains its lath shape and is slightly clouded by spinel microcryst inclusions. Blade-like inclusions of spinel and biotite oriented along plagioclase cleavage planes are present in some thin sections. In Type 1b, relict plagioclase is largely consumed by metamorphic phases in coronas. Igneous clinopyroxene (≤ 2.5 cm in 1a, ≤ 1.25 cm in 1b) in these samples is heavily clouded to nearly opaque due to the exsolution of ilmenite microcrysts. Relict Fe-Ti oxides (≤ 1 cm) are largely ilmenite with patches of magnetite, which have fine exsolution lamellae of ilmenite and probably spinel. Larger crystals may be skeletal and are typically rimmed by primary biotite. Former igneous olivine (≤ 1 cm in 1a, ≤ 0.5 cm in 1b) is replaced in every thin section by two varieties of pseudomorph. The vast majority of olivine is replaced by a symplectite of orthopyroxene grains hosting fine, closely-spaced vermicular intergrowths of ilmenite with minor magnetite (Figure 3.3). In some Type 1b samples, this pseudomorph may look like a single opaque oxide crystal. The curved fractures characteristic of olivine are preserved and separate orthopyroxene crystals of differing optical orientation that host differently oriented ilmenite vermicules.

Less commonly, olivine is replaced by a material with the vivid red-orange appearance of "iddingsite", which retains relict olivine fractures and has an embayed form (Figure 3.4). Backscattered electron (BSE) images revealed that this pseudomorph is composed of an aggregate of small (< 100 μm), irregular, strongly zoned crystals (Figure 3.5). In Type 1a, the replaced olivine is almost entirely included within relict clinopyroxene, whereas in Type 1b, "iddingsite" replaced closely spaced olivine crystals.

Euhedral accessory apatite (up to nearly 1 cm long) is commonly included within relict clinopyroxene, biotite, and plagioclase, and uncommonly in olivine pseudomorphs and Fe-Ti oxides. Where it is included in plagioclase, apatite typically has a thin rim of garnet. Baddeleyite (up to 0.3 mm) forms inclusions in plagioclase and biotite in Type 1 samples and is surrounded by a zircon reaction rim; this association was used to determine the ages of igneous crystallization and metamorphism of the Algonquin metagabbro suite (Davidson and van Breemen, 1988).

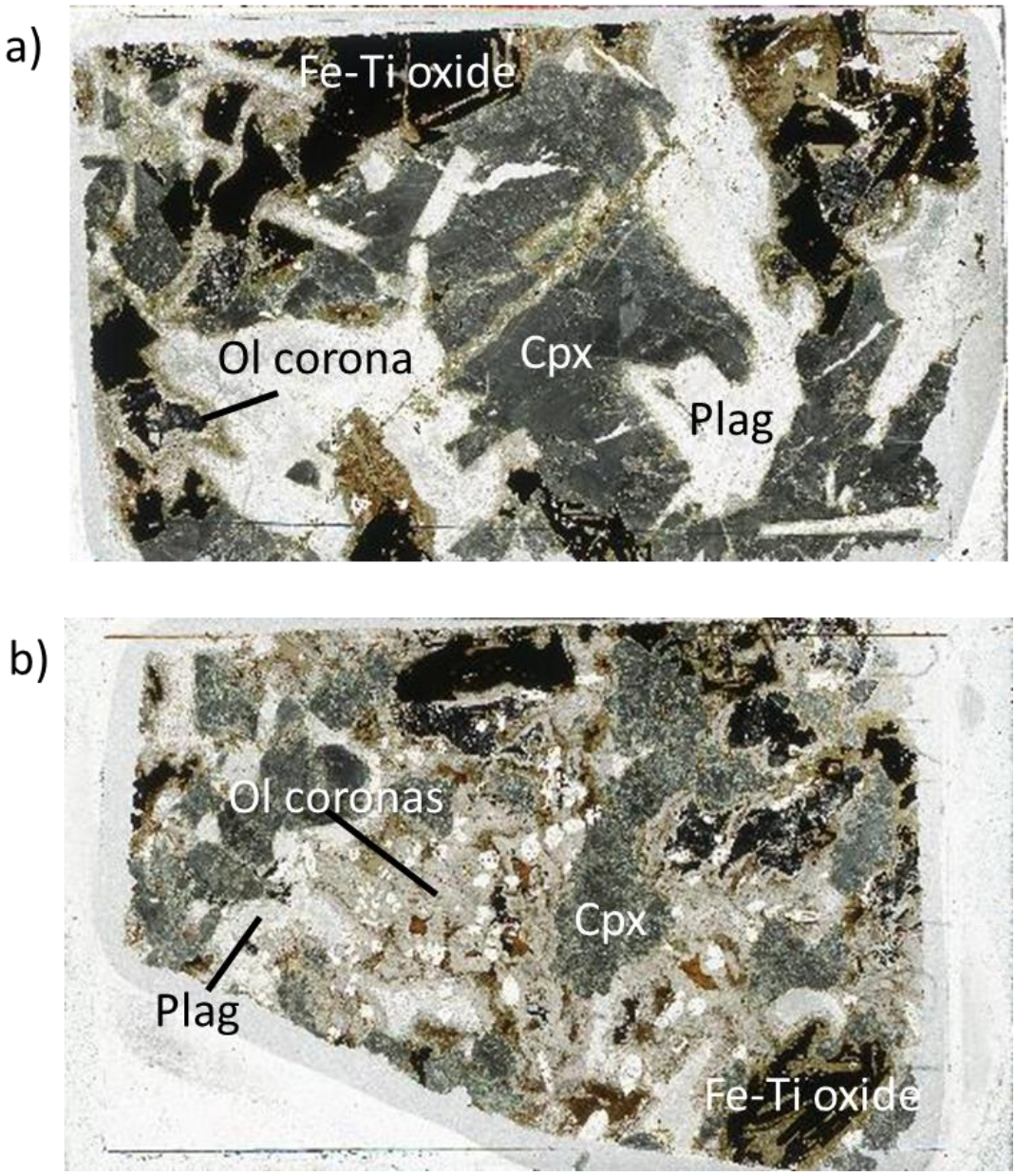

Figure 3.2: Type 1 corona textures, shown in thin section scans (field of view approximately 30 mm). A) Type 1a exhibits a coarse-grained relict ophitic to sub-ophitic texture. B) In Type 1b, little plagioclase remains and mafic phases are more abundant and finer-grained than Type 1a.

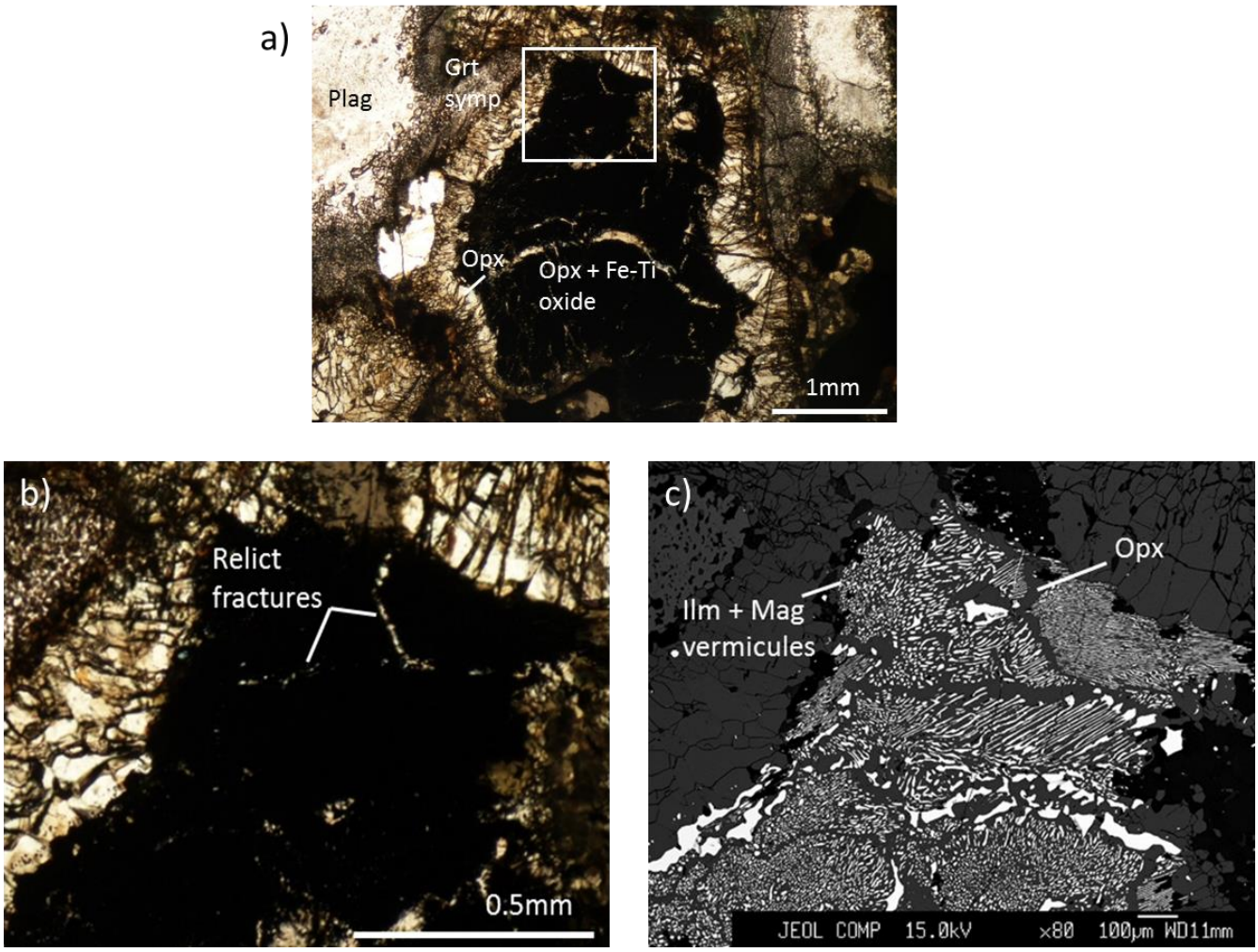

Figure 3.3: Opx + Fe-Ti oxide symplectite pseudomorph after olivine in Type 1a (JKEM-12). (A, B) plane polarized light (PPL) image; C) back scattered electron (BSE) image. Field of view in A) is ca. 5 mm, all images from a single polished section (thicker than normal sections). The pseudomorph appears opaque in section due to the high density of oxide vermicules (A, B). The BSE image of the polished section surface captures the intricate intergrowths. Vermicules have multiple orientations in a single pseudomorph, and appear in clusters separated by relict fractures.

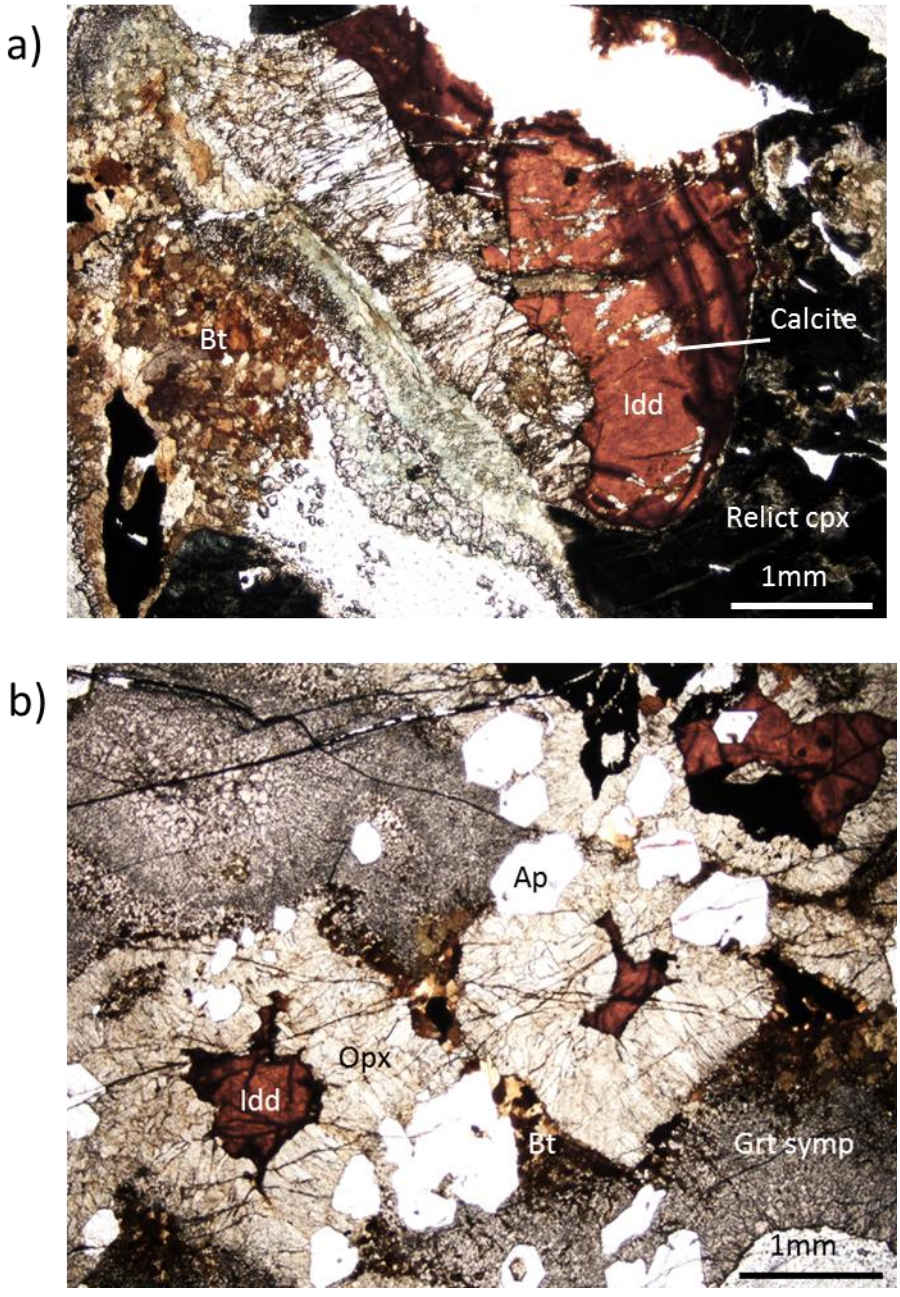

Figure 3.4: "Iddingsite" pseudomorphs after olivine in PPL in A) Type 1a, included within relict clinopyroxene (JKEM-14a) and B) Type 1b, surrounded by broad coronas (JKEM-01). Field of view for each ca. 6.25 mm. The pseudomorphs have a brilliant, slightly mottled red-orange colour with dark relict fractures. The pseudomorph in the upper right of B) consists of both "iddingsite" and opx + Fe-Ti oxide symplectite.

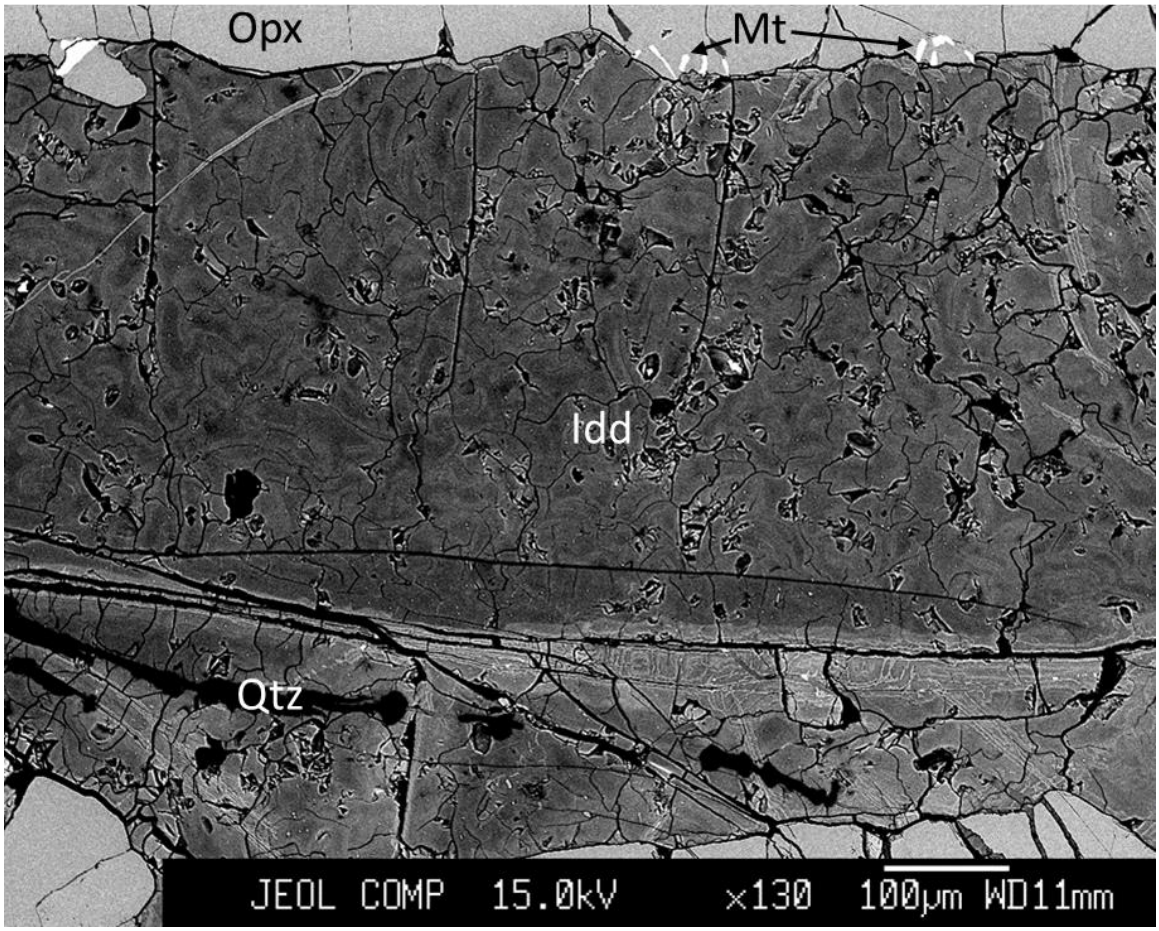

Figure 3.5: BSE image of an "iddingsite" aggregate in Type 1b. Each crystal is zoned with a darker core and paler rim. Sharp, irregular grain boundaries separate the crystals (JKEM-01).

Metamorphism of Type 1 samples formed broadly concentric coronitic shells of metamorphic phases between original olivine and plagioclase and between relict Fe-Ti oxides and plagioclase. In Type 1a, coronas associated with olivine pseudomorphs range from 0.75 to 2 mm wide with well-defined boundaries between each shell. Starting at the olivine pseudomorph and ending with relict plagioclase, the typical assemblage is orthopyroxene ± clinopyroxene, amphibole ± biotite, and garnet symplectite (Figure 3.6a). The orthopyroxene shell has a consistent width within a corona and consists of

elongated crystals (≤ 0.5 mm long) radiating outward from the centre of the former olivine crystal. The adjacent clinopyroxene shell is variable in continuity and width and is formed of equigranular grains (≤ 0.2 mm), commonly with very fine exsolution lamellae, probably of orthopyroxene. Amphibole and biotite crystals in the next shell are of similar shape and size to the clinopyroxene. The outermost shell consists of garnet symplectite, with a band of clean, monomineralic garnet in contact with relict plagioclase. Garnet grains increase in size from ca. 20 to 100 μm towards the plagioclase and are finely intergrown with amphibole + plagioclase + clinopyroxene + orthopyroxene (1-50 μm).

In Type 1b samples, coronas around olivine pseudomorphs are broader (≤ 3 mm wide), with concentric shells of orthopyroxene and garnet + biotite + orthopyroxene (Figure 3.6b). The orthopyroxene and garnet intergrowths that form the bulk of the corona are significantly wider than those in Type 1a and clinopyroxene and amphibole are absent from the corona. Garnet, biotite, and orthopyroxene are equigranular (ca. 0.1 mm) in the inner part of the shell, which is dominated by coarser garnet closer to plagioclase. Coronas between Fe-Ti oxides and plagioclase are similar in Types 1a and 1b. The typical shell sequence is amphibole ± biotite surrounded by garnet symplectite; these layers are nearly identical to the outer two layers of the olivine corona in Type 1a (Figure 3.7). The most obvious difference is that biotite is more abundant around Fe-Ti oxides, probably reflecting its original distribution in the gabbroic protolith.

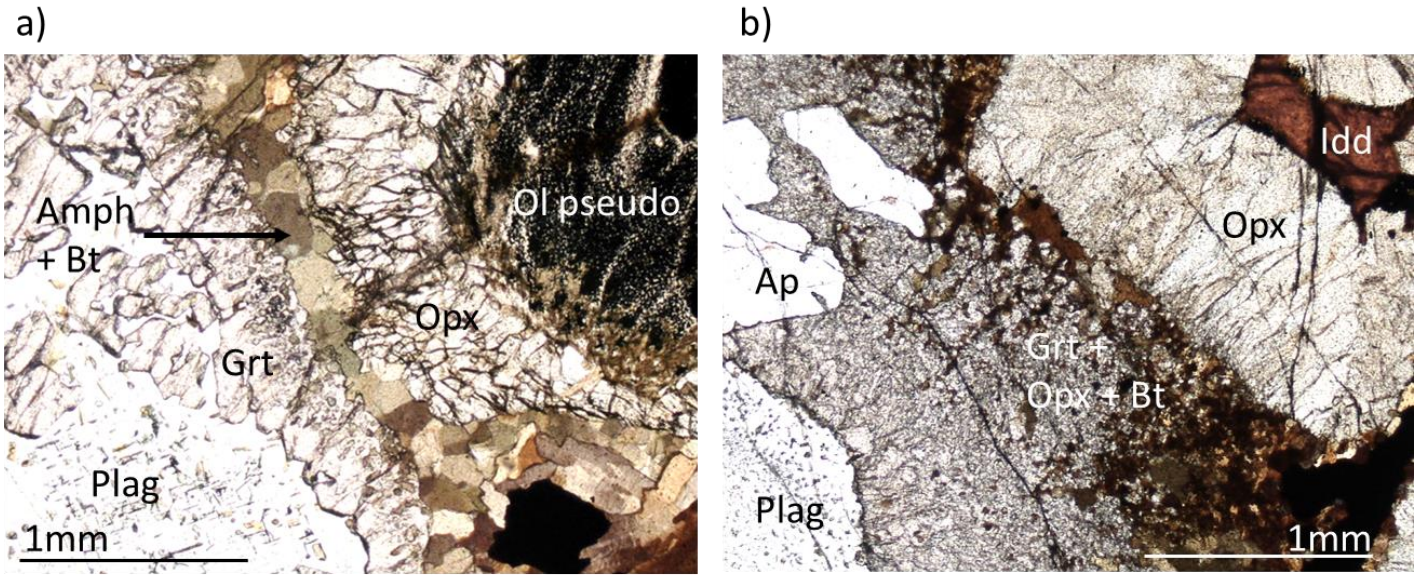

Figure 3.6: Coronas associated with olivine pseudomorphs in PPL. A) Type 1a, surrounding an orthopyroxene + Fe-Ti oxide symplectite (JKEM-17) and B) Type 1b, surrounding "iddingsite" (JKEM-01). Field of view ca. 2.5 mm for each. Compared to Type 1a, Type 1b coronas are typically broader, contain more biotite, and have a finer-grained symplectite.

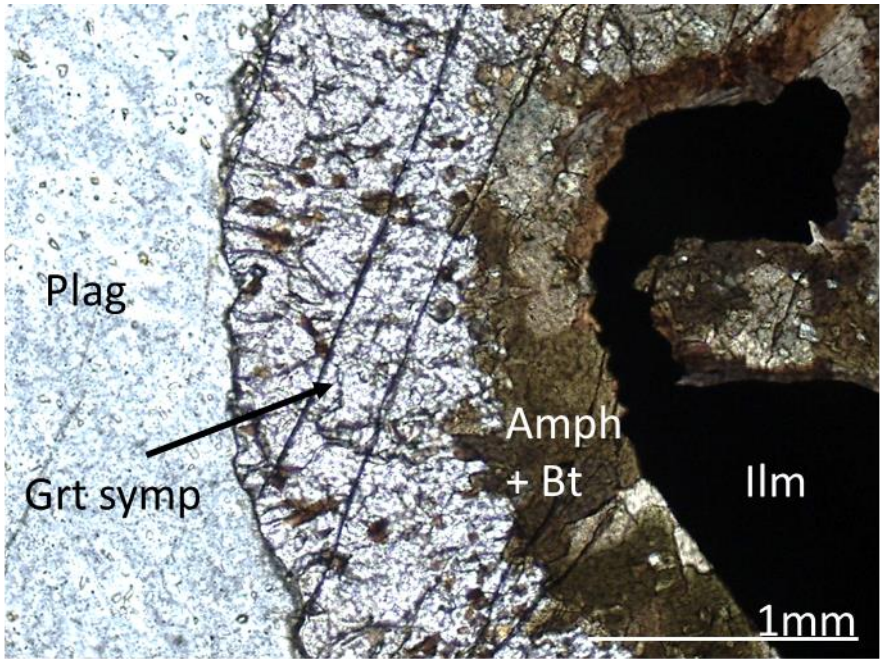

Figure 3.7: Type 1 Fe-Ti oxide corona in PPL (JKEM-1). Field of view ca. 2.5 mm. Biotite and amphibole rim the Fe-Ti oxide (largely ilmenite) with an outer garnet symplectite shell. The adjacent plagioclase exhibits spinel clouding.

3.4.2 Mineral Chemistry

Mineral compositions for all samples were determined using the JEOL 8200 Superprobe in the Robert M. MacKay Laboratory at Dalhousie University, operating at an accelerating voltage of 15.0 kV and a beam current of approximately $2.00 * 10^{-8}$ A, with a minimum spot size of 2 μm. The full set of analyses is presented in Appendix A.

Microprobe spot analyses were acquired from three Type 1a and two Type 1b samples, along with chemical maps showing the distribution of Al, Ca, K, Mg, and Ti in two Type 1a olivine pseudomorph coronas and one Fe-Ti oxide corona (Figures 3.8, 3.9, and 3.10). Table 3.1 lists the end members and abbreviations used below. Average EMP analyses for each phase are provided in Table 3.2 for Type 1a and Table 3.3 for Type 1b.

Mineral	**Formula**	**Endmembers**
Amphibole (Amph)	$NaCa_2[(Mg,Fe^{2+})_4Al]Si_6Al_2O_{22}(OH)_2$	Pargasite (Prg), Ferropargasite (Fpg)
	$NaCa_2[(Mg,Fe^{2+})_4Fe^{3+}]Si_6Al_2O_{22}(OH)_2$	Magnesiohastingsite (Mhs), Hastingsite (Hsg)
Biotite (Bt)	$K_2(Fe^{2+},Mg)_6[Si_6Al_2O_{20}](OH)_4$	Annite (Ann), Phlogopite (Phl)
Clinopyroxene (Cpx)	$Ca(Mg,Fe^{2+})Si_2O_6$	Diopside (Di), Hedenbergite (Hd)
Garnet (Grt)	$(Mg,Fe^{2+},Mn,Ca)_3Al_2Si_3O_{12}$	Pyrope (Prp), Almandine (Alm), Spessartine (Sps), Grossular (Grs)
Orthopyroxene (Opx)	$(Mg,Fe^{2+})SiO_3$	Enstatite (En), Ferrosilite (Fs)
Plagioclase (Plag)	$Na(AlSi_3O_8)$ - $Ca(Al_2Si_2O_8)$	Albite (Ab), Anorthite (An)
Ilmenite	$FeTiO_3$ - Fe_2O_3	Ilmenite (Ilm), Hematite (Hem)
Magnetite	$Fe^{2+}Fe^{3+}{}_2O_4$ - Fe_2TiO_4	Magnetite (Mt), Ulvöspinel (Usp)
Iddingsite		Iddingsite (Idd)

Table 3.1: List of important minerals, their chemical formulas, endmembers, and abbreviations.

Orthopyroxene

Orthopyroxene in Type 1 rocks is the main component of the innermost shell of olivine pseudomorphs coronas and is rare in the outer garnet symplectite shell. In Type 1a, orthopyroxene compositions after olivine are consistently $En_{48}Fs_{52}$. Symplectite orthopyroxenes are more magnesian, averaging $En_{53}Fs_{47}$. Type 1b orthopyroxenes show virtually no variation, averaging $En_{45}Fs_{55}$.

Clinopyroxene

In Type 1 samples, both recrystallized relict clinopyroxene and clinopyroxene in inner and symplectic coronitic shells were analysed. The composition of the crystals can be described in terms of the Di and Hd components, although a small sodic component, typically ranging from 0.8 to 1.4% Na_2O, is also present. Recrystallized relict clinopyroxene in Type 1a samples shows the largest variation in composition, $Di_{55-70}Hd_{45-30}$. Symplectite clinopyroxenes have a similar range, whereas inner shell clinopyroxene is more restricted, $Di_{65-70}Hd_{35-30}$. In Type 1b samples, no clinopyroxene is found within coronas. Recrystallized relict crystals and clinopyroxene associated with recrystallized relict biotite have nearly identical average compositions of $Di_{58}Hd_{42}$, near the Fe-rich end of the Type 1a range.

Amphibole

In Type 1 samples, metamorphic amphibole is the main component of the coronitic shell in contact with the garnet symplectite, and is also an important part of the symplectite. For amphibole shells in Type 1a olivine pseudomorph and Fe-Ti oxide

coronas, amphiboles are classified as magnesiohastingsite (after Leake et al., 1997). Amphiboles associated with Fe-Ti oxide coronas are slightly more Fe-rich than the others, plotting near the magnesiohastingsite-hastingsite boundary. Amphibole is rare in the Type 1b samples analyzed, where it is associated with Fe-Ti oxide coronas and relict clinopyroxene and has a titanian ferropargasite composition.

Biotite

Some large biotites in Type 1 samples are interpreted to be relict igneous crystals, but biotite is also common in coronas, particularly those surrounding Fe-Ti oxides. Type 1a relict biotite crystals average $Ann_{57}Phl_{43}$, with ca. 5.1% TiO_2. Biotites in coronas, both in the inner shell and symplectite, are more magnesian, averaging $Ann_{47}Phl_{53}$, with average TiO_2 content of 4.2%. In one Type 1a sample, metamorphic biotite inclusions in plagioclase were large enough to be analyzed. These crystals average $Ann_{54}Phl_{46}$ and 2.0% TiO_2. Relict biotite in Type 1b samples is more Fe- and Ti-rich than in Type 1a, with one crystal averaging $Ann_{61}Phl_{39}$ and 6.0% TiO_2. Biotites in a corona surrounding an olivine pseudomorph average $Ann_{54}Phl_{46}$ and 6.2% TiO_2, with a consistent composition across the corona. In the Fe-Ti oxide corona analyzed, biotites in garnet symplectite average $Ann_{52}Phl_{48}$ and 5.5% TiO_2, whereas those in the inner shell average $Ann_{57}Phl_{43}$ and 6.1% TiO_2.

Garnet

In Type 1 samples, garnet is the main component of the symplectic coronitic shell. The average garnet composition in Type 1a samples is $Prp_{14}Alm_{65}Grs_{18}$ and

$Prp_{11}Alm_{67}Grs_{18}$ in Type 1b samples. Chemical variation between garnets in olivine pseudomorph coronas and Fe-Ti oxide coronas is negligible; although individual grains are not zoned, there is slight zonation across the shell in Type 1a. Generally, garnets in the inner part of the symplectite have higher Fe/(Fe + Mg) than those close to plagioclase, and the clean outer garnet is generally enriched in Ca (Figures 3.8-3.10, Mg and Ca maps). The chemical compositions of Type 1b garnets are remarkably homogeneous in all settings.

Plagioclase

Type 1 samples preserve relict igneous plagioclase as well as some metamorphic plagioclase within coronas. Traverses of five to seven analyses were conducted across three relict crystals in Type 1a samples to investigate zonation. Two showed possible relict igneous zonation, from cores somewhat less calcic than expected from gabbro (An_{42-46}) to more sodic rims (An_{16-28}). The composition of the third crystal ranged from An_{35-40}, with possible weak zoning and a slightly albite-enriched core. Relict plagioclase adjacent to the outer reaches of coronas also showed a typical range of An_{35-40}. In one Type 1a sample, antiperthite was observed in several plagioclase grains, i.e. sodic plagioclase hosting exsolution lamellae of potassium feldspar. Metamorphic plagioclase in Type 1a is more sodic and displays a smaller compositional range (An_{15-25}) than the relict crystals. In Type 1b samples, igneous plagioclase crystals are largely consumed by coronas and therefore do not show primary zonation. Both textural settings of plagioclase in these rocks have similar compositions, typically An_{10-15}, and in contrast to Type 1a contain a small Or component (Or_{1-6}).

Olivine Pseudomorphs

Type 1 samples preserve two varieties of olivine pseudomorph: vermicular intergrowths of ilmenite and magnetite hosted by orthopyroxene, and an iddingsite-like material. In the former, more common, pseudomorph, orthopyroxene composition generally matches that of the adjacent orthopyroxene shell. In Type 1a samples, pure ilmenite accounts for > 90% of the opaque vermicules. Analyses of associated magnetite are dominantly Fe_3O_4 with a small amount of Al_2O_3 and TiO_2. Analyses of pseudomorph Fe-Ti oxides are indistinguishable from those of relict primary Fe-Ti oxides. In one Type 1b sample, variable Ti:Fe indicates that ilmenite and magnetite are too finely intergrown (< 2 μm) to be resolved with the microprobe beam.

One "iddingsite" aggregate was analyzed in a Type 1b sample; a summary of the results is given in Table 3.4. Each crystal is strongly zoned with a chemically and texturally distinct core and rim. A systematic chemical variation in Fe:Si averages 0.55:1 for cores and 0.63:1 for rims. The consistently low totals (ca. 90%) are attributed to H_2O within the crystal structure.

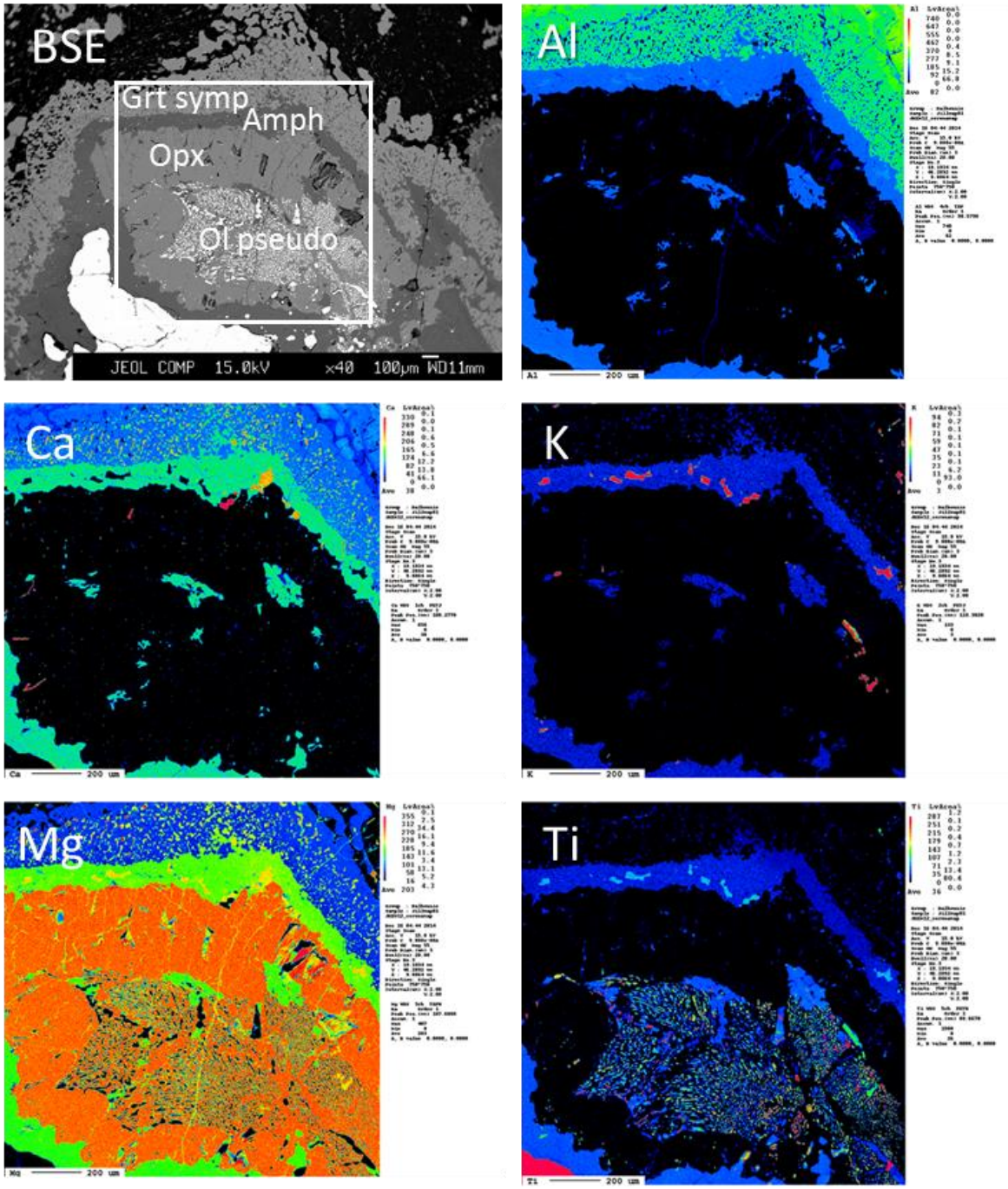

Figure 3.8: BSE image of a Type 1 olivine pseudomorph corona (top left) with chemical maps (Al, Ca, K, Mg, Ti) (JKEM-12). Scale bar on maps = 200 µm. The chemically homogeneous orthopyroxene shell is surrounded by a shell of mainly amphibole. Symplectite garnet is weakly zoned in the Mg and Ca maps, with increasing Mg and Ca toward plagioclase.

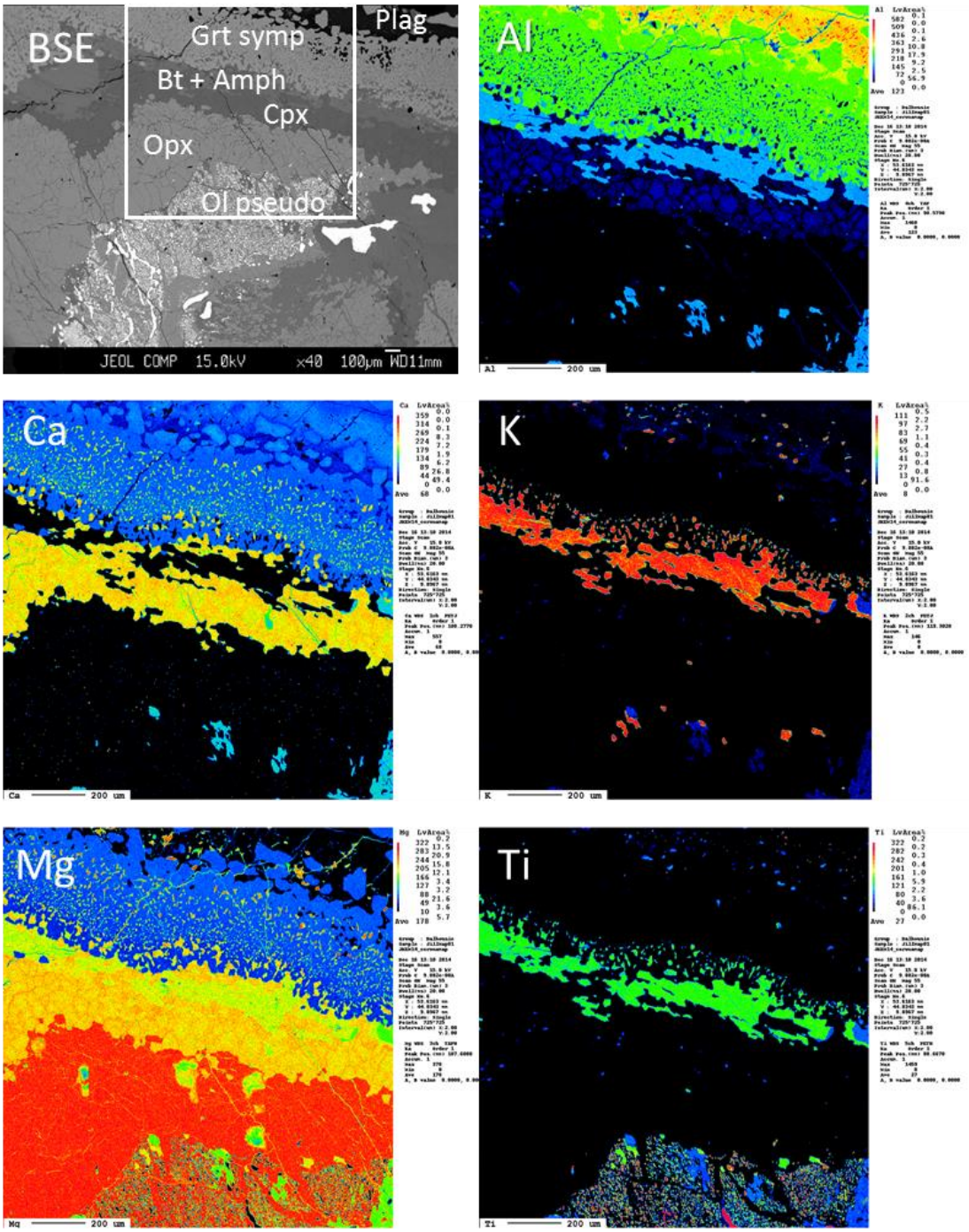

Figure 3.9: BSE image of a Type 1 olivine pseudomorph corona (top left) with chemical maps (Al, Ca, K, Mg, Ti) (JKEM-14a). Scale bar on maps = 200 µm. Adjacent to the typical orthopyroxene shell is a clinopyroxene + biotite shell with minor amphibole. Al and Ca maps show depletion of these elements in plagioclase near garnet. Clinopyroxene crystals have cores relatively enriched in Al (typically correlated with Na enrichment) and rims relatively enriched in Mg.

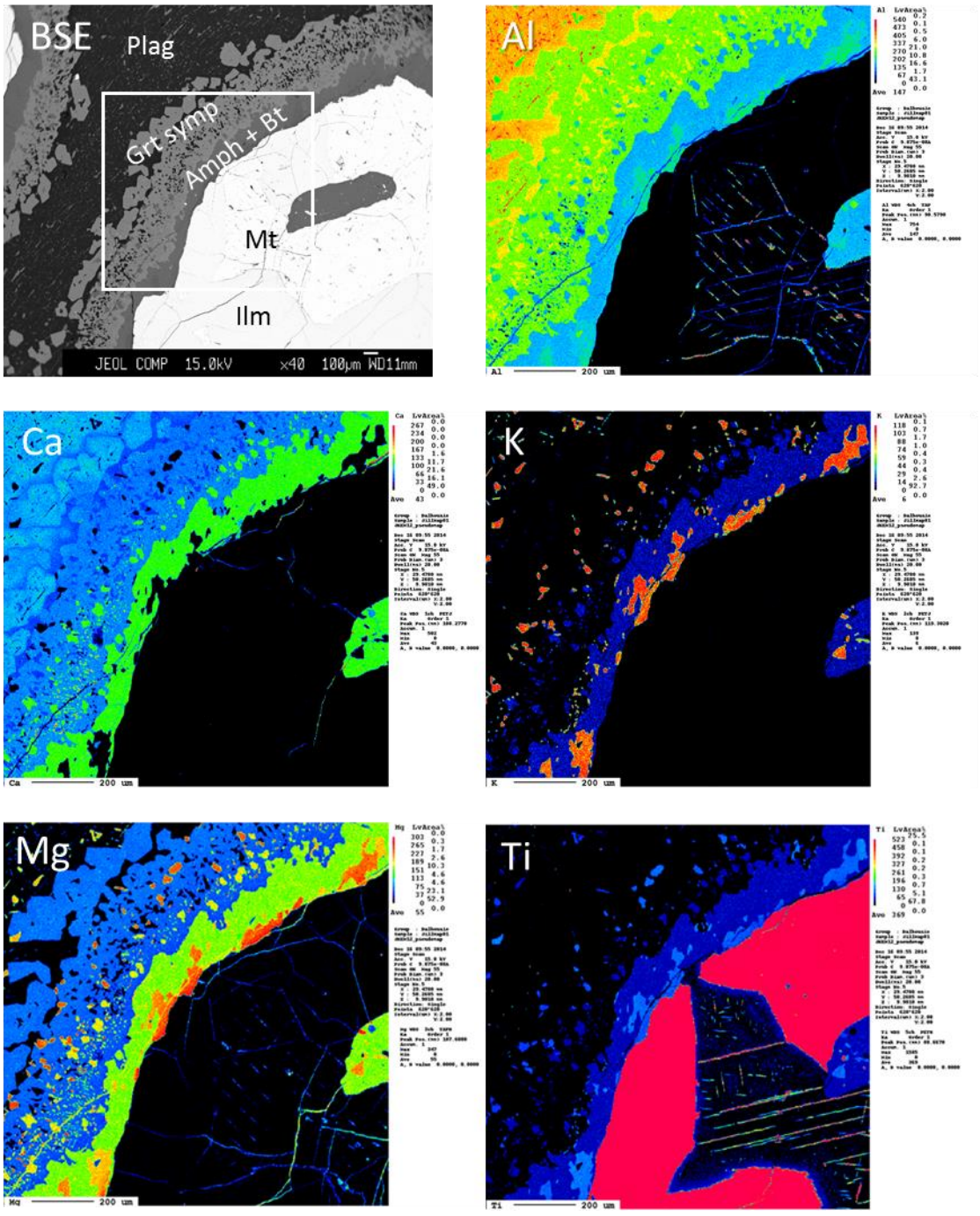

Figure 3.10: BSE image of a Type 1 Fe-Ti oxide corona (top left) with chemical maps (Al, Ca, K, Mg, Ti) (JKEM-12). Scale bar on maps = 200 µm. The Ti map shows ilmenite exsolution lamellae in magnetite and the Al map shows an Al-rich set of lamellae in magnetite (likely a type of spinel). Biotite, shown in red on the K map, is adjacent to the Fe-Ti oxide.

	Orthopyroxene		Clinopyroxene			Amphibole	
	Inner cor	Ol symp	Recrys	Inner cor	Symp	Ol corona	Ilm corona
SiO_2	51.54	52.14	52.49	52.54	52.56	42.38	41.40
TiO_2	0.05	0.05	0.15	0.08	0.07	1.32	1.53
Al_2O_3	0.57	0.49	1.66	2.38	2.28	12.21	12.67
Cr_2O_3	0.01	0.05	0.01	0.00	0.01	0.00	0.00
FeO	31.76	28.89	13.25	11.48	12.44	17.25	18.03
MnO	0.44	0.37	0.23	0.16	0.12	0.09	0.05
MgO	16.27	18.52	11.03	11.45	10.99	10.36	9.46
CaO	0.41	0.35	20.65	21.26	20.96	11.09	10.86
Na_2O	0.01	0.01	1.09	1.14	1.15	2.58	2.72
K_2O	0.02	0.02	0.02	0.02	0.05	0.94	0.91
ZrO_2	0.00	0.00	0.01	0.00	0.00	0.00	0.00
Total	101.10	100.89	100.60	100.51	100.62	98.23	97.64

	Biotite			Garnet	Plagioclase			
	Relict	Corona	Plag inc	Corona	Core[1]	Rim[1]	Near cor	Symp
SiO_2	36.21	36.35	33.67	37.78	58.55	62.61	58.61	63.87
TiO_2	5.12	4.09	2.09	0.04	0.00	0.00	0.00	0.00
Al_2O_3	13.94	14.62	18.47	21.24	26.75	23.77	26.21	22.78
Cr_2O_3	0.01	0.00	0.00	0.04	0.00	0.00	0.00	0.00
FeO	22.03	18.88	20.43	29.91	0.01	0.11	0.13	0.62
MnO	0.01	0.02	0.03	1.35	0.00	0.00	0.00	0.00
MgO	9.41	12.13	9.79	3.69	0.00	0.01	0.00	0.05
CaO	0.00	0.04	0.08	6.38	8.28	4.94	8.12	3.98
Na_2O	0.09	0.27	0.06	0.01	6.79	8.69	6.96	9.28
K_2O	9.36	9.17	9.26	0.03	0.18	0.24	0.14	0.19
ZrO_2	0.00	0.00	0.00	0.01	0.00	0.01	0.01	0.00
Total	96.18	95.58	93.88	100.48	100.57	100.37	100.19	100.77

Table 3.2: Average EMP analyses for corona-forming phases in Type 1a.
Cor = corona, symp = symplectite, inc = inclusion, recrys = recrystallized.
[1] From plagioclase showing relict igneous zonation.

	Orthopyroxene	Clinopyroxene		Amphibole	Biotite				Garnet	Plagioclase
	Ol corona	Recrys	With bt	Ilm corona	Relict	Ol corona	Ilm inner cor	Ilm symp	Corona	Relict & symp
SiO_2	51.51	51.70	51.18	40.98	35.53	36.22	35.99	36.34	37.18	64.67
TiO_2	0.03	0.15	0.00	2.77	6.01	6.18	6.15	5.53	0.04	0.04
Al_2O_3	0.53	2.15	1.79	11.57	13.31	13.94	14.06	13.78	20.70	21.99
Cr_2O_3	0.02	0.01	0.00	0.00	0.00	0.00	0.01	0.09	0.05	0.00
FeO	32.64	15.02	14.46	20.67	22.96	20.97	21.73	20.46	30.28	0.28
MnO	0.51	0.30	0.13	0.18	0.00	0.04	0.05	0.10	1.80	0.02
MgO	15.43	9.59	9.76	7.48	8.31	9.86	9.36	10.60	2.88	0.01
CaO	0.49	20.31	20.45	10.75	0.03	0.02	0.02	0.08	6.55	2.92
Na_2O	0.02	1.30	1.05	2.48	0.04	0.21	0.15	0.05	0.02	9.57
K_2O	0.03	0.01	0.01	1.62	9.56	9.38	9.57	9.67	0.04	0.46
ZrO_2	0.01	0.02	0.00	0.01	0.00	0.00	0.01	0.02	0.01	0.00
Total	101.22	100.54	98.84	98.56	95.75	96.83	97.10	96.72	99.53	99.96

Table 3.3: Average EMP analyses for corona-forming phases in Type 1b. Abbreviations same as Table 3.2.

	Cores		Rims	
	Average	St. Dev.	Average	St. Dev.
SiO_2	55.50	1.08	52.38	0.89
TiO_2	0.04	0.02	0.04	0.03
Al_2O_3	0.03	0.01	0.02	0.02
Cr_2O_3	0.03	0.02	0.05	0.03
FeO	30.26	0.82	33.11	0.73
MnO	0.39	0.04	0.37	0.03
MgO	2.68	0.14	2.52	0.11
CaO	1.53	0.09	1.52	0.07
Na_2O	0.03	0.01	0.02	0.01
K_2O	0.16	0.04	0.20	0.03
ZrO_2	0.00	0.01	0.01	0.01
Total	90.66	0.40	90.24	0.61

Table 3.4: Average core and rim EMP analyses from “iddingsite”.

3.5 Type 2

3.5.1 Textural Features

Type 2 samples, which are spatially associated with clinopyroxene + plagioclase-bearing veins, represent a progression of reactions and textural reworking relative to Type 1 (Figures 3.1, 3.11). Relict igneous phases, particularly plagioclase and clinopyroxene, show signs of breakdown and recrystallization. Where relict plagioclase is preserved, spinel dust is absent and the blade-like inclusions of spinel and biotite are larger. Plagioclase has recrystallized to a mosaic of inclusion-free polygonal grains, and in some crystals, is partially replaced by idioblastic garnet (0.5 to 1 mm) at the outer margins of coronas. Relict clinopyroxene is variably recrystallized at its edges in a similar fashion to plagioclase. The polygonal grains are inclusion-free and strongly resemble those in the Type 1a olivine corona clinopyroxene shell. Many relict clinopyroxene crystals have fewer ilmenite lamellae than those of Type 1 and are thus more translucent. The outer margins are partially replaced by amphibole. Fe-Ti oxide crystals are more embayed or have broken down into separate, irregular, smaller crystals partly consumed by amphibole and biotite. Olivine pseudomorphs in Type 2 are mosaics of equant orthopyroxene variably replaced by clinopyroxene that lack ilmenite and magnetite vermicules ($\leq$ 100 μm) (Figure 3.12).

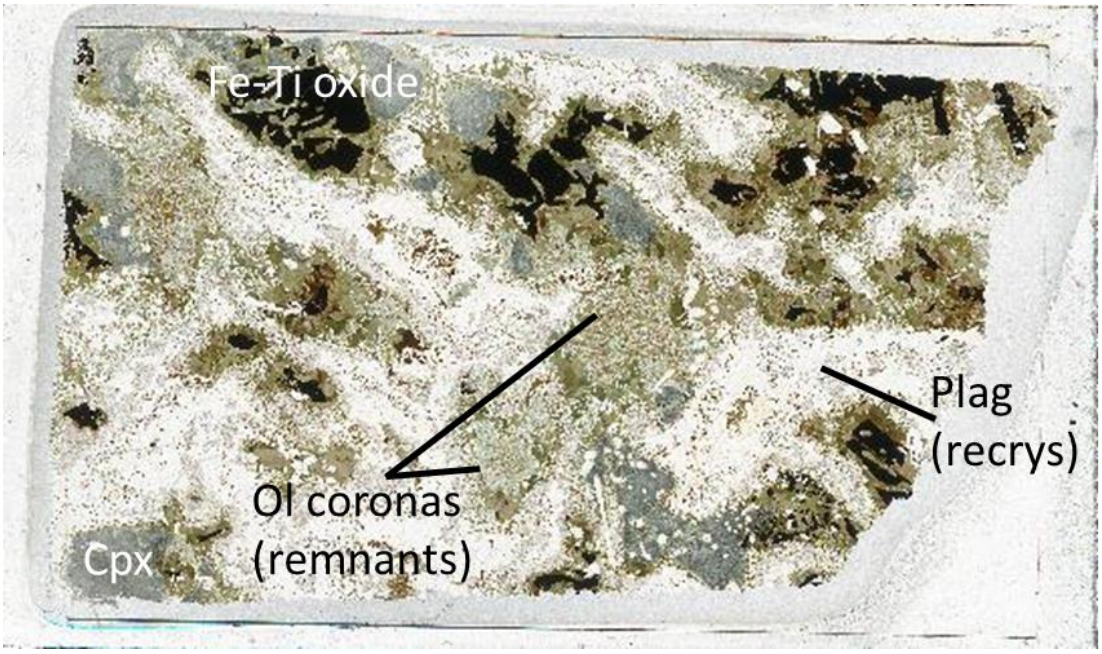

Figure 3.11: Type 2 textures in thin section (field of view = 30 mm). Relict igneous texture is partially overprinted by mafic phases and plagioclase has recrystallized to a lath-shaped mosaic. Orthopyroxene + clinopyroxene aggregates replace olivine pseudomorphs.

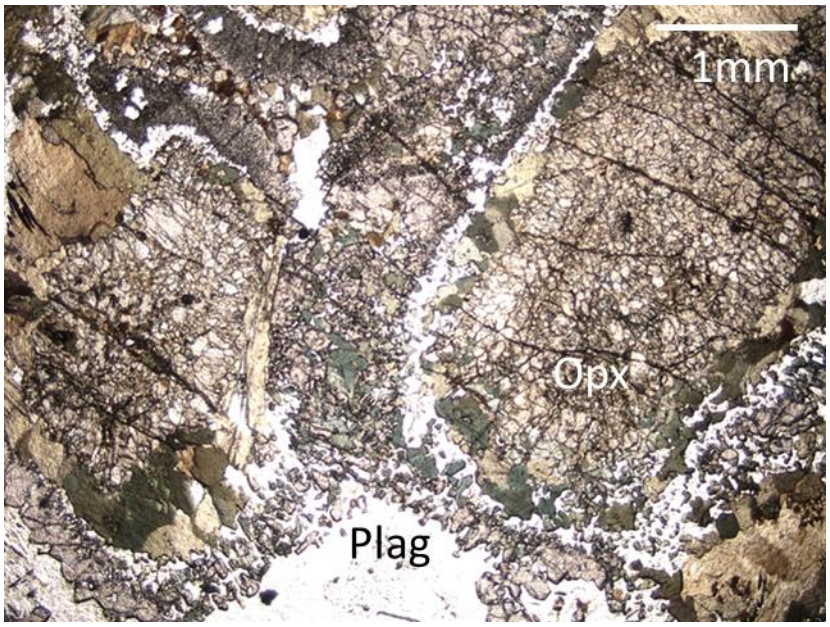

Figure 3.12: Orthopyroxene mosaics after olivine in Type 2 (JKEM-14b). Field of view ca. 6.25 mm. Orthopyroxene crystals are equant, in contrast to the radiating crystals in Type 1.

Coronas in Type 2 samples show breakdown and changes in the mineral assemblages relative to Type 1. Olivine pseudomorph coronas typically have an orthopyroxene core surrounded by shells of amphibole, plagioclase moat, and garnet or garnet symplectite (Figure 3.13a). The orthopyroxene shell is texturally indistinguishable from the olivine pseudomorph and forms an equigranular aggregate at the core of Type 2 coronas. Clinopyroxene, where present, is intergrown with orthopyroxene in the mosaics. Orthopyroxene is progressively replaced by clinopyroxene + plagioclase in further reacted samples (Figure 3.13b). The amphibole shell is similar to that of Type 1, but its embayed contact with the plagioclase moat suggests instability between the amphibole and plagioclase. This is true of the garnet shell as well; the garnet in the symplectite is more texturally broken down than in Type 1 and comprises radiating, xenoblastic crystals of garnet, amphibole, and plagioclase in some coronas (Figure 3.12). Locally, garnet crystals have amalgamated into a monomineralic band with individual crystals zoned from core to rim (Figure 3.14). These two textures may coexist within a single corona. Coronas associated with Fe-Ti oxides have the same assemblages as Type 1, but also display a plagioclase moat between the two shells (Figure 3.13b). Garnet textures are similar to those in the olivine coronas.

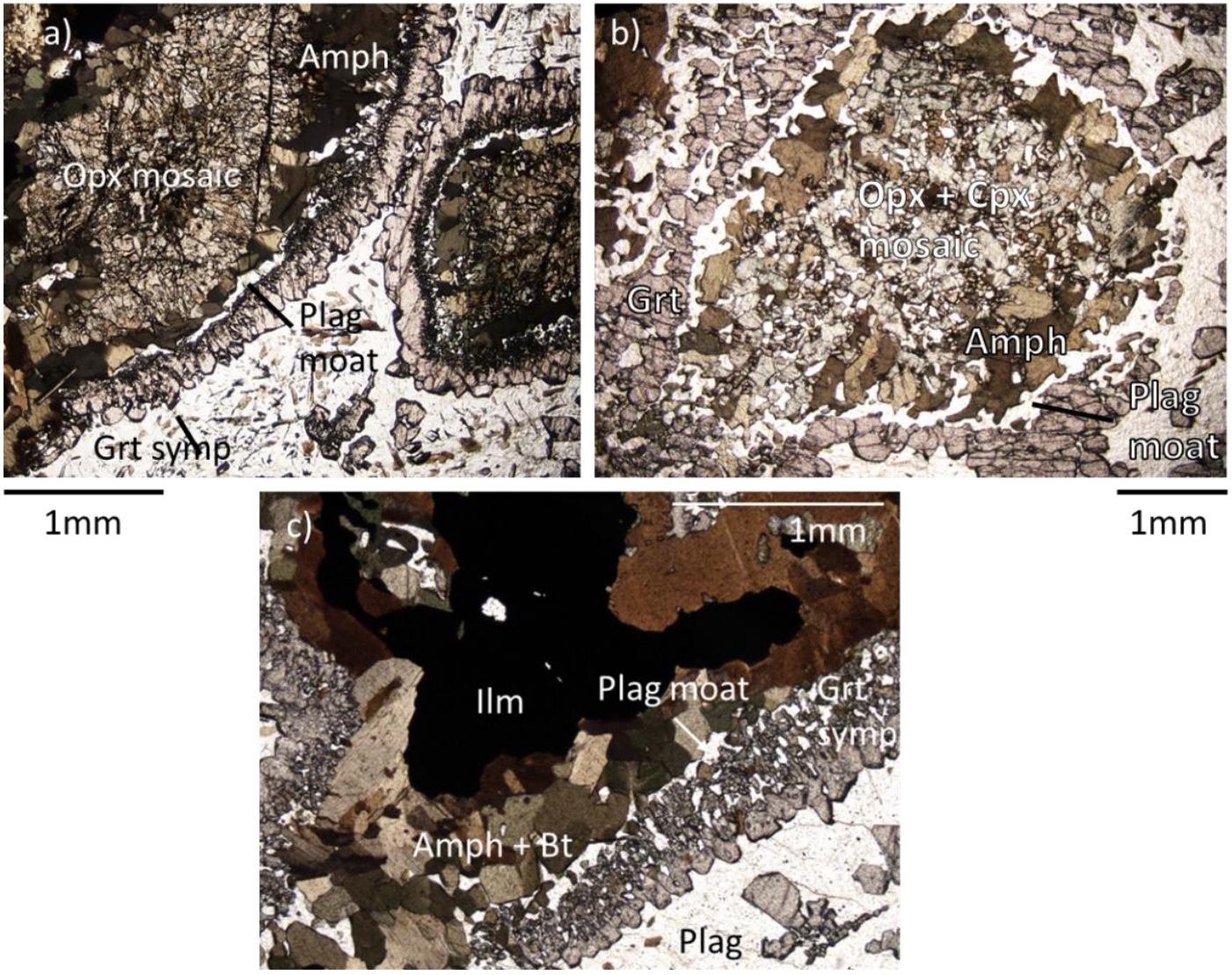

Figure 3.13: Typical Type 2 corona textures. A) Corona around an orthopyroxene mosaic (JKEM-14b). Field of view ca. 4 mm. B) A Type 2 corona. Orthopyroxene is partially replaced by clinopyroxene, plagioclase, and amphibole (JKEM-16). Field of view ca. 6.25 mm. C) Corona around a Fe-Ti oxide (JKEM-11). Field of view ca. 2.5 mm. In all three coronas, embayed garnet and amphibole are separated from each other by a plagioclase moat.

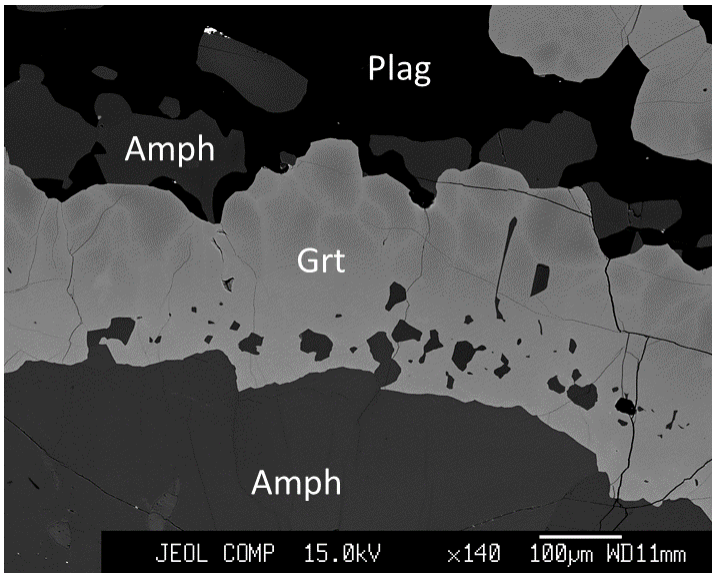

Figure 3.14: BSE image of amalgamated, zoned garnet in a Fe-Ti corona (JKEM-14b). Inner shell garnet is not zoned and hosts inclusions of amphibole. No plagioclase moat is present in this corona.

3.5.2 Mineral Chemistry

The chemical data summarized here were obtained from two Type 2 samples, JKEM-14b and JKEM-15b, the latter with more advanced textural and mineralogical reworking. Table 3.5 lists average compositions for each phase.

Orthopyroxene

In Type 2 rocks, orthopyroxene forms mosaics after olivine but is typically absent from the symplectic coronitic shell. In JKEM-14b, however, orthopyroxene is a small component of the symplectite in the olivine pseudomorph corona, with an average of $En_{59}Fs_{41}$. The composition of mosaic orthopyroxene is consistent within samples but differs slightly between the two. JKEM-14b mosaics average $En_{55}Fs_{45}$, whereas those in JKEM-15b average $En_{51}Fs_{49}$.

Clinopyroxene

Corona clinopyroxene is common in JKEM-15b but virtually absent from JKEM-14b, save for one orthopyroxene-cored corona almost entirely included within relict clinopyroxene. As in Type 1 samples, the clinopyroxenes typically contain ca. 1.0% Na_2O. JKEM-14b clinopyroxenes average $Di_{80}Hd_{20}$ whereas $Di_{76}Hd_{24}$ is the average for JKEM-15b; these are more magnesian than Type 1.

Amphibole

The distribution of amphibole in Type 2 samples is similar to Type 1 samples. Symplectite amphiboles are consistently classified as magnesiohastingsites in both types of coronas; those in the inner shell of olivine pseudomorph coronas fall into the same category with a slightly different composition (Table 3.5). Fe-Ti oxide corona amphiboles have a slightly higher Al component and are therefore pargasites. Outside one Fe-Ti oxide corona, amphibole adjacent garnet is also pargasitic.

Biotite

In Type 2 samples, relict igneous biotite is not preserved and all analyses are from inner corona biotite near igneous Fe-Ti oxides and inclusions in plagioclase. Compositions are significantly different between the two Type 2 samples examined. In JKEM-14b, inner corona biotites average $Ann_{30}Phl_{70}$ and 2.2% TiO_2 whereas those in JKEM-15b have averages of $Ann_{47}Phl_{53}$ and 3.5% TiO_2. Biotite inclusions in plagioclase typically contain ca. 3.0% TiO_2 in both samples and average $Ann_{53}Phl_{47}$ in JKEM-15b.

Two biotite inclusions in JKEM-14b are slightly more magnesian than those in JKEM-15b.

Garnet

Garnet in Type 2 symplectic coronitic shells is commonly zoned. Cores are more Ca-rich with an average of $Prp_{17}Alm_{53}Grs_{28}$; garnet rims average $Prp_{17}Alm_{58}Grs_{23}$. Unzoned crystals are relatively more Fe-rich, with compositions averaging $Prp_{19}Alm_{61}Grs_{18}$.

Plagioclase

Type 2 samples saw the proliferation of metamorphic plagioclase, with the introduction of an albitic moat in coronas and the recrystallization of relict plagioclase. Igneous crystals are preserved in JKEM-14b and a traverse across one revealed zoning from a calcic core (An_{48}) to sodic rims (An_{22-26}). Relict plagioclase near the outer shell of coronas averages An_{32}. Recrystallized relict plagioclase outside coronas in JKEM-15 has compositions of An_{9-20}. Metamorphic plagioclase within coronas has a consistent range of An_{14-22} between the two samples.

	Orthopyroxene			Clinopyroxene		Amphibole		
	Ol symp	14b mosaic	15b mosaic	14b corona	15b corona	Symp	Ol corona	Ilm corona
SiO_2	52.32	51.67	51.70	52.08	52.04	41.67	42.05	40.26
TiO_2	0.03	0.04	0.04	0.12	0.12	1.22	1.27	1.51
Al_2O_3	0.87	0.73	0.67	2.47	2.37	13.77	12.65	14.07
Cr_2O_3	0.05	0.01	0.03	0.00	0.07	0.01	0.04	0.01
FeO	25.98	28.06	29.68	8.74	10.61	14.50	16.60	17.06
MnO	0.30	0.36	0.36	0.14	0.14	0.09	0.10	0.09
MgO	20.84	19.06	17.31	13.02	12.32	11.72	10.63	9.25
CaO	0.25	0.29	0.46	22.29	22.13	10.90	10.86	11.16
Na_2O	0.00	0.00	0.01	0.98	1.04	2.83	2.85	2.80
K_2O	0.03	0.03	0.02	0.02	0.07	0.57	0.73	0.93
ZrO_2	0.05	0.01	0.00	0.00	0.01	0.03	0.02	0.01
Total	100.71	100.26	100.30	99.86	100.94	97.31	97.79	97.14

	Biotite			Garnet			Plagioclase				
	14b ilm cor	15b ilm cor	Plag inc	Core	Rim	Unzoned	Core[1]	Rim	Rel near cor	Rec near cor	Moat
SiO_2	36.67	35.79	33.73	37.56	37.32	37.41	55.75	62.02	60.24	64.56	63.82
TiO_2	2.17	3.50	3.05	0.07	0.06	0.06	0.00	0.00	0.00	0.00	0.00
Al_2O_3	17.17	14.97	17.39	21.43	21.27	21.17	28.22	23.85	24.93	21.58	22.32
Cr_2O_3	0.00	0.02	0.02	0.01	0.00	0.07	0.00	0.00	0.00	0.00	0.00
FeO	12.57	18.39	18.84	24.30	26.64	28.19	0.02	0.20	0.14	0.08	0.38
MnO	0.01	0.04	0.01	0.69	1.04	1.02	0.00	0.00	0.00	0.00	0.00
MgO	16.60	11.76	10.51	4.48	4.24	4.91	0.00	0.00	0.02	0.01	0.02
CaO	0.00	0.03	0.04	10.73	8.54	6.62	10.08	5.18	6.43	3.03	3.69
Na_2O	0.41	0.32	0.18	0.01	0.01	0.01	5.97	8.78	7.98	9.89	9.56
K_2O	9.10	9.04	8.80	0.02	0.03	0.03	0.07	0.14	0.11	0.18	0.16
ZrO_2	0.00	0.02	0.01	0.03	0.01	0.03	0.01	0.00	0.00	0.00	0.00
Total	94.70	93.89	92.57	99.33	99.16	99.53	100.13	100.17	99.88	99.33	99.96

Table 3.5: Average EMP analyses for corona-forming phases in Type 2.
Rel = relict, Rec = recrystallized
[1] Single analysis rather than average.

3.6 Type 3

3.6.1 Textural Features

Type 3 samples show the highest degree of textural reworking (Figure 3.15). Most of these samples are located near both types of veins and pegmatite described in the previous chapter; however, several adjacent samples appear to have no relation to veins or other evidence of fluid infiltration in the plane of the outcrop.

Igneous phases and coronas are recrystallized or replaced to such a degree that they may be unrecognizable (Figure 3.15a). In some samples, relict clinopyroxene locally retains a roughly rectangular shape, with its edges partially consumed by amphibole and plagioclase (Figure 3.16). Clinopyroxene in the most texturally reworked rocks is largely replaced by amphibole, plagioclase, and orthopyroxene, leaving only irregular blebs of the original mineral, recognizable by small ilmenite inclusions. Plagioclase is completely recrystallized to granoblastic aggregates (grains ca. 1 mm) in Type 3 samples, although the original lath shape can be identified in some samples. Relict Fe-Ti oxides are largely replaced by amphibole and biotite. In one sample, Fe-Ti oxides within approximately 3 cm of a clinopyroxene + plagioclase-bearing vein have a titanite reaction rim or are symplectically intergrown with titanite (Figure 3.17). Remnants of olivine coronas in these samples are difficult to identify; orthopyroxene has been largely replaced by irregular, granular clinopyroxene, amphibole, and plagioclase (Figure 3.16). Clinopyroxene replacing relict igneous clinopyroxene typically has a single optical orientation and ilmenite inclusions, whereas those replacing olivine coronas have multiple orientations and few inclusions. Small quartz blebs are found as included in plagioclase and have replaced relict clinopyroxene along with plagioclase.

Type 3 samples are divided into two subtypes based on the abundance of garnet. In Type 3a, whether plagioclase aggregates have a lath shape or not, they are partially or largely replaced by idioblastic garnet (ca. 1 mm), locally associated with biotite of similar size (Figure 3.18). Type 3b is characterized by a distinct lack or deficiency of garnet and recrystallized aggregates of plagioclase; these rocks constitute a small proportion of Type 3 samples.

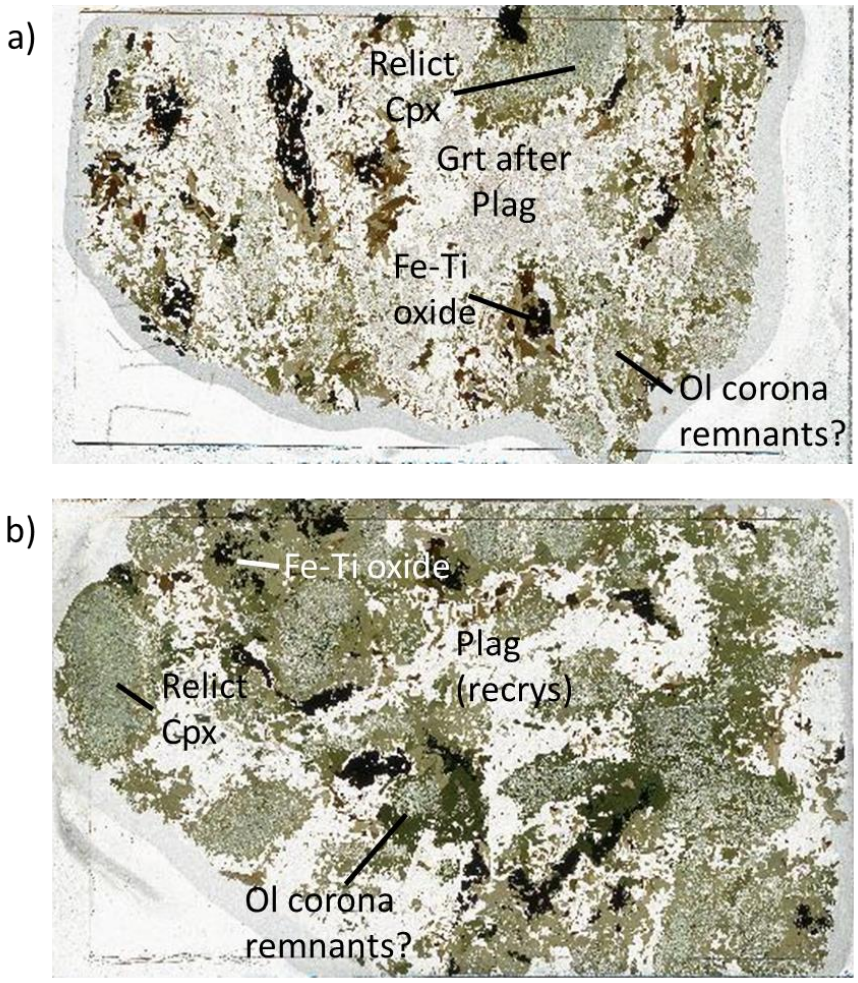

Figure 3.15: Type 3 textures in thin section (field of view = 30 mm). A) Type 3a textures (JKEM-10) and B) Type 3b textures (JKEM-07). Relict igneous texture and coronas are largely overprinted in these samples by later metamorphic phases. Type 3a is distinguished from Type 3b by its abundant garnet.

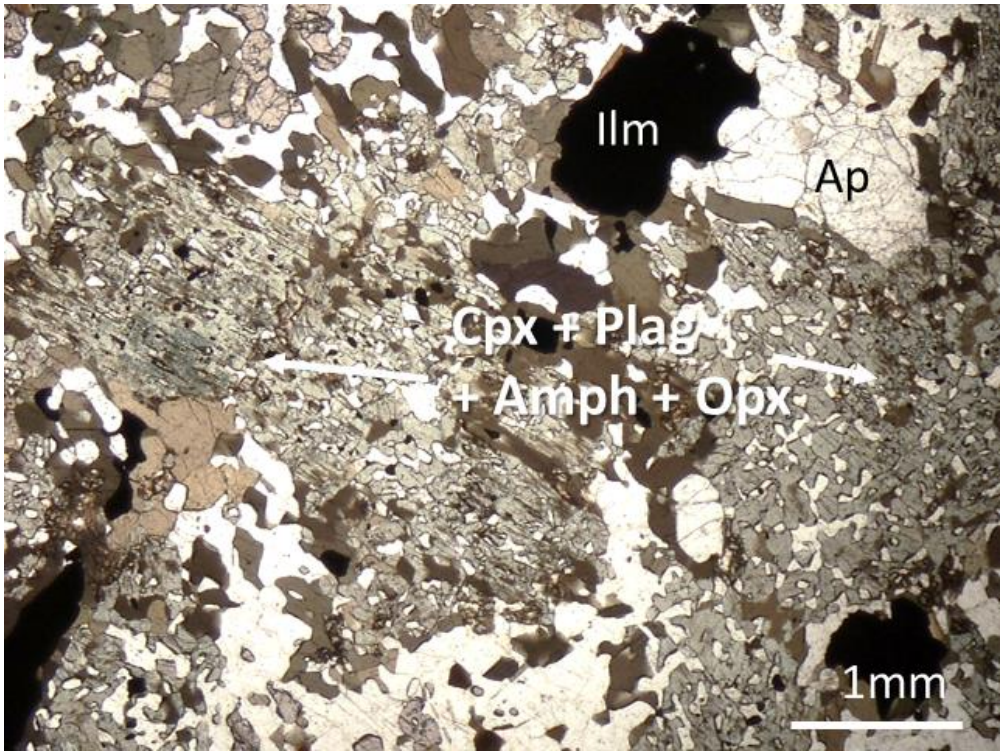

Figure 3.16: Remnants of relict clinopyroxene (left) and remnants of an olivine corona (right) in Type 3a (JKEM-09), both replaced by cpx + amph + plag + opx. Field of view ca. 6.25 mm. Relict clinopyroxene retains ilmenite inclusions and a somewhat rectangular shape.

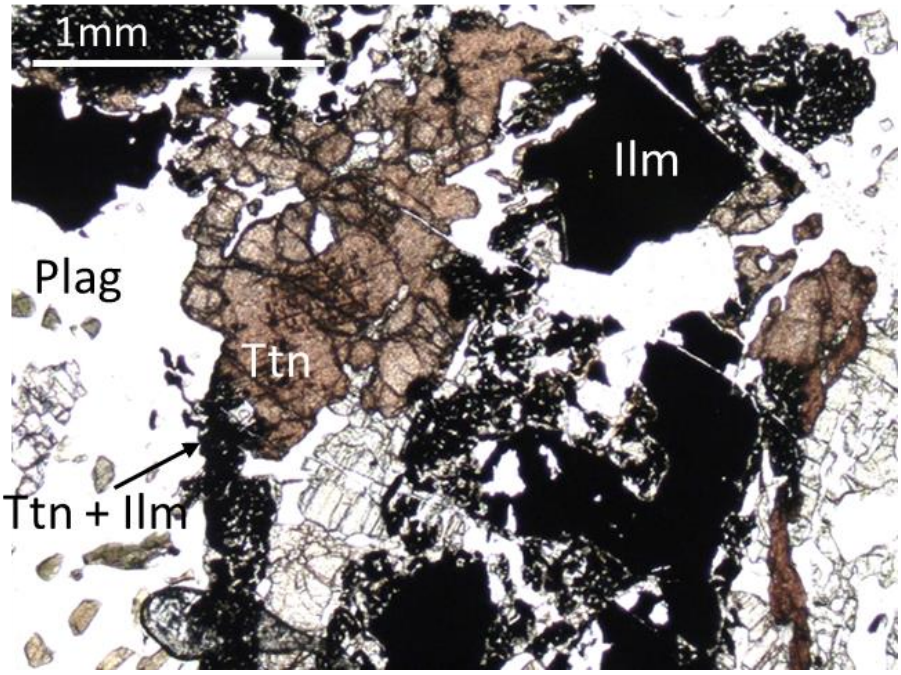

Figure 3.17: Fe-Ti oxide and titanite symplectite close to a clinopyroxene + plagioclase-bearing vein (JKEM-13c). Field of view ca. 2.5 mm. Ilmenite has a thin rim of titanite.

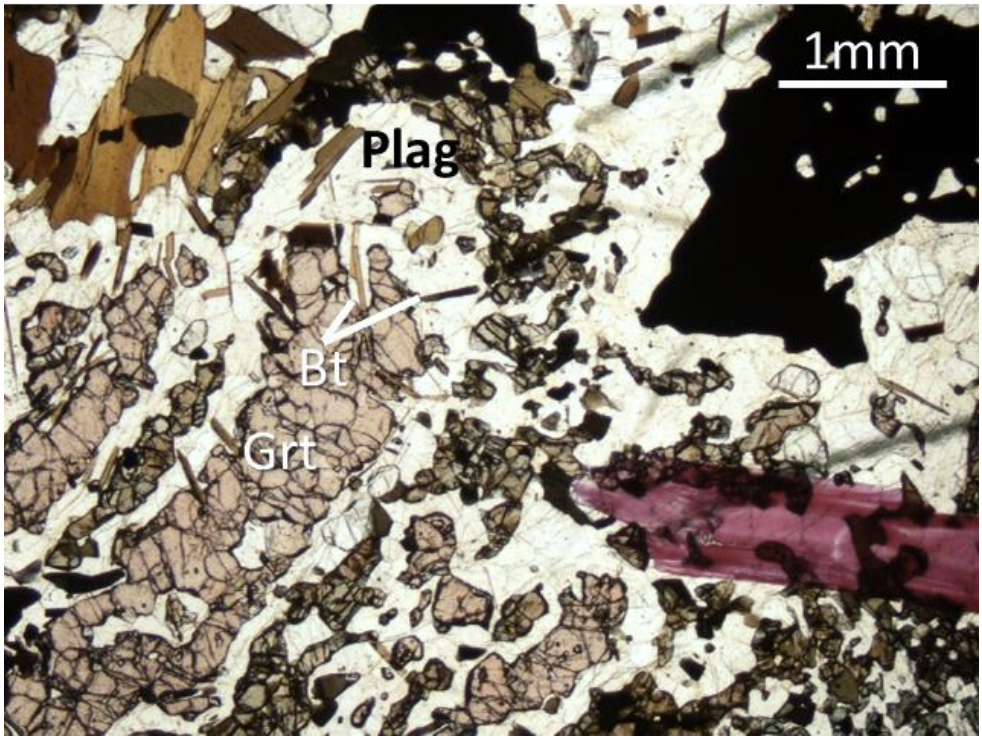

Figure 3.18: Garnet replacing recrystallized plagioclase in Type 3a (JKEM-10). Field of view ca. 6.25 mm. The aggregate of garnet retains the elongated, lath-like shape of plagioclase. Skeletal biotite is included within and radiates from garnet. Purple mark in the lower right is ink.

3.6.2 Mineral Chemistry

Presented below is a summary of the chemical data obtained from a representative Type 3a sample. Average EMP analyses for each phase are presented in Table 3.6.

Orthopyroxene

Orthopyroxenes in Type 3 samples are dispersed throughout the rock and are typically found near clinopyroxene blebs. These crystals have an average composition of $En_{44}Fs_{56}$.

Clinopyroxene

Recrystallized clinopyroxene after primary clinopyroxene and within the remnants of an olivine pseudomorph corona was analyzed. In addition to being texturally similar, crystals in the two settings are chemically identical, averaging $Di_{65}Hd_{35}$. These clinopyroxenes are less sodic than the previous types, typically only containing ca. 0.6% Na_2O.

Amphibole

Amphibole is a major component of Type 3 rocks, as it replaces most of the mafic phases. Analyses were taken from those replacing clinopyroxene, orthopyroxene, and Fe-Ti oxide. The compositions of amphiboles varies only slightly and all are ferropargasites.

Biotite

In Type 3 samples, biotite is found near the remnants of igneous Fe-Ti oxides and garnet clusters. Biotites analyzed near an oxide average $Ann_{54}Phl_{46}$ with a Ti content of 4.5% TiO_2. Those reacting with garnet had two compositions, $Ann_{50}Phl_{50}$ with ca. 3.0-3.4% TiO_2 and $Ann_{56}Phl_{44}$ with ca. 4.4% TiO_2; these biotites are texturally indistinguishable.

Garnet

In Type 3a, garnet crystals form clusters replacing recrystallized relict plagioclase. These garnets show no zoning and have a consistent composition averaging $Prp_{15}Alm_{64}Grs_{18}$.

Plagioclase

Type 3 samples contain only recrystallized metamorphic plagioclase, and both those rimming garnet clusters and those replacing mafic phases were analyzed. The two settings have similar compositions, averaging An_{20}.

	Orthopyroxene	**Clinopyroxene**	**Amphibole**	**Biotite**			**Garnet**	**Plagioclase**
	All	All	All	Near ilm	Near grt1[1]	Near grt2[1]	All	All
SiO_2	51.31	52.65	42.31	36.02	36.41	36.00	37.42	63.55
TiO_2	0.05	0.04	1.79	4.48	3.18	4.46	0.01	0.00
Al_2O_3	0.45	1.21	11.29	14.12	14.31	14.40	20.83	23.03
Cr_2O_3	0.03	0.02	0.05	0.08	0.00	0.00	0.02	0.00
FeO	32.99	12.58	19.80	21.00	20.09	21.60	29.55	0.15
MnO	0.66	0.25	0.15	0.09	0.01	0.04	1.63	0.00
MgO	14.75	11.17	8.20	10.07	11.26	9.52	3.72	0.02
CaO	0.53	22.52	11.47	0.05	0.14	0.02	6.10	4.34
Na_2O	0.01	0.65	1.99	0.17	0.09	0.08	0.01	9.10
K_2O	0.03	0.03	1.36	9.47	8.90	9.60	0.03	0.33
ZrO_2	0.01	0.00	0.02	0.06	0.00	0.00	0.00	0.00
Total	100.82	101.11	98.44	95.62	94.39	95.71	99.32	100.52

Table 3.6: Average EMP analyses for corona-forming phases in Type 3.
[1]Two different compositions of biotite found in association with the same garnet aggregate.

3.7 Summary

The Emsdale metagabbro preserves three general stages of textural evolution, with Type 1 the least evolved and Type 3 the most. This observation is supported by progressive grain size reduction, recrystallization, and breakdown of igneous phases (Figure 3.19). Coronas are progressively obscured by likely late metamorphic amphibole and plagioclase, and are unidentifiable in some Type 3 samples.

Mafic phases are generally enriched in Fe, reflecting the high-Fe bulk composition typical of Algonquin metagabbros (Grant, 1987). Type 1b mafic minerals are particularly Fe- and Ti-rich compared to the other types. Type 2 samples show the largest variation in mineral composition of the three types; Type 3 phases have remarkable chemical homogeneity. In comparison to Type 1 and Type 3 samples, Type 2 mafic phases are slightly enriched in Mg, resulting either from compositional heterogeneity in the metagabbro body or a higher grade metamorphic assemblage.

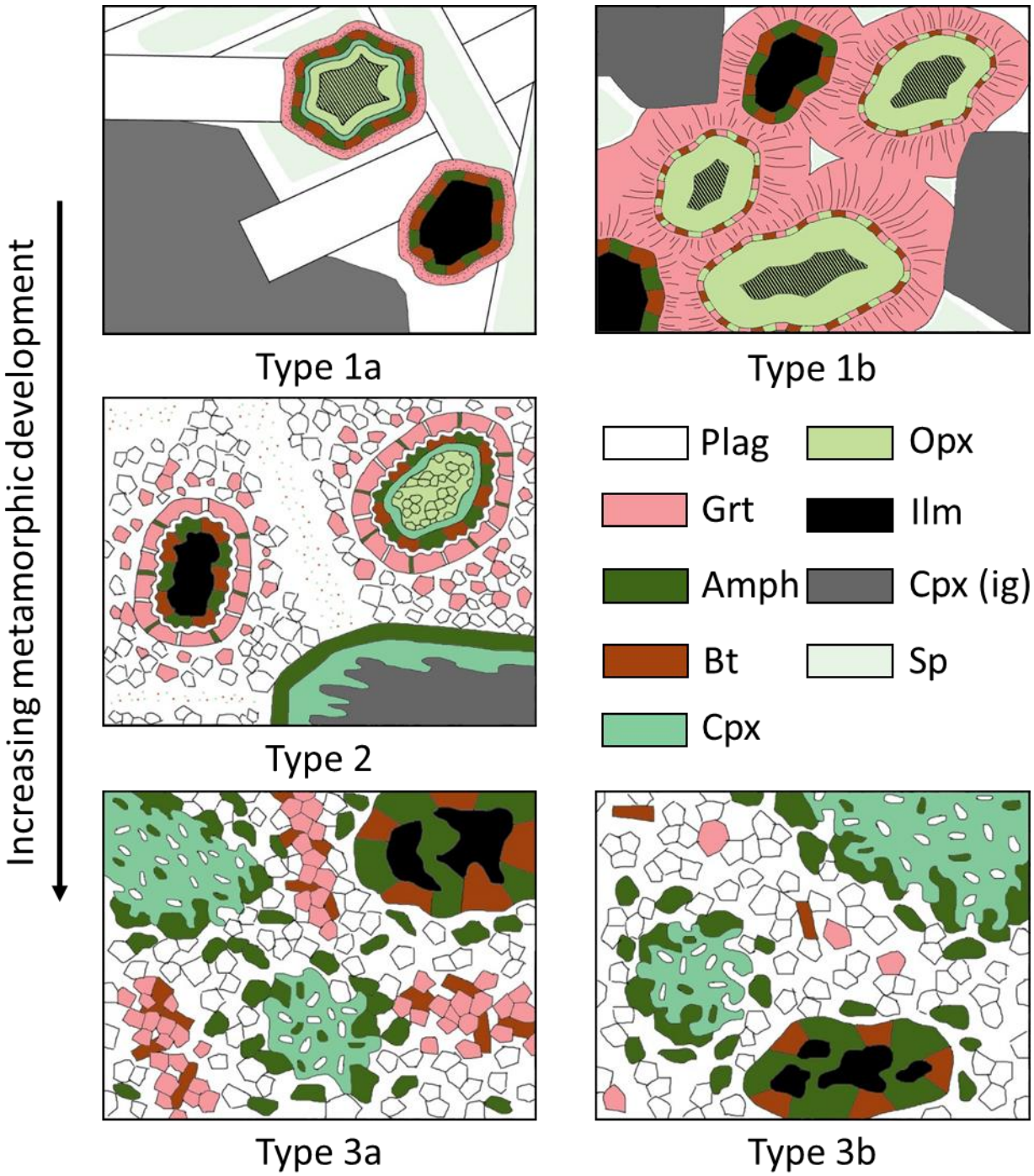

Figure 3.19: Schematic diagrams of Types 1a, 1b, 2, 3a, and 3b coronas. With increasing metamorphic development and textural reworking, coronas are increasingly overprinted by later phases. Igneous plagioclase and clinopyroxene are progressively recrystallized, becoming granoblastic in Type 3.

Chapter 4: Thermobarometry

4.1 Methods

Estimating pressures and temperatures using "conventional" thermobarometry (Powell and Holland, 2008) is based on pressure- or temperature- sensitive chemical exchanges between minerals that have reached equilibrium. The relationships between mineral compositions and P-T conditions may be determined experimentally using natural or synthetic minerals (e.g. Ellis and Green, 1979; Ravna 2000a; Ravna 2000b). Alternatively, methods such as Thermocalc (Powell and Holland, 1994) and TWQ (Berman, 1991) are based on internally consistent thermodynamic databases for a variety of minerals and calculate P-T estimates for a given assemblage using a set of independent reactions. Average P-T is calculated from the intersections of these reactions on a P-T plot, which vary according to the endmember activities of a particular assemblage.

One goal of this study is to determine the metamorphic P-T conditions for the Emsdale coronite, targeting minerals that grew together and achieved equilibrium during metamorphism. Although corona structures provide a variety of metamorphic phases potentially suitable for P-T calculations, the corona itself is a disequilibrium feature. Instability between olivine and plagioclase or between Fe-Ti oxides and plagioclase caused a series of incomplete reactions. Discrete subdomains of equilibrium must therefore be defined in order to apply thermobarometers to coronites. Each type of Emsdale coronite poses a different set of challenges for identifying equilibrium assemblages. In general, where a granoblastic texture is observed with chemical homogeneity, equilibrium conditions are assumed. In this case, mineral composition

averages were used. Within coronas, only phases in mutual contact are considered to have reached equilibrium, either between two shells or within the symplectite. A garnet just outside the symplectite would not be paired with plagioclase within the symplectite. The analyses were chosen based on their proximity to one another and their likelihood of representing peak conditions for that sample, based on comparison of measured compositions with expected high P-T compositions (Figure 4.1). For example, the most albitic plagioclase and most grossular-rich garnets were chosen to obtain the peak pressure.

As reviewed by Powell and Holland (2008), thermobarometric estimates are subject to many sources of uncertainty. These include identification of the peak metamorphic assemblage, retrograde cation exchange, and unknown Fe^{3+} in EMP analyses. Peak metamorphic conditions may not be represented by all the minerals present in a corona. Some phases may have been inherited from an earlier assemblage, whereas others may have been introduced during retrogression. During slow cooling of the Emsdale metagabbro, chemical exchange, particularly involving Fe-Mg, between some minerals formerly in equilibrium may have continued. This would result in P-T estimates lower than peak conditions, or minimum estimates, as these minerals re-equilibrated along the retrograde path. In addition, the electron microprobe measures only Fe_{total}; Fe^{2+} and Fe^{3+} cannot be differentiated using EMP data alone. Fe^{3+} can be calculated stoichiometrically in minerals with a known cation:oxygen ratio, but this method assumes that EMP analyses provide stoichiometrically balanced compositions, which is not always the case. This leads to a potential source of uncertainty for

thermobarometers relying on Fe^{2+} exchange, since the assumption that $Fe^{2+} = Fe_{total}$ overestimates the concentration of Fe available to exchange with Mg.

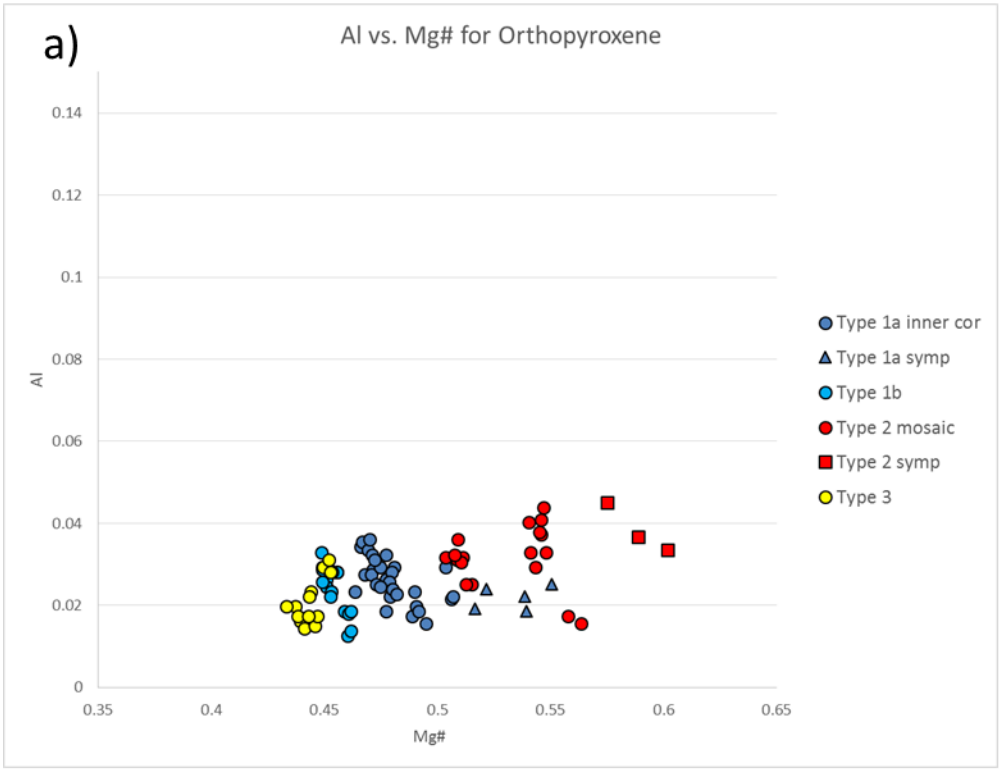

Higher Al, higher Mg = higher temperature

Higher Na = higher pressure
Higher Mg = higher temperature

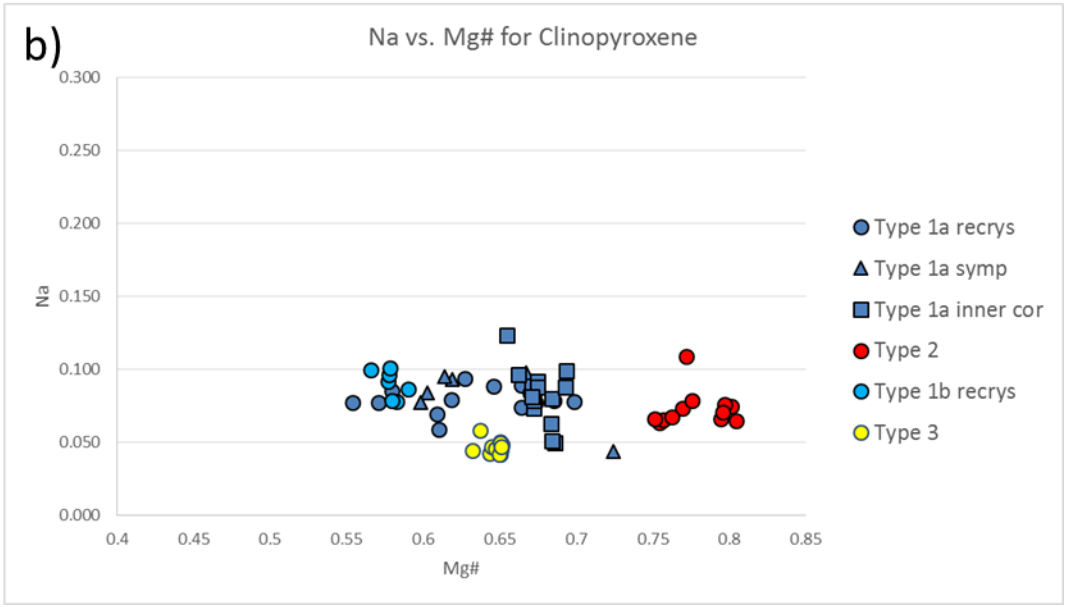

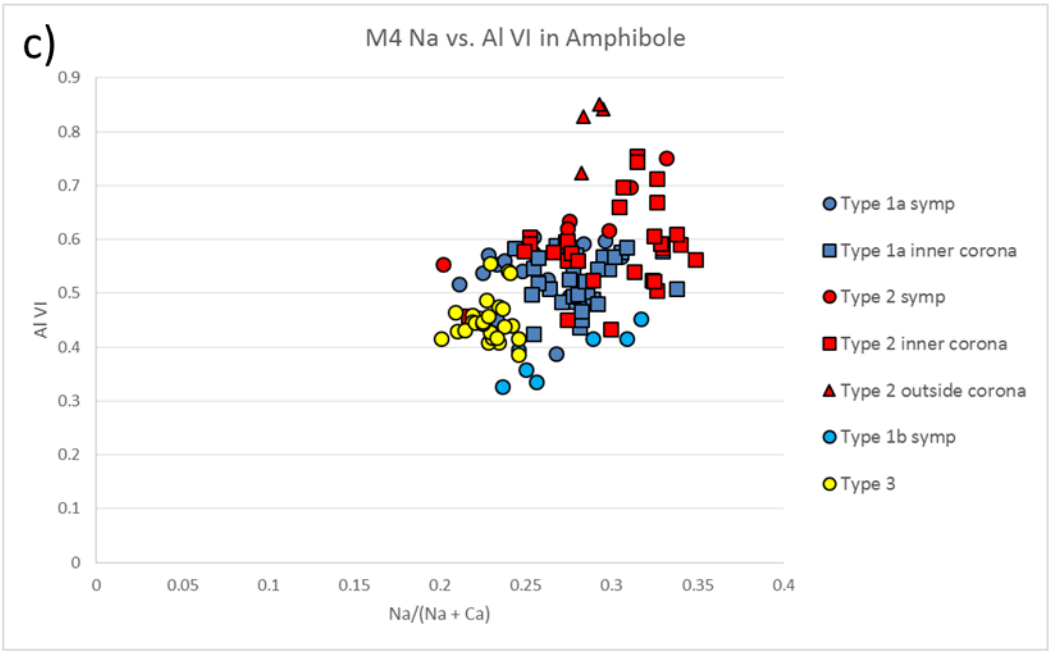

Higher M4 Na = higher pressure
Higher Al VI = higher temperature

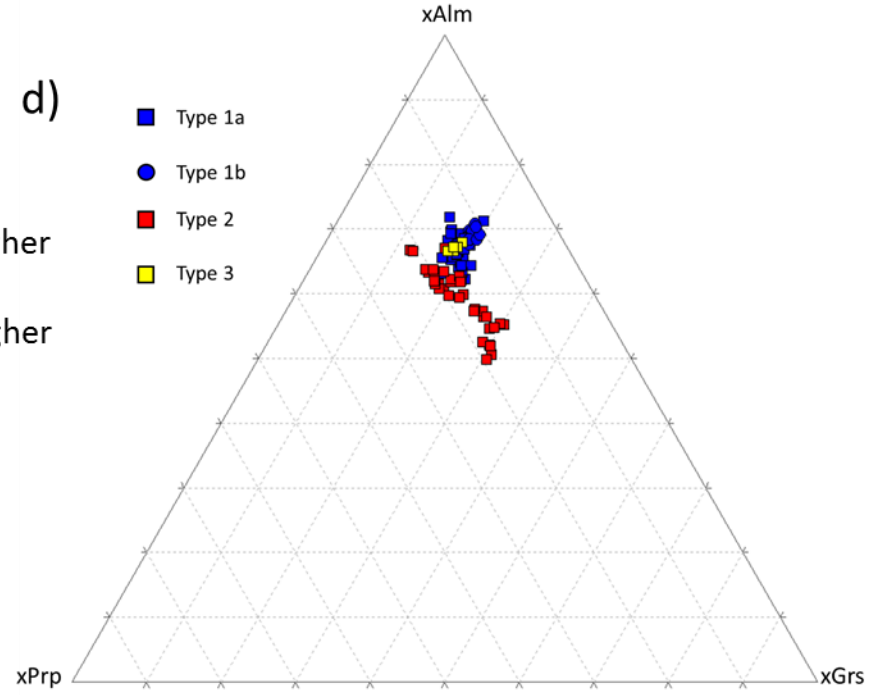

Higher xGrs = higher pressure
Higher xPrp = higher temperature

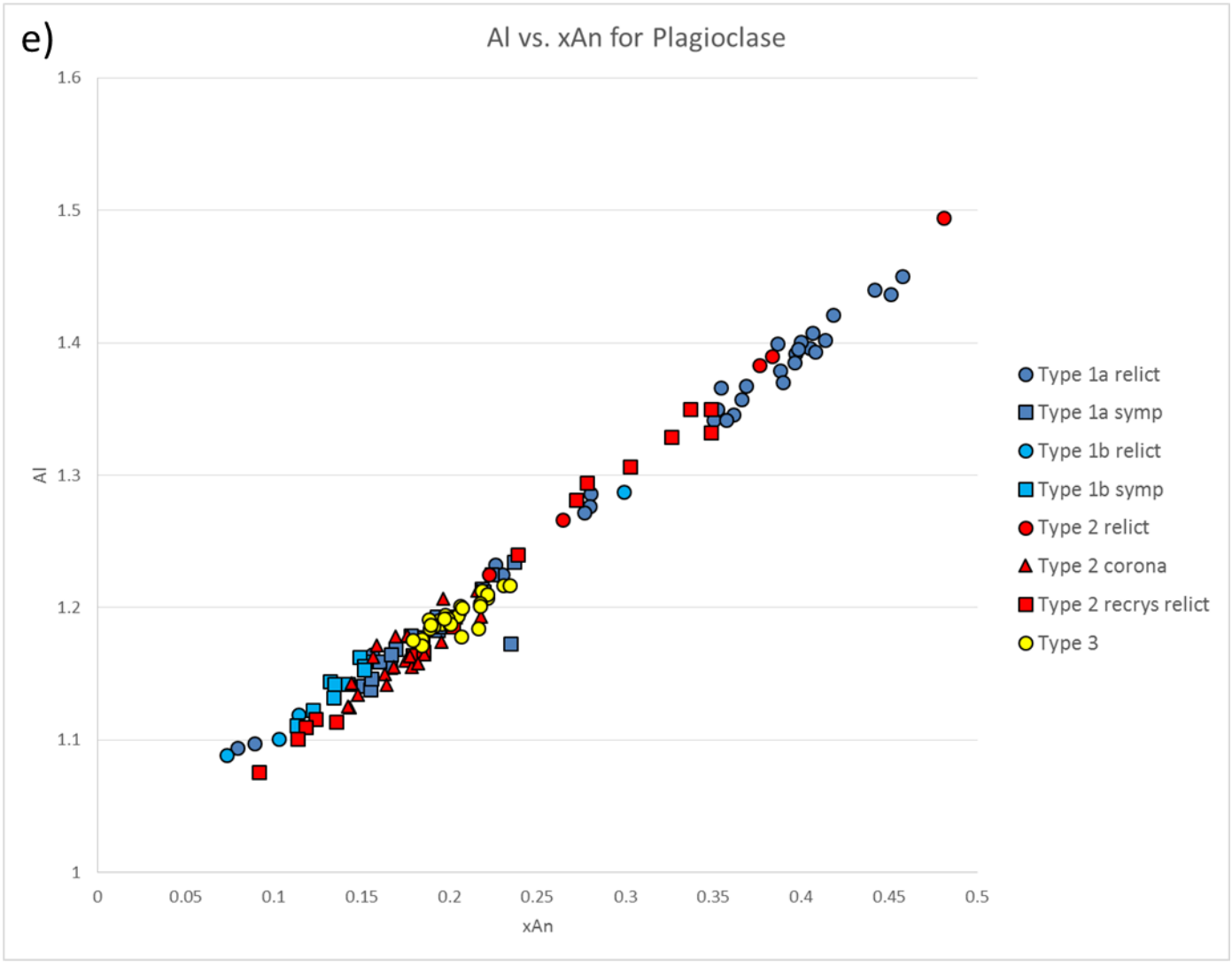

Figure 4.1: Compositional plots to compare EMP analyses of A) orthopyroxene, Al vs. Mg#, B) clinopyroxene, Na vs. Mg#, C) amphibole, M4 site Na vs. Al^{VI}, D) garnet, xAlm vs. xGrs vs. xPrp, and E) plagioclase, Al vs. xAn. These plots were used qualitatively to evaluate assemblages that represent peak P-T conditions for each type; the approach for each mineral is noted next to each graph. Only relative compositions were of interest, therefore instrument error, which would be the same for each analysis, is omitted. The very low contents of Al in orthopyroxene and Na in clinopyroxene would be subject to considerable error.

4.2 Type 1

4.2.1 Approach

In Type 1a samples, where coronas are best preserved and no granoblastic textures are present, equilibrium is assumed within the garnet symplectite corona shell and between adjacent shells. Minerals in the symplectite show little compositional variation within a single corona and likely grew simultaneously. The symplectite-producing reaction calculated by Grant (1988) (Table 5.1) indicates that plagioclase, together with mobile Mg, Fe, and H_2O, could produce all components of the symplectite through a single reaction, consistent with the equilibrium interpretation. Orthopyroxene-clinopyroxene and the amphibole-garnet pair in adjacent shells were considered to have formed in equilibrium, although the two pairs may not have formed at the same time.

A similar approach was less useful for Type 1b samples. In JKEM-01, the only multi-phase coronitic shell analyzed has the assemblage orthopyroxene + garnet + biotite; in the absence of plagioclase, this assemblage is not well suited for thermobarometry. In JKEM-02, a Fe-Ti oxide corona and adjacent plagioclase + garnet + biotite symplectite and an amphibole shell were analyzed. Garnet and biotite in contact and amphibole and plagioclase in contact are considered to represent equilibrium.

4.2.2 Results

The P-T results presented here are from a single olivine pseudomorph corona in a representative Type 1a sample, JKEM-12. In this corona, opx, cpx, amph, and grt + amph + opx + cpx + plag symplectite shells are well developed (Figure 4.2). Table 4.1 lists the

analyses used for thermobarometry, and Table 4.2 lists the results for each thermobarometer.

The following thermometers rely on Fe^{2+}-Mg exchange and are therefore subject to retrograde cation exchange, especially between small crystals. The orthopyroxene-clinopyroxene thermometer (Wells, 1977) was applied to assemblages within the symplectite and in adjacent shells. Results from both settings are similar, giving 845 ± 70°C and 828 ± 70°C respectively. Within the symplectite, however, garnet-clinopyroxene thermometers yielded much lower temperatures of 554 ± 100°C (Ravna, 2000b) and 627 ± 50°C (Ellis and Green, 1979) for an assumed P = 10 kb. Amphibole-garnet assemblages gave even lower temperatures. The contact between the garnet-bearing and hornblende shells yielded 538 ± 50°C (Ravna, 2000a) and 589 ± 50°C (Graham and Powell, 1984), with garnet and hornblende in the symplectite lower still at 499 ± 50°C (Ravna, 2000a) and 569 ± 50°C (Graham and Powell, 1984). These data suggest either retrograde cation exchange between garnet and amphibole, garnet and amphibole did not form in equilibrium, or both.

The other thermobarometers use exchanges involving Ca, Al, and Si, which are less susceptible to retrograde cation exchange then Fe^{2+}-Mg. Hornblende-plagioclase thermometry in the symplectite (Blundy and Holland, 1990) gave relatively higher temperatures of 732 ± 75°C at 10 kb and 759 ± 75°C at 15 kb. The garnet-hornblende-plagioclase-quartz barometers (Kohn and Spear, 1990) were applied to the symplectite shell, giving 8.68 ± 0.5 kb at 500°C, 9.18 ± 0.5 kb at 650°C, and 9.86 ± 0.5 kb at 850°C for the Mg endmember reaction, and 7.99 ± 0.5 kb at 500°C, 9.32 ± 0.5 kb at 650°C, and 11.1 ± 0.5 kb at 850°C for the Fe endmember reaction.

These multireaction thermobarometers require equilibrium among all minerals in the calculation, which may not be true in this case. Both Thermocalc (Powell and Holland, 1994) and TWQ (Berman, 1991; Berman 2007) computed average pressures and temperatures using the reactions listed in Table 4.2 with the same symplectite phases, the latter without amphibole. Relative to the other thermobarometers, Thermocalc produced high estimates, 15.8 ± 3.2 kb and 977 ± 122°C. TWQ estimates are more comparable at 10.7 ± 0.7 kb and 685 ± 65°C.

Coronas in Type 1b typically lack plagioclase in their symplectites; the abundant plagioclase in JKEM-02 made it more suitable for thermobarometry (Figure 4.3). The garnet-biotite thermometer (Spear, 1993) at 10 kb gave 674 ± 50°C and hornblende-plagioclase estimates are 747 ± 75°C at 10 kb and 766 ± 75°C at 15 kb. Garnet-hornblende-plagioclase-quartz pressure estimates are 11.2 ± 0.5 kb for the Mg endmember reaction and 11.8 ± 0.5 kb for the Fe endmember reaction. The analyses used for these P-T estimates were used in Thermocalc, which produced 15.4 ± 2.6 kb at 963 ± 172°C.

The broad variation in P-T estimates from Type 1 samples is likely a result of the uncertainties outlined in section 4.1; cation exchange and changes in the corona mineral assemblage during retrogression have led to inconsistent results. Amphibole in the olivine corona is likely a retrograde phase that replaced clinopyroxene, causing garnet-hornblende thermometers to give low temperatures. The low garnet-clinopyroxene temperatures in the symplectite may be due to retrograde Fe-Mg exchange. Clinopyroxene grains in symplectite are very small (1-50 μm) and enveloped by garnet, making the crystals vulnerable to exchange. Retrograde chemical exchange in the

symplectite may explain the similarly low temperature calculated by TWQ and the garnet-biotite thermometer in JKEM-02. Thermocalc results are most likely unusable, as the estimates are substantially higher than the others and have large errors; disequilibrium between amphibole and the other phases is the probable cause. Therefore, the most reliable temperature estimate for Type 1 samples is given by the orthopyroxene-clinopyroxene thermometer. This assemblage was likely least affected by retrograde metamorphism, as it is relatively coarse-grained and closely adjacent rims were avoided during analysis. Therefore, orthopyroxene-clinopyroxene is interpreted to represent near-peak temperature conditions. Pressure estimates for the symplectite from garnet-plagioclase-hornblende-quartz barometers and TWQ are in general agreement. However, the incorporation of quartz in the reactions for each method lends uncertainty to these pressures; no quartz is found in JKEM-12, indicating that the activity of quartz was less than 1. The pressures calculated are therefore minimum estimates.

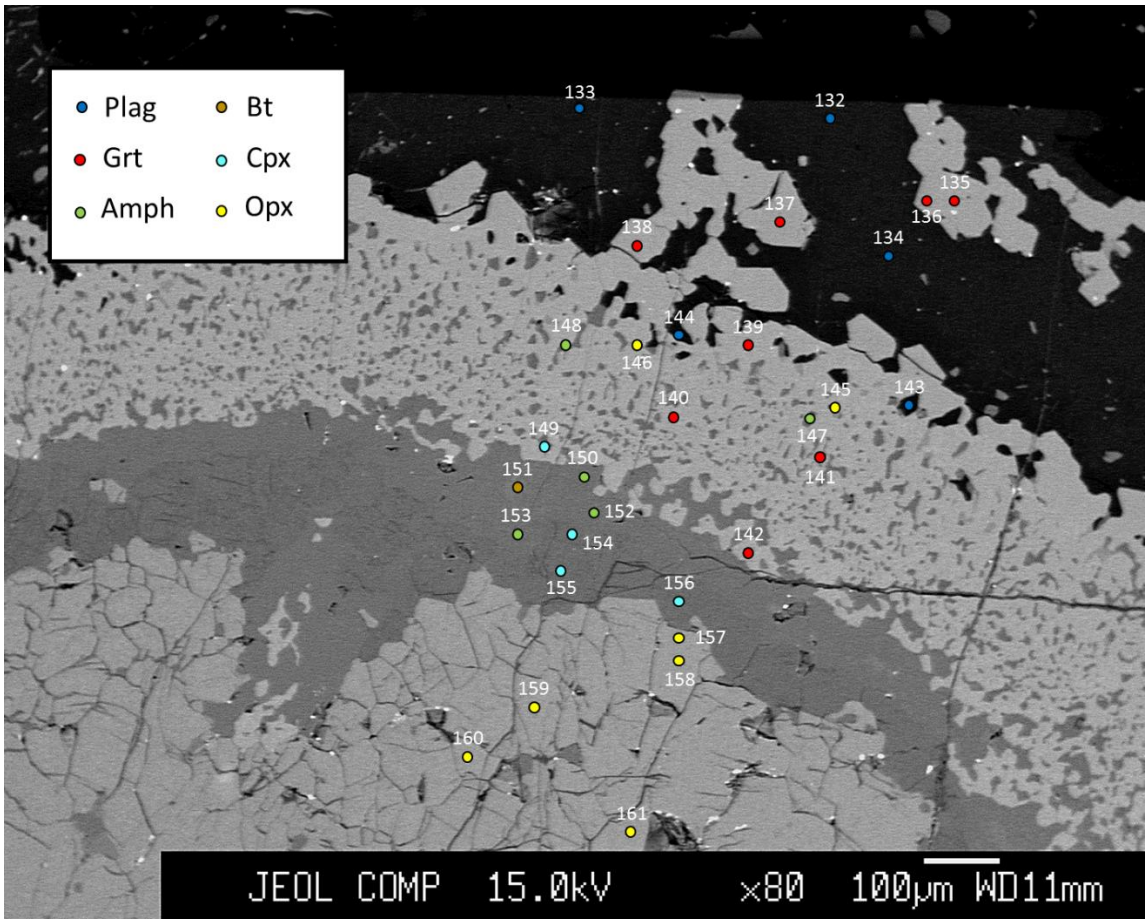

Figure 4.2: Locations of EMP point analyses in an olivine corona in Type 1a (JKEM-12). BSE image, numbers are analysis numbers; full analyses in Table 4.1 (used for P-T calculation) and Appendix.

	Orthopyroxene			Clinopyroxene	
No.	**145**	**Av. 157-161**		**149**	**Av. 154-156**
SiO_2	52.09	51.58 ± 0.16		53.38	52.36 ± 0.17
TiO_2	0.09	0.03 ± 0.01		0.06	0.07 ± 0.02
Al_2O_3	0.50	0.58 ± 0.06		0.91	2.29 ± 0.40
Cr_2O_3	0.06	0.02 ± 0.01		0.06	0.00
FeO	28.73	31.76 ± 0.11		11.07	11.67 ± 0.21
MnO	0.36	0.43 ± 0.02		0.19	0.15 ± 0.01
MgO	18.83	16.39 ± 0.07		13.06	11.59 ± 0.30
CaO	0.36	0.45 ± 0.04		22.26	21.17 ± 0.36
Na_2O	0.03	0.01 ± 0.01		0.62	1.07 ± 0.18
K_2O	0.03	0.01 ± 0.01		0.05	0.01 ± 0.01
ZrO_2	101.07	101.26 ± 0.14		101.66	100.39 ± 0.08
Si	1.973	1.981 ± 0.004		1.968	1.957 ± 0.007
Ti	0.002	0.001		0.002	0.002 ± 0.001
Al	0.022	0.026 ± 0.002		0.040	0.101 ± 0.018
Cr	0.031*	0.011* ± 0.008		0.068*	0.060* ± 0.010
($Fe^{3+,1}$)					
Fe	0.879	1.009 ± 0.007		0.274	0.305 ± 0.006
Mn	0.011	0.014 ± 0.001		0.006	0.005
Mg	1.063	0.938 ± 0.004		0.718	0.646 ± 0.017
Ca	0.015	0.018 ± 0.001		0.879	0.848 ± 0.014
Na	0.002	0.000		0.044	0.077 ± 0.013
K	0.001	0.001		0.002	0.000
Total	4.000	4.000		4.000	4.000
MgM1*	0.529	0.473	MgM1*	0.667	0.599
MgM2*	0.532	0.467	MgM2*	0.051	0.048
Mg#*	0.547	0.482	Mg#*	0.724	0.679
Fe# *	0.453	0.518	Mg#	0.678	
Al^{VI}*	0.000	0.007	Fe#	0.322	
			Al^{VI}*	0.008	0.057
			Fe/Mg	0.476	

	Amphibole			Garnet			Plagioclase
No.	**147**	**153**		**140**	**142**		**143**
SiO_2	43.67	42.87		38.83	38.61		63.96
TiO_2	0.52	1.05		0.08	0.10		0.00
Al_2O_3	11.69	11.60		20.93	21.21		22.76
Cr_2O_3	0.03	0.00		0.11	0.08		0.00
FeO	15.34	18.01		29.67	30.18		0.76
MnO	0.12	0.08		1.33	1.45		0.03
MgO	12.50	10.10		3.70	3.42		0.00
CaO	11.20	11.17		6.86	6.47		3.90
Na_2O	2.24	2.43		0.00	0.00		9.44
K_2O	0.88	1.03		0.03	0.03		0.21
Total	98.19	98.31		101.54	101.55		101.07
Si	6.475	6.445		3.030	3.019		2.807
Ti	0.058	0.117		0.005	0.006		0.000
Al	2.042	2.054		1.926	1.955		1.178
Cr	0.005	0.000		0.006	0.005		0.000
($Fe^{3+,1}$)							
Fe	1.902	2.266		1.937	1.974		0.028
Mn	0.016	0.009		0.088	0.096		0.001
Mg	2.762	2.263		0.431	0.398		0.000
Ca	1.778	1.799		0.574	0.541		0.183
Na	0.644	0.708		0.000	0.000		0.803
K	0.168	0.198		0.004	0.004		0.012
Total	15.852	15.859		7.999	7.998		5.013
Fe/Mg	0.689	1.001	xPrp	0.14	0.13	xAn	0.18
Mg#	0.592		xAlm	0.64	0.66	xAb	0.80
Fe#	0.408		xSps	0.03	0.03		
xT1Si	0.619		xGrs	0.19	0.18		
xT1Al	0.381		Fe#	0.818	0.832		
			Mg#	0.182	0.168		
			Fe/Mg	4.496	4.955		

Table 4.1: EMP analyses used in PT calculations from a Type 1a olivine corona (Figure 4.2).
[1] A * in the Cr row indicates that Fe^{3+} is reported instead of Cr. A * next to a calculated value indicates that it was calculated with Fe^{3+} and Fe^{2+} separate. Otherwise, Fe^{tot} was used.

Thermobarometer	Analyses Used	Pressure (kb)	Temperature (°C)	Comment
Opx/Cpx	Opx 145, Cpx 149	N/A	845 ± 70	
Opx/Cpx	Opx 157-161 av., Cpx 154-156 av.	N/A	828 ± 70	
Grt/Cpx[1]	Grt 140, Cpx 149	*10*	554 ± 100	
Grt/Cpx[2]	Grt 140, Cpx 149	*10*	627 ± 50	
Grt/Hbl[1]	Grt 140, Amph 147	N/A	499 ± 50	
Grt/Hbl[1]	Grt 142, Amph 153	N/A	538 ± 50	
Grt/Hbl[2]	Grt 140, Amph 147	N/A	569 ± 50	
Grt/Hbl[2]	Grt 142, Amph 153	N/A	589 ± 50	
Hbl/Plag	Amph 147, Plag 143	*10, 15*	732, 759 ± 75	Ed-Ri reaction
Grt/Plag/Hbl/Qtz	Grt 140, Plag 143, Amph 147	8.68, 9.18, 9.86 ± 0.5	*500, 650, 850*	Mg endmember
Grt/Plag/Hbl/Qtz	Grt 140, Plag 143, Amph 147	7.99, 9.32, 11.1 ± 0.5	*500, 650, 850*	Fe endmember
Thermocalc	Opx 145, Cpx 149, Amph 147, Grt 140, Plag 143	15.8 ± 3.2	977 ± 122	
TWQ	Opx 145, Cpx 149, Grt 140, Plag 143	10.7 ± 0.7	685 ± 65	

Reactions used by Thermocalc:

Grs + En = 2Di + CaTs

CaTs + 2Fs = Hd + Alm

Ts + 4En = 2Prp + Tr

$2CaTs + 2Fact = 2Grs + 5Fs + 2Qtz + 2H_2O$

3Di + 4Ts + 10Fs = 3CaTs + 5Prp + 4Fact

10Grs + 5Alm + 3Ts = 9Di + 21CaTs + 3Fact

$6CaTs + 2Tr + 9Fs = 10Di + 6Alm + 2Qtz + 2H_2O$

Reactions used by TWQ:

2Alm + Grs + 3Qtz = 6Fs + 3An

Alm + 3En = Prp + 3Fs

3Qtz + Prp + 2Grs = 3An + 3Di

Table 4.2: P-T Estimates from Type 1a analyses (Table 4.1).
Cpx[1] Ravna, 2000b
Cpx[2] Ellis & Green, 1979
Hbl[1] Ravna, 2000a
Hbl[2] Graham & Powell, 1984
Italics – used in calculation, not a result

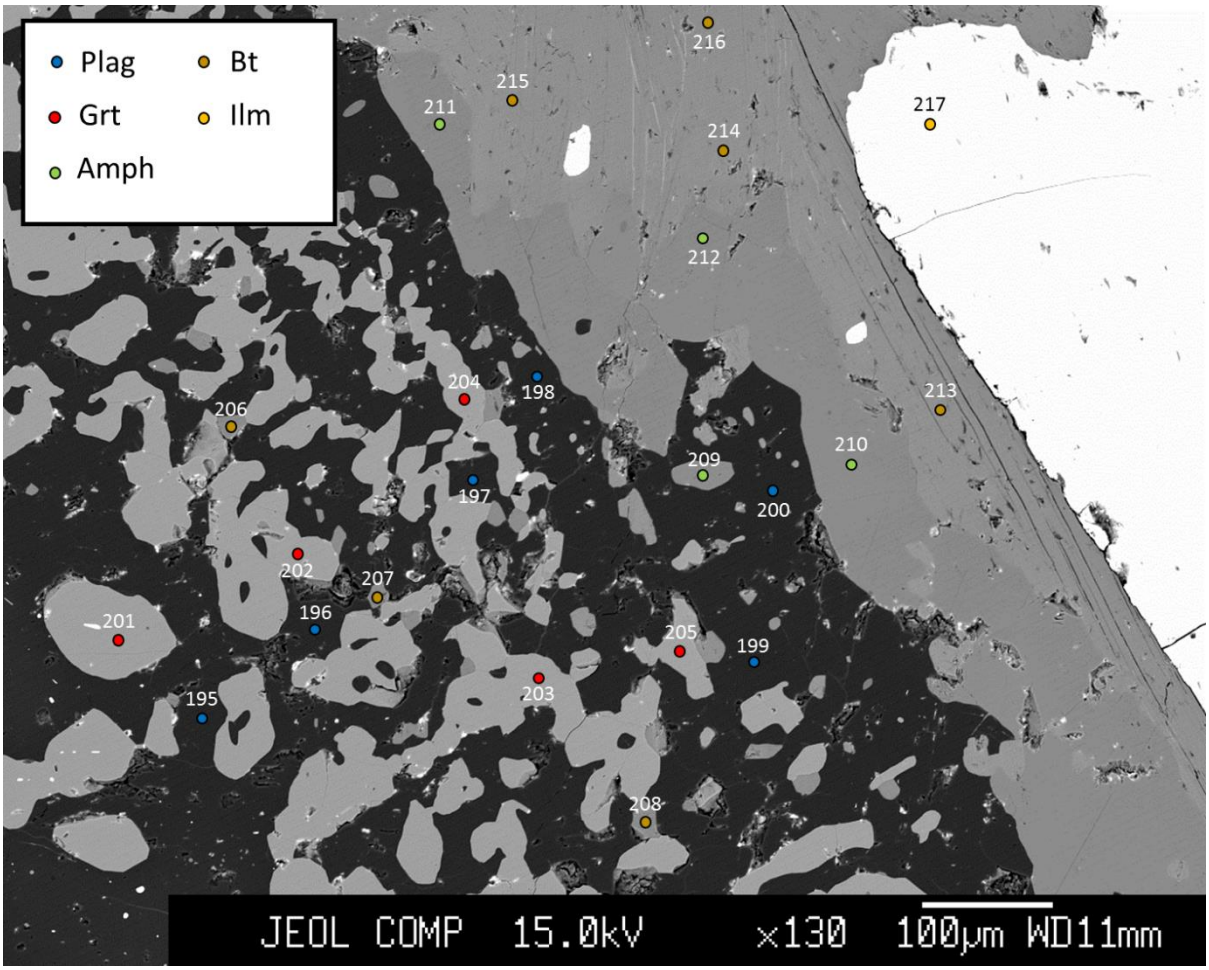

Figure 4.3: Locations of EMP point analyses in an ilmenite corona in Type 1b (JKEM-02). BSE image, numbers are analysis numbers; full analyses in Table 4.3 (used for P-T calculation) and Appendix.

	Amphibole		Biotite		Garnet		Plagioclase
No.	**209**		**208**		**201**		**199**
SiO_2	40.11		36.02		37.25		65.43
TiO_2	3.07		5.53		0.07		0.00
Al_2O_3	11.28		13.67		20.88		21.67
Cr_2O_3	0.08		0.07		0.10		0.00
FeO	20.67		20.73		30.00		0.23
MnO	0.20		0.08		1.84		0.03
MgO	7.03		10.24		3.23		0.00
CaO	10.64		0.09		6.70		2.58
Na_2O	2.30		0.05		0.01		9.98
K_2O	1.68		9.68		0.04		0.38
ZrO_2	0.00		0.04		0.02		0.00
Total	97.05		96.20		100.13		100.29
Si	6.254		5.518		2.974		2.875
Ti	0.359		0.638		0.004		0.000
Al	2.072		2.468		1.964		1.122
Cr	0.009		0.009		0.006		0.000
Fe	2.696		2.655		2.003		0.008
Mn	0.025		0.011		0.125		0.001
Mg	1.633		2.336		0.384		0.000
Ca	1.778		0.015		0.574		0.122
Na	0.695		0.015		0.001		0.850
K	0.334		1.892		0.005		0.021
Zr	0.000		0.002		0.001		0.000
Total	15.856		15.563		8.041		4.999
Mg#	0.377	Mg/Fe	0.880	xPrp	0.12	xAn	0.12
Fe#	0.623			xAlm	0.65	xAb	0.86
xT1Si	0.563			xSps	0.04		
xT1Al	0.438			xGrs	0.19		
				Mg/Fe	0.192		

Table 4.3: EMP analyses used in PT calculations from a Type 1b ilmenite corona (Figure 4.3).

Thermobarometer	Analyses Used	Pressure (kb)	Temperature (°C)	Comment
Grt/Bt	Grt 201, Bt 208	*10*	674 ± 50	
Hbl/Plag	Amph 209, Plag 199	*10, 15*	747, 766 ± 75	Ed-Ri reaction
Grt/Plag/Hbl/Qtz	Grt 201, Plag 199, Amph 209	11.2 ± 0.5	*700*	Mg endmember
Grt/Plag/Hbl/Qtz	Grt 201, Plag 199, Amph 209	11.8 ± 0.5	*700*	Fe endmember
Thermocalc	Grt 201, Bt 208, Amph 209, Plag 199	15.4 ± 2.6	963 ± 172	

Reactions used by Thermocalc:
2Prp + 4Grs + 3Ts + 12Qtz = 3Tr + 12An
6Tr + 21An = 10Prp + 11Grs + 27Qtz + 6H2O
6Fact + 21An = 11Grs + 10Alm + 27Qtz + 6H2O
5Phl + 3Fact = 5Ann + 3Tr
4Prp + 8Grs + 9Ts + 6Ab = 3Tr + 6Prg

Table 4.4: P-T Estimates from Type 1b analyses (Table 4.3).
Italics – used in calculation, not a result

4.3 Type 2

4.3.1 Approach

For coronas preserved in JKEM-14b, the Type 1a approach was used. Pressure estimates used symplectite garnet and hornblende with the adjacent plagioclase moat, as its high albite content indicates formation under relatively high pressure conditions. In JKEM-15b, garnet symplectites are absent and interpreted to have been replaced by monomineralic garnet; therefore, the inner assemblage of opx + cpx + amph + plag was used for P-T estimation. The inner shells of the olivine corona are more texturally variable than in JKEM-14b and the Type 1a samples, allowing the assemblage to coexist in contact with one another. Several orthopyroxene crystals are partly replaced by amphibole and plagioclase, which suggests that not all phases formed a single equilibrium assemblage.

4.3.2 Results

Type 2 is represented by JKEM-15b, in which corona shells are no longer concentric or continuous, orthopyroxene mosaics replace the olivine pseudomorphs, and albitic plagioclase has proliferated throughout the coronas (Figure 4.4). All thermobarometers (Table 4.6) applied to Type 1a were used with analyses (Table 4.5) from JKEM-15b, with the exception of garnet-clinopyroxene thermometers, as these minerals were most likely not in equilibrium.

Orthopyroxene-clinopyroxene thermometry used an average of the mosaic orthopyroxene along with a clinopyroxene interpreted to represent peak conditions, giving 880 ± 70°C. Garnet-hornblende thermometers produced lower temperatures of 709 ± 50°C (Ravna, 2000a) and 703 ± 50°C (Graham and Powell, 1984).

Hornblende-plagioclase estimates are comparable at 720 ± 75°C at 10 kb and 754 ± 75°C at 15 kb. The two garnet-plagioclase-hornblende-quartz barometers gave similar estimates, with 11.9 ± 0.5 kb at 700°C and 13.1 ± 0.5 kb at 850°C for the Mg endmember reaction and 11.5 ± 0.5 kb at 700°C and 13.1 ± 0.5 kb at 850°C for the Fe endmember reaction.

Thermocalc and TWQ used nearly the same set of analyses from across the corona. Average P-T estimates from Thermocalc are 17.9 ± 4.1 kb and 1078 ± 167°C and from TWQ are 15.0 ± 1.0 kb at 909 ± 80°C, 15.9 ± 1.0 kb at 870 ± 80°C, and 16.6 ± 1.0 kb at 817 ± 80°C.

Type 2 P-T estimates are subject to the same sources of error as Type 1 with additional uncertainty resulting from difficulty in unambiguously identifying the peak equilibrium assemblage. These samples represent the transition from Type 1 to Type 3,

and therefore likely preserve remnants of the Type 1 assemblages partially overprinted by intermediate assemblages. The peak temperature is probably best represented by the opx + cpx assemblage, diagnostic of granulite facies conditions. The clinopyroxene analysis used (Table 4.5) is relatively sodic compared to those typical of Type 2 (Table 3.3) and is interpreted to represent the peak P clinopyroxene composition. However, peak pressure is not well constrained in Type 2 samples, because minerals required to obtain robust P estimates such as garnet, plagioclase, and clinopyroxene probably did not form in equilibrium.

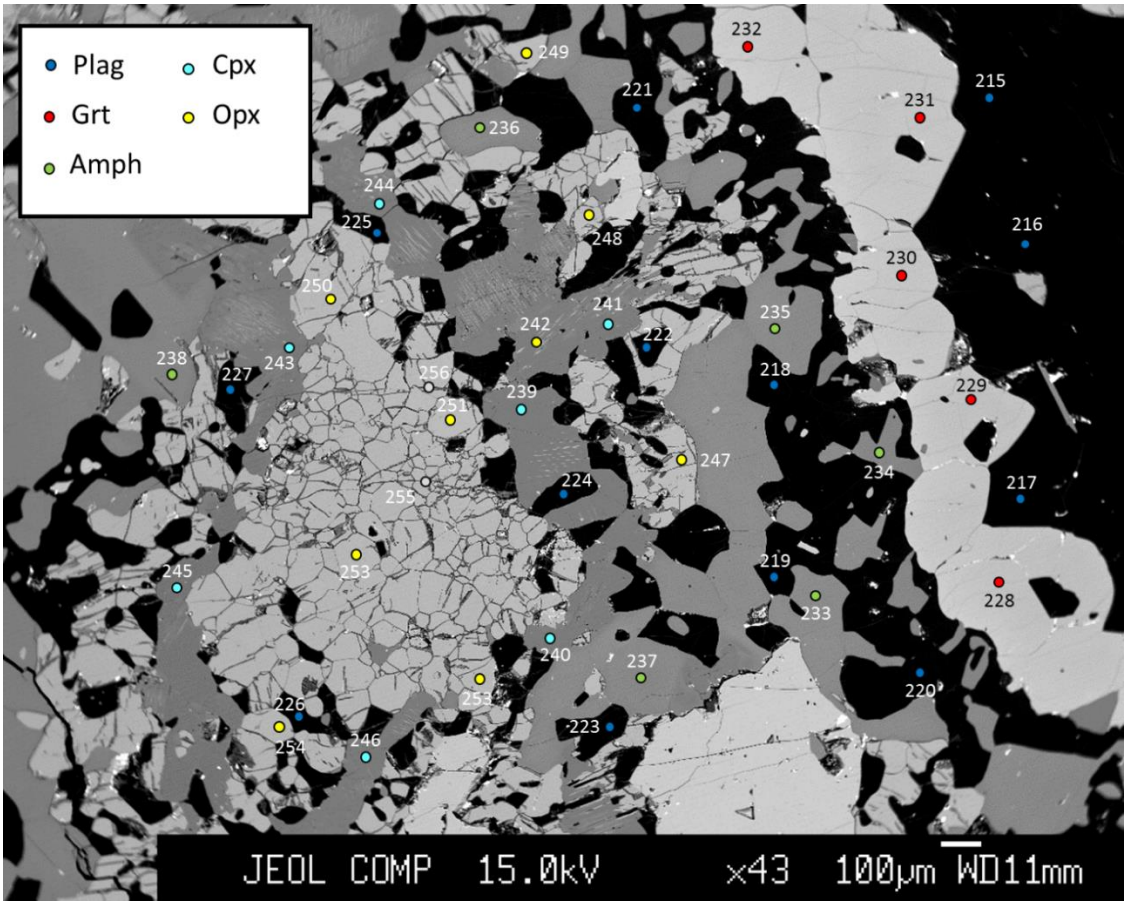

Figure 4.4: Locations of EMP point analyses around an olivine mosaic in Type 2 (JKEM-15b). BSE image, numbers are analysis numbers; full analyses in Table 4.5 (used for P-T calculation) and Appendix.

	Orthopyroxene		Clinopyroxene
No.	**249**	**Av. 247-254**	**239**
SiO_2	52.10	51.70 ± 0.30	50.027
TiO_2	0.04	0.04 ± 0.01	0.198
Al_2O_3	0.56	0.67 ± 0.08	4.547
Cr_2O_3	0.00	0.03 ± 0.02	0.09
FeO	29.57	29.68 ± 0.15	11.633
MnO	0.33	0.36 ± 0.02	0.137
MgO	17.61	17.31 ± 0.18	11.619
CaO	0.40	0.46 ± 0.04	19.959
Na_2O	0.01	0.01	1.506
K_2O	0.01	0.02 ± 0.01	0.155
ZrO_2	0.00	0.00 ± 0.01	0.007
Total	100.62	100.30 ± 0.29	99.878
Si	1.992	1.988 ± 0.005	1.867
Ti	0.001	0.001	0.006
Al	0.025	0.030 ± 0.004	0.200
Cr ($Fe^{3+,1}$)	0.000	0.001* ± 0.004	0.172*
Fe	0.946	0.953 ± 0.004	0.191
Mn	0.011	0.012 ± 0.001	0.004
Mg	1.004	0.993 ± 0.007	0.646
Ca	0.016	0.019 ± 0.002	0.798
Na	0.001	0.001	0.109
K	0.001	0.001	0.007
Zr	0.000	0.000	0.000
Total	3.996	4.000	4.000
MgM1*		0.499	MgM1* 0.583
MgM2*		0.494	MgM2* 0.069
Mg#*		0.510	Mg#* 0.772
Fe# *		0.490	Al^{VI}* 0.067
Al^{VI}*		0.019	

	Amphibole		Garnet		Plagioclase
No.	**234**		**229**		**219**
SiO_2	41.45		37.79		65.10
TiO_2	0.95		0.09		0.00
Al_2O_3	13.05		21.05		21.69
Cr_2O_3	0.09		0.09		0.00
FeO	16.57		27.36		0.20
MnO	0.09		0.74		0.00
MgO	10.23		5.03		0.00
CaO	11.29		7.40		3.07
Na_2O	2.90		0.02		10.00
K_2O	0.88		0.04		0.23
ZrO_2	0.00		0.03		0.00
Total	97.51		99.64		100.28
Si	6.265		2.983		2.864
Ti	0.108		0.005		0.000
Al	2.325		1.958		1.125
Cr	0.012		0.006		0.000
(*Fe^{3+})					
Fe	2.095		1.806		0.007
Mn	0.012		0.049		0.000
Mg	2.305		0.592		0.000
Ca	1.829		0.626		0.145
Na	0.851		0.002		0.853
K	0.170		0.004		0.013
Zr	0.000		0.001		0.000
Total	15.974		8.034		5.006
Fe/Mg	0.909	xPrp	0.193	xAn	0.143
Mg#	0.524	xAlm	0.588	xAb	0.844
Fe#	0.476	xSps	0.016		
xT1Si	0.558	xGrs	0.204		
xT1Al	0.443	Fe/Mg	3.053		

Table 4.5: EMP analyses used in PT calculations from the remnants of a Type 2 olivine corona (Fig. 4.4).
[1] A * has the same significance as in Table 4.1

Thermobarometer	Analyses Used	Pressure (kb)	Temperature (°C)	Comment
Opx/Cpx	Opx 247-254 av., Cpx 239	N/A	880 ± 70	
Grt/Hbl[1]	Grt 229, Amph 234	N/A	709 ± 50	
Grt/Hbl[2]	Grt 229, Amph 234	N/A	703 ± 50	
Hbl/Plag	Amph 234, Plag 219	*10, 15*	720, 754 ± 75	Ed-Ri reaction
Grt/Plag/Hbl/Qtz	Grt 229, Amph 234, Plag 219	11.9, 13.1 ± 0.5	*700, 850*	Mg endmember
Grt/Plag/Hbl/Qtz	Grt 229, Amph 234, Plag 219	11.5, 13.1 ± 0.5	*700, 850*	Fe endmember
Thermocalc	Opx 249, Cpx 239, Amph 234, Grt 229, Plag 219	17.9 ± 4.1	1078 ± 167	
TWQ	Opx 249, Cpx 239, Grt 229, Plag 219	15.0, 15.9, 16.6 ± 1.0	909, 870, 817 ± 80	

Reactions used by Thermocalc:
CaTs + Qtz = An
En + MgTs = Prp
2Prp + Grs + 3Qtz = 3En + 3An
3MgTs + 3Di = 2Prp + Grs
3Fs + 3CaTs = Grs + 2Alm
3Hd + 3CaTs = 2Grs + Alm
9En + 6Prg + 18An = 14Prp + 10Grs +6Ab + $6H_2O$
Reactions used by TWQ:
2Alm + Grs + 3Qtz = 6Fs + 3An
Alm + 3En = Prp + 3Fs
3Qtz + Prp + 2Grs = 3An + 3Di

Table 4.6: P-T Estimates from Type 2 analyses (Table 4.5).
Grt/Hbl[1] Ravna, 2000a
Grt/Hbl[2] Graham & Powell, 1984
Italics – used in calculation, not a result

4.4 Type 3

4.4.1 Approach

Type 3 samples are characterized by equigranular assemblages containing amphibole, plagioclase, and pyroxene; corona textures are largely obliterated. The combination of the near-granoblastic texture, with mutual contacts among all phases, and compositional homogeneity of specific phases, suggests that these samples are well equilibrated. Therefore, average compositions were used for calculating P-T estimates. However, the textures and mineral assemblage also indicate that the P-T conditions likely represent retrograde conditions relative to Type 1 and Type 2 samples.

4.4.2 Results

JKEM-10 is a Type 3a sample with the textural and chemical equilibrium features described above (Figure 4.5a). Garnet in this sample is restricted to clusters rimmed by plagioclase (Figure 4.5b). Averages of EMP analyses (Table 4.7) were used to estimate pressure and temperature (Table 4.8).

The orthopyroxene-clinopyroxene temperature, 755 ± 70°C, is higher but comparable to garnet-clinopyroxene temperatures of 618 ± 100°C (Ravna, 2000b) and 679 ± 50°C (Ellis and Green, 1979) at 9.5 kb and garnet-hornblende temperatures of 706 ± 50°C (Ravna, 2000a) and 678 ± 50°C (Graham and Powell, 1984).

Hornblende-plagioclase temperatures are similar with 702 ± 75°C at 10 kb and 679 ± 75°C at 15 kb. Pressure estimates from the two garnet-plagioclase-hornblende-quartz barometers are in general agreement, the Mg endmember reaction giving 8.33 ±

0.5 kb at 600°C and 8.73 ± 0.5 kb at 750°C and the Fe endmember reaction giving 8.27 ± 0.5 kb at 600°C and 9.49 ± 0.5 kb at 750°C.

Thermocalc estimates are comparatively high, with 14.4 ± 2.4 kb and 1029 ± 116°C, whereas TWQ calculated similar results to the other thermobarometers, 10.7 ± 0.07 kb and 793 ± 8°C.

Of the three types, Type 3 P-T estimates are subject to the least uncertainty. Amphibole is clearly part of the Type 3 peak assemblage, which exhibits clear evidence of reaching equilibrium. However, equilibrium between garnet and orthopyroxene + clinopyroxene + amphibole is difficult to demonstrate, as garnet is rarely in contact with the assemblage. The relatively slightly low temperatures obtained from garnet + clinopyroxene and garnet + amphibole may reflect this uncertainty. As in Types 1 and 2 samples, Thermocalc gives unrealistically high P-T estimates with large errors, which are not consistent with the evidence for textural and chemical equilibrium in this sample.

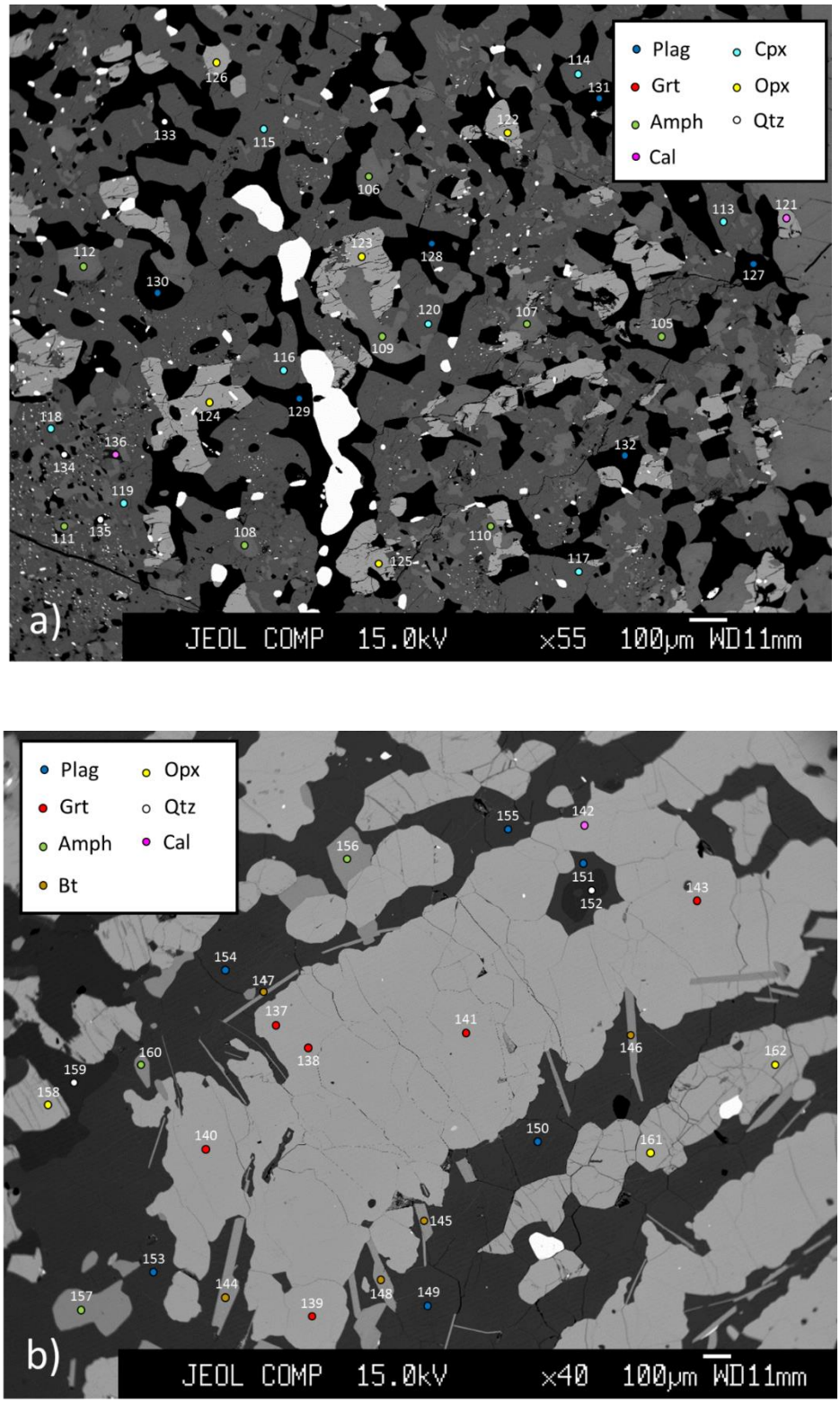

Figure 4.5: Locations of EMP analyses in Type 3a (JKEM-10), from phases A) replacing relict clinopyroxene and B) replacing recrystallized plagioclase. BSE images, numbers are analysis numbers; full analyses in Table 4.7 (used for P-T calculation) and Appendix.

	Orthopyroxene		Clinopyroxene		Amphibole	
No.	**All av.**		**All av.**		**All av.**	
SiO_2	51.31	± 0.20	52.65	± 0.20	42.31	± 0.54
TiO_2	0.05	± 0.02	0.04	± 0.03	1.79	± 0.19
Al_2O_3	0.45	± 0.12	1.21	± 0.17	11.29	± 0.57
Cr_2O_3	0.03	± 0.01	0.02	± 0.02	0.05	± 0.03
FeO	32.99	± 0.24	12.58	± 0.18	19.80	± 0.20
MnO	0.66	± 0.07	0.25	± 0.03	0.15	± 0.04
MgO	14.75	± 0.29	11.17	± 0.14	8.20	± 0.19
CaO	0.53	± 0.04	22.52	± 0.22	11.47	± 0.12
Na_2O	0.01	± 0.01	0.65	± 0.06	1.99	± 0.09
K_2O	0.03	± 0.01	0.03	± 0.01	1.36	± 0.10
ZrO_2	0.01	± 0.02	0.00	± 0.01	0.02	± 0.03
Total	100.82	± 0.43	101.11	± 0.23	98.44	± 0.28
Si	1.999	± 0.008	1.970	± 0.005	6.429	± 0.076
Ti	0.002	± 0.001	0.001	± 0.001	0.204	± 0.022
Al	0.021	± 0.006	0.053	± 0.008	2.022	± 0.103
Cr	0.000*		0.053*	± 0.007	0.006	± 0.003
($Fe^{3+,1}$)						
Fe	1.075	± 0.010	0.341	± 0.007	2.517	± 0.028
Mn	0.022	± 0.003	0.008	± 0.001	0.020	± 0.005
Mg	0.857	± 0.013	0.623	± 0.007	1.858	± 0.040
Ca	0.022	± 0.002	0.903	± 0.008	1.868	± 0.018
Na	0.001	± 0.001	0.047	± 0.004	0.587	± 0.026
K	0.002	± 0.001	0.001		0.264	± 0.019
Zr	0.000		0.000		0.001	± 0.002
Total	4.000		4.000		15.778	± 0.038

MgM1*	0.434		MgM1*	0.597	Fe/Mg	1.355
MgM2*	0.424		MgM2*	0.027	Mg#	0.425
Mg#*	0.444		Mg#*	0.647	Fe#	0.575
Fe# *	0.556		Mg#	0.613	xT1Si	0.608
Al^{VI}*	0.020		Fe#	0.387	xT1Al	0.393
			Al^{VI}*	0.023		
			Fe/Mg	0.632		

	Garnet			Plagioclase	
No.	**All av.**			**All av.**	
SiO_2	37.42	± 0.15		63.56	± 0.45
TiO_2	0.01	± 0.02		0.00	± 0.01
Al_2O_3	20.83	± 0.05		22.98	± 0.27
Cr_2O_3	0.02	± 0.02		0.00	
FeO	29.55	± 0.19		0.17	± 0.18
MnO	1.63	± 0.17		0.00	
MgO	3.72	± 0.24		0.02	± 0.07
CaO	6.10	± 0.10		4.31	± 0.32
Na_2O	0.01	± 0.01		9.10	± 0.17
K_2O	0.03	± 0.01		0.33	± 0.07
ZrO_2	0.00			0.01	± 0.02
Total	99.32	± 0.23		100.48	± 0.35
Si	2.996	± 0.007		2.800	± 0.014
Ti	0.001	± 0.001		0.000	
Al	1.965	± 0.008		1.193	± 0.013
Cr	0.001	± 0.001		0.000	
(*Fe^{3+})					
Fe	1.978	± 0.009		0.006	± 0.007
Mn	0.111	± 0.011		0.000	
Mg	0.444	± 0.028		0.001	± 0.005
Ca	0.523	± 0.010		0.203	± 0.015
Na	0.001	± 0.001		0.778	± 0.013
K	0.003	± 0.001		0.019	± 0.004
Zr	0.000			0.000	
Total	8.023	± 0.005		5.001	± 0.005
xPrp	0.145		xAn	0.203	
xAlm	0.647		xAb	0.778	
xSps	0.0363				
xGrs	0.171				
Fe#	0.817				
Mg#	0.183				
Fe/Mg	4.472				

Table 4.7: EMP analyses used in PT calculations from Type 3a.
[1] A * has the same significance as in Table 4.1.

Thermobarometer	Analyses Used	Pressure (kb)	Temperature (°C)	Comment
Opx/Cpx	Opx av., Cpx av.	N/A	755 ± 70	
Grt/Cpx[1]	Grt av., Cpx av.	*9.5*	618 ± 100	
Grt/Cpx[2]	Grt av., Cpx av.	*9.5*	679 ± 50	
Grt/Hbl[1]	Grt av., Amph av.	N/A	706 ± 50	
Grt/Hbl[2]	Grt av., Amph av.	N/A	678 ± 50	
Hbl/Plag	Amph av., Plag av.	*10, 15*	702, 679 ± 75	Ed-Tr reaction
Grt/Plag/Hbl/Qtz	Grt av., Plag av., Amph av.	8.33, 8.73 ± 0.5	*600, 750*	Mg endmember
Grt/Plag/Hbl/Qtz	Grt av., Plag av., Amph av.	8.27, 9.49 ± 0.5	*600, 750*	Fe endmember
Thermocalc	Opx av., Cpx av., Amph av., Grt av., Plag av.	14.4 ± 2.4	1029 ± 116	
TWQ	Opx av., Cpx av., Grt av., Plag av.	10.7 ± 0.07	793 ± 8	

Reactions used by Thermocalc:
CaTs + Qtz = An
En + MgTs = Prp
2Prp + Grs + 3Qtz = 3En + 3An
3MgTs + 3Di = 2Prp + Grs
3Fs + 3CaTs = Grs + 2Alm
Alm + 3Hd = Grs + 3Fs
4En + Ts = 2Prp + Tr
8Alm + 6Fact = 2Grs + 27Fs + 6An + 6H2O
5Prp + 3Fact = 5Alm + 3Tr
11Prp + 4Grs + 3Tr + 3Ab = 18En + 3Prg + 12An
Reactions used by TWQ:
2Alm + Grs + 3Qtz = 6Fs + 3An
Alm + 3En = Prp + 3Fs
3Qtz + Prp + 2Grs = 3An + 3Di

Table 4.8: P-T Estimates from Type 3a analyses (Table 4.7).
Cpx[1] Ravna, 2000b
Cpx[2] Ellis & Green, 1979
Hbl[1] Ravna, 2000a
Hbl[2] Graham & Powell, 1984
Italics – used in calculation, not a result

4.5 P-T Path of Metamorphism

The mineral assemblages, textures, and P-T estimates are all consistent with the interpretation that Types 1, 2, and 3 represent three sequential stages in the metamorphic history of the Emsdale metagabbro. The early-stage coronas and well-preserved gabbroic textures of Type 1a indicate prograde evolution to granulite facies conditions, whereas the highly reworked and amphibole-rich Type 3a samples indicate retrogression to amphibolite. P-T estimates from Types 1, 2, and 3 samples therefore represent early, intermediate, and late stages respectively on the P-T-t path for the Emsdale metagabbro.

Table 4.9 lists the P-T estimates deemed most reliable from Type 1a, 2, and 3a samples analyzed by EMP. Prograde conditions prior to Type 1a have been inferred by analyzing an approximate "early" assemblage of opx + cpx + grt + adjacent plag (discussed further in chapter 5) using TWQ, which gave lower P-T estimates than Type 1a. Type 1a peak temperature is likely underestimated by TWQ and best represented by the orthopyroxene-clinopyroxene estimates of approximately 800 ± 70°C. Pressures for Type 1a samples average 10.9 ± 0.5 kb. Type 2 pressures may be overestimated by TWQ, but in general are at least 1 kb higher than Type 1a at 12.9 ± 0.5 kb, with peak temperature likely close to 880 ± 70°C. Despite uncertainties in the P-T results, Type 2 likely records peak or near-peak P-T granulite facies conditions. TWQ results are considered to be most reliable for Type 3a; pressure averages at 9.6 ± 0.5 kb with temperature likely around 770 ± 70°C. Results from the orthopyroxene-clinopyroxene thermometer and TWQ produced a relatively narrow temperature range of less than 200°C (not including uncertainty) among all types, with the highest temperatures

obtained from Type 2 sample JKEM-15b, and somewhat lower temperatures from Types 1a and 3a. These results suggest a near-isothermal P-T evolution.

The P-T estimates were used to construct a P-T-t path of for the Emsdale coronite (Figure 4.6), though the considerable overlap in temperatures lends uncertainty to its position. However, the P-T path clearly indicates that pressure increased to peak conditions and decreased during the retrograde path over a relatively small range of temperatures.

Figure 4.7a compares Emsdale coronite P-T estimates with those calculated by Grant (1987) using olivine-plagioclase-garnet barometry and garnet-clinopyroxene and garnet-orthopyroxene thermometry for other Algonquin metagabbros. Her results are from a larger number of samples and show less variation than the Emsdale coronite but lower P-T conditions; the only overlap is with the earliest prograde and latest retrograde estimates. Grant reported that pressure estimates were relatively low for samples with plagioclase moats, in contrast to the relatively high pressures of Type 2 samples. An explanation may lie in Grant's use of olivine-plagioclase-garnet barometry for all pressure estimates. Olivine coronas form by disequilibrium between olivine and plagioclase, suggesting that this assemblage is not suitable for thermobarometry. In addition, Grant likely used now-outdated thermometer calibrations. This interpretation is supported by the agreement between the Emsdale coronite P-T path and more recent thermobarometric data from Timmermann (1998) calculated using TWQ (Figure 4.7b). Two P-T paths in Timmermann's study were from samples in the McClintock and southern Huntsville subdomains of the Algonquin Domain (Figure 2.1). Both overlap with the Emsdale coronite P-T range, and all three paths indicate decompression

accompanied by a relatively small decrease in temperature. The “hairpin” shape of the Emsdale P-T-t path suggests burial and exhumation within the deep levels (ca. 30km) of a large, hot, long-lasting orogen, in which elevated temperatures were maintained in the thick crust for a prolonged period of time (e.g. Culshaw et al. 1997; Jamieson et al. 2010).

Type (Sample)	Thermobarometer	Pressure (kb)	Temperature (°C)
"Early" (JKEM-12)	TWQ	8.4 ± 0.4	777 ± 63
Type 1a (JKEM-12)	Opx/Cpx	N/A	845 ± 70
Type 1a (JKEM-12)	Opx/Cpx	N/A	828 ± 70
Type 1a (JKEM-12)	Grt/Plag/Hbl/Qtz	9.86 ± 0.5	*850*
Type 1a (JKEM-12)	Grt/Plag/Hbl/Qtz	11.1 ± 0.5	*850*
Type 1a (JKEM-12)	TWQ	10.7 ± 0.7	685 ± 65
Type 1a (JKEM-14a)	Opx/Cpx	N/A	808 ± 70
Type 1a (JKEM-14a)	Grt/Plag/Hbl/Qtz	10.6 ± 0.5	*850*
Type 1a (JKEM-14a)	Grt/Plag/Hbl/Qtz	11.8 ± 0.5	*850*
Type 1a (JKEM-15a)	Opx/Cpx	N/A	790 ± 70
Type 1a (JKEM-15a)	Grt/Plag/Hbl/Qtz	10.6 ± 0.5	*850*
Type 1a (JKEM-15a)	Grt/Plag/Hbl/Qtz	11.7 ± 0.5	*850*
Type 2 (JKEM-14b)	Opx/Cpx	N/A	765 ± 70
Type 2 (JKEM-14b)	Grt/Plag/Hbl/Qtz	12.6 ± 0.5	*850*
Type 2 (JKEM-14b)	Grt/Plag/Hbl/Qtz	12.7 ± 0.5	*850*
Type 2 (JKEM-15b)	Opx/Cpx	N/A	880 ± 70
Type 2 (JKEM-15b)	Grt/Plag/Hbl/Qtz	13.1 ± 0.5	*850*
Type 2 (JKEM-15b)	Grt/Plag/Hbl/Qtz	13.1 ± 0.5	*850*
Type 2 (JKEM-15b)	TWQ	15.0-16.6 ± 1.0	817-909 ± 80
Type 3a (JKEM-10)	Opx/Cpx	N/A	755 ± 70
Type 3a (JKEM-10)	Grt/Plag/Hbl/Qtz	8.73 ± 0.5	*750*
Type 3a (JKEM-10)	Grt/Plag/Hbl/Qtz	9.49 ± 0.5	*750*
Type 3a (JKEM-10)	TWQ	10.7 ± 0.07	793 ± 8

Table 4.9: Summary of reliable P-T estimates from six samples analyzed by EMP.
Italics – used in calculation, not a result

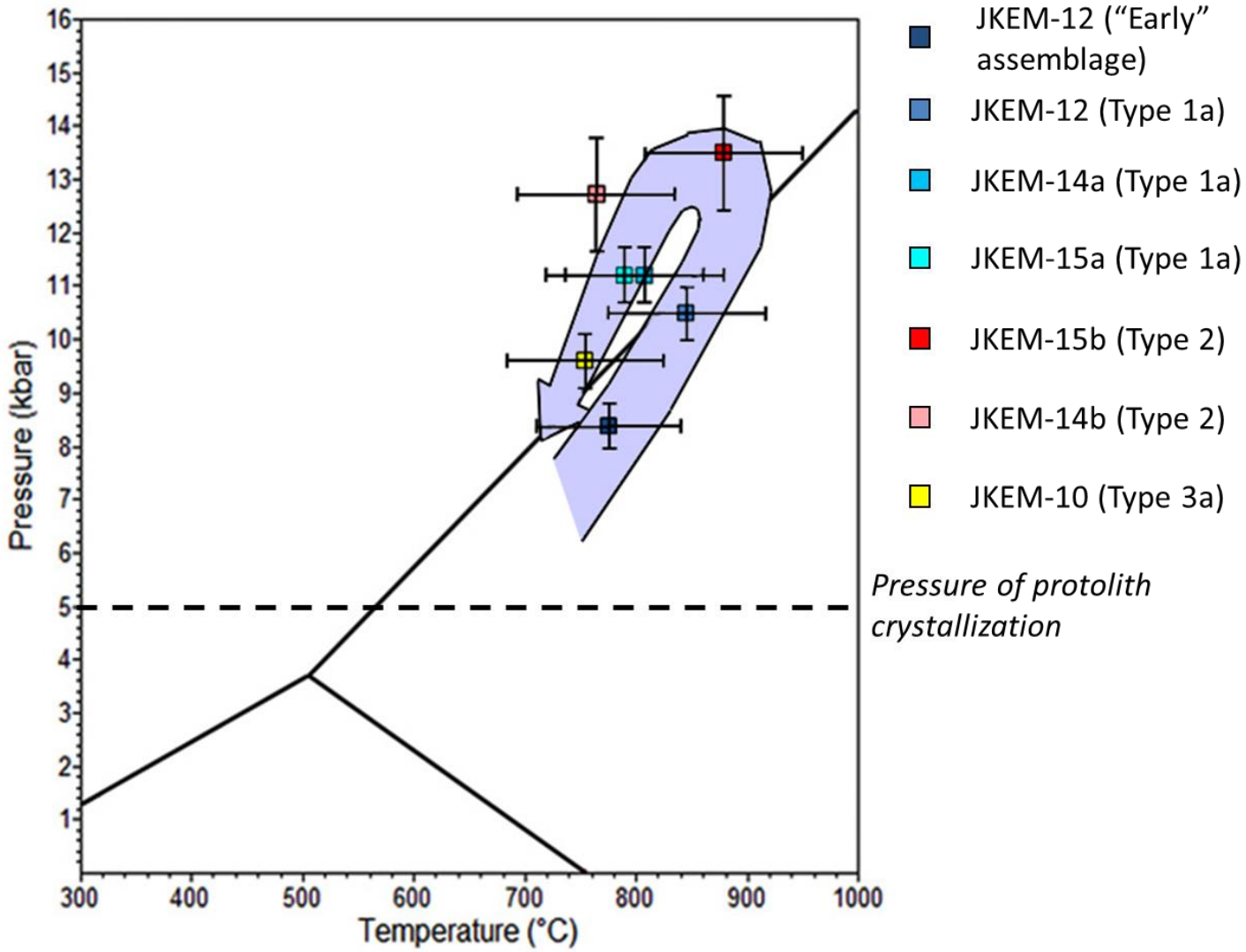

Figure 4.6: Pressure and temperature plot with P-T estimates from Table 4.9 and the suggested P-T-t path of metamorphism. Despite temperature overlap between the samples, pressures are well-resolved. Type 2 represents peak metamorphic conditions and Types 1a and 3a P-T estimates were used to approximate the prograde and retrograde paths respectively. Pressure of protolith crystallization is discussed in chapter 5.

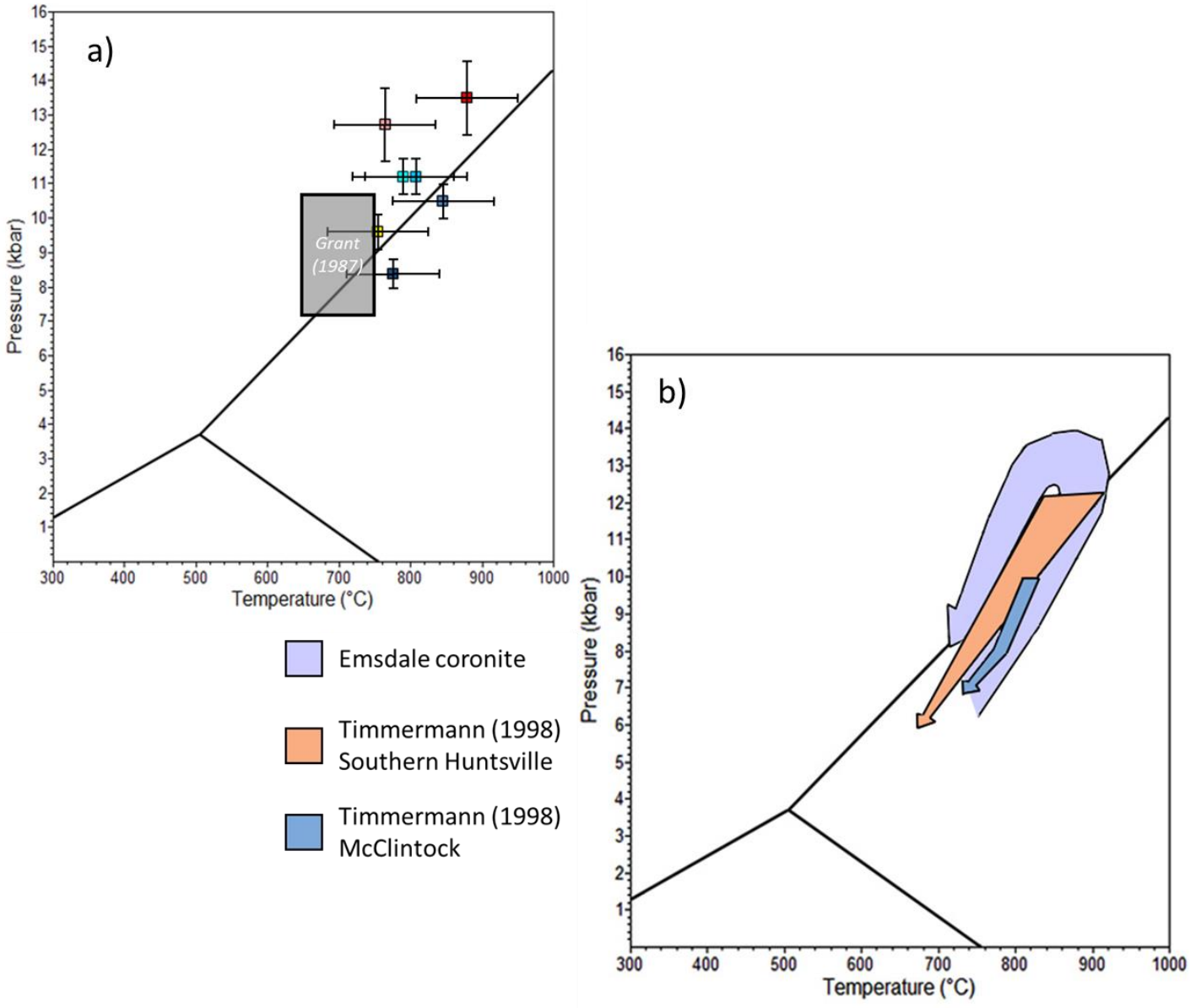

Figure 4.7: Comparisons between Emsdale metagabbro P-T data and P-T data from previous work. A) P-T estimates from this study are plotted with the P-T range reported by Grant (1987) for Algonquin metagabbros from all domains of her study. Grant's results were less variable and are lower than those of this study. B) Emsdale metagabbro suggested P-T path superimposed by two paths from Timmermann (1998) from the Algonquin Domain. The Timmermann paths have no prograde component, but all three show a similar retrograde evolution.

Chapter 5: Petrologic Interpretation and Discussion

5.1 Introduction

Results presented in the previous chapters have been used to interpret the metamorphic history of the Emsdale metagabbro from protolith to the most retrogressed stage preserved. The mineralogical and textural changes during the prograde and retrograde paths (5.3, 5.4) are inferred from previous work (Grant, 1987) in conjunction with the findings of this study. Possible mechanisms of formation of the olivine pseudomorphs observed in this coronite are discussed (5.5).

5.2 Protolith Conditions

The olivine gabbro protoliths of the Algonquin metagabbros were intruded into polycyclic Laurentian crust at ca. 1150-1160 Ma (Davidson and van Breemen, 1988; Heaman and LeCheminant, 1993). The well-preserved igneous features of the metagabbros allow inferences to be made about the igneous development of the protolith though petrographic and geochemical analyses (Grant, 1987). Grant modelled the fractionation of major phases during the crystallization of the olivine gabbros (refer to Grant, 1987 for results); however, only broad, qualitative estimates could be made for the depth of gabbro intrusion and therefore the pressure conditions prior to metamorphism.

Using the geochemical data collected by Grant (1987), I conducted a study to model the igneous development of Algonquin metagabbro protoliths and constrain their intrusion depth (Kendrick, 2014, unpublished). The MELTS web applet (Ghiorso and Sack, 1995; Asimow and Ghiorso, 1998) was employed to model liquids produced by

fractional crystallization during cooling of a mantle-derived melt at 5 kb, 7.5 kb, and 10 kb. The compositions of melts produced were compared to Grant's bulk composition data from unaltered, quenched Algonquin metagabbro samples. The best chemical match between the model and the data was found at a pressure of 5 kb. In addition, the modelled fractionating assemblage of clinopyroxene (Ti-rich) + plagioclase + olivine + minor spinel at 5 kb closely approximates the inferred assemblage in the gabbroic protoliths; at higher pressures, orthopyroxene crystallized in place of olivine, contradicting the assemblage of the Emsdale metagabbro and the observations of Grant (1987). Therefore, the protolith of the Emsdale metagabbro likely intruded at a depth corresponding to approximately 5 kb, or around 15 km. After crystallization, the gabbro remained at these conditions until the onset of crustal thickening and metamorphism accompanying the Ottawan phase of the Grenvillian orogeny. The 5 kb protolith pressure is shown with the with the inferred P-T path (Figure 4.6) for comparison. Pressures of metamorphism for Types 1 to 3 were considerably higher than the likely pressure of gabbro crystallization.

5.3 Prograde Reactions and Textural Evolution

The earliest stages of reaction are not preserved in the Emsdale coronite but can be inferred from other members of the Algonquin metagabbro suite. G86-12, a coronite sample not part of this study, was collected in Algonquin Park (Figure 2.1), approximately 80 km east of the study site; this sample is presented here solely for comparison. Preliminary petrographic observations reveal that this coronite has a well preserved igneous texture with early stages of corona formation between plagioclase and olivine and between plagioclase and Fe-Ti oxides. In this sample, relict olivine is largely

unreacted aside from granoblastic orthopyroxene replacing its outer edges (Figure 5.1). Fe-Ti oxides are commonly surrounded by recrystallized biotite and rimmed by a band of granoblastic amphibole (Figure 5.2). During early development, the Emsdale coronite likely shared the features of G86-12 and passed through unpreserved intermediate stages before reaching the earliest preserved stage, Type 1.

Work by Grant (1987) includes the most extensive study of the Algonquin metagabbro suite. Her least evolved samples resemble Type 1a of this study mineralogically and texturally, with olivine corona assemblages of opx + cpx, ± amph + grt-cpx or grt-amph symplectite (Figure 5.3); unlike Type 1a, Grant's samples preserved igneous olivine at the cores of coronas. Grant described a spinel-bearing symplectite in three samples, in some cases coexisting metastably with a garnet-bearing symplectite. She reported that the garnet-bearing symplectites showed no sign of replacing those bearing spinel and that most samples appeared never to have contained spinel in their coronas; therefore, the different symplectites likely do not represent two sequential stages of development. The existence of the two symplectite types can instead be attributed to differences in pressure conditions (Grant, 1987). Coronites containing only garnet-bearing symplectites, such as the Emsdale metagabbro, likely passed quickly through the spinel stability field to garnet-forming pressures. Grant's samples suggested that the next developmental stage after the symplectite was the formation of monomineralic garnet adjacent to plagioclase, which is present in all Type 1 samples. The "early" opx + cpx + grt symp + plag assemblage added to the P-T path of metamorphism (Figure 4.6) is probably analogous to a stage just before Type 1; all phases in the symplectite were fine-grained with no monomineralic garnet.

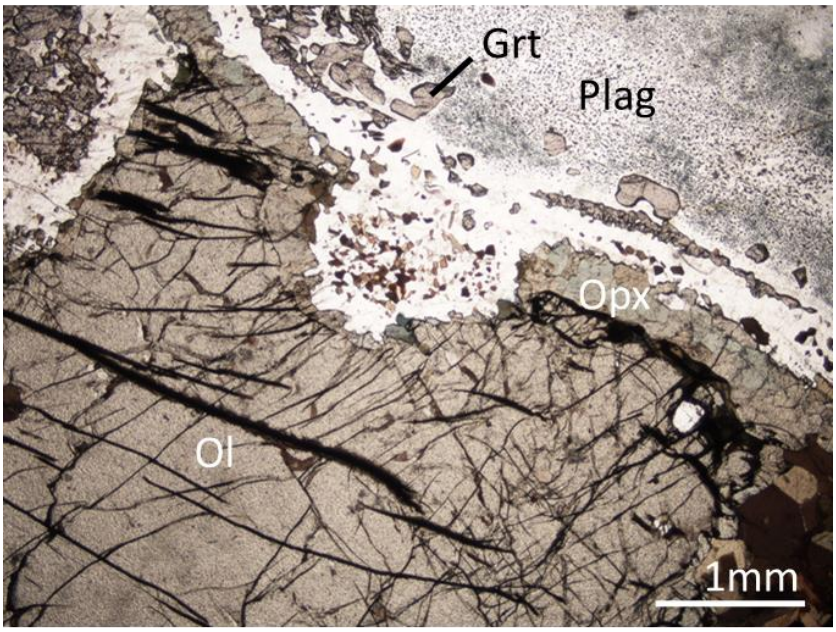

Figure 5.1: Relict olivine with an orthopyroxene rim in PPL (G86-12). Field of view ca. 6.25 mm. Relict plagioclase is clear close to orthopyroxene and otherwise clouded by spinel. A small amount of garnet replaces plagioclase near olivine.

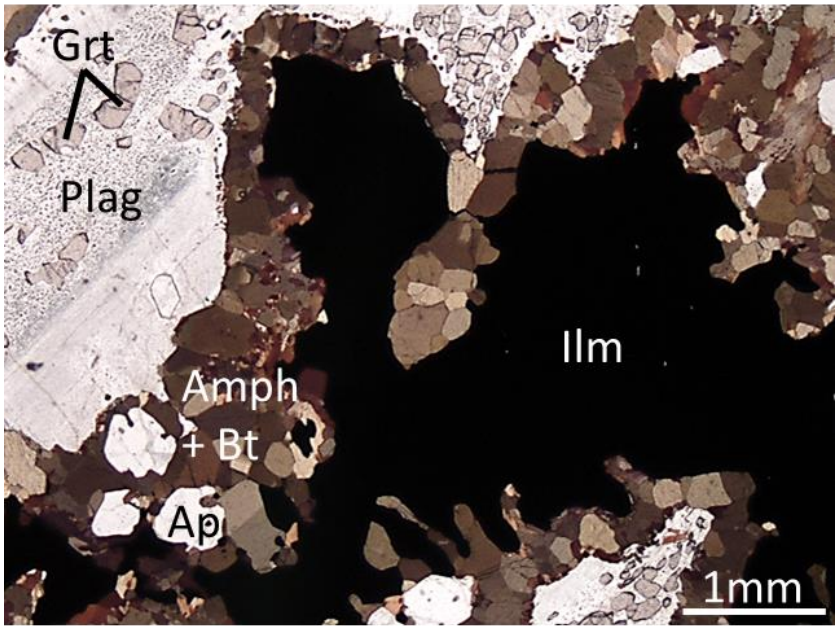

Figure 5.2: Fe-Ti oxide rimmed by amphibole + biotite in PPL (G86-12). Field of view ca. 6.25 mm. Garnet is present but does not form a shell.

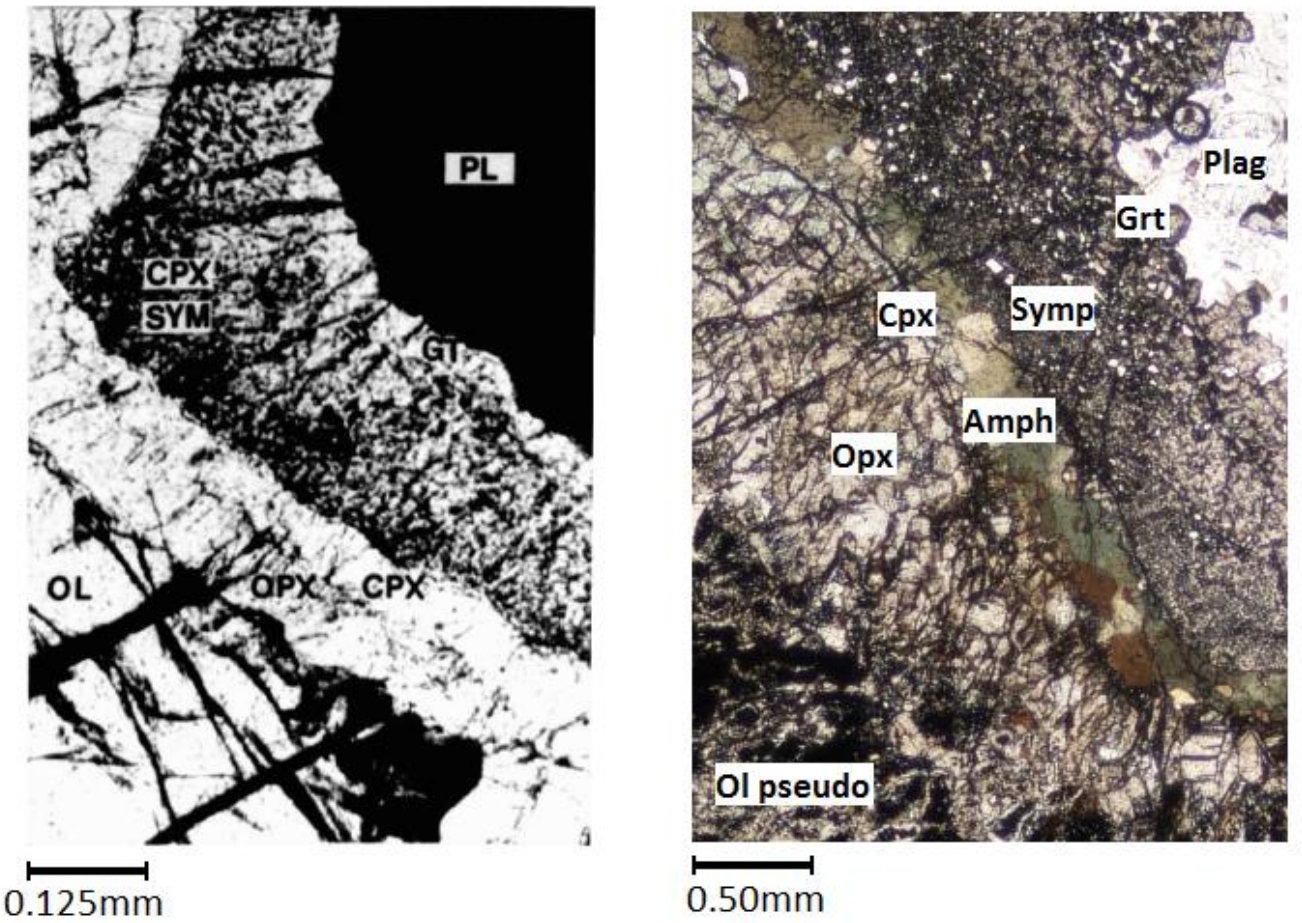

Figure 5.3: Olivine coronas in early stages of formation. Complete coronitic sequences from Grant (1987) (left) and from Type 1a of this study (right) are texturally similar. The major differences between the two are the presence of amphibole and biotite and the discontinuity of the clinopyroxene shell in Type 1a.

Grant (1987, 1988) proposed that progression until this stage was entirely diffusion-controlled. Based on the oxide components of corona-forming minerals in her work (Table 5.1), she proposed a set of diffusion-driven reactions responsible for forming each corona shell, assuming single-stage, steady-state growth (Table 5.2). To test Grant's reactions, average mineral compositions from Type 1a samples of the present study (Table 5.1) were substituted into them. In all reactions, the calculated Al, Ca, and Si components balanced, whereas the Mg and Fe components generally did not in reactions involving olivine, orthopyroxene, and garnet. Failure of Grant's reactions to predict the

Mg and Fe components of Emsdale metagabbro coronas can be attributed to differences in metagabbro bulk composition. The coronas Grant used to model the reactions developed in an Mg-rich metagabbro, whereas the Emsdale metagabbro shows evidence of being relatively Fe-rich based on the compositions and modal proportions of its mafic phases. Olivine in the Emsdale coronite may have been more Fe-rich than those Grant (1988) used to calculate the reactions.

Oxide components used in Grant (1988)						
DMS-8	MgO	FeO	SiO2	$AlO_{1.5}$	CaO	$NaO_{0.5}$
Ol	1.20	0.80	1.00			
Opx	1.36	0.64	1.96	0.07		
Cpx	0.75	0.23	1.95	0.15	0.85	0.08
Grt	0.95	1.50	3.00	2.00	0.55	
Symp	1.10	1.36	3.13	1.72	0.70	0.02
An38			10.50	5.48	1.54	2.40
"Plag 1"			3.09	1.70	1.00	0.40
"Plag 2"			2.79	1.70	1.00	0.40
DMS-13A	MgO	FeO	SiO2	$AlO_{1.5}$	CaO	$NaO_{0.5}$
Ol	1.10	0.90	1.00			
Opx	1.30	0.70	1.98	0.05		
Cpx	0.75	0.23	1.96	0.15	0.85	0.08
Amph	2.90	1.40	6.20	2.60	1.80	0.90
Grt	0.86	1.60	3.00	2.00	0.54	
Symp	1.00	1.40	3.14	1.74	0.67	0.08
Average Type 1a						
	MgO	FeO	SiO2	$AlO_{1.5}$	CaO	$NaO_{0.5}$
Ol	1.15	0.85	1.00			
Opx	0.93	1.02	1.98	0.03		
Cpx	0.64	0.36	1.97	0.10	0.85	0.08
Amph	2.13	2.31	6.31	2.22	1.78	0.79
Grt	0.43	1.98	2.99	1.98	0.54	

Table 5.1: Average oxide components for olivine corona-forming minerals in work by Grant (1988) and Emsdale metagabbro Type 1a. Olivine components in Type 1a are an average of those used by Grant.

Interface	Reaction
Ol/Opx	4.65 Ol + 0.21 SiO_2 + 0.09 $A1O_{1.5}$ → 2.42 Opx + 2.00 MgO + 2.45 FeO
Opx/Cpx	0.84 Opx + 0.06 $AlO_{1.5}$ + 0.86 CaO + 0.15 $NaO_{0.5}$ + 0.36 SiO_2 → 1.04 Cpx + 0.33 MgO + 0.32 FeO
Cpx/Amph	0.31 Cpx + 0.03 FeO + 0.05 $AlO_{1.5}$ + 0.09 $NaO_{0.5}$ + 0.05 H_2O → 0.05 Amph + 0.11 MgO + 0.30 SiO2 + 0.17 CaO
Amph/Symp	0.22 Grt + 0.06 Amph + 0.17 MgO + 0.13 SiO_2 + 0.11 CaO + 0.19 $NaO_{0.5}$ + H_2O → 0.19 Amph + 0.14 FeO + 0.14 $A1O_{1.5}$
Plag/Symp	2.26 [$Na_{0.4}CaAl_{1.7}Si_{3.09}$] + 2.89 MgO + 2.84 FeO + H_2O → 0.37 Amph + 1.44 Grt + 0.40 SiO_2 + 0.02 $A1O_{l.5}$ + 0.82 CaO + 0.50 $NaO_{0.5}$
Overall	4.65 Ol + 2.26 [$Na_{0.4}$,$CaAl_{l.7}$,$Si_{3.09}$] + H_2O → 1.58 Opx + 0.74 Cpx + 0.55 Amph + 1.21 Grt

Table 5.2: Reactions calculated by Grant (1988) using her oxide mineral compositions in Table 5.1.

Based on research by Grant (1987, 1988) and examination of samples from other Algonquin metagabbro bodies, the early evolution of the Emsdale metagabbro can be inferred. Instability of coexisting igneous olivine and plagioclase initiated diffusion, leading to the reactions listed in Table 5.2, with a similar process at work between igneous Fe-Ti oxides and plagioclase. Work by Grant (1988) focused entirely on the process of olivine corona growth, which will be the focus here as well. Fe and Mg were liberated from olivine and diffused toward plagioclase, where Si, Al, Ca, and Na were released and diffused toward olivine (Grant, 1988). Grant considered spinel clouding of plagioclase to be an important early step in the process; the released Fe and Mg allowed spinel to grow, which in turn liberated additional Ca essential for corona formation. Si and Al were slow-moving components, with Al as the slowest and its mobility potentially controlling the rate of corona formation (Grant, 1988). This hypothesis is reflected by the

step-like distribution of Al within coronas, where the innermost shell contains little to no Al and the outer symplectite shell has Al values closer to plagioclase (Grant, 1987, 1988; Figures 3.8 and 3.9 Al maps). Grant hypothesized that as long as the components listed above were able to continue diffusing, the corona would continue to grow. As the coronas grew larger, the chemical gradients became smaller and spread over a larger distance, which eventually slowed diffusion to a stop (Grant, 1988). Another driving factor for diffusion identified by Grant was temperature; higher temperature facilitates diffusion and low temperatures provide insufficient energy to drive diffusion. As temperature variation is small between the three types of Emsdale coronite, the coronas in Type 1 were likely limited by diffusion length-scale rather than temperature.

Grant (1988) considered the formation of the different corona shells to be a single-stage, steady-state process during post-crystallization cooling of the gabbro body. This assumption implies that rather than growing in succession, the shells grew simultaneously and that each shell maintained a constant mineral composition during corona development. However, textures from Emsdale coronite Type 1a olivine coronas do not fully support these assumptions. The clinopyroxene shell is typically discontinuous and uneven, showing evidence of consumption by the adjacent amphibole layer. In addition, most thermometers incorporating amphibole produced temperatures that are likely retrograde. Amphibole should therefore not be included in corona-forming reactions in the Emsdale coronite, as it is almost certainly a retrograde phase. The original corona assemblage of opx + cpx + symplectic grt potentially grew by single-stage, steady-state diffusion as modelled by Grant (1988); assemblages and textures in Type 1a coronas neither support nor refute this hypothesis.

The corona mineral chemistry of Type 1a supports Grant's (1987) argument that the coronas in Algonquin metagabbros are not late igneous features. She reasoned that residual melt present after the crystallization of the main igneous phases would be enriched in incompatible elements; therefore, coronas forming from this melt should be enriched in elements such as Ti. Corona mineral compositions in Grant's samples, like those in the Emsdale metagabbro, did not show the expected enrichment. However, Grant's hypothesis of corona growth during slow post-crystallization cooling is not supported. Her assumption was that coronas formed at pressures controlled solely by depth of the gabbro intrusion, and ceased to grow when the body cooled below a certain temperature. The estimated pressure at which the gabbro protoliths crystallized is approximately 5 kb (Kendrick, 2014, unpublished), considerably lower than pressure estimates for coronas in Type 1a or those calculated by Grant (1987) (Table 4.9, Figure 4.6). The pressure discrepancy between the protolith and Type 1a indicates that lithostatic pressure during intrusion was not sufficient to initiate corona formation. Thus in the Emsdale coronite, corona growth was an entirely prograde metamorphic process related to orogenesis.

5.4 Evolution from Type 1 to Type 3

As described in chapter 3, the Emsdale metagabbro hosts a range of textures classified into three types. After the diffusion-controlled growth of coronas preserved in Type 1 samples, Type 2 marks the onset of textural reworking at peak metamorphism causing both coronas and igneous phases to be obscured. A similar progression was reported by Grant (1987) in samples she classified as medium-grained. Igneous olivine

was completely replaced by an orthopyroxene mosaic, whereas in coarser-grained samples, olivine survived initial stages of reworking. In general, both types of samples showed grt + cpx symplectite overprinted by clean garnet that extended into igneous plagioclase as idioblastic crystals, and a plagioclase moat between the clinopyroxene and symplectite shells (Grant, 1987).

The plagioclase moat may have formed by several possible mechanisms. McLelland and Whitney (1980) presented two explanations: igneous zonation or displacement of albitic plagioclase from outside the corona to the inside. Their igneous zonation hypothesis is based on the assumption that garnet will not form where plagioclase is albite-rich, or Al-poor. Igneous plagioclase is typically zoned toward sodic rims, which McLelland and Whitney proposed were adjacent to igneous olivine and Fe-Ti oxides at the time of corona formation. Garnet would therefore not form close to olivine and oxides, as it would be restricted to the calcic plagioclase cores. This mechanism cannot explain the plagioclase moats seen in Algonquin metagabbros, as samples preserving early corona formation clearly show garnet in contact with the mafic corona shells with no albite-rich moat. The other suggestion by McLelland and Whitney is based on volume (V) changes of reactions outside and within the corona. Their proposed garnet-forming reaction within the corona has a negative ΔV, whereas their reaction for spinel formation in the outer plagioclase produces albite and can have a positive ΔV. Albite formed outside the corona may therefore be displaced toward the volume deficiency created within the corona. Grant (1987) adopted this explanation for Algonquin metagabbros, as the plagioclase moat is present in samples where garnet has proliferated. Cox and Indares (1999) suggested that the plagioclase moats in their coronas

grew during decompression, based on the breakdown of the jadeite component in adjacent clinopyroxene. This mechanism would suggest that the rock had attained at least near-eclogite facies metamorphic grade; the Emsdale coronite bears no evidence of high-pressure metamorphism. In Type 2 samples, the embayed contacts between the moat and amphibole and the moat and garnet suggest that plagioclase may have formed simply by breakdown of these two phases. Na could be supplied by the amphibole, and both garnet and amphibole could provide Ca and Al in a general decompression reaction of

$$\text{Garnet} + \text{Amphibole(1)} = \text{Plagioclase} + \text{Amphibole(2)},$$

where amphibole 1 and 2 are different compositions of amphibole.

Type 3 rocks represent the most retrogressed portions of the outcrop. The igneous texture of the gabbro protolith has been almost entirely overprinted by later metamorphic phases, and former igneous plagioclase has undergone extensive grain size reduction. Olivine coronas have been replaced by granoblastic amph + plag + cpx + opx, and amph + bt partially replace magmatic Fe-Ti oxides. Type 3 samples appear to have been evolving toward granoblastic amphibolites or garnet amphibolites with an assemblage of amph + plag + bt + qtz ± grt. The variety of textures and assemblages in Type 3a and 3b described in chapter 3 is among those described by Grant (1987). She observed that the garnet content varied between retrogressed samples depending on locality; those from the Opeongo and Kawagama subdomains were garnet-poor, similar to Type 3b. Samples studied by Grant from near pegmatite dykes and localized shear zones in particular lacked garnet, which she attributed to fluid influx - variable fluid activity affected the end product achieved through retrogression. Granulites with little to no amphibole and garnet pseudomorphs after plagioclase were the endpoint in less hydrous systems, whereas

samples similar to Type 3 represented a greater degree of hydration. Analysis of a Type 3a sample reveals evidence of significant fluid influx. Aside from the proliferation of amphibole, calcite is found in several textural settings. Skeletal biotite associated with garnet and plagioclase may have formed from the small blades included in plagioclase alongside spinel in Types 1 and 2; biotite growth appears to have been enhanced whereas spinel has disappeared. Spinel was likely converted to the garnet and biotite aggregates replacing plagioclase in Type 3a by a general reaction of

$$\text{Spinel} + \text{Plagioclase} + \text{Fluid} = \text{Garnet} + \text{Biotite}.$$

Despite representing different developmental stages in the metamorphic history of the Emsdale coronite, Types 1, 2 and 3 coexist within a single metagabbro body due to local variations in fluid availability (Figure 3.1). Fluids introduced by the pegmatite dyke, quartz veins, and the clinopyroxene + plagioclase-bearing veins accelerated reactions and facilitated textural reworking. The cross-cutting nature of veins and pegmatite suggests that their intrusion postdated crystallization of the igneous protolith and was likely synchronous with metamorphism. Type 2 assemblages and samples transitional between Types 1 and 2 support this hypothesis, as it appears that prior to fluid introduction, all samples had likely developed Type 1 coronas. Therefore, the injection of veins must have postdated corona formation, which was a prograde metamorphic process (Figure 4.6). Type 2 likely preserves the approximate P-T conditions at the time of vein intrusion.

5.5 Pseudomorphs After Olivine

As described in chapter 3, olivine in all samples is replaced by either an orthopyroxene + ilmenite + magnetite symplectite, or more rarely, “iddingsite” (Ch.3).

This section focuses mainly on the former, which has not been reported previously in the Grenville Province.

5.5.1 Hypotheses of Previous Workers

In one of the earliest studies to report orthopyroxene + oxide symplectites after olivine, Frodesen (1968) described "a granular aggregate of orthopyroxene with large amounts of iron ore" replacing igneous olivine. He suggested that these pseudomorphs and the outer symplectite shell of the coronas formed coevally by alteration later in the metamorphic history of the metagabbro. Recently Gallien et al. (2012) studied an Argentinian coronite and reported orthopyroxene + magnetite symplectites after olivine. They proposed that the oxidation of fayalite produced magnetite and excess silica, which in turn reacted with forsterite to form enstatite. This mechanism appears to be feasible for that example, although no source of mobile oxygen was proposed. Van Lamoen (1979) argued against the olivine oxidation hypothesis for orthopyroxene + magnetite symplectites from Finland, stating that the above reaction could not produce the orthopyroxene composition observed in the symplectites. In his coronite samples, olivine was partly replaced by the symplectite, which was only found where igneous opaque oxides and olivine were in contact. Van Lamoen (1979) suggested that excess Fe produced by the formation of orthopyroxene from olivine was trapped within the orthopyroxene shell by the adjacent opaque oxides. With the addition of an Al and Ti-bearing fluid of unidentified origin, magnetite of the composition observed by van Lamoen was formed. Claeson (1998) reported orthopyroxene + magnetite + spinel symplectite pseudomorphs only in samples rich in igneous Fe-Ti oxides, and attributed

their formation to grain-boundary diffusion of a late igneous fluid. In the study by Zeck et al. (1982), replacement of olivine by the orthopyroxene + ilmenite ± magnetite symplectite was restricted to portions of the olivine crystal that were adjacent to an igneous Fe-Ti oxide. They proposed that corona growth between Fe-Ti oxides and plagioclase was therefore related to orthopyroxene symplectite formation. A fluid phase bearing K and Si, perhaps of late igneous origin, reacted with Fe-Ti oxides to produce the biotite and hornblende coronitic shells and caused a release of Ti (Zeck et al., 1982). The Ti-rich fluid then reacted with olivine to form orthopyroxene + ilmenite.

5.5.2 Pseudomorphs in the Emsdale Metagabbro

Unlike many of the studies above, the oxides in the pseudomorphs observed in Emsdale Type 1 samples are always dominated by ilmenite. To consider the stability of the symplectite assemblage, olivine, ilmenite, orthopyroxene, and magnetite were plotted on a ternary diagram in terms of Fe + Mg, Ti, and Si components in Figure 5.4a. The red tie line connects the two phases initially in equilibrium, magmatic olivine and ilmenite. This assemblage became unstable in the coronite as orthopyroxene replaced olivine (Figure 5.4b). A shift from ilmenite + olivine to ilmenite + orthopyroxene left excess Fe + Mg, as olivine has higher (Fe + Mg):Si than orthopyroxene. As a consequence, some magnetite formed, giving a general reaction of

$$Fe_2SiO_4\,(Fa) + FeTiO_3\,(Ilm) = FeSiO_3\,(Fs) + Fe_3O_4\,(Mt) + FeTiO_3.$$

The symplectite phases therefore coexist stably; however, their distribution must be explained. A Ti-bearing assemblage directly replaces olivine, which contains little to no Ti itself. The possibility of the symplectites being derived solely from olivine, as

suggested by Gallien et al. (2012), can be eliminated; the necessary amount of Ti could not possibly be produced from olivine alone. The orthopyroxene symplectites must therefore form by interaction between olivine and an external phase bearing Ti. Claeson (1998) and Zeck et al. (1982) identified the external reactant phase as late igneous fluid, which was thought to mobilize Ti from magmatic Fe-Ti oxides. In the Emsdale coronite, however, igneous fluid could not have been a factor, because corona formation was almost certainly a prograde metamorphic process. Had the orthopyroxene symplectite pseudomorph replaced olivine during the latest stages of igneous crystallization, the formation of an inclusion-free orthopyroxene shell during metamorphism would have been impossible. Sometime after the growth of the orthopyroxene shell, the embayed remnants of igneous olivine were replaced by the pseudomorph.

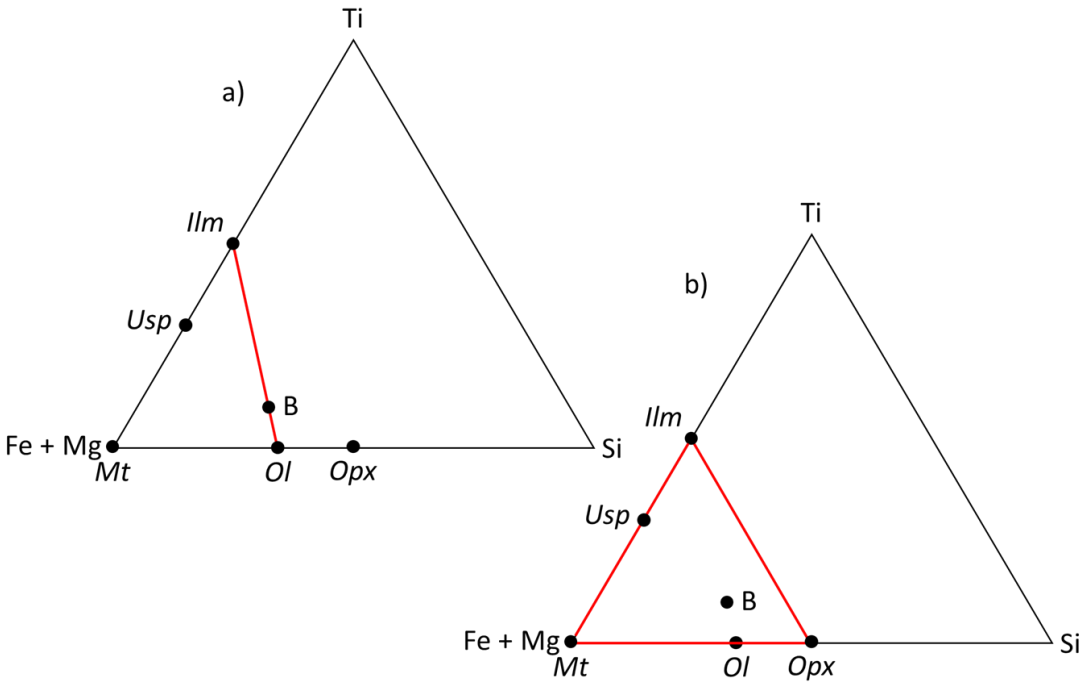

Figure 5.4: Ternary diagrams for the (Fe + Mg)-Ti-Si system, a) before metamorphism and b) post-metamorphism. A) The tie line connects ilmenite and olivine, originally a stable assemblage prior to metamorphism. B) The tie line previously between ilmenite and olivine shifts to orthopyroxene, releasing Fe as a consequence. To compensate, magnetite becomes part of the stable assemblage. B = approximate bulk composition of the symplectite; ulvöspinel has been added for reference.

The general immobility of Ti (Cann, 1970) is an important factor when considering its source. One possible solution is that the igneous olivine may have contained magmatic ilmenite inclusions. Although Fe-Ti oxides are typically late-crystallizing phases, Pang et al. (2008) reported Fe-Ti oxide inclusions within cumulus olivine in layered intrusions. In Type 1 samples, however, olivine crystallized with or before Fe-Ti oxide, as the two are either adjacent to one another or, less commonly, olivine is included within large Fe-Ti oxides.

Alternatively, Zeck et al. (1982) described orthopyroxene symplectites that formed only in olivine very near magmatic Fe-Ti oxides, suggesting that some mobility of Ti between neighbouring crystals was possible. In Type 1 olivine coronas, the orthopyroxene shell, representing the original extent of the olivine crystal, is typically within 2 mm of an igneous Fe-Ti oxide. Through thin section examination, this association was confirmed for approximately 73% of 98 orthopyroxene + ilmenite symplectite pseudomorphs. As thin sections provide information only about a 2D plane through a rock, this implies that for a single symplectite cut on a single plane, there is a 73% chance that a Fe-Ti oxide is less than 2 mm away from the olivine pseudomorph. A symplectite can be cut on a large number of planes, each with a 73% chance of revealing a nearby Fe-Ti oxide. The probability that an oxide is present on at least one plane is very high; if only five planes are considered, the chance becomes 99.9%. Therefore, every orthopyroxene + ilmenite + magnetite symplectite in Type 1 samples most likely formed within 2 mm of a magmatic Fe-Ti oxide. If Ti were released from ilmenite by reaction or interaction with a fluid, mobility on the millimeter scale would have been sufficient for it to reach olivine.

In reflected light and BSE images, magmatic ilmenite crystals in Emsdale metagabbro show evidence of patchy replacement by magnetite with fine exsolution lamellae, probably ilmenite and spinel (Figures 3.10 and 5.5). Coexisting ilmenite and magnetite are solid solutions of ilmenite and hematite (IlmHem) and magnetite ulvöspinel (MtUsp) respectively; the proportions of these endmembers depends on the oxygen fugacity (fO_2) and temperature of the system (Spencer and Lindsley, 1981), by the reaction

$$Fe_2TiO_4\ (Usp) + Fe_2O_3\ (Hem) = FeTiO_3\ (Ilm) + Fe_3O_4\ (Mt).\ (1)$$

The variation in compositions of the coexisting solid solutions with respect to fO_2 and temperature is illustrated in Figure 5.6. As fO_2 increases at constant temperature, hematite increases in IlmHem and magnetite increases in MtUsp. Therefore, an igneous olivine + ilmenite assemblage experiencing a fO_2 increase would break down by

$$6\ Fe_2SiO_4\ (Fa) + FeTiO_3 + O_2 = 6\ FeSiO_3\ (Fs) + Fe_3O_4 + Fe_2O_3 + Fe_2TiO_4.\ (2)$$

Olivine is replaced by orthopyroxene and magnetite replaces ilmenite; ulvöspinel and hematite are also produced but remain in solid solution with magnetite and ilmenite respectively. If reactions (1) and (2) are combined, the result is

$$6\ Fe_2SiO_4 + FeTiO_3 + O_2 = 6\ FeSiO_3 + 2\ Fe_3O_4 + FeTiO_3,\ (3)$$

producing the orthopyroxene + ilmenite + magnetite symplectite assemblage. Ilmenite remains unchanged during this reaction and can be removed, leaving

$$6\ Fe_2SiO_4 + O_2 = 6\ FeSiO_3 + 2\ Fe_3O_4.\ (4)$$

Ilmenite is therefore neither gained nor lost in the overall reaction, simply transferred from the magmatic assemblage on the reactants side of (3) to the symplectite on the products side (3). The replacement of magmatic ilmenite by magnetite caused by

increased fO_2 releases ilmenite, which recrystallizes with orthopyroxene in the pseudomorph only millimeters away. This process explains both the orthopyroxene + ilmenite + magnetite pseudomorphs after olivine and the magnetite replacement after magmatic ilmenite in the Emsdale coronite. Metamorphic fluids associated with vein intrusions could have raised the fO_2 of the system, initiating reaction (2). The lack of Fe-Ti oxide vermicules in most Type 2 orthopyroxene mosaics after olivine suggests that Type 2 textures developed before the Fe-Ti oxide pseudomorph. Olivine close to veins was replaced by the orthopyroxene mosaics, whereas Fe-Ti oxide pseudomorphs formed later in drier parts of the metagabbro; ilmenite transfer was likely a relatively slow process compared to mosaic development.

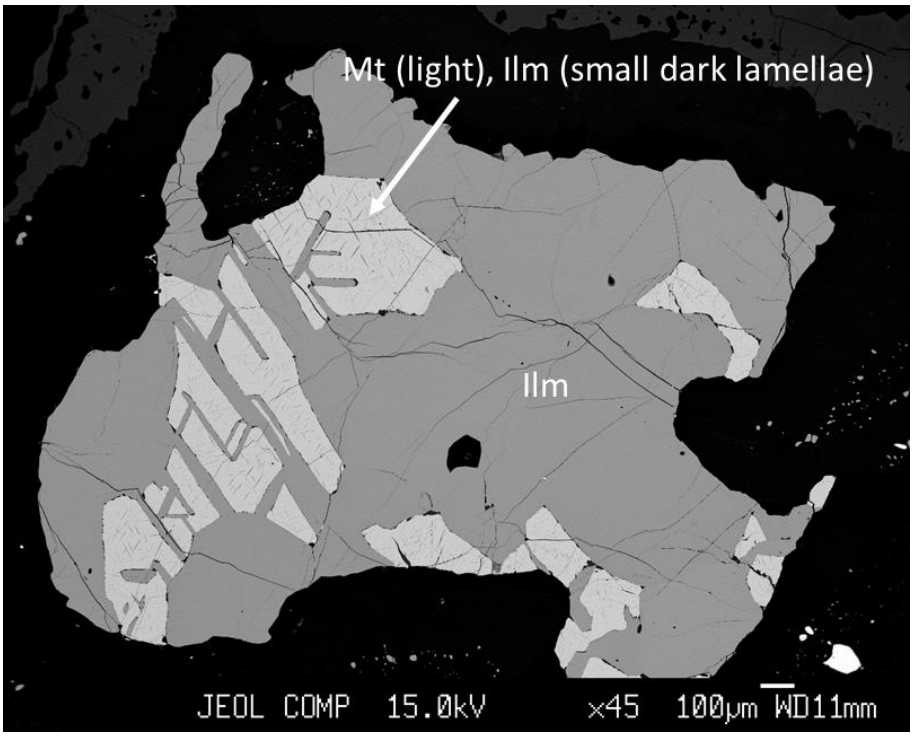

Figure 5.5: BSE image of a magmatic Fe-Ti oxide in a Type 2 sample (JKEM-14b). The darker ilmenite is replaced by patches of lighter magnetite with complex intergrowths of the two. Magnetite hosts fine, discontinuous ilmenite exsolution lamellae. Ilmenite composition is $Ilm_{93}Hem_{7}$, magnetite composition is $Mt_{99}Usp_{1}$. All coronite types have similar compositions of Fe-Ti oxides; they have likely all been reset along the retrograde path.

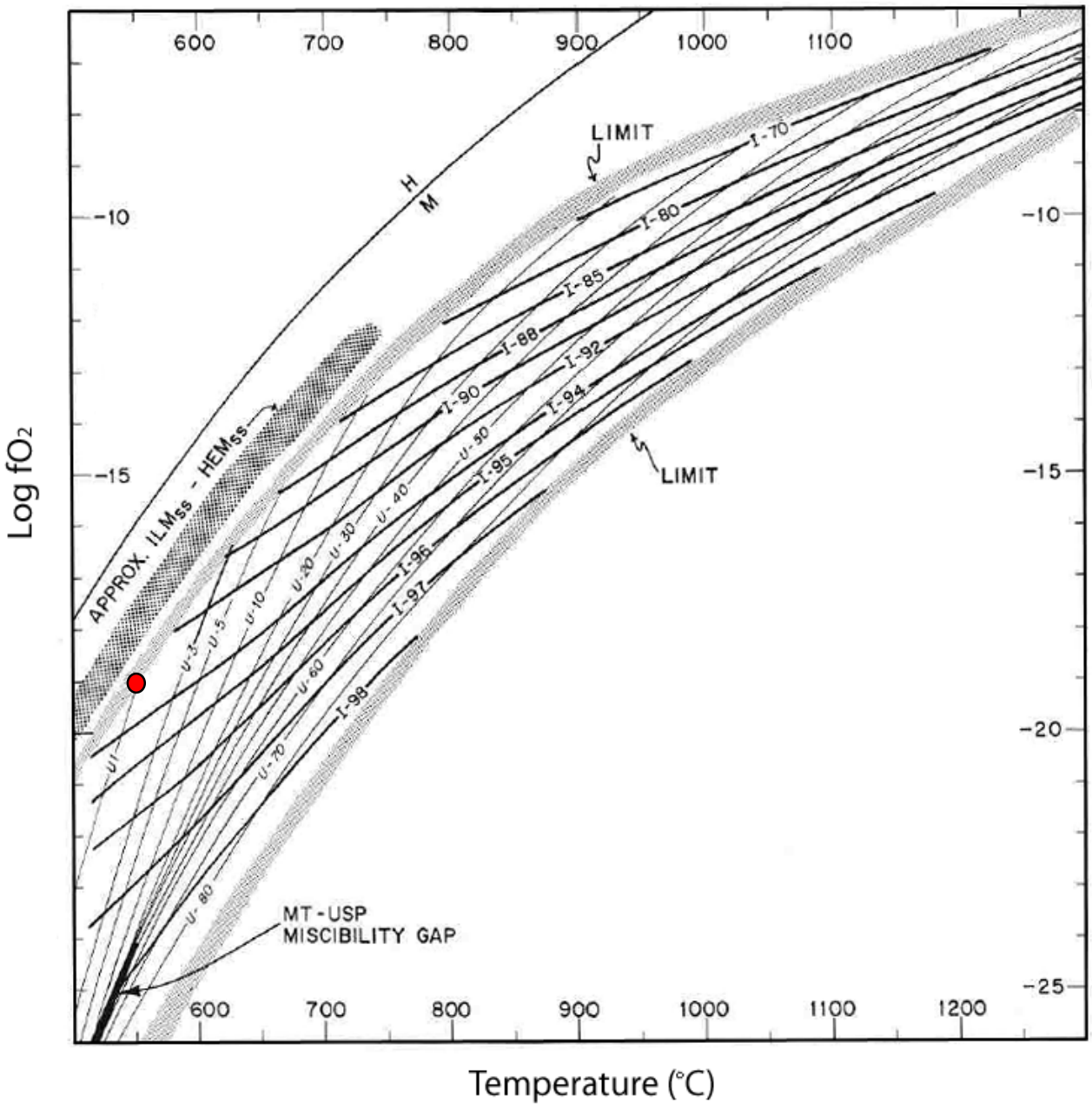

Figure 5.6: A log fO_2 vs. temperature plot with ulvöspinel-magnetite (U) and ilmenite-hematite (I) isopleths (Spencer and Lindsley, 1981). As log fO_2 increases, the ulvöspinel component of MtUsp and the ilmenite component of IlmHem decrease in favour of the oxidized phases magnetite and hematite. The composition of the Fe-Ti oxides in Figure 5.5 is plotted on the graph in red; the corresponding low temperature indicates retrograde conditions.

5.5.3 “Iddingsite”

“Iddingsite” pseudomorphs likely represent olivine crystals that were shielded from igneous Fe-Ti oxides by other phases, and thus could not be infiltrated by mobilized ilmenite. Examples of this pseudomorph are never adjacent to oxides in the plane of the thin section. In one section, “iddingsite” aggregates are nearly entirely included within relict clinopyroxene, which would likely provide sufficient 3D shielding. The pseudomorph is more common in cumulate thin sections, where the abundant olivine and clinopyroxene may have separated many olivine crystals from magmatic Fe-Ti oxides. The brilliant red-orange colour of the “iddingsite” may indicate the presence of hematite, perhaps formed by oxidation of Fe released by olivine in response to elevated fO_2 during metamorphism (Goff, 1996). Whether the “iddingsite” is a single phase or a homogeneous aggregate of very finely intergrown alteration products remains unknown. Given the near complete lack of literature about iddingsite in metaplutonic settings, further work is required to explain its presence in the Emsdale coronite.

5.6 Summary

The Emsdale coronite preserves a large portion of its metamorphic history in a single outcrop. Figure 5.7 summarizes the multistage textural evolution of the metagabbro, incorporating stages inferred from sample G86-12 and Grant (1987, 1988) with those observed in Types 1, 2, and 3. Corona-forming reactions were diffusion-driven and were likely similar to those proposed by Grant (1988). Grant suggested that these reactions began after crystallization of the protolith but before metamorphism, which is not true of the Emsdale coronite. Corona formation was initiated by prograde

metamorphism and the entire body likely reached the stage preserved in Type 1. Near peak metamorphism, veins were intruded into the metagabbro and textural reworking commenced in the adjacent rock. Metagabbro not affected by veins, including Type 1 samples, retained its igneous texture and preserve little development beyond the prograde path. Grain boundary diffusion of fluids, however, increased fO_2 sufficiently in Type 1 to form pseudomorphs after olivine by the processes described in section 5.5; clinopyroxene was replaced by amphibole during retrogression. In metagabbro near veins, including Types 2 and 3, igneous phases were progressively recrystallized and overprinted by metamorphic phases. Type 2 retains coronas at a more advanced stage and higher P-T conditions relative to Type 1, as reactions were facilitated by fluid influx and no longer diffusion-controlled. In samples most affected by veins, Type 3, granoblastic amphibole has proliferated and retrograde conditions were preserved as the metagabbro evolved toward amphibolite ± garnet.

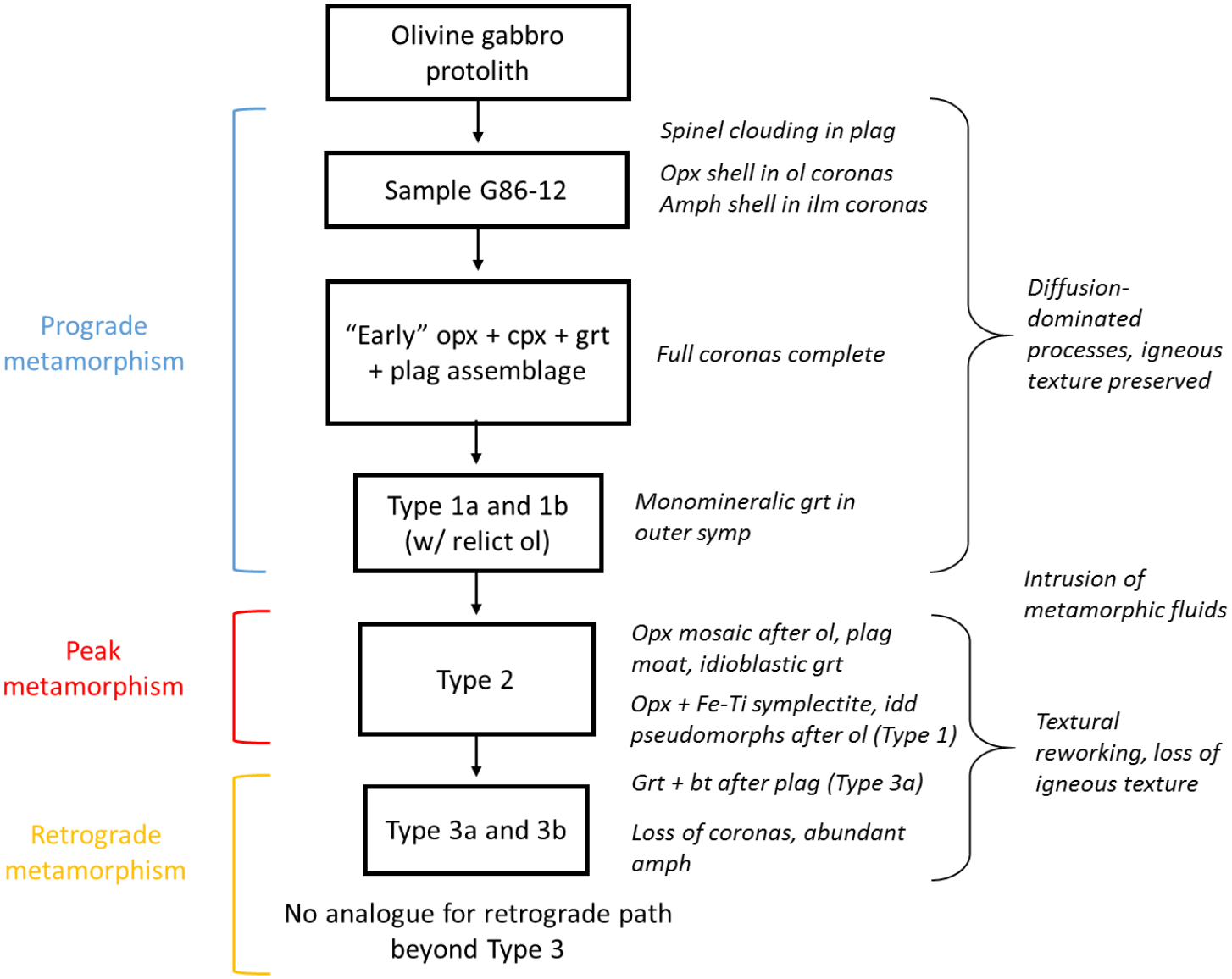

Figure 5.7: Flow chart of the inferred and observed stages of textural evolution of the Emsdale metagabbro, with their timing relative to the P-T path of metamorphism. The early prograde evolution was inferred from sample G86-12 and work by Grant (1987). Types 1 to 3 preserve textural evolution from prograde, peak, and retrograde metamorphism.

Chapter 6: Conclusions and Further Work

6.1 Conclusions

6.1.1 Significance to the Grenville Province

- A P-T path of metamorphism was constructed from a single, coherent body within the Novar subdomain that experienced the entire range of conditions suggested by this path with little to no internal deformation.
- The Ottawan Orogeny caused an increase in pressure in the Emsdale metagabbro to a peak of 13.0 ± 1.0 kb at 880 ± 70°C over a relatively small temperature range, and a subsequent decrease in pressure with minimal cooling.
- The P-T path indicates burial and exhumation deep within the thick, hot crust of the Grenville Orogen, where cooling was very slow.

6.1.2 Significance to Coronite Research

- Coronas in the Emsdale metagabbro developed during prograde metamorphism by diffusion-controlled reactions (cf. Joesten, 1986; Grant 1987).
- Injection of veins near peak metamorphism initiated a different set of reactions in the adjacent rock, causing coronas and igneous texture to be overprinted and peak metamorphic assemblages to be preserved.
- Orthopyroxene + ilmenite + magnetite symplectites after olivine formed by reactions associated with oxidation of olivine (cf. Zeck et al., 1982; van Lamoen, 1979).

6.2 Future Work

The results of this study indicate that further research is required on metamorphic fluids in the Grenville Province and pseudomorphs after olivine in high-grade metaplutonic settings. The absence of orthopyroxene + ilmenite + magnetite symplectites and iddingsite from other Algonquin metagabbros may have implications for the composition and distribution of metamorphic fluid in the region. Other coherent mafic bodies proximal to major shear zones should be examined for evidence of similar alteration. The new hypothesis for replacement of olivine by orthopyroxene + ilmenite + magnetite symplectite should be tested further in other rocks exhibiting this phenomenon. The hypothesis could be strengthened by a quantitative analysis in which the volume of magmatic ilmenite replaced by magnetite and the volume of ilmenite in an adjacent pseudomorph are calculated; in theory, these volumes should be approximately equal. In addition, further work is required to understand iddingsite pseudomorphs after olivine in metaplutonic settings. Its structure, composition, and conditions required for formation should be investigated.

References

Ashworth, J.R. 1986. The role of magmatic reaction, diffusion, and annealing in the evolution of coronitic microstructure in troctolitic gabbro from Risör, Norway: a discussion. Mineralogical Magazine, **50**: 469-473.

Asimow, P.D. and Ghiorso, M.S. 1998. Algorithmic modifications extending MELTS to calculate subsolidus phase relations. American Mineralogist, **83**: 1127-1131.

Berman, R.G. 1991. Thermobarometry using multiequilibrium calculations: A new technique, with petrological applications. The Canadian Mineralogist, **29**: 833-855.

Berman, R.G. 2007. WinTWQ (version 2.3): A software package for performing internally-consistent thermobarometric calculations. Geological Survey of Canada, Open File 5462, (ed. 2.32). doi: 10.4095/223425.

Bethune, K.M. and Davidson, A. 1997. Grenvillian metamorphism of the Sudbury diabase dyke-swarm: from protolith to two-pyroxene - garnet coronite. The Canadian Mineralogist, **35**: 1191-1220.

Blundy, J.D. and Holland T.J.B. 1990. Calcic amphibole equilibria and a new amphibole-plagioclase geothermometer. Contributions to Mineralogy and Petrology, **104**: 208-224. doi: 10.1007/BF00306444.

Bruno, M., Messiga, B., Rebay, G., and Rubbo, M. 2004. High pressure coronites in the western Alps: a record of reaction pathways. Periodico di Mineralogia, **73**: 97-107.

Cann, J.R. 1970. Rb, Sr, Y, Zr and Nb in some ocean floor basaltic rocks. Earth and Planetary Science Letters, **10**: 7-11.

Carr, S.D., Easton, R.M., Jamieson, R.A., and Culshaw, N.G. 2000. Geologic transect across the Grenville orogen of Ontario and New York. Canadian Journal of Earth Sciences, **37**(2-3): 193-216. doi:10.1139/cjes-37-2-3-193.

Claeson, D.T. 1998. Coronas, reaction rims, symplectites and emplacement depth of the Rymmen gabbro, Transscandinavian Igneous Belt, southern Sweden. Mineralogical Magazine, **62**: 743-757.

Cox R. A. and Indares A. 1999. Transformation of Fe–Ti gabbro to coronite, eclogite and amphibolite in the Baie du Nord segment, Manicouagan Imbricate Zone, eastern Grenville Province. Journal of Metamorphic Geology, **17**: 537-555. doi:10.1046/j.1525-1314.1999.00216.x

Culshaw, N.G., Davidson, A., and Nadeau, L. 1983. Structural subdivisions of the Grenville Province in the Parry Sound – Algonquin region, Ontario. *In* Current Research, Part B, Geological Survey of Canada, paper 83-1B: 243-252.

Culshaw, N.G., Jamieson, R.A., Ketchum, J.W.F., Wodicka, N., Corrigan, D. and Reynolds, P.H. 1997. Transect across the northwestern Grenville orogen, Georgian Bay, Ontario: polystage convergence and extension in the lower orogenic crust. Tectonics, **16**: 966-982. doi:10.1029/97TC02285.

Davidson, A. 1991. Metamorphism and tectonic setting of gabbroic and related rocks in the Central Gneiss Belt, Grenville Province, Ontario. Geological Association of Canada, Toronto '91 Committee, Field Trip A2: Guidebook, Sudbury, ON.

Davidson, A., and Grant, S.M. 1986. Reconnaissance geology of western and central Algonquin Park and detailed study of coronitic olivine metagabbro, central Gneiss Belt, Grenville Province of Ontario. In Current Research, Part B, Geological Survey of Canada, paper 86-1B: 837-848.

Davidson, A. and van Breemen, O. 1988. Baddeleyite-zircon relationships in coronitic metagabbro, Grenville Province, Ontario: implications for geochronology. Contributions to Mineralogy and Petrology, **100**: 291-299. doi:10.1007/BF003 79740.

Dudàs, F.Ö., Davidson, A., and Bethune, K.M., 1994. Age of the Sudbury diabase dykes and their metamorphism in the Grenville Province, Ontario. *In* Radiogenic age and isotopic studies, Report 8, Geological Survey of Canada, Paper 94-F, pp. 97-106.

Ellis, D.J., and Green, D.H. 1979. An experimental study of the effect of Ca upon garnet-clinopyroxene Fe-Mg exchange equilibria. Contributions to Mineralogy and Petrology, **71**: 13-22.

Foster, J.G.J. 2012. Tectonometamorphic evolution of the Kiosk Domain, Central Gneiss Belt, Grenville Province, Ontario: Constraints from geochronology and thermobarometry. MSc. Thesis, Department of Earth Sciences, Dalhousie University, Halifax, N.S.

Frodesen, S. 1968. Coronas around olivine in a small gabbro intrusion, Bamble Area, South Norway. Norsk Geologisk Tidsskrift, **48**: 201-206.

Gallien, F., Mogessie, A., Hauzenberger, C.A., Bjerg, E., Delpino, S., and Castro de Machuca, B. 2012. On the origin of multi-layer coronas between olivine and plagioclase at the gabbro–granulite transition, Valle Fértil–La Huerta Ranges, San Juan Province, Argentina. Journal of Metamorphic Geology, **30**: 281-301. doi:10.1111/j.1525-1314.2011.00967.x.

Ghiorso, M.S., and Sack, R.O. 1995. Chemical mass transfer in magmatic processes IV. A revised and internally consistent thermodynamic model for the interpretation and extrapolation of liquid-solid equilibria in magmatic systems at elevated temperatures and pressures. Contributions to Mineralogy and Petrology, **119**: 197-212.

Goff, F. 1996. Vesicle cylinders in vapor-differentiated basalt flows. Journal of Volcanology and Geothermal Research, **71**: 167-185.

Graham, C.M. and Powell, R. 1984. A garnet-hornblende geothermometer: calibration, testing, and application to the Pelona Schist, Southern California. Journal of Metamorphic Geology, **2**: 13-31. doi: 10.1111/j.1525-1314.1984.tb00282.x.

Grant, S.M. 1987. The petrology and structural relations of metagabbros from the western Grenville Province, Canada. Ph.D. thesis, Department of Geology, University of Leicester, Leicester, U.K.

Grant, S.M. 1988. Diffusion models for corona formation in metagabbros from the Western Grenville Province, Canada. Contributions to Mineralogy and Petrology, **98**: 49-63. doi:10.1007/BF00371909.

Heaman, L.M. and LeCheminant, A.N. 1993. Paragenesis and U-Pb systematics of baddeleyite(ZrO2). Chemical Geology, **110**: 95-129. doi: 10.1016/0009-2541(93)90249-I.

Jamieson, R.A, Beaumont, C., Nguyen, M.H., and Culshaw, N.G. 2007. Syn-convergent ductile flow in the variable-strength continental crust: numerical models with application to the western Grenville orogeny. Tectonics, **26**: TC5005,doi:10.1029/2006TC0022036.

Jamieson, R.A., Beaumont, C., Warren C.J., and Nguyen, M.H. 2010. The Grenville Orogen explained? Applications and limitations of integrating numerical models with geological and geophysical data. Canadian Journal of Earth Sciences, **47**: 517-539. doi:10.1139/E09-070.

Joesten, R. 1986. The role of magmatic reaction, diffusion and annealing in the evolution of coronitic microstructure in troctolitic gabbro from Risör, Norway. Mineralogical Magazine, **50**: 441-467. doi:10.1180/minmag.1986.050.357.08.

Johnson, C.D. and Carlson, W.D. 1990. The origin of olivine-plagioclase coronas in metagabbros from the Adirondack Mountains, New York. Journal of Metamorphic Geology, **8**: 697-717. doi:10.1111/j.1525-1314.1990.tb00496.x.

Kendrick, J.L. 2014. An assessment of the origin of Algonquin metagabbro using melt fractionation modelling and minor and trace element comparisons. Unpublished class project, ERTH 4510, Dalhousie University.

Ketchum, J.W.F. and Davidson, A. 2000. Crustal architecture and tectonic assembly of the Central Gneiss Belt, southwestern Grenville Province, Canada: a new interpretation. Canadian Journal of Earth Sciences, **37**: 217-234. doi:10.1139/e98-099.

Kohn, M.J. and Spear, F.S. 1990. Two new geobarometers for garnet amphibolites, with applications to southeastern Vermont. American Mineralogist, **75**: 89-96.

van Lamoen, H. 1979. Coronas in olivine gabbros and iron ores from Susimäki and Riuttamaa, Finland. Contributions to Mineralogy and Petrology, **68**: 259-268.

Leake, B.E., Woolley, A.R., Arps, C.E.S., Birch, W.D., Gilbert, M.C., Grice, J.D., Hawthorne, F.C., Kato, A., Kisch, H.J., Krivovichev, V.G., Linthout, K., Laird, J., Mandarino, J.A., Maresch, W.V., Nickel, E.H., Rock, N.M.S., Schumacher, J.C., Smith, D.C., Stephenson, N.C.N., Ungaretti, L., Whittaker, E.J.W., and Youzhi, G. 1997. Nomenclature of amphiboles: Report of the Subcommittee on Amphiboles of the International Mineralogical Association, Commission on New Minerals and Mineral Names. American Mineralogist, **82**: 1019–1037.

Marsh, J.H. and Culshaw, N.G. 2014. Timing and conditions of high-pressure metamorphism in the western Grenville Province: Constraints from accessory mineral composition and phase equilibrium modeling. Lithos, **200-201**: 402-417. doi:10.1016/j.lithos.2014.04.016.

McLelland J.M and Whitney, P.R. 1980. Compositional controls on spinel clouding and garnet formation in plagioclase of olivine metagabbros, Adirondack Mountains, New York. Contributions to Mineralogy and Petrology, **73**: 243-251.

Murthy, M.V.N. 1958. Coronites from India and their bearing on the origin of coronas. Bulletin of the Geological Society of America, **68**: 23-38.

Nadeau, L. 1990. Tectonic, thermal and magmatic evolution of the Central Gneiss Belt, Hunsville region, southwestern Grenville orogeny. Ph.D. thesis, Carelton University, Ottawa, Ont.

Pang, K.N., Li, C., Zhou, M.F. and Ripley, E.M. 2008. Abundant Fe–Ti oxide inclusions in olivine from the Panzhihua and Hongge layered intrusions, SW China: evidence for early saturation of Fe–Ti oxides in ferrobasaltic magma. Contributions to Mineralogy and Petrology, **156**: 307-321. doi: 10.1007/s00410-008-0287-z.

Powell, R. and Holland T. 1994. Optimal geothermometry and geobarometry. American Mineralogist, **79**: 120-133.

Powell, R. and Holland, T.J.B. 2008. On thermobarometry. Journal of Metamorphic

Geology, **26**: 155-179. doi:10.1111/j.1525-1314.2007.00756.x.

Ravna, E. K. 2000a. Distribution of Fe^{2+} and Mg between coexisting garnet and hornblende in synthetic and natural systems: An empirical calibration of the garnet–hornblende Fe–Mg geothermometer. Lithos, **53**: 265-277. doi:10.1016/S0024-4937(00)00029-3.

Ravna, E. K. 2000b. The garnet–clinopyroxene Fe^{2+}–Mg geothermometer: an updated calibration. Journal of Metamorphic Geology, **18**: 211-219. doi: 10.1046/j.1525-1314.2000.00247.x.

Rivers, T. 1997. Lithotectonic elements of the Grenville Province: review and tectonic implications. Precambrian Research, **86**: 117-154. doi: 10.1016/S0301-9268(97)00038-7.

Rivers, T., Culshaw, N., Hynes, A., Indares, A., Jamieson, R. A., and Martignole, J. 2012. The Grenville Orogen – A post Lithoprobe perspective. *In* Tectonic Styles in Canada: The Lithoprobe Perspective. *Edited* by J.A. Percival, F.A. Cook, and R.M. Clowes. Geological Society of Canada Special Paper, 49: 97-236.

Rivers, T., Ketchum, J., Indares, A., and Hynes, A. 2002. The High Pressure belt in the Grenville Province: architecture, timing, and exhumation. Canadian Journal of Earth Sciences, **39**: 867-893. doi:10.1139/E02-025.

Rivers T., Martignole, J., Gower, C.F., and Davidson, A. 1989. New tectonic divisions of the Grenville Province, southeast Candian Shield. Tectonics, **8**: 63-84. doi:10.1029/ TC008i001p00063.

Sapountzis, E.S. 1975. Coronas from the Thessaloniki gabbros (North Greece). Contributions to Mineralogy and Petrology, **51**: 197-203. doi:10.1007/BF00372079.

Spear, F.S. 1993. Metamorphic phase equilibria and pressure-temperature-time paths. Mineralogical Society of America, Washington, D.C.

Spencer, K.J and Lindsley, D.H. 1981. A solution model for coexisting iron-titanium oxides. American Mineralogist, **66**: 1189-1201.

Timmermann, H. 1998. Geology, metamorphism, and U-Pt geochronology in the Central Geniss Belt between Huntsville and Haliburton, southwestern Grenville Province, Ontario. Ph.D. thesis, Department of Earth Sciences, Dalhousie University, Halifax, N.S.

Wells, P.R.A. 1977. Pyroxene thermometry in simple and complex systems. Contributions to Mineralogy and Petrology, **62**: 129-139.

Wynne-Edwards, H.R. 1972. The Grenville Province. *In* Variations in Tectonic Styles in Canada. *Edited* by R. A. Price and R. J. W. Douglas. Geological Association of Canada, Special Paper 11, St. John's, NL. pp. 263-334.

Zeck, H.P., Shenouda, H.H., Rønsbo, J.G., and Poorter, R.P.E. 1982. Hypersthene-ilmenite(/magnetite) symplectites in coronitic olivine-gabbronorites. Lithos, **15**: 173-182.

Appendix

Appendix A: EMP analyses

Note:

- cal = calcite, zrn = zircon, bdd = baddeleyite, pyrr = pyrrhotite unk = unknown, (inf) = inferred
- JKEM-12, 14a, 15a = Type 1a, JKEM-01, 02 = Type 1b, JKEM-14b, 15b = Type 2, JKEM-10 = Type 3a
- Zr was not analyzed in samples JKEM-12 and JKEM-14a.

Sample	JKEM-12	JKEM-12	JKEM-12	JKEM-12	JKEM-12	JKEM-12	JKEM-12	JKEM-12	JKEM-12	JKEM-12	JKEM-12	JKEM-12	JKEM-12
Mineral	opx	opx	opx	opx	opx	opx	opx	opx	opx	opx	opx	opx	opx
No.	145	146	157	158	159	160	161	166	167	169	171	172	174
Weight %													
SiO2	52.09	52.52	51.64	51.80	51.37	51.53	51.58	51.34	51.40	51.36	51.29	51.44	51.23
TiO2	0.09	0.06	0.03	0.03	0.02	0.01	0.04	0.07	0.06	0.00	0.00	0.00	0.00
Al2O3	0.50	0.42	0.65	0.58	0.62	0.57	0.49	0.71	0.68	0.56	0.61	0.63	0.76
Cr2O3	0.06	0.06	0.03	0.02	0.02	0.03	0.00	0.00	0.00	0.00	0.00	0.00	0.00
FeO	28.73	28.87	31.64	31.79	31.70	31.74	31.93	32.11	32.27	32.27	32.28	32.19	32.53
MnO	0.36	0.39	0.43	0.40	0.44	0.46	0.43	0.41	0.41	0.39	0.36	0.39	0.41
MgO	18.83	18.95	16.44	16.29	16.41	16.34	16.47	16.04	16.20	16.23	15.93	16.10	15.92
CaO	0.36	0.36	0.39	0.47	0.48	0.42	0.46	0.30	0.31	0.33	0.29	0.30	0.32
Na2O	0.03	0.01	0.01	0.01	0.01	0.00	0.00	0.00	0.00	0.00	0.00	0.00	0.00
K2O	0.03	0.03	0.02	0.01	0.02	0.02	0.00	0.00	0.00	0.01	0.01	0.01	0.00
ZrO2	0.00	0.00	0.00	0.00	0.00	0.00	0.00	0.00	0.00	0.00	0.00	0.00	0.00
Total	101.07	101.67	101.27	101.41	101.09	101.13	101.39	100.97	101.33	101.14	100.77	101.06	101.17
No.	145	146	157	158	159	160	161	166	167	169	171	172	174
Cations, O = 6													
Si	1.977	1.981	1.983	1.987	1.979	1.984	1.981	1.981	1.978	1.981	1.985	1.984	1.978
Ti	0.002	0.002	0.001	0.001	0.001	0.001	0.001	0.002	0.002	0.000	0.000	0.000	0.000
Al	0.022	0.019	0.029	0.026	0.028	0.026	0.022	0.032	0.031	0.025	0.028	0.029	0.034
Cr	0.002	0.002	0.001	0.001	0.001	0.001	0.000	0.000	0.000	0.000	0.000	0.000	0.000
Fe	0.912	0.911	1.016	1.020	1.021	1.022	1.026	1.037	1.039	1.041	1.045	1.038	1.050
Mn	0.011	0.013	0.014	0.013	0.014	0.015	0.014	0.013	0.013	0.013	0.012	0.013	0.013
Mg	1.065	1.066	0.941	0.931	0.942	0.938	0.943	0.923	0.929	0.934	0.919	0.926	0.916
Ca	0.015	0.014	0.016	0.019	0.020	0.017	0.019	0.013	0.013	0.014	0.012	0.013	0.013
Na	0.002	0.001	0.001	0.001	0.001	0.000	0.000	0.000	0.000	0.000	0.000	0.000	0.000
K	0.001	0.001	0.001	0.001	0.001	0.001	0.000	0.000	0.000	0.000	0.001	0.001	0.000
Zr	0.000	0.000	0.000	0.000	0.000	0.000	0.000	0.000	0.000	0.000	0.000	0.000	0.000
Total	4.010	4.009	4.003	4.000	4.007	4.005	4.007	4.001	4.006	4.007	4.001	4.002	4.005

Sample	JKEM-12	JKEM-12	JKEM-12	JKEM-12	JKEM-12	JKEM-12	JKEM-12	JKEM-12	JKEM-12	JKEM-14a	JKEM-14a	JKEM-14a	JKEM-14a
Mineral	opx	opx	opx	opx	opx	opx	opx	opx	opx	opx	opx	opx	opx
No.	176	180	189	229	230	231	236	237	260	328	329	330	331
Weight %													
SiO2	51.06	51.25	51.86	51.42	51.60	51.22	50.18	51.32	51.08	51.08	51.72	51.09	52.08
TiO2	0.00	0.00	0.00	0.00	0.00	0.07	0.36	0.08	0.19	0.09	0.05	0.01	0.02
Al2O3	0.77	0.73	0.43	0.71	0.41	0.61	0.51	0.54	0.79	0.53	0.46	0.78	0.54
Cr2O3	0.00	0.00	0.00	0.01	0.00	0.00	0.03	0.00	0.00	0.02	0.04	0.00	0.00
FeO	32.37	31.95	29.90	31.81	32.05	32.03	33.06	32.14	32.06	33.21	31.87	31.73	31.40
MnO	0.40	0.36	0.36	0.41	0.43	0.47	0.46	0.46	0.45	0.52	0.50	0.51	0.43
MgO	15.90	15.85	17.92	16.29	16.41	15.97	16.04	16.30	15.96	14.79	15.82	15.75	16.41
CaO	0.29	0.29	0.40	0.40	0.39	0.37	0.33	0.37	0.32	0.52	0.41	0.45	0.41
Na2O	0.00	0.00	0.00	0.01	0.01	0.00	0.02	0.00	0.01	0.00	0.00	0.02	0.03
K2O	0.01	0.02	0.01	0.00	0.01	0.02	0.03	0.02	0.02	0.01	0.02	0.03	0.03
ZrO2	0.00	0.00	0.00	0.00	0.00	0.00	0.00	0.00	0.00	0.00	0.00	0.00	0.00
Total	100.79	100.45	100.89	101.05	101.30	100.76	101.02	101.23	100.87	100.78	100.90	100.38	101.33
No.	176	180	189	229	230	231	236	237	260	328	329	330	331
Cations, O = 6													
Si	1.978	1.987	1.982	1.981	1.985	1.982	1.953	1.978	1.975	1.989	1.996	1.984	1.994
Ti	0.000	0.000	0.000	0.000	0.000	0.002	0.011	0.002	0.005	0.003	0.002	0.001	0.001
Al	0.035	0.034	0.019	0.032	0.019	0.028	0.023	0.025	0.036	0.024	0.021	0.036	0.024
Cr	0.000	0.000	0.000	0.000	0.000	0.000	0.001	0.000	0.000	0.001	0.001	0.000	0.000
Fe	1.049	1.036	0.956	1.025	1.031	1.037	1.076	1.036	1.037	1.082	1.028	1.030	1.006
Mn	0.013	0.012	0.012	0.013	0.014	0.016	0.015	0.015	0.015	0.017	0.016	0.017	0.014
Mg	0.918	0.916	1.021	0.935	0.941	0.922	0.930	0.936	0.920	0.859	0.910	0.911	0.937
Ca	0.012	0.012	0.016	0.016	0.016	0.016	0.014	0.016	0.013	0.022	0.017	0.019	0.017
Na	0.000	0.000	0.000	0.001	0.001	0.000	0.001	0.000	0.001	0.000	0.000	0.001	0.002
K	0.001	0.001	0.001	0.000	0.001	0.001	0.001	0.001	0.001	0.001	0.001	0.002	0.002
Zr	0.000	0.000	0.000	0.000	0.000	0.000	0.000	0.000	0.000	0.000	0.000	0.000	0.000
Total	4.006	3.998	4.007	4.003	4.007	4.003	4.025	4.008	4.003	3.997	3.992	4.001	3.996

Sample	JKEM-14a	JKEM-14a	JKEM-14a	JKEM-14a	JKEM-14a	JKEM-15a	JKEM-15a	JKEM-15a	JKEM-15a	JKEM-15a	JKEM-15a	JKEM-15a	JKEM-15a
Mineral	opx	opx	opx	opx	opx	opx	opx	opx	opx	opx	opx	opx	opx
No.	333	334	369	370	371	27	28	31	32	33	66	84	94
Weight %													
SiO2	51.29	51.52	52.05	51.84	51.90	51.92	52.10	51.60	52.04	52.10	52.26	51.29	51.96
TiO2	0.06	0.07	0.06	0.02	0.01	0.10	0.07	0.06	0.07	0.08	0.00	0.00	0.09
Al2O3	0.44	0.50	0.65	0.52	0.51	0.34	0.41	0.52	0.39	0.43	0.56	0.74	0.54
Cr2O3	0.00	0.00	0.01	0.00	0.00	0.00	0.02	0.02	0.00	0.01	0.05	0.00	0.08
FeO	33.97	33.16	31.92	31.50	31.47	30.59	30.89	30.69	31.16	31.02	27.55	30.61	29.39
MnO	0.55	0.56	0.41	0.44	0.43	0.47	0.51	0.49	0.52	0.47	0.33	0.34	0.41
MgO	14.35	15.10	16.19	16.33	16.42	16.82	16.76	16.53	16.71	16.77	18.92	16.74	17.98
CaO	0.53	0.47	0.46	0.45	0.49	0.32	0.38	0.48	0.43	0.47	0.31	0.33	0.30
Na2O	0.03	0.02	0.02	0.02	0.03	0.01	0.02	0.02	0.02	0.03	0.00	0.01	0.03
K2O	0.03	0.04	0.02	0.02	0.01	0.03	0.03	0.02	0.03	0.03	0.01	0.00	0.05
ZrO2	0.00	0.00	0.00	0.00	0.00	0.00	0.00	0.00	0.03	0.01	0.00	0.00	0.01
Total	101.25	101.43	101.78	101.16	101.28	100.61	101.19	100.42	101.40	101.41	99.98	100.05	100.84
No.	333	334	369	370	371	27	28	31	32	33	66	84	94
Cations, O = 6													
Si	1.994	1.991	1.988	1.991	1.990	1.997	1.994	1.991	1.991	1.991	1.992	1.984	1.983
Ti	0.002	0.002	0.002	0.001	0.001	0.003	0.002	0.002	0.002	0.002	0.000	0.000	0.002
Al	0.020	0.023	0.029	0.024	0.023	0.016	0.019	0.023	0.017	0.020	0.025	0.034	0.024
Cr	0.000	0.000	0.000	0.000	0.000	0.000	0.001	0.001	0.000	0.001	0.001	0.000	0.002
Fe	1.105	1.072	1.020	1.012	1.009	0.984	0.989	0.991	0.997	0.992	0.878	0.991	0.938
Mn	0.018	0.018	0.013	0.014	0.014	0.015	0.017	0.016	0.017	0.016	0.010	0.011	0.013
Mg	0.832	0.870	0.922	0.935	0.939	0.964	0.956	0.951	0.953	0.955	1.075	0.965	1.023
Ca	0.022	0.019	0.019	0.019	0.020	0.013	0.016	0.020	0.018	0.019	0.013	0.013	0.013
Na	0.002	0.001	0.001	0.002	0.002	0.001	0.001	0.001	0.001	0.002	0.000	0.001	0.002
K	0.001	0.002	0.001	0.001	0.001	0.002	0.001	0.001	0.001	0.001	0.001	0.000	0.002
Zr	0.000	0.000	0.000	0.000	0.000	0.000	0.000	0.000	0.001	0.000	0.000	0.000	0.000
Total	3.995	3.997	3.996	3.999	3.999	3.994	3.995	3.997	3.999	4.000	3.995	3.999	4.004

Sample	JKEM-15a	JKEM-15a	JKEM-15a	JKEM-01	JKEM-01	JKEM-01	JKEM-01	JKEM-01	JKEM-01	JKEM-01	JKEM-01	JKEM-01	JKEM-01
Mineral	opx	opx	opx	opx	opx	opx	opx	opx	opx	opx	opx	opx	opx
No.	113	115	118	34	35	36	41	42	43	47	48	54	55
Weight %													
SiO2	52.48	52.05	51.46	51.76	51.59	51.66	51.05	51.45	51.26	51.13	51.16	51.09	51.43
TiO2	0.05	0.07	0.08	0.00	0.02	0.00	0.05	0.10	0.05	0.06	0.12	0.11	0.02
Al2O3	0.48	0.66	0.48	0.32	0.37	0.40	0.49	0.57	0.50	0.46	0.49	1.01	0.58
Cr2O3	0.04	0.07	0.05	0.00	0.00	0.02	0.06	0.05	0.06	0.02	0.07	0.05	0.05
FeO	30.02	30.18	29.91	31.73	31.72	31.62	33.43	33.19	33.27	33.44	33.27	32.93	32.74
MnO	0.38	0.42	0.37	0.48	0.57	0.47	0.57	0.57	0.57	0.56	0.58	0.55	0.54
MgO	17.26	17.17	17.24	16.41	16.31	16.35	14.61	14.66	14.59	14.61	14.65	15.13	15.06
CaO	0.35	0.45	1.03	0.45	0.53	0.47	0.52	0.50	0.51	0.50	0.56	0.43	0.59
Na2O	0.04	0.05	0.05	0.04	0.02	0.02	0.02	0.02	0.02	0.04	0.03	0.03	0.03
K2O	0.02	0.02	0.02	0.03	0.03	0.04	0.02	0.03	0.03	0.04	0.04	0.03	0.03
ZrO2	0.00	0.00	0.05	0.00	0.02	0.04	0.04	0.01	0.01	0.02	0.04	0.04	0.06
Total	101.12	101.13	100.74	101.22	101.17	101.08	100.86	101.15	100.86	100.86	100.99	101.39	101.13
No.	113	115	118	34	35	36	41	42	43	47	48	54	55
Cations, O = 6													
Si	1.999	1.987	1.977	1.990	1.987	1.989	1.990	1.994	1.994	1.992	1.990	1.974	1.991
Ti	0.001	0.002	0.002	0.000	0.001	0.000	0.002	0.003	0.001	0.002	0.004	0.003	0.001
Al	0.022	0.029	0.022	0.014	0.017	0.018	0.022	0.026	0.023	0.021	0.022	0.046	0.026
Cr	0.001	0.002	0.002	0.000	0.000	0.001	0.002	0.001	0.002	0.001	0.002	0.001	0.002
Fe	0.956	0.964	0.961	1.021	1.021	1.018	1.090	1.076	1.083	1.090	1.082	1.064	1.060
Mn	0.012	0.014	0.012	0.016	0.019	0.016	0.019	0.019	0.019	0.019	0.019	0.018	0.018
Mg	0.980	0.977	0.987	0.940	0.936	0.938	0.849	0.847	0.847	0.848	0.849	0.871	0.869
Ca	0.014	0.018	0.043	0.019	0.022	0.020	0.022	0.020	0.021	0.021	0.023	0.018	0.025
Na	0.003	0.004	0.004	0.003	0.001	0.001	0.002	0.001	0.002	0.003	0.002	0.002	0.002
K	0.001	0.001	0.001	0.002	0.001	0.002	0.001	0.002	0.002	0.002	0.002	0.001	0.002
Zr	0.000	0.000	0.001	0.000	0.001	0.001	0.001	0.000	0.000	0.001	0.001	0.001	0.001
Total	3.991	3.997	4.012	4.005	4.005	4.003	3.998	3.990	3.993	3.999	3.995	4.000	3.997

Sample	JKEM-01	JKEM-01	JKEM-01	JKEM-01	JKEM-01	JKEM-01	JKEM-01	JKEM-01	JKEM-01	JKEM-01	JKEM-01	JKEM-01	JKEM-01
Mineral	opx	opx	opx	opx	opx	opx	opx	opx	opx	opx	opx	opx	opx
No.	56	57	58	59	60	61	62	63	64	65	84	85	86
Weight %													
SiO2	51.33	51.29	51.33	51.62	51.17	51.60	51.66	51.46	51.61	51.34	51.44	51.54	51.75
TiO2	0.05	0.04	0.02	0.03	0.03	0.04	0.01	0.03	0.04	0.11	0.00	0.03	0.03
Al2O3	0.65	0.54	0.51	0.63	0.64	0.72	0.57	0.64	0.62	0.61	0.28	0.41	0.30
Cr2O3	0.04	0.07	0.07	0.06	0.00	0.01	0.00	0.00	0.00	0.00	0.00	0.00	0.00
FeO	33.12	32.92	32.95	32.86	32.98	32.94	33.11	33.00	32.73	32.47	32.51	32.52	32.49
MnO	0.55	0.56	0.51	0.53	0.55	0.51	0.54	0.51	0.48	0.49	0.45	0.49	0.46
MgO	15.16	15.17	15.31	15.20	15.19	15.04	15.15	15.09	15.37	15.23	15.55	15.45	15.64
CaO	0.52	0.59	0.54	0.50	0.51	0.54	0.52	0.51	0.45	0.52	0.36	0.43	0.44
Na2O	0.02	0.04	0.03	0.02	0.01	0.02	0.02	0.00	0.01	0.01	0.01	0.02	0.01
K2O	0.02	0.01	0.01	0.02	0.02	0.02	0.04	0.02	0.05	0.05	0.05	0.04	0.03
ZrO2	0.01	0.00	0.01	0.05	0.00	0.00	0.00	0.00	0.00	0.00	0.01	0.00	0.00
Total	101.48	101.23	101.29	101.52	101.09	101.43	101.60	101.26	101.36	100.82	100.66	100.93	101.14
No.	56	57	58	59	60	61	62	63	64	65	84	85	86
Cations, O = 6													
Si	1.984	1.986	1.986	1.990	1.984	1.990	1.991	1.990	1.990	1.990	1.997	1.995	1.997
Ti	0.001	0.001	0.001	0.001	0.001	0.001	0.000	0.001	0.001	0.003	0.000	0.001	0.001
Al	0.029	0.025	0.023	0.029	0.029	0.033	0.026	0.029	0.028	0.028	0.013	0.019	0.014
Cr	0.001	0.002	0.002	0.002	0.000	0.000	0.000	0.000	0.000	0.000	0.000	0.000	0.000
Fe	1.070	1.066	1.066	1.059	1.069	1.063	1.067	1.067	1.055	1.052	1.055	1.052	1.049
Mn	0.018	0.018	0.017	0.017	0.018	0.017	0.018	0.017	0.016	0.016	0.015	0.016	0.015
Mg	0.873	0.875	0.883	0.873	0.878	0.865	0.870	0.869	0.883	0.880	0.899	0.892	0.899
Ca	0.022	0.025	0.022	0.020	0.021	0.022	0.022	0.021	0.019	0.022	0.015	0.018	0.018
Na	0.001	0.003	0.002	0.001	0.001	0.002	0.001	0.000	0.001	0.001	0.001	0.002	0.001
K	0.001	0.001	0.001	0.001	0.001	0.001	0.002	0.001	0.002	0.002	0.002	0.002	0.002
Zr	0.000	0.000	0.000	0.001	0.000	0.000	0.000	0.000	0.000	0.000	0.000	0.000	0.000
Total	4.001	4.001	4.003	3.995	4.002	3.994	3.997	3.995	3.996	3.996	3.998	3.997	3.996

Sample	JKEM-01	JKEM-01	JKEM-01	JKEM-01	JKEM-02	JKEM-02	JKEM-02	JKEM-14b	JKEM-14b	JKEM-14b	JKEM-14b	JKEM-14b	JKEM-14b
Mineral	opx	opx	opx	opx	opx	opx	opx	opx	opx	opx	opx	opx	opx
No.	87	88	89	96	181	224	225	49	50	52	66	67	68
Weight %													
SiO2	51.77	51.75	51.64	51.33	50.41	50.53	50.61	52.83	52.02	52.11	51.59	51.37	51.66
TiO2	0.00	0.00	0.03	0.02	0.00	0.08	0.05	0.02	0.03	0.02	0.06	0.00	0.05
Al2O3	0.40	0.41	0.49	0.62	0.54	0.51	0.55	0.77	0.83	1.01	0.97	0.90	0.89
Cr2O3	0.00	0.00	0.00	0.00	0.00	0.04	0.04	0.05	0.09	0.03	0.00	0.00	0.01
FeO	32.47	32.60	32.99	32.72	35.77	35.66	35.68	25.25	25.92	26.77	28.09	28.19	28.63
MnO	0.48	0.48	0.48	0.48	0.69	0.74	0.77	0.28	0.30	0.32	0.31	0.35	0.33
MgO	15.57	15.69	15.30	15.23	13.14	13.21	13.11	21.42	20.81	20.31	19.02	18.99	18.87
CaO	0.42	0.45	0.43	0.50	0.49	0.55	0.51	0.25	0.24	0.26	0.27	0.27	0.24
Na2O	0.01	0.03	0.02	0.02	0.00	0.01	0.01	0.00	0.00	0.00	0.00	0.02	0.00
K2O	0.03	0.01	0.04	0.03	0.01	0.01	0.02	0.03	0.02	0.03	0.04	0.03	0.04
ZrO2	0.01	0.02	0.02	0.01	0.00	0.01	0.05	0.05	0.07	0.03	0.02	0.00	0.01
Total	101.16	101.44	101.44	100.95	101.04	101.36	101.38	100.93	100.32	100.88	100.37	100.12	100.73
No.	87	88	89	96	181	224	225	49	50	52	66	67	68
Cations, O = 6													
Si	1.997	1.993	1.993	1.989	1.985	1.983	1.985	1.972	1.964	1.963	1.966	1.965	1.966
Ti	0.000	0.000	0.001	0.001	0.000	0.002	0.001	0.001	0.001	0.001	0.002	0.000	0.001
Al	0.018	0.019	0.022	0.028	0.025	0.023	0.025	0.034	0.037	0.045	0.044	0.041	0.040
Cr	0.000	0.000	0.000	0.000	0.000	0.001	0.001	0.001	0.002	0.001	0.000	0.000	0.000
Fe	1.048	1.050	1.064	1.061	1.178	1.171	1.171	0.788	0.818	0.843	0.895	0.902	0.911
Mn	0.016	0.016	0.016	0.016	0.023	0.025	0.025	0.009	0.010	0.010	0.010	0.011	0.011
Mg	0.895	0.901	0.880	0.880	0.771	0.773	0.766	1.192	1.171	1.140	1.081	1.083	1.071
Ca	0.017	0.019	0.018	0.021	0.021	0.023	0.022	0.010	0.010	0.010	0.011	0.011	0.010
Na	0.001	0.002	0.001	0.001	0.000	0.001	0.001	0.000	0.000	0.000	0.000	0.001	0.000
K	0.002	0.001	0.002	0.001	0.001	0.001	0.001	0.001	0.001	0.001	0.002	0.001	0.002
Zr	0.000	0.001	0.001	0.000	0.000	0.000	0.001	0.001	0.001	0.001	0.001	0.000	0.000
Total	3.994	4.000	3.998	3.997	4.003	4.003	3.999	4.009	4.015	4.015	4.012	4.016	4.012

Sample	JKEM-14b	JKEM-14b	JKEM-14b	JKEM-14b	JKEM-14b	JKEM-14b	JKEM-14b	JKEM-15b	JKEM-15b	JKEM-15b	JKEM-15b	JKEM-15b	JKEM-15b
Mineral	opx	opx	opx	opx	opx	opx	opx	opx	opx	opx	opx	opx	opx
No.	69	70	71	73	74	137	138	247	248	249	250	251	252
Weight %													
SiO2	51.83	51.48	51.71	51.71	51.75	51.81	51.78	51.16	51.44	52.10	51.99	51.63	51.73
TiO2	0.01	0.05	0.04	0.04	0.04	0.05	0.07	0.05	0.04	0.04	0.05	0.06	0.04
Al2O3	0.74	0.83	0.84	0.73	0.65	0.35	0.39	0.70	0.80	0.56	0.56	0.69	0.70
Cr2O3	0.02	0.01	0.01	0.03	0.02	0.00	0.00	0.04	0.01	0.00	0.02	0.04	0.04
FeO	28.09	28.07	28.21	28.36	28.31	27.09	27.52	30.01	29.53	29.57	29.62	29.78	29.62
MnO	0.35	0.35	0.33	0.35	0.32	0.46	0.45	0.37	0.35	0.33	0.38	0.34	0.37
MgO	19.11	18.92	18.95	18.76	18.89	19.61	19.46	17.06	17.17	17.61	17.47	17.31	17.36
CaO	0.27	0.25	0.27	0.19	0.26	0.42	0.42	0.52	0.44	0.40	0.48	0.49	0.46
Na2O	0.00	0.00	0.00	0.00	0.00	0.00	0.00	0.01	0.02	0.01	0.01	0.01	0.00
K2O	0.03	0.03	0.04	0.03	0.03	0.04	0.03	0.03	0.02	0.01	0.03	0.02	0.04
ZrO2	0.00	0.01	0.00	0.04	0.02	0.03	0.00	0.00	0.00	0.00	0.00	0.02	0.00
Total	100.46	99.99	100.38	100.25	100.29	99.86	100.11	99.94	99.82	100.62	100.60	100.39	100.35
No.	69	70	71	73	74	137	138	247	248	249	250	251	252
Cations, O = 6													
Si	1.973	1.970	1.971	1.975	1.976	1.979	1.976	1.979	1.985	1.992	1.990	1.984	1.986
Ti	0.001	0.001	0.001	0.001	0.001	0.002	0.002	0.001	0.001	0.001	0.001	0.002	0.001
Al	0.033	0.037	0.038	0.033	0.029	0.016	0.017	0.032	0.036	0.025	0.025	0.031	0.032
Cr	0.001	0.000	0.001	0.001	0.001	0.000	0.000	0.001	0.001	0.000	0.001	0.001	0.001
Fe	0.895	0.898	0.899	0.906	0.904	0.865	0.878	0.971	0.953	0.946	0.949	0.957	0.951
Mn	0.011	0.011	0.011	0.011	0.010	0.015	0.014	0.012	0.011	0.011	0.012	0.011	0.012
Mg	1.085	1.079	1.077	1.069	1.075	1.117	1.107	0.984	0.988	1.004	0.997	0.991	0.994
Ca	0.011	0.010	0.011	0.008	0.011	0.017	0.017	0.022	0.018	0.016	0.020	0.020	0.019
Na	0.000	0.000	0.000	0.000	0.000	0.000	0.000	0.001	0.001	0.001	0.001	0.001	0.000
K	0.002	0.002	0.002	0.001	0.002	0.002	0.001	0.001	0.001	0.001	0.001	0.001	0.002
Zr	0.000	0.000	0.000	0.001	0.000	0.001	0.000	0.000	0.000	0.000	0.000	0.001	0.000
Total	4.012	4.010	4.010	4.007	4.010	4.012	4.014	4.004	3.997	3.996	3.997	4.000	3.998

Sample	JKEM-15b	JKEM-15b	JKEM-10	JKEM-10	JKEM-10	JKEM-10	JKEM-10	JKEM-10	JKEM-10	JKEM-10	JKEM-10	JKEM-10	JKEM-10
Mineral	opx	opx	opx	opx	opx	opx	opx	opx	opx	opx	opx	opx	opx
No.	253	254	122	123	124	125	126	158	161	162	178	179	180
Weight %													
SiO2	51.76	51.78	51.13	51.36	51.08	51.02	51.14	51.36	51.50	51.33	51.13	51.72	51.34
TiO2	0.02	0.05	0.03	0.02	0.05	0.05	0.06	0.04	0.06	0.06	0.09	0.03	0.05
Al2O3	0.67	0.71	0.35	0.31	0.43	0.37	0.42	0.48	0.62	0.68	0.64	0.33	0.51
Cr2O3	0.03	0.07	0.03	0.04	0.03	0.03	0.03	0.00	0.04	0.02	0.02	0.05	0.04
FeO	29.70	29.66	32.91	33.00	33.40	32.93	33.26	32.82	32.84	32.52	32.91	33.16	33.30
MnO	0.34	0.38	0.73	0.74	0.75	0.69	0.75	0.68	0.55	0.52	0.60	0.64	0.64
MgO	17.37	17.15	14.46	14.61	14.55	14.41	14.25	14.66	15.24	15.05	15.06	14.96	14.90
CaO	0.43	0.50	0.51	0.52	0.50	0.50	0.56	0.56	0.50	0.58	0.55	0.43	0.54
Na2O	0.01	0.01	0.00	0.01	0.00	0.00	0.00	0.02	0.01	0.00	0.03	0.02	0.03
K2O	0.02	0.01	0.05	0.04	0.04	0.04	0.06	0.01	0.04	0.02	0.02	0.03	0.03
ZrO2	0.01	0.00	0.00	0.00	0.00	0.00	0.00	0.00	0.06	0.01	0.00	0.00	0.00
Total	100.36	100.30	100.21	100.64	100.83	100.03	100.53	100.64	101.45	100.78	101.03	101.36	101.38
No.	253	254	122	123	124	125	126	158	161	162	178	179	180
Cations, O = 6													
Si	1.987	1.989	2.002	2.002	1.992	2.001	1.999	1.999	1.987	1.991	1.984	2.000	1.988
Ti	0.001	0.001	0.001	0.001	0.001	0.001	0.002	0.001	0.002	0.002	0.002	0.001	0.001
Al	0.031	0.032	0.016	0.014	0.020	0.017	0.020	0.022	0.028	0.031	0.029	0.015	0.023
Cr	0.001	0.002	0.001	0.001	0.001	0.001	0.001	0.000	0.001	0.001	0.001	0.002	0.001
Fe	0.953	0.953	1.078	1.076	1.089	1.081	1.087	1.068	1.060	1.055	1.068	1.072	1.078
Mn	0.011	0.012	0.025	0.025	0.025	0.023	0.025	0.022	0.018	0.017	0.020	0.021	0.021
Mg	0.994	0.982	0.844	0.849	0.845	0.842	0.830	0.851	0.877	0.870	0.871	0.862	0.860
Ca	0.018	0.020	0.022	0.022	0.021	0.021	0.023	0.023	0.021	0.024	0.023	0.018	0.022
Na	0.001	0.001	0.000	0.001	0.001	0.000	0.000	0.002	0.001	0.000	0.002	0.001	0.002
K	0.001	0.000	0.002	0.002	0.002	0.002	0.003	0.001	0.002	0.001	0.001	0.002	0.001
Zr	0.000	0.000	0.000	0.000	0.000	0.000	0.000	0.000	0.001	0.000	0.000	0.000	0.000
Total	3.998	3.993	3.991	3.992	3.997	3.989	3.991	3.990	3.997	3.992	4.002	3.994	4.000

Sample	JKEM-10	JKEM-10
Mineral	opx	opx
No.	181	182
Weight %		
SiO2	51.52	51.37
TiO2	0.07	0.08
Al2O3	0.38	0.38
Cr2O3	0.05	0.03
FeO	32.82	32.98
MnO	0.67	0.63
MgO	14.88	14.70
CaO	0.55	0.55
Na2O	0.03	0.02
K2O	0.03	0.02
ZrO2	0.00	0.02
Total	100.99	100.77
No.	181	182
Cations, O = 6		
Si	1.998	1.999
Ti	0.002	0.002
Al	0.017	0.017
Cr	0.001	0.001
Fe	1.064	1.073
Mn	0.022	0.021
Mg	0.860	0.853
Ca	0.023	0.023
Na	0.002	0.001
K	0.002	0.001
Zr	0.000	0.001
Total	3.992	3.992

Sample	JKEM-12	JKEM-12	JKEM-12	JKEM-12	JKEM-12	JKEM-12	JKEM-12	JKEM-12	JKEM-12	JKEM-12	JKEM-12	JKEM-12	JKEM-14a
Mineral	cpx	cpx	cpx	cpx	cpx	cpx	cpx	cpx	cpx	cpx	cpx	cpx	cpx
No.	149	154	155	156	218	250	251	252	254	255	256	262	291
Weight %													
SiO2	53.38	52.56	52.30	52.24	52.63	52.35	51.93	52.43	51.45	52.16	52.49	51.08	52.04
TiO2	0.06	0.07	0.05	0.09	0.00	0.11	0.55	0.12	0.04	0.04	0.06	0.14	0.00
Al2O3	0.91	1.84	2.62	2.40	1.35	1.76	1.87	1.70	1.75	1.91	1.38	2.08	2.44
Cr2O3	0.06	0.00	0.00	0.00	0.00	0.00	0.00	0.00	0.00	0.01	0.00	0.00	0.00
FeO	11.07	11.43	11.81	11.78	11.26	13.00	13.14	12.40	13.44	13.54	13.98	13.28	12.90
MnO	0.19	0.16	0.15	0.15	0.11	0.22	0.34	0.31	0.22	0.20	0.23	0.18	0.00
MgO	13.06	11.91	11.30	11.57	12.10	11.07	11.97	12.09	5.58	10.44	10.83	5.64	10.36
CaO	22.26	21.56	20.85	21.11	22.00	20.46	19.87	20.22	21.10	21.15	21.16	20.89	20.45
Na2O	0.62	0.87	1.23	1.11	0.69	1.22	1.08	1.09	0.42	0.95	0.81	0.56	1.14
K2O	0.05	0.01	0.00	0.01	0.00	0.02	0.04	0.03	0.04	0.04	0.03	0.01	0.03
ZrO2	0.00	0.00	0.00	0.00	0.00	0.00	0.00	0.00	0.00	0.00	0.00	0.00	0.00
Total	101.66	100.41	100.30	100.45	100.14	100.21	100.78	100.39	94.05	100.42	100.97	93.84	99.37
No.	149	154	155	156	218	250	251	252	254	255	256	262	291
Cations, O = 6													
Si	1.978	1.972	1.965	1.961	1.981	1.979	1.954	1.973	2.074	1.976	1.981	2.062	1.981
Ti	0.002	0.002	0.001	0.002	0.000	0.003	0.016	0.004	0.001	0.001	0.002	0.004	0.000
Al	0.040	0.082	0.116	0.106	0.060	0.079	0.083	0.076	0.083	0.085	0.061	0.099	0.109
Cr	0.002	0.000	0.000	0.000	0.000	0.000	0.000	0.000	0.000	0.000	0.000	0.000	0.000
Fe	0.343	0.359	0.371	0.370	0.354	0.411	0.413	0.391	0.453	0.429	0.441	0.448	0.410
Mn	0.006	0.005	0.005	0.005	0.004	0.007	0.011	0.010	0.007	0.006	0.007	0.006	0.000
Mg	0.721	0.666	0.633	0.648	0.679	0.624	0.671	0.678	0.335	0.589	0.609	0.339	0.588
Ca	0.884	0.867	0.839	0.849	0.887	0.829	0.801	0.815	0.911	0.858	0.856	0.904	0.833
Na	0.044	0.064	0.089	0.081	0.050	0.089	0.079	0.080	0.033	0.070	0.059	0.044	0.084
K	0.002	0.001	0.000	0.001	0.000	0.001	0.002	0.001	0.002	0.002	0.002	0.001	0.002
Zr	0.000	0.000	0.000	0.000	0.000	0.000	0.000	0.000	0.000	0.000	0.000	0.000	0.000
Total	4.023	4.018	4.021	4.024	4.015	4.022	4.030	4.027	3.900	4.016	4.018	3.907	4.007

Sample	JKEM-14a	JKEM-14a	JKEM-14a	JKEM-14a	JKEM-14a	JKEM-14a	JKEM-14a	JKEM-14a	JKEM-14a	JKEM-14a	JKEM-14a	JKEM-14a	JKEM-14a
Mineral	cpx	cpx	cpx	cpx	cpx	cpx	cpx	cpx	cpx	cpx	cpx	cpx	cpx
No.	294	305	306	310	311	312	313	357	358	364	365	366	367
Weight %													
SiO2	52.36	52.72	52.68	52.26	52.28	53.14	53.26	52.42	52.35	52.85	52.46	52.37	52.64
TiO2	0.00	0.19	0.13	0.29	0.09	0.11	0.10	0.05	0.07	0.00	0.11	0.11	0.09
Al2O3	1.97	2.62	2.67	0.83	0.97	0.86	1.75	2.68	2.66	2.95	2.53	2.33	2.45
Cr2O3	0.00	0.00	0.00	0.01	0.00	0.00	0.00	0.00	0.00	0.00	0.00	0.00	0.00
FeO	12.95	13.11	13.00	15.31	15.08	15.82	12.96	11.97	12.04	12.10	11.75	11.43	11.62
MnO	0.00	0.16	0.15	0.27	0.25	0.29	0.21	0.19	0.18	0.18	0.15	0.13	0.12
MgO	10.34	10.53	10.44	10.06	10.01	10.24	10.96	11.07	11.12	10.83	11.27	11.38	11.42
CaO	20.77	20.74	20.60	20.41	20.36	19.80	20.93	20.79	21.13	19.93	21.03	21.53	21.45
Na2O	1.05	1.29	1.32	1.06	1.16	1.07	1.10	1.35	1.25	1.72	1.27	1.02	1.10
K2O	0.10	0.05	0.05	0.01	0.02	0.02	0.02	0.02	0.03	0.01	0.02	0.02	0.01
ZrO2	0.00	0.00	0.00	0.00	0.00	0.00	0.00	0.00	0.00	0.00	0.00	0.00	0.00
Total	99.54	101.42	101.02	100.50	100.21	101.36	101.28	100.54	100.82	100.58	100.58	100.32	100.90
No.	294	305	306	310	311	312	313	357	358	364	365	366	367
Cations, O = 6													
Si	1.991	1.969	1.973	1.993	1.997	2.006	1.990	1.967	1.961	1.978	1.966	1.967	1.966
Ti	0.000	0.005	0.004	0.008	0.002	0.003	0.003	0.001	0.002	0.000	0.003	0.003	0.002
Al	0.088	0.115	0.118	0.037	0.043	0.038	0.077	0.118	0.118	0.130	0.112	0.103	0.108
Cr	0.000	0.000	0.000	0.000	0.000	0.000	0.000	0.000	0.000	0.000	0.000	0.000	0.000
Fe	0.412	0.410	0.407	0.488	0.482	0.499	0.405	0.376	0.377	0.379	0.368	0.359	0.363
Mn	0.000	0.005	0.005	0.008	0.008	0.009	0.007	0.006	0.006	0.006	0.005	0.004	0.004
Mg	0.586	0.586	0.583	0.572	0.570	0.576	0.610	0.619	0.621	0.604	0.630	0.637	0.636
Ca	0.846	0.830	0.827	0.833	0.833	0.801	0.838	0.836	0.848	0.799	0.845	0.866	0.859
Na	0.077	0.094	0.095	0.078	0.086	0.078	0.079	0.098	0.091	0.125	0.092	0.074	0.079
K	0.005	0.002	0.002	0.001	0.001	0.001	0.001	0.001	0.001	0.001	0.001	0.001	0.001
Zr	0.000	0.000	0.000	0.000	0.000	0.000	0.000	0.000	0.000	0.000	0.000	0.000	0.000
Total	4.006	4.016	4.014	4.019	4.023	4.012	4.009	4.022	4.025	4.021	4.022	4.016	4.018

Sample	JKEM-14a	JKEM-15a	JKEM-15a	JKEM-15a	JKEM-15a	JKEM-15a	JKEM-15a	JKEM-15a	JKEM-15a	JKEM-15a	JKEM-15a	JKEM-02	JKEM-02
Mineral	cpx	cpx	cpx	cpx	cpx	cpx	cpx	cpx	cpx	cpx	cpx	cpx	cpx
No.	368	34	35	36	37	38	125	126	127	128	129	174	175
Weight %													
SiO2	52.54	53.32	52.58	52.37	52.30	52.41	52.64	52.59	53.03	52.59	51.72	51.14	51.22
TiO2	0.12	0.08	0.16	0.11	0.08	0.12	0.17	0.15	0.11	0.09	0.18	0.00	0.00
Al2O3	2.31	1.00	3.16	2.55	2.95	2.83	1.65	2.16	1.43	2.31	2.60	1.70	1.88
Cr2O3	0.00	0.00	0.00	0.02	0.02	0.00	0.03	0.01	0.00	0.04	0.03	0.00	0.00
FeO	11.89	11.29	11.05	11.29	10.99	11.12	11.81	12.28	11.72	10.84	13.61	14.44	14.49
MnO	0.16	0.17	0.17	0.19	0.16	0.20	0.20	0.20	0.17	0.18	0.19	0.11	0.14
MgO	11.38	12.16	11.02	11.30	11.27	11.39	11.32	11.33	11.55	11.75	10.81	9.81	9.72
CaO	21.08	22.31	21.02	21.22	21.06	21.44	21.60	20.76	21.21	21.61	19.56	20.43	20.47
Na2O	1.22	0.71	1.34	1.12	1.37	1.23	1.03	1.24	1.16	1.08	1.28	1.05	1.06
K2O	0.01	0.03	0.02	0.03	0.04	0.04	0.02	0.02	0.01	0.03	0.03	0.00	0.01
ZrO2	0.00	0.00	0.00	0.00	0.00	0.01	0.05	0.01	0.03	0.05	0.03	0.00	0.00
Total	100.71	101.05	100.51	100.21	100.25	100.77	100.53	100.75	100.43	100.56	100.02	98.68	99.00
No.	368	34	35	36	37	38	125	126	127	128	129	174	175
Cations, O = 6													
Si	1.968	1.989	1.964	1.967	1.961	1.958	1.979	1.972	1.991	1.967	1.961	1.980	1.977
Ti	0.003	0.002	0.004	0.003	0.002	0.004	0.005	0.004	0.003	0.002	0.005	0.000	0.000
Al	0.102	0.044	0.139	0.113	0.130	0.124	0.073	0.095	0.064	0.101	0.116	0.077	0.085
Cr	0.000	0.000	0.000	0.001	0.001	0.000	0.001	0.000	0.000	0.001	0.001	0.000	0.000
Fe	0.373	0.352	0.345	0.355	0.344	0.347	0.371	0.385	0.368	0.339	0.432	0.467	0.468
Mn	0.005	0.005	0.005	0.006	0.005	0.006	0.007	0.007	0.005	0.006	0.006	0.004	0.005
Mg	0.635	0.676	0.613	0.633	0.630	0.634	0.634	0.634	0.646	0.655	0.611	0.566	0.559
Ca	0.847	0.892	0.842	0.854	0.846	0.858	0.870	0.834	0.853	0.866	0.795	0.848	0.847
Na	0.089	0.052	0.097	0.082	0.100	0.089	0.075	0.090	0.085	0.078	0.094	0.079	0.079
K	0.001	0.001	0.001	0.002	0.002	0.002	0.001	0.001	0.001	0.001	0.001	0.000	0.001
Zr	0.000	0.000	0.000	0.000	0.000	0.000	0.001	0.000	0.001	0.001	0.001	0.000	0.000
Total	4.022	4.014	4.010	4.015	4.021	4.022	4.018	4.021	4.016	4.018	4.022	4.021	4.021

Sample	JKEM-02	JKEM-02	JKEM-02	JKEM-02	JKEM-02	JKEM-02	JKEM-02	JKEM-14b	JKEM-14b	JKEM-14b	JKEM-14b	JKEM-14b	JKEM-15b
Mineral	cpx	cpx	cpx	cpx	cpx	cpx	cpx	cpx	cpx	cpx	cpx	cpx	cpx
No.	176	219	220	221	222	223	227	132	133	134	135	136	239
Weight %													
SiO2	51.26	51.87	51.73	51.69	51.68	51.55	51.84	51.90	52.31	51.97	52.21	52.01	50.03
TiO2	0.00	0.18	0.14	0.16	0.12	0.14	0.14	0.11	0.11	0.11	0.12	0.15	0.20
Al2O3	1.15	2.10	2.04	2.26	2.25	2.08	1.73	2.69	2.29	2.73	2.29	2.33	4.55
Cr2O3	0.00	0.00	0.00	0.00	0.03	0.00	0.01	0.00	0.00	0.00	0.00	0.00	0.09
FeO	16.73	15.13	14.98	14.97	15.24	14.77	14.40	8.74	8.80	8.71	8.68	8.79	11.63
MnO	0.12	0.31	0.31	0.29	0.34	0.28	0.28	0.12	0.14	0.14	0.15	0.16	0.14
MgO	8.47	9.40	9.68	9.56	9.52	9.79	9.98	12.84	13.23	12.83	13.13	13.06	11.62
CaO	20.21	20.22	20.24	20.33	20.14	20.62	20.69	22.35	22.22	22.19	22.62	22.10	19.96
Na2O	0.98	1.36	1.25	1.31	1.38	1.18	1.05	1.04	0.93	1.06	0.91	0.98	1.51
K2O	0.00	0.02	0.01	0.00	0.01	0.01	0.02	0.00	0.02	0.02	0.03	0.02	0.16
ZrO2	0.00	0.00	0.00	0.07	0.01	0.01	0.02	0.00	0.01	0.00	0.00	0.00	0.01
Total	98.92	100.58	100.39	100.64	100.70	100.41	100.13	99.79	100.05	99.75	100.13	99.59	99.88
No.	176	219	220	221	222	223	227	132	133	134	135	136	239
Cations, O = 6													
Si	1.999	1.974	1.972	1.966	1.966	1.965	1.977	1.943	1.952	1.945	1.949	1.951	1.892
Ti	0.000	0.005	0.004	0.004	0.004	0.004	0.004	0.003	0.003	0.003	0.003	0.004	0.005
Al	0.053	0.094	0.091	0.101	0.101	0.094	0.077	0.119	0.101	0.121	0.101	0.103	0.203
Cr	0.000	0.000	0.000	0.000	0.001	0.000	0.000	0.000	0.000	0.000	0.000	0.000	0.002
Fe	0.545	0.481	0.478	0.476	0.485	0.471	0.459	0.274	0.275	0.272	0.271	0.276	0.368
Mn	0.004	0.010	0.010	0.010	0.011	0.009	0.009	0.004	0.004	0.004	0.005	0.005	0.004
Mg	0.492	0.533	0.550	0.542	0.540	0.556	0.568	0.716	0.736	0.716	0.731	0.730	0.655
Ca	0.845	0.824	0.827	0.829	0.821	0.842	0.845	0.897	0.889	0.890	0.905	0.888	0.809
Na	0.074	0.100	0.092	0.097	0.101	0.088	0.077	0.076	0.067	0.077	0.065	0.071	0.110
K	0.000	0.001	0.001	0.000	0.001	0.001	0.001	0.000	0.001	0.001	0.001	0.001	0.007
Zr	0.000	0.000	0.000	0.001	0.000	0.000	0.001	0.000	0.000	0.000	0.000	0.000	0.000
Total	4.012	4.023	4.025	4.026	4.030	4.028	4.018	4.032	4.028	4.030	4.031	4.030	4.057

Sample	JKEM-15b	JKEM-15b	JKEM-15b	JKEM-15b	JKEM-15b	JKEM-15b	JKEM-15b	JKEM-10	JKEM-10	JKEM-10	JKEM-10	JKEM-10	JKEM-10
Mineral	cpx	cpx	cpx	cpx	cpx	cpx	cpx	cpx	cpx	cpx	cpx	cpx	cpx
No.	240	241	242	243	244	245	246	113	114	115	116	117	118
Weight %													
SiO2	52.37	52.02	51.89	52.10	52.62	52.38	52.78	52.69	52.41	52.43	52.41	52.99	52.54
TiO2	0.08	0.18	0.07	0.12	0.09	0.09	0.08	0.00	0.00	0.01	0.03	0.00	0.04
Al2O3	1.57	2.42	0.72	2.38	1.81	1.94	1.95	1.05	1.36	1.24	1.26	1.01	1.27
Cr2O3	0.09	0.11	0.13	0.07	0.08	0.08	0.01	0.02	0.02	0.05	0.04	0.02	0.03
FeO	10.66	10.78	27.90	10.33	10.40	10.34	10.15	12.41	12.92	12.74	12.54	12.45	12.77
MnO	0.14	0.13	0.37	0.15	0.16	0.16	0.14	0.26	0.28	0.29	0.28	0.24	0.28
MgO	12.47	12.49	16.89	12.25	12.37	12.56	12.46	11.27	10.99	11.06	11.03	11.32	11.08
CaO	22.52	22.00	2.62	22.52	22.87	22.38	22.68	22.69	22.20	22.50	22.51	22.56	22.49
Na2O	0.89	1.03	0.16	1.11	0.92	0.94	0.93	0.58	0.61	0.64	0.70	0.59	0.65
K2O	0.04	0.10	0.03	0.04	0.04	0.05	0.03	0.04	0.04	0.04	0.03	0.04	0.04
ZrO2	0.00	0.02	0.00	0.00	0.03	0.00	0.00	0.00	0.00	0.00	0.01	0.00	0.02
Total	100.82	101.29	100.78	101.08	101.38	100.93	101.20	100.99	100.82	100.98	100.84	101.21	101.20
No.	240	241	242	243	244	245	246	113	114	115	116	117	118
Cations, O = 6													
Si	1.960	1.937	1.982	1.942	1.956	1.954	1.960	1.982	1.977	1.975	1.976	1.987	1.975
Ti	0.002	0.005	0.002	0.004	0.002	0.002	0.002	0.000	0.000	0.000	0.001	0.000	0.001
Al	0.069	0.106	0.032	0.104	0.079	0.085	0.085	0.046	0.061	0.055	0.056	0.044	0.056
Cr	0.002	0.003	0.004	0.002	0.002	0.002	0.000	0.001	0.001	0.001	0.001	0.001	0.001
Fe	0.334	0.335	0.891	0.322	0.323	0.323	0.316	0.390	0.407	0.401	0.395	0.391	0.401
Mn	0.005	0.004	0.012	0.005	0.005	0.005	0.004	0.008	0.009	0.009	0.009	0.008	0.009
Mg	0.695	0.694	0.962	0.681	0.685	0.698	0.690	0.632	0.618	0.621	0.620	0.632	0.621
Ca	0.903	0.878	0.107	0.899	0.911	0.895	0.903	0.914	0.897	0.908	0.910	0.907	0.906
Na	0.064	0.074	0.012	0.080	0.067	0.068	0.067	0.042	0.044	0.047	0.051	0.043	0.047
K	0.002	0.005	0.002	0.002	0.002	0.002	0.001	0.002	0.002	0.002	0.001	0.002	0.002
Zr	0.000	0.001	0.000	0.000	0.001	0.000	0.000	0.000	0.000	0.000	0.000	0.000	0.001
Total	4.036	4.043	4.006	4.042	4.034	4.035	4.029	4.018	4.016	4.020	4.019	4.014	4.021

Sample	JKEM-10	JKEM-10	JKEM-10	JKEM-10	JKEM-10	JKEM-10	JKEM-10	JKEM-10
Mineral	cpx	cpx	cpx	cpx	cpx	cpx	cpx	cpx
No.	119	120	172	173	174	175	176	177
Weight %								
SiO2	52.51	52.62	52.55	52.58	52.96	52.80	52.88	52.72
TiO2	0.00	0.06	0.08	0.09	0.07	0.08	0.04	0.05
Al2O3	1.10	1.22	1.60	1.30	1.31	1.15	0.91	1.12
Cr2O3	0.03	0.02	0.04	0.00	0.01	0.00	0.01	0.00
FeO	12.59	12.58	12.83	12.58	12.49	12.31	12.58	12.32
MnO	0.28	0.28	0.26	0.21	0.22	0.24	0.24	0.22
MgO	11.18	11.16	10.98	11.17	11.20	11.29	11.45	11.27
CaO	22.64	22.55	21.93	22.63	22.78	22.66	22.50	22.58
Na2O	0.60	0.63	0.81	0.68	0.69	0.63	0.58	0.65
K2O	0.02	0.04	0.02	0.02	0.02	0.03	0.02	0.02
ZrO2	0.00	0.00	0.00	0.02	0.00	0.00	0.00	0.00
Total	100.94	101.16	101.09	101.27	101.75	101.17	101.22	100.95
No.	119	120	172	173	174	175	176	177
Cations, O = 6								
Si	1.978	1.977	1.974	1.973	1.976	1.981	1.984	1.982
Ti	0.000	0.002	0.002	0.002	0.002	0.002	0.001	0.001
Al	0.049	0.054	0.071	0.058	0.058	0.050	0.040	0.050
Cr	0.001	0.001	0.001	0.000	0.001	0.000	0.000	0.000
Fe	0.397	0.395	0.403	0.395	0.390	0.386	0.395	0.388
Mn	0.009	0.009	0.008	0.007	0.007	0.007	0.008	0.007
Mg	0.628	0.625	0.615	0.625	0.623	0.631	0.641	0.632
Ca	0.914	0.908	0.883	0.910	0.911	0.911	0.905	0.909
Na	0.044	0.046	0.059	0.049	0.050	0.046	0.042	0.047
K	0.001	0.002	0.001	0.001	0.001	0.002	0.001	0.001
Zr	0.000	0.000	0.000	0.001	0.000	0.000	0.000	0.000
Total	4.020	4.019	4.018	4.021	4.018	4.016	4.016	4.018

Sample	JKEM-12	JKEM-12	JKEM-12	JKEM-12	JKEM-12	JKEM-12	JKEM-12	JKEM-12	JKEM-12	JKEM-12	JKEM-12	JKEM-12	JKEM-12
Mineral	amph	amph	amph	amph	amph	amph	amph	amph	amph	amph	amph	amph	amph
No.	147	148	150	152	153	179	190	191	194	196	212	213	214
Weight %													
SiO2	43.67	42.89	42.30	42.02	42.87	41.28	42.59	42.36	40.46	40.95	41.82	43.41	42.44
TiO2	0.52	0.43	1.00	0.96	1.05	1.59	0.99	1.17	1.73	1.64	1.96	0.52	1.05
Al2O3	11.69	12.43	12.04	12.10	11.60	12.68	12.19	12.26	13.04	13.02	12.78	11.67	12.00
Cr2O3	0.03	0.03	0.04	0.01	0.00	0.00	0.00	0.00	0.00	0.00	0.00	0.00	0.00
FeO	15.34	16.37	17.79	17.86	18.01	18.96	16.44	17.48	18.97	18.61	16.94	16.42	16.91
MnO	0.12	0.15	0.14	0.10	0.08	0.05	0.08	0.07	0.05	0.08	0.05	0.10	0.11
MgO	12.50	11.56	10.17	10.09	10.10	8.94	10.87	10.26	8.60	8.70	10.16	11.51	11.00
CaO	11.20	11.15	11.20	11.19	11.17	10.56	11.16	11.01	10.96	10.86	10.90	11.11	11.18
Na2O	2.24	2.34	2.47	2.38	2.43	2.86	2.30	2.47	2.55	2.57	2.67	2.32	2.64
K2O	0.88	1.07	1.13	1.06	1.03	0.80	1.17	1.01	1.08	1.09	1.06	1.00	0.76
ZrO2	0.00	0.00	0.00	0.00	0.00	0.00	0.00	0.00	0.00	0.00	0.00	0.00	0.00
Total	98.19	98.41	98.29	97.77	98.31	97.71	97.78	98.09	97.43	97.52	98.33	98.05	98.07
No.	147	148	150	152	153	179	190	191	194	196	212	213	214
Cations, O = 23													
Si	6.475	6.389	6.371	6.362	6.445	6.279	6.396	6.369	6.196	6.247	6.268	6.484	6.366
Ti	0.058	0.048	0.113	0.108	0.117	0.182	0.110	0.131	0.200	0.189	0.221	0.058	0.117
Al	2.042	2.183	2.137	2.157	2.054	2.272	2.157	2.174	2.353	2.341	2.259	2.054	2.121
Cr	0.005	0.005	0.005	0.002	0.000	0.000	0.000	0.000	0.000	0.000	0.000	0.000	0.000
Fe	1.902	2.040	2.240	2.261	2.266	2.413	2.065	2.199	2.429	2.374	2.123	2.052	2.121
Mn	0.016	0.018	0.018	0.012	0.009	0.007	0.009	0.009	0.007	0.012	0.007	0.012	0.014
Mg	2.762	2.567	2.284	2.277	2.263	2.029	2.433	2.300	1.964	1.978	2.270	2.562	2.459
Ca	1.778	1.780	1.806	1.815	1.799	1.723	1.796	1.773	1.799	1.776	1.750	1.778	1.796
Na	0.644	0.676	0.722	0.699	0.708	0.842	0.669	0.722	0.757	0.759	0.775	0.672	0.766
K	0.168	0.202	0.219	0.205	0.198	0.154	0.225	0.193	0.212	0.212	0.202	0.191	0.145
Zr	0.000	0.000	0.000	0.000	0.000	0.000	0.000	0.000	0.000	0.000	0.000	0.000	0.000
Total	15.852	15.909	15.916	15.898	15.859	15.902	15.865	15.872	15.916	15.888	15.877	15.861	15.905

Sample	JKEM-12	JKEM-12	JKEM-12	JKEM-12	JKEM-12	JKEM-12	JKEM-12	JKEM-12	JKEM-12	JKEM-12	JKEM-12	JKEM-12	JKEM-12
Mineral	amph	amph	amph	amph	amph	amph	amph	amph	amph	amph	amph	amph	amph
No.	215	216	217	219	220	221	223	224	225	226	227	228	232
Weight %													
SiO2	42.19	41.51	41.33	42.47	42.42	41.31	41.23	41.31	40.85	41.40	41.61	41.62	41.01
TiO2	0.96	1.63	1.85	0.76	1.18	1.88	1.74	1.85	1.72	1.78	1.50	1.75	1.70
Al2O3	12.61	12.40	12.46	12.05	11.82	12.38	12.39	12.54	12.73	12.24	12.45	12.21	12.56
Cr2O3	0.00	0.00	0.00	0.00	0.00	0.00	0.00	0.00	0.00	0.00	0.00	0.00	0.06
FeO	16.57	17.79	18.35	18.00	18.37	18.85	18.40	18.79	19.00	18.97	18.94	18.97	18.83
MnO	0.06	0.08	0.08	0.07	0.08	0.07	0.09	0.07	0.09	0.09	0.07	0.07	0.06
MgO	10.72	10.03	9.36	10.07	10.00	8.98	9.03	9.01	8.90	9.06	9.12	9.07	8.84
CaO	11.12	10.92	10.84	11.15	11.07	10.89	10.82	10.92	10.67	10.93	10.86	10.81	10.91
Na2O	2.46	2.68	2.68	2.41	2.59	2.74	2.68	2.72	2.76	2.72	2.68	2.71	2.70
K2O	1.12	0.91	0.94	1.08	0.81	0.93	0.98	0.94	0.98	0.77	0.93	0.86	0.98
ZrO2	0.00	0.00	0.00	0.00	0.00	0.00	0.00	0.00	0.00	0.00	0.00	0.00	0.00
Total	97.82	97.94	97.89	98.06	98.34	98.02	97.36	98.15	97.70	97.96	98.16	98.08	97.66
No.	215	216	217	219	220	221	223	224	225	226	227	228	232
Cations, O = 6													
Si	6.341	6.274	6.268	6.406	6.387	6.272	6.291	6.263	6.233	6.288	6.304	6.311	6.256
Ti	0.108	0.184	0.212	0.085	0.133	0.214	0.200	0.212	0.198	0.202	0.170	0.200	0.196
Al	2.233	2.210	2.226	2.141	2.098	2.217	2.229	2.240	2.289	2.192	2.222	2.183	2.259
Cr	0.000	0.000	0.000	0.000	0.000	0.000	0.000	0.000	0.000	0.000	0.000	0.000	0.007
Fe	2.084	2.249	2.328	2.270	2.314	2.394	2.348	2.381	2.424	2.410	2.401	2.406	2.404
Mn	0.007	0.012	0.012	0.009	0.009	0.009	0.012	0.009	0.012	0.012	0.009	0.009	0.007
Mg	2.401	2.261	2.116	2.263	2.245	2.031	2.054	2.036	2.024	2.052	2.061	2.052	2.010
Ca	1.792	1.769	1.762	1.803	1.787	1.773	1.769	1.773	1.743	1.780	1.764	1.757	1.783
Na	0.718	0.787	0.789	0.706	0.754	0.805	0.794	0.798	0.817	0.803	0.787	0.798	0.800
K	0.216	0.175	0.182	0.207	0.156	0.179	0.191	0.182	0.191	0.150	0.179	0.166	0.191
Zr	0.000	0.000	0.000	0.000	0.000	0.000	0.000	0.000	0.000	0.000	0.000	0.000	0.000
Total	15.902	15.923	15.893	15.891	15.884	15.898	15.888	15.893	15.932	15.891	15.900	15.884	15.914

Sample	JKEM-12	JKEM-12	JKEM-12	JKEM-14a	JKEM-14a	JKEM-14a	JKEM-14a	JKEM-14a	JKEM-14a	JKEM-15a	JKEM-15a	JKEM-15a	JKEM-15a
Mineral	amph	amph	amph	amph	amph	amph	amph	amph	amph	amph	amph	amph	amph
No.	233	234	235	354	355	361	372	373	374	30	39	40	41
Weight %													
SiO2	41.53	41.41	41.62	42.00	42.37	41.31	41.41	41.61	41.52	43.49	41.53	41.84	41.68
TiO2	1.81	1.93	1.64	2.84	2.34	2.26	2.14	2.47	1.81	1.71	1.17	1.63	0.98
Al2O3	11.83	12.15	12.29	11.96	12.25	12.38	13.16	12.94	13.43	10.91	12.60	12.33	12.59
Cr2O3	0.00	0.01	0.03	0.00	0.00	0.00	0.00	0.00	0.00	0.00	0.00	0.00	0.00
FeO	18.48	18.79	19.03	16.16	16.06	19.15	18.38	18.19	18.35	17.39	17.47	17.73	17.32
MnO	0.11	0.12	0.09	0.09	0.07	0.07	0.11	0.08	0.09	0.08	0.10	0.11	0.10
MgO	9.38	9.22	9.16	10.39	10.68	8.54	8.97	9.03	9.11	10.42	9.74	9.58	10.03
CaO	11.02	10.91	10.78	11.18	11.24	11.06	10.96	11.06	11.14	11.12	11.02	11.06	11.09
Na2O	2.60	2.69	2.76	2.56	2.34	2.63	2.87	3.11	3.01	2.51	2.59	2.65	2.68
K2O	1.03	0.94	0.82	1.33	1.55	1.22	0.90	0.49	0.59	0.78	1.03	0.95	0.95
ZrO2	0.00	0.00	0.00	0.00	0.00	0.00	0.00	0.00	0.00	0.00	0.01	0.00	0.00
Total	97.80	98.17	98.22	98.51	98.90	98.60	98.89	98.99	99.04	98.40	97.24	97.87	97.42
No.	233	234	235	354	355	361	372	373	374	30	39	40	41
Cations, O = 6													
Si	6.316	6.279	6.304	6.281	6.302	6.256	6.217	6.226	6.212	6.502	6.314	6.325	6.318
Ti	0.207	0.221	0.186	0.320	0.262	0.258	0.242	0.278	0.205	0.193	0.133	0.186	0.113
Al	2.121	2.171	2.194	2.107	2.148	2.210	2.328	2.282	2.367	1.923	2.259	2.197	2.249
Cr	0.000	0.000	0.005	0.000	0.000	0.000	0.000	0.000	0.000	0.000	0.000	0.000	0.000
Fe	2.351	2.383	2.410	2.022	1.996	2.427	2.307	2.277	2.295	2.174	2.222	2.243	2.197
Mn	0.014	0.016	0.012	0.012	0.009	0.009	0.014	0.009	0.012	0.009	0.012	0.014	0.014
Mg	2.128	2.084	2.068	2.316	2.369	1.927	2.006	2.015	2.031	2.321	2.206	2.157	2.268
Ca	1.796	1.773	1.750	1.792	1.792	1.794	1.762	1.773	1.785	1.780	1.794	1.792	1.803
Na	0.766	0.791	0.810	0.743	0.674	0.771	0.835	0.902	0.874	0.729	0.764	0.777	0.787
K	0.200	0.182	0.159	0.253	0.294	0.237	0.173	0.094	0.113	0.150	0.200	0.182	0.184
Zr	0.000	0.000	0.000	0.000	0.000	0.000	0.000	0.000	0.000	0.000	0.000	0.000	0.000
Total	15.900	15.902	15.898	15.847	15.849	15.891	15.884	15.856	15.893	15.783	15.902	15.875	15.932

Sample	JKEM-15a	JKEM-15a	JKEM-15a	JKEM-15a	JKEM-15a	JKEM-15a	JKEM-15a	JKEM-15a	JKEM-15a	JKEM-15a	JKEM-15a	JKEM-15a	JKEM-15a
Mineral	amph	amph	amph	amph	amph	amph	amph	amph	amph	amph	amph	amph	amph
No.	42	43	57	58	59	60	80	81	82	83	85	86	87
Weight %													
SiO2	42.69	43.01	43.04	43.16	43.66	44.23	41.25	41.20	41.48	41.17	41.48	41.27	41.65
TiO2	0.78	0.99	0.47	0.60	0.55	0.39	1.49	1.55	1.50	1.40	1.46	1.39	1.31
Al2O3	12.24	12.44	12.50	12.12	12.05	11.74	12.70	12.97	12.74	12.81	13.02	13.02	12.80
Cr2O3	0.00	0.00	0.00	0.00	0.00	0.00	0.00	0.00	0.00	0.00	0.00	0.00	0.00
FeO	16.93	16.59	16.24	15.64	15.46	15.03	18.39	18.27	18.03	17.78	17.84	17.67	16.97
MnO	0.09	0.05	0.10	0.09	0.08	0.11	0.04	0.03	0.04	0.03	0.04	0.03	0.01
MgO	10.71	11.07	11.40	11.71	11.83	12.57	9.35	9.11	9.35	9.32	9.66	9.48	10.18
CaO	10.95	11.06	11.03	11.27	11.13	11.18	10.73	10.86	10.86	10.76	10.91	10.81	10.68
Na2O	2.48	2.62	2.59	2.62	2.54	2.49	2.83	2.87	2.86	2.90	2.90	2.83	2.79
K2O	0.87	0.85	0.84	0.80	0.76	0.70	0.83	0.84	0.78	0.81	0.83	0.86	0.80
ZrO2	0.00	0.01	0.02	0.00	0.00	0.00	0.00	0.00	0.00	0.00	0.00	0.00	0.00
Total	97.73	98.69	98.23	98.02	98.04	98.42	97.62	97.69	97.62	96.98	98.14	97.33	97.18
No.	42	43	57	58	59	60	80	81	82	83	85	86	87
Cations, O = 6													
Si	6.415	6.387	6.410	6.429	6.481	6.521	6.270	6.256	6.291	6.281	6.254	6.268	6.304
Ti	0.087	0.110	0.053	0.067	0.062	0.044	0.170	0.177	0.170	0.161	0.166	0.159	0.150
Al	2.169	2.178	2.194	2.128	2.107	2.040	2.275	2.321	2.277	2.305	2.314	2.330	2.284
Cr	0.000	0.000	0.000	0.000	0.000	0.000	0.000	0.000	0.000	0.000	0.000	0.000	0.000
Fe	2.128	2.061	2.022	1.948	1.918	1.854	2.337	2.321	2.286	2.268	2.249	2.245	2.148
Mn	0.012	0.007	0.012	0.012	0.009	0.014	0.005	0.002	0.005	0.005	0.005	0.002	0.000
Mg	2.399	2.452	2.532	2.601	2.617	2.762	2.118	2.061	2.114	2.118	2.171	2.146	2.298
Ca	1.764	1.760	1.762	1.799	1.771	1.764	1.748	1.766	1.764	1.760	1.762	1.760	1.732
Na	0.722	0.754	0.748	0.759	0.731	0.711	0.835	0.844	0.840	0.858	0.849	0.833	0.821
K	0.166	0.161	0.159	0.152	0.143	0.131	0.161	0.163	0.150	0.159	0.159	0.166	0.154
Zr	0.000	0.000	0.002	0.000	0.000	0.000	0.000	0.000	0.000	0.000	0.000	0.000	0.000
Total	15.861	15.870	15.893	15.893	15.842	15.842	15.918	15.914	15.898	15.916	15.930	15.907	15.893

Sample	JKEM-15a	JKEM-01	JKEM-01	JKEM-02	JKEM-02	JKEM-02	JKEM-02	JKEM-02	JKEM-02	JKEM-14b	JKEM-14b	JKEM-14b	JKEM-14b
Mineral	amph	amph	amph	amph	amph	amph	amph	amph	amph	amph	amph	amph	amph
No.	88	40	95	183	185	209	210	211	212	47	48	51	60
Weight %													
SiO2	41.68	41.13	41.43	40.86	40.51	40.11	41.00	41.09	40.86	42.38	41.00	42.02	41.80
TiO2	1.41	2.94	2.68	2.79	2.58	3.07	2.85	2.81	2.66	1.20	1.11	1.21	1.54
Al2O3	12.80	12.28	12.31	12.03	11.87	11.28	11.51	11.58	11.63	13.54	12.65	13.33	12.78
Cr2O3	0.00	0.01	0.00	0.00	0.00	0.08	0.09	0.09	0.00	0.04	0.02	0.00	0.00
FeO	16.85	20.14	19.35	21.66	21.68	20.67	20.84	20.60	20.57	14.63	15.76	14.34	16.20
MnO	0.00	0.13	0.08	0.10	0.07	0.20	0.21	0.21	0.12	0.08	0.11	0.09	0.12
MgO	10.04	7.77	8.29	6.65	6.69	7.03	7.50	7.52	7.42	11.86	11.85	11.94	10.80
CaO	10.81	10.90	11.22	10.20	10.51	10.64	10.77	10.78	10.70	10.84	9.63	10.73	10.54
Na2O	2.77	2.71	2.64	3.20	2.94	2.30	2.53	2.48	2.44	2.89	2.78	2.87	2.91
K2O	0.82	1.47	1.59	0.68	1.19	1.68	1.59	1.64	1.62	0.62	0.52	0.59	0.66
ZrO2	0.00	0.01	0.02	0.00	0.00	0.00	0.02	0.00	0.00	0.03	0.01	0.05	0.00
Total	97.18	99.48	99.60	98.18	98.03	97.05	98.90	98.79	98.00	98.11	95.44	97.19	97.35
No.	88	40	95	183	185	209	210	211	212	47	48	51	60
Cations, O = 6													
Si	6.309	6.217	6.233	6.274	6.256	6.254	6.263	6.274	6.286	6.272	6.272	6.274	6.293
Ti	0.161	0.334	0.304	0.322	0.299	0.359	0.329	0.322	0.308	0.133	0.127	0.136	0.175
Al	2.284	2.187	2.183	2.178	2.160	2.072	2.072	2.084	2.109	2.362	2.282	2.346	2.268
Cr	0.000	0.002	0.000	0.000	0.000	0.009	0.012	0.012	0.000	0.005	0.002	0.000	0.000
Fe	2.132	2.546	2.436	2.783	2.801	2.696	2.663	2.631	2.647	1.810	2.015	1.792	2.038
Mn	0.000	0.016	0.012	0.014	0.009	0.025	0.028	0.028	0.016	0.009	0.014	0.012	0.014
Mg	2.266	1.750	1.858	1.523	1.541	1.633	1.707	1.711	1.702	2.617	2.700	2.659	2.424
Ca	1.753	1.764	1.808	1.679	1.739	1.778	1.762	1.764	1.764	1.720	1.578	1.718	1.700
Na	0.814	0.794	0.771	0.955	0.879	0.695	0.750	0.736	0.727	0.830	0.826	0.830	0.849
K	0.159	0.283	0.306	0.133	0.235	0.334	0.308	0.320	0.317	0.117	0.101	0.113	0.127
Zr	0.000	0.000	0.002	0.000	0.000	0.000	0.002	0.000	0.000	0.002	0.000	0.002	0.000
Total	15.877	15.895	15.914	15.861	15.921	15.856	15.898	15.884	15.877	15.882	15.918	15.884	15.888

Sample	JKEM-14b	JKEM-14b	JKEM-14b	JKEM-14b	JKEM-14b	JKEM-14b	JKEM-14b	JKEM-14b	JKEM-14b	JKEM-14b	JKEM-14b	JKEM-14b	JKEM-14b
Mineral	amph	amph	amph	amph	amph	amph	amph	amph	amph	amph	amph	amph	amph
No.	61	62	63	64	65	75	76	89	90	91	92	110	111
Weight %													
SiO2	41.92	42.27	41.83	42.15	41.99	42.18	42.11	40.98	42.45	41.59	41.23	42.93	41.53
TiO2	1.52	1.43	1.45	1.63	1.36	1.31	1.25	0.32	0.27	0.26	0.40	1.16	1.23
Al2O3	13.09	13.06	13.03	13.03	12.63	12.76	12.80	15.11	13.99	15.02	15.23	13.30	14.41
Cr2O3	0.00	0.00	0.02	0.00	0.01	0.00	0.00	0.00	0.00	0.00	0.00	0.00	0.00
FeO	15.93	16.07	16.28	16.34	16.11	15.88	16.07	15.31	15.12	14.64	14.96	13.72	13.55
MnO	0.07	0.10	0.09	0.11	0.09	0.10	0.08	0.07	0.06	0.05	0.06	0.08	0.11
MgO	10.85	10.99	10.82	10.88	10.93	10.92	11.10	10.50	11.58	11.20	10.62	12.47	11.76
CaO	10.60	10.63	10.41	10.45	10.36	10.60	10.72	11.37	11.63	11.54	11.49	11.43	11.47
Na2O	2.90	2.78	2.84	2.86	2.94	2.89	2.86	2.61	2.51	2.52	2.56	2.79	2.76
K2O	0.68	0.61	0.67	0.61	0.59	0.54	0.56	0.92	0.79	0.89	0.97	0.33	0.63
ZrO2	0.03	0.00	0.01	0.05	0.04	0.02	0.01	0.00	0.00	0.00	0.00	0.04	0.05
Total	97.59	97.93	97.45	98.11	97.04	97.18	97.54	97.18	98.39	97.71	97.52	98.25	97.50
No.	61	62	63	64	65	75	76	89	90	91	92	110	111
Cations, O = 6													
Si	6.284	6.307	6.286	6.288	6.332	6.339	6.314	6.162	6.284	6.192	6.166	6.311	6.171
Ti	0.173	0.161	0.163	0.182	0.154	0.147	0.140	0.037	0.030	0.028	0.044	0.129	0.138
Al	2.312	2.298	2.307	2.291	2.245	2.259	2.261	2.680	2.440	2.636	2.684	2.305	2.525
Cr	0.000	0.000	0.002	0.000	0.000	0.000	0.000	0.000	0.000	0.000	0.000	0.000	0.000
Fe	1.996	2.006	2.047	2.040	2.031	1.996	2.015	1.925	1.872	1.824	1.870	1.686	1.684
Mn	0.009	0.014	0.012	0.014	0.012	0.014	0.009	0.009	0.007	0.007	0.007	0.009	0.014
Mg	2.424	2.443	2.424	2.420	2.454	2.445	2.482	2.353	2.555	2.486	2.367	2.732	2.604
Ca	1.702	1.700	1.677	1.670	1.674	1.707	1.723	1.831	1.845	1.840	1.842	1.801	1.826
Na	0.844	0.805	0.828	0.828	0.858	0.842	0.830	0.759	0.720	0.727	0.743	0.796	0.796
K	0.129	0.115	0.129	0.117	0.113	0.104	0.106	0.175	0.150	0.170	0.186	0.062	0.120
Zr	0.002	0.000	0.000	0.002	0.002	0.000	0.000	0.000	0.000	0.000	0.000	0.002	0.002
Total	15.875	15.847	15.877	15.854	15.875	15.852	15.882	15.932	15.902	15.909	15.909	15.836	15.882

Sample	JKEM-14b	JKEM-14b	JKEM-14b	JKEM-14b	JKEM-14b	JKEM-14b	JKEM-14b	JKEM-14b	JKEM-14b	JKEM-14b	JKEM-14b	JKEM-15b	JKEM-15b
Mineral	amph	amph	amph	amph	amph	amph	amph	amph	amph	amph	amph	amph	amph
No.	112	113	114	115	116	117	118	139	140	141	142	233	234
Weight %													
SiO2	40.17	39.91	40.28	40.33	40.54	40.29	39.76	42.87	44.14	41.98	43.51	41.78	41.45
TiO2	1.38	1.42	1.41	1.69	1.35	1.42	1.39	0.90	0.77	1.17	0.94	1.22	0.95
Al2O3	15.36	15.20	15.09	14.44	14.23	14.52	14.96	12.41	10.65	12.40	11.15	12.41	13.05
Cr2O3	0.00	0.00	0.00	0.00	0.00	0.00	0.00	0.00	0.00	0.00	0.00	0.08	0.09
FeO	14.99	16.14	16.33	16.20	16.19	16.07	16.52	15.02	15.37	15.44	14.83	17.36	16.57
MnO	0.08	0.07	0.08	0.09	0.06	0.09	0.07	0.07	0.10	0.08	0.07	0.12	0.09
MgO	10.44	9.48	9.60	9.83	9.95	9.80	9.49	11.80	12.34	11.38	12.30	10.15	10.23
CaO	11.29	11.34	11.28	11.30	11.37	11.24	11.36	11.56	11.22	11.33	11.72	11.24	11.29
Na2O	2.90	2.69	2.77	2.66	2.76	2.68	2.74	2.48	2.21	2.56	2.34	2.86	2.90
K2O	0.72	0.98	0.92	1.00	0.78	1.01	0.99	0.71	0.63	0.76	0.66	0.87	0.88
ZrO2	0.02	0.02	0.00	0.00	0.01	0.00	0.00	0.00	0.00	0.01	0.00	0.01	0.00
Total	97.35	97.23	97.75	97.54	97.23	97.13	97.27	97.79	97.41	97.09	97.52	98.08	97.51
No.	112	113	114	115	116	117	118	139	140	141	142	233	234
Cations, O = 6													
Si	6.033	6.042	6.065	6.090	6.132	6.104	6.035	6.383	6.585	6.323	6.491	6.300	6.265
Ti	0.156	0.161	0.159	0.191	0.154	0.161	0.159	0.101	0.087	0.133	0.106	0.138	0.108
Al	2.719	2.712	2.680	2.569	2.537	2.592	2.677	2.178	1.872	2.201	1.960	2.206	2.325
Cr	0.000	0.000	0.000	0.000	0.000	0.000	0.000	0.000	0.000	0.000	0.000	0.009	0.012
Fe	1.884	2.042	2.056	2.047	2.047	2.036	2.098	1.870	1.918	1.946	1.849	2.190	2.095
Mn	0.009	0.009	0.009	0.012	0.009	0.012	0.009	0.009	0.012	0.009	0.009	0.014	0.012
Mg	2.337	2.141	2.155	2.213	2.245	2.215	2.148	2.620	2.744	2.555	2.735	2.282	2.305
Ca	1.817	1.840	1.822	1.829	1.842	1.824	1.847	1.845	1.794	1.829	1.872	1.817	1.829
Na	0.846	0.789	0.807	0.780	0.810	0.789	0.805	0.715	0.639	0.750	0.676	0.835	0.851
K	0.138	0.189	0.177	0.191	0.150	0.196	0.193	0.133	0.120	0.145	0.127	0.168	0.170
Zr	0.002	0.002	0.000	0.000	0.000	0.000	0.000	0.000	0.000	0.000	0.000	0.000	0.000
Total	15.944	15.930	15.932	15.921	15.928	15.930	15.974	15.856	15.773	15.893	15.826	15.960	15.974

Sample	JKEM-15b	JKEM-15b	JKEM-15b	JKEM-15b	JKEM-15b	JKEM-15b	JKEM-15b	JKEM-15b	JKEM-15b	JKEM-10	JKEM-10	JKEM-10	JKEM-10
Mineral	amph	amph	amph	amph	amph	amph	amph	amph	amph	amph	amph	amph	amph
No.	235	236	237	238	280	281	282	283	284	100	101	102	105
Weight %													
SiO2	42.15	41.82	43.30	41.92	40.10	40.41	39.86	40.53	40.87	42.60	42.23	42.57	42.72
TiO2	1.11	0.98	1.07	0.97	1.64	1.61	1.70	1.50	1.44	2.03	2.09	1.97	1.75
Al2O3	12.32	12.65	11.06	12.50	13.25	13.15	13.59	13.23	13.12	10.94	11.08	10.65	10.67
Cr2O3	0.06	0.08	0.08	0.07	0.04	0.04	0.03	0.01	0.00	0.05	0.05	0.05	0.05
FeO	16.95	17.61	17.30	17.67	18.01	18.24	18.11	17.93	17.87	19.91	19.73	19.71	19.60
MnO	0.12	0.12	0.13	0.11	0.10	0.09	0.10	0.12	0.11	0.15	0.14	0.14	0.17
MgO	10.21	10.18	10.64	10.10	8.66	8.73	8.50	8.89	8.85	8.15	8.21	8.32	8.38
CaO	11.15	11.35	11.29	11.35	10.96	11.02	10.88	10.99	10.99	11.56	11.47	11.58	11.32
Na2O	2.83	2.82	2.71	2.81	2.85	3.00	2.94	2.88	2.86	2.02	2.00	2.05	1.93
K2O	0.90	0.90	0.83	0.92	0.88	0.87	0.90	0.88	0.98	1.40	1.43	1.25	1.28
ZrO2	0.06	0.00	0.10	0.00	0.05	0.02	0.00	0.00	0.02	0.00	0.00	0.00	0.01
Total	97.84	98.51	98.51	98.41	96.55	97.16	96.60	96.96	97.11	98.80	98.42	98.27	97.86
No.	235	236	237	238	280	281	282	283	284	100	101	102	105
Cations, O = 6													
Si	6.353	6.284	6.481	6.307	6.178	6.189	6.141	6.205	6.245	6.454	6.422	6.477	6.514
Ti	0.124	0.110	0.120	0.110	0.191	0.184	0.196	0.173	0.166	0.230	0.239	0.225	0.200
Al	2.187	2.240	1.953	2.215	2.406	2.374	2.468	2.387	2.362	1.955	1.987	1.909	1.916
Cr	0.007	0.009	0.009	0.009	0.005	0.005	0.002	0.000	0.000	0.007	0.007	0.007	0.005
Fe	2.137	2.213	2.167	2.224	2.321	2.337	2.332	2.295	2.284	2.523	2.509	2.507	2.500
Mn	0.016	0.016	0.016	0.014	0.014	0.012	0.014	0.016	0.014	0.018	0.018	0.018	0.023
Mg	2.293	2.279	2.374	2.266	1.990	1.994	1.950	2.031	2.017	1.840	1.861	1.886	1.904
Ca	1.801	1.826	1.812	1.831	1.808	1.808	1.796	1.803	1.801	1.877	1.868	1.888	1.849
Na	0.826	0.821	0.787	0.819	0.851	0.890	0.879	0.853	0.849	0.591	0.589	0.603	0.570
K	0.173	0.173	0.159	0.175	0.175	0.170	0.177	0.173	0.191	0.271	0.276	0.242	0.248
Zr	0.005	0.000	0.007	0.000	0.002	0.002	0.000	0.000	0.002	0.000	0.000	0.000	0.000
Total	15.921	15.974	15.886	15.971	15.939	15.964	15.957	15.937	15.932	15.767	15.776	15.764	15.730

Sample	JKEM-10	JKEM-10	JKEM-10	JKEM-10	JKEM-10	JKEM-10	JKEM-10	JKEM-10	JKEM-10	JKEM-10	JKEM-10	JKEM-10	JKEM-10
Mineral	amph	amph	amph	amph	amph	amph	amph	amph	amph	amph	amph	amph	amph
No.	106	107	108	109	110	111	112	156	157	160	166	167	168
Weight %													
SiO2	43.20	42.66	42.26	42.86	43.28	42.71	42.79	41.57	41.79	41.68	43.00	42.66	42.54
TiO2	1.48	1.71	1.70	1.61	1.44	1.59	1.63	1.52	1.75	1.66	1.89	1.69	1.91
Al2O3	10.59	10.88	11.02	10.71	10.26	10.83	10.98	12.27	12.18	12.42	11.13	10.95	11.19
Cr2O3	0.08	0.07	0.09	0.09	0.07	0.02	0.05	0.00	0.00	0.02	0.05	0.02	0.07
FeO	19.66	20.03	20.43	19.80	19.69	19.69	19.92	19.75	19.62	19.49	19.50	19.91	19.94
MnO	0.14	0.17	0.16	0.14	0.13	0.17	0.13	0.12	0.08	0.11	0.13	0.14	0.16
MgO	8.33	8.22	7.93	8.34	8.69	8.24	8.18	8.06	7.90	8.07	8.49	8.44	8.15
CaO	11.55	11.61	11.72	11.63	11.55	11.50	11.51	11.32	11.53	11.40	11.63	11.47	11.37
Na2O	1.82	1.95	1.96	1.92	1.77	1.92	1.93	2.13	2.04	2.04	1.92	1.92	2.02
K2O	1.20	1.40	1.30	1.29	1.17	1.33	1.33	1.44	1.47	1.49	1.25	1.29	1.32
ZrO2	0.00	0.02	0.01	0.00	0.00	0.03	0.00	0.00	0.00	0.00	0.00	0.00	0.00
Total	98.05	98.69	98.57	98.38	98.05	98.03	98.46	98.19	98.36	98.38	98.98	98.50	98.67
No.	106	107	108	109	110	111	112	156	157	160	166	167	168
Cations, O = 6													
Si	6.567	6.472	6.438	6.509	6.578	6.509	6.495	6.337	6.355	6.332	6.475	6.475	6.447
Ti	0.168	0.196	0.193	0.184	0.163	0.182	0.186	0.175	0.200	0.189	0.214	0.193	0.216
Al	1.898	1.946	1.978	1.918	1.838	1.946	1.964	2.206	2.183	2.224	1.973	1.957	1.999
Cr	0.009	0.007	0.012	0.012	0.009	0.002	0.007	0.000	0.000	0.002	0.005	0.002	0.007
Fe	2.500	2.542	2.604	2.514	2.502	2.509	2.530	2.519	2.496	2.477	2.456	2.528	2.528
Mn	0.018	0.023	0.021	0.018	0.016	0.021	0.016	0.016	0.012	0.014	0.016	0.018	0.021
Mg	1.888	1.858	1.801	1.888	1.969	1.872	1.852	1.831	1.792	1.829	1.904	1.909	1.842
Ca	1.881	1.888	1.914	1.893	1.879	1.877	1.872	1.849	1.879	1.856	1.877	1.865	1.847
Na	0.536	0.573	0.577	0.566	0.522	0.568	0.566	0.630	0.603	0.603	0.561	0.564	0.593
K	0.232	0.271	0.253	0.251	0.228	0.260	0.258	0.281	0.285	0.288	0.242	0.251	0.255
Zr	0.000	0.002	0.000	0.000	0.000	0.002	0.000	0.000	0.000	0.000	0.000	0.000	0.000
Total	15.700	15.778	15.792	15.755	15.704	15.750	15.748	15.845	15.806	15.815	15.725	15.764	15.757

Sample	JKEM-10	JKEM-10	JKEM-10	JKEM-10	JKEM-10	JKEM-10	JKEM-10	JKEM-10	JKEM-10
Mineral	amph	amph	amph	amph	amph	amph	amph	amph	amph
No.	169	170	171	200	201	202	203	204	205
Weight %									
SiO2	42.39	42.47	41.95	41.88	41.77	41.51	41.71	41.67	41.68
TiO2	1.67	1.85	1.97	1.83	1.80	1.83	2.02	2.13	1.94
Al2O3	11.12	11.66	11.44	11.66	11.94	11.95	11.63	11.58	11.75
Cr2O3	0.05	0.00	0.02	0.06	0.07	0.07	0.07	0.06	0.06
FeO	19.97	19.62	19.71	20.01	19.82	19.80	19.89	19.96	19.71
MnO	0.13	0.12	0.12	0.20	0.21	0.21	0.21	0.19	0.21
MgO	8.27	8.39	8.13	8.19	8.00	8.02	8.00	8.07	8.11
CaO	11.41	11.56	11.54	11.37	11.37	11.40	11.38	11.22	11.38
Na2O	2.00	2.05	2.03	2.04	2.04	2.07	2.09	2.15	2.04
K2O	1.35	1.29	1.39	1.39	1.53	1.46	1.43	1.50	1.43
ZrO2	0.00	0.00	0.00	0.06	0.08	0.08	0.07	0.08	0.08
Total	98.34	99.00	98.31	98.69	98.62	98.41	98.52	98.61	98.38
No.	169	170	171	200	201	202	203	204	205
Cations, O = 6									
Si	6.449	6.403	6.387	6.362	6.348	6.325	6.350	6.341	6.348
Ti	0.191	0.209	0.225	0.209	0.205	0.209	0.232	0.244	0.223
Al	1.994	2.072	2.054	2.086	2.139	2.146	2.088	2.077	2.109
Cr	0.007	0.000	0.002	0.007	0.009	0.009	0.009	0.007	0.007
Fe	2.542	2.473	2.509	2.542	2.519	2.523	2.532	2.542	2.509
Mn	0.016	0.014	0.016	0.025	0.028	0.028	0.028	0.023	0.028
Mg	1.875	1.886	1.845	1.854	1.812	1.822	1.817	1.831	1.840
Ca	1.861	1.868	1.884	1.849	1.852	1.861	1.856	1.831	1.856
Na	0.589	0.600	0.600	0.600	0.603	0.612	0.619	0.635	0.600
K	0.262	0.248	0.271	0.269	0.297	0.285	0.278	0.292	0.276
Zr	0.000	0.000	0.000	0.005	0.005	0.005	0.005	0.007	0.007
Total	15.785	15.776	15.794	15.808	15.815	15.826	15.817	15.829	15.806

Sample	JKEM-12	JKEM-12	JKEM-12	JKEM-12	JKEM-12	JKEM-12	JKEM-12	JKEM-12	JKEM-12	JKEM-12	JKEM-12	JKEM-12	JKEM-14a
Mineral	bt	bt	bt	bt	bt	bt	bt	bt	bt	bt	bt	bt	bt
No.	151	186	195	197	198	199	200	204	222	241	242	244	279
Weight %													
SiO2	36.45	36.16	35.81	35.92	36.26	36.37	36.10	33.95	36.03	33.63	33.85	33.25	36.01
TiO2	3.62	2.24	4.54	3.59	3.68	3.92	4.15	2.42	4.49	1.84	1.73	2.38	4.92
Al2O3	14.64	15.37	14.62	15.74	15.29	15.18	15.05	18.51	14.46	18.82	18.73	17.84	14.03
Cr2O3	0.04	0.00	0.00	0.00	0.00	0.00	0.00	0.00	0.00	0.00	0.00	0.00	0.00
FeO	19.45	18.60	20.06	17.76	17.50	18.51	18.71	20.00	20.05	20.97	19.93	20.82	22.13
MnO	0.06	0.02	0.03	0.00	0.00	0.00	0.01	0.03	0.01	0.02	0.02	0.04	0.00
MgO	12.43	12.91	11.04	12.65	12.65	12.29	11.92	9.90	11.27	9.96	10.16	9.15	9.44
CaO	0.10	0.04	0.09	0.04	0.00	0.03	0.00	0.07	0.07	0.05	0.08	0.11	0.00
Na2O	0.21	0.04	0.28	0.33	0.29	0.32	0.30	0.05	0.32	0.06	0.06	0.07	0.08
K2O	9.57	10.00	9.04	9.32	9.41	9.39	9.44	9.22	9.33	9.68	9.29	8.86	9.31
ZrO2	0.00	0.00	0.00	0.00	0.00	0.00	0.00	0.00	0.00	0.00	0.00	0.00	0.00
Total	96.57	95.37	95.51	95.36	95.08	96.02	95.67	94.15	96.04	95.03	93.83	92.51	95.92
No.	151	186	195	197	198	199	200	204	222	241	242	244	279
Cations, O = 22													
Si	5.509	5.520	5.482	5.445	5.507	5.496	5.487	5.267	5.493	5.210	5.269	5.280	5.546
Ti	0.411	0.257	0.524	0.409	0.420	0.447	0.473	0.282	0.515	0.213	0.202	0.284	0.570
Al	2.609	2.765	2.638	2.814	2.737	2.704	2.695	3.386	2.598	3.436	3.436	3.337	2.548
Cr	0.004	0.000	0.000	0.000	0.000	0.000	0.000	0.000	0.000	0.000	0.000	0.000	0.000
Fe	2.460	2.374	2.570	2.253	2.224	2.339	2.378	2.596	2.556	2.717	2.594	2.765	2.851
Mn	0.007	0.002	0.004	0.000	0.000	0.000	0.002	0.002	0.000	0.002	0.002	0.004	0.000
Mg	2.801	2.937	2.519	2.858	2.864	2.768	2.702	2.290	2.561	2.301	2.358	2.167	2.167
Ca	0.018	0.007	0.015	0.007	0.000	0.004	0.000	0.013	0.011	0.009	0.013	0.018	0.000
Na	0.062	0.013	0.081	0.099	0.086	0.095	0.088	0.015	0.095	0.018	0.018	0.020	0.022
K	1.846	1.947	1.764	1.804	1.824	1.811	1.830	1.824	1.815	1.914	1.844	1.795	1.830
Zr	0.000	0.000	0.000	0.000	0.000	0.000	0.000	0.000	0.000	0.000	0.000	0.000	0.000
Total	15.728	15.825	15.598	15.690	15.664	15.664	15.657	15.675	15.644	15.822	15.739	15.673	15.534

Sample	JKEM-14a	JKEM-14a	JKEM-14a	JKEM-14a	JKEM-14a	JKEM-14a	JKEM-14a	JKEM-14a	JKEM-14a	JKEM-14a	JKEM-14a	JKEM-14a	JKEM-14a
Mineral	bt	bt	bt	bt	bt	bt	bt	bt	bt	bt	bt	bt	bt
No.	280	281	282	283	284	285	286	287	288	290	293	314	315
Weight %													
SiO2	36.24	36.33	36.55	36.31	35.71	36.45	36.36	36.28	35.56	36.33	36.24	36.14	36.49
TiO2	4.99	5.14	5.00	5.02	4.90	5.05	5.09	5.09	4.87	5.17	5.12	5.80	5.21
Al2O3	14.03	13.94	14.12	14.07	13.91	14.00	13.99	13.95	13.82	13.80	13.91	12.30	13.69
Cr2O3	0.00	0.00	0.00	0.00	0.00	0.00	0.00	0.00	0.00	0.00	0.00	0.02	0.03
FeO	21.88	22.21	21.94	21.91	21.62	22.11	21.88	21.51	21.89	21.80	22.02	26.26	21.95
MnO	0.00	0.00	0.00	0.00	0.00	0.00	0.00	0.00	0.00	0.00	0.00	0.09	0.04
MgO	9.54	9.46	9.67	9.42	9.48	9.44	9.49	9.40	9.45	9.30	9.36	6.20	9.47
CaO	0.00	0.00	0.00	0.00	0.00	0.00	0.00	0.00	0.00	0.00	0.00	0.27	0.02
Na2O	0.08	0.08	0.08	0.05	0.06	0.05	0.04	0.06	0.08	0.06	0.05	0.42	0.20
K2O	9.35	9.43	9.53	9.65	9.02	9.43	9.53	9.38	8.53	9.32	9.35	8.54	9.47
ZrO2	0.00	0.00	0.00	0.00	0.00	0.00	0.00	0.00	0.00	0.00	0.00	0.00	0.00
Total	96.10	96.59	96.88	96.43	94.70	96.53	96.37	95.67	94.20	95.77	96.04	96.05	96.58
No.	280	281	282	283	284	285	286	287	288	290	293	314	315
Cations, O = 6													
Si	5.562	5.557	5.564	5.562	5.557	5.573	5.568	5.584	5.557	5.592	5.570	5.672	5.581
Ti	0.576	0.592	0.572	0.579	0.574	0.581	0.585	0.590	0.572	0.598	0.592	0.684	0.601
Al	2.537	2.515	2.534	2.541	2.550	2.523	2.526	2.532	2.545	2.504	2.519	2.275	2.468
Cr	0.000	0.000	0.000	0.000	0.000	0.000	0.000	0.000	0.000	0.000	0.000	0.002	0.004
Fe	2.809	2.842	2.794	2.807	2.814	2.827	2.803	2.770	2.860	2.807	2.829	3.445	2.807
Mn	0.000	0.000	0.000	0.000	0.000	0.000	0.000	0.000	0.000	0.000	0.000	0.011	0.004
Mg	2.185	2.158	2.196	2.149	2.198	2.152	2.165	2.156	2.202	2.134	2.145	1.450	2.160
Ca	0.000	0.000	0.000	0.000	0.000	0.000	0.000	0.000	0.000	0.000	0.000	0.046	0.002
Na	0.022	0.022	0.022	0.013	0.018	0.015	0.011	0.018	0.022	0.018	0.015	0.128	0.062
K	1.830	1.839	1.850	1.885	1.791	1.839	1.861	1.841	1.701	1.830	1.833	1.709	1.848
Zr	0.000	0.000	0.000	0.000	0.000	0.000	0.000	0.000	0.000	0.000	0.000	0.000	0.000
Total	15.523	15.528	15.532	15.539	15.503	15.512	15.519	15.492	15.462	15.486	15.506	15.422	15.541

Sample	JKEM-14a	JKEM-14a	JKEM-14a	JKEM-14a	JKEM-14a	JKEM-14a	JKEM-14a	JKEM-14a	JKEM-15a	JKEM-15a	JKEM-15a	JKEM-15a	JKEM-01
Mineral	bt	bt	bt	bt	bt	bt	bt	bt	bt	bt	bt	bt	bt
No.	318	319	332	356	359	360	362	363	114	77	78	79	44
Weight %													
SiO2	36.51	35.82	36.54	37.13	36.81	37.08	35.85	36.21	36.80	36.55	36.58	36.26	36.26
TiO2	5.74	5.46	4.88	5.09	5.34	5.39	5.11	4.08	4.02	3.34	3.47	3.34	6.62
Al2O3	13.95	13.89	14.33	13.98	13.92	14.17	13.89	13.72	14.88	14.80	15.00	14.14	14.06
Cr2O3	0.03	0.03	0.00	0.00	0.00	0.00	0.00	0.00	0.04	0.00	0.00	0.00	0.06
FeO	22.84	22.78	20.49	17.75	19.98	19.71	20.68	20.31	18.88	16.76	17.62	18.59	21.47
MnO	0.05	0.04	0.02	0.04	0.03	0.05	0.02	0.02	0.03	0.00	0.00	0.00	0.06
MgO	9.19	9.05	10.99	12.59	10.86	11.46	10.54	11.79	12.58	13.43	13.23	13.08	9.14
CaO	0.00	0.01	0.04	0.05	0.10	0.09	0.04	0.02	0.02	0.00	0.00	0.00	0.16
Na2O	0.21	0.25	0.25	0.05	0.26	0.29	0.35	0.25	0.35	0.34	0.42	0.32	0.28
K2O	9.51	9.57	9.34	9.76	8.99	9.29	8.38	8.68	9.44	8.57	9.23	8.40	9.41
ZrO2	0.00	0.00	0.00	0.00	0.00	0.00	0.00	0.00	0.03	0.00	0.00	0.00	0.02
Total	98.04	96.90	96.88	96.43	96.27	97.53	94.86	95.07	97.04	93.79	95.56	94.12	97.53
No.	318	319	332	356	359	360	362	363	114	77	78	79	44
Cations, O = 6													
Si	5.522	5.496	5.524	5.573	5.575	5.540	5.526	5.564	5.509	5.579	5.524	5.570	5.482
Ti	0.653	0.629	0.554	0.574	0.607	0.605	0.592	0.471	0.453	0.383	0.394	0.385	0.752
Al	2.486	2.512	2.554	2.473	2.484	2.497	2.526	2.486	2.625	2.662	2.671	2.559	2.506
Cr	0.004	0.004	0.000	0.000	0.000	0.000	0.000	0.000	0.004	0.000	0.000	0.000	0.007
Fe	2.889	2.924	2.592	2.229	2.530	2.464	2.666	2.609	2.365	2.138	2.226	2.387	2.715
Mn	0.007	0.004	0.002	0.004	0.004	0.007	0.002	0.002	0.004	0.000	0.000	0.000	0.007
Mg	2.072	2.070	2.475	2.816	2.451	2.552	2.422	2.699	2.807	3.056	2.979	2.994	2.059
Ca	0.000	0.002	0.007	0.007	0.015	0.013	0.007	0.002	0.002	0.000	0.000	0.000	0.026
Na	0.064	0.075	0.073	0.013	0.075	0.086	0.103	0.075	0.101	0.101	0.123	0.095	0.081
K	1.835	1.872	1.802	1.870	1.738	1.771	1.648	1.701	1.804	1.670	1.780	1.646	1.815
Zr	0.000	0.000	0.000	0.000	0.000	0.000	0.000	0.000	0.002	0.000	0.000	0.000	0.002
Total	15.532	15.589	15.585	15.561	15.479	15.534	15.492	15.611	15.679	15.589	15.697	15.635	15.455

Sample	JKEM-01	JKEM-01	JKEM-01	JKEM-01	JKEM-01	JKEM-01	JKEM-01	JKEM-01	JKEM-01	JKEM-01	JKEM-01	JKEM-01	JKEM-01
Mineral	bt	bt	bt	bt	bt	bt	bt	bt	bt	bt	bt	bt	bt
No.	66	67	68	69	70	71	72	73	74	90	91	92	93
Weight %													
SiO2	35.73	36.49	36.25	36.18	35.57	36.24	36.13	36.40	36.04	36.40	36.62	36.14	36.45
TiO2	6.11	6.36	6.26	6.14	6.13	6.10	6.15	6.25	6.18	6.13	6.19	6.24	6.17
Al2O3	13.73	14.07	14.12	13.89	13.90	14.12	14.05	14.11	13.98	13.84	13.84	13.89	13.82
Cr2O3	0.00	0.00	0.00	0.00	0.00	0.00	0.00	0.00	0.00	0.00	0.00	0.00	0.00
FeO	20.73	21.12	20.90	20.86	20.84	21.03	20.84	21.09	20.82	21.14	21.04	21.04	21.13
MnO	0.05	0.05	0.04	0.02	0.03	0.06	0.03	0.06	0.06	0.04	0.06	0.03	0.04
MgO	9.72	9.95	9.87	9.72	9.70	9.87	9.78	9.75	9.77	10.00	10.12	9.83	9.90
CaO	0.01	0.01	0.00	0.01	0.04	0.08	0.00	0.01	0.02	0.00	0.03	0.02	0.03
Na2O	0.21	0.22	0.20	0.21	0.26	0.22	0.19	0.23	0.19	0.19	0.21	0.26	0.21
K2O	8.81	9.66	9.68	9.31	9.23	9.48	9.46	9.34	9.07	9.53	9.64	9.23	9.50
ZrO2	0.00	0.00	0.00	0.01	0.00	0.00	0.00	0.00	0.00	0.00	0.00	0.01	0.01
Total	95.09	97.94	97.30	96.35	95.69	97.20	96.63	97.23	96.13	97.27	97.74	96.69	97.26
No.	66	67	68	69	70	71	72	73	74	90	91	92	93
Cations, O = 6													
Si	5.511	5.485	5.482	5.518	5.471	5.487	5.498	5.502	5.502	5.509	5.513	5.496	5.515
Ti	0.708	0.719	0.713	0.704	0.711	0.695	0.704	0.711	0.711	0.697	0.702	0.715	0.702
Al	2.495	2.493	2.517	2.497	2.519	2.519	2.519	2.515	2.515	2.468	2.455	2.488	2.466
Cr	0.000	0.000	0.000	0.000	0.000	0.000	0.000	0.000	0.000	0.000	0.000	0.000	0.000
Fe	2.675	2.655	2.644	2.660	2.680	2.662	2.651	2.666	2.658	2.675	2.649	2.675	2.675
Mn	0.007	0.007	0.004	0.002	0.004	0.009	0.004	0.007	0.007	0.004	0.009	0.004	0.004
Mg	2.235	2.231	2.224	2.211	2.224	2.229	2.218	2.196	2.224	2.257	2.270	2.229	2.233
Ca	0.002	0.002	0.000	0.002	0.007	0.013	0.000	0.002	0.002	0.000	0.004	0.002	0.004
Na	0.062	0.062	0.057	0.062	0.077	0.064	0.057	0.068	0.055	0.055	0.062	0.077	0.062
K	1.734	1.852	1.868	1.811	1.813	1.830	1.835	1.800	1.767	1.841	1.852	1.791	1.835
Zr	0.000	0.000	0.000	0.000	0.000	0.000	0.000	0.000	0.000	0.000	0.000	0.000	0.000
Total	15.431	15.508	15.510	15.468	15.508	15.510	15.486	15.468	15.440	15.510	15.517	15.479	15.497

Sample	JKEM-01	JKEM-02	JKEM-02	JKEM-02	JKEM-02	JKEM-02	JKEM-02	JKEM-02	JKEM-02	JKEM-02	JKEM-02	JKEM-02	JKEM-02
Mineral	bt	bt	bt	bt	bt	bt	bt	bt	bt	bt	bt	bt	bt
No.	94	167	168	169	170	171	184	213	214	215	216	206	207
Weight %													
SiO2	36.42	35.07	35.80	35.55	35.79	35.46	35.35	36.19	35.96	36.09	35.72	36.47	36.53
TiO2	6.10	5.86	6.20	5.99	6.07	5.97	6.08	6.16	6.16	6.34	5.92	5.60	5.46
Al2O3	13.83	13.07	13.49	13.37	13.48	13.14	13.83	14.04	14.14	13.86	14.22	13.76	13.91
Cr2O3	0.00	0.00	0.00	0.00	0.00	0.00	0.00	0.00	0.04	0.00	0.00	0.10	0.11
FeO	20.97	22.78	23.19	23.10	23.29	22.43	22.81	22.07	21.67	21.69	21.48	20.39	20.25
MnO	0.03	0.00	0.00	0.00	0.00	0.00	0.00	0.05	0.05	0.06	0.04	0.13	0.09
MgO	10.03	8.19	8.40	8.34	8.37	8.25	8.40	9.41	9.29	9.15	9.59	10.66	10.91
CaO	0.04	0.13	0.00	0.00	0.00	0.00	0.00	0.08	0.00	0.00	0.00	0.09	0.07
Na2O	0.22	0.09	0.05	0.06	0.00	0.00	0.22	0.17	0.17	0.14	0.14	0.05	0.05
K2O	9.45	9.28	9.62	9.62	9.69	9.57	9.39	9.48	9.51	9.64	9.66	9.51	9.82
ZrO2	0.00	0.00	0.00	0.00	0.00	0.00	0.00	0.00	0.02	0.00	0.00	0.01	0.00
Total	97.09	94.47	96.73	96.04	96.69	94.82	96.06	97.64	97.02	96.96	96.77	96.76	97.19
No.	94	167	168	169	170	171	184	213	214	215	216	206	207
Cations, O = 6													
Si	5.515	5.531	5.513	5.520	5.520	5.562	5.474	5.480	5.476	5.502	5.454	5.531	5.518
Ti	0.695	0.695	0.717	0.700	0.704	0.704	0.708	0.702	0.706	0.728	0.680	0.638	0.620
Al	2.468	2.429	2.449	2.446	2.451	2.429	2.523	2.506	2.537	2.490	2.559	2.460	2.477
Cr	0.000	0.000	0.000	0.000	0.000	0.000	0.000	0.000	0.004	0.000	0.000	0.011	0.013
Fe	2.655	3.005	2.988	3.001	3.003	2.941	2.955	2.794	2.759	2.765	2.743	2.585	2.559
Mn	0.004	0.000	0.000	0.000	0.000	0.000	0.000	0.007	0.007	0.007	0.004	0.015	0.011
Mg	2.264	1.925	1.927	1.929	1.923	1.929	1.938	2.123	2.108	2.079	2.185	2.411	2.457
Ca	0.007	0.022	0.000	0.000	0.000	0.000	0.000	0.013	0.000	0.000	0.000	0.015	0.011
Na	0.064	0.026	0.013	0.020	0.000	0.000	0.064	0.051	0.051	0.040	0.042	0.015	0.013
K	1.824	1.868	1.892	1.905	1.907	1.914	1.855	1.833	1.846	1.874	1.881	1.839	1.892
Zr	0.000	0.000	0.000	0.000	0.000	0.000	0.000	0.000	0.002	0.000	0.000	0.000	0.000
Total	15.499	15.503	15.501	15.523	15.508	15.481	15.519	15.510	15.495	15.486	15.550	15.523	15.574

Sample	JKEM-02	JKEM-14b	JKEM-14b	JKEM-14b	JKEM-14b	JKEM-14b	JKEM-14b	JKEM-15b	JKEM-15b	JKEM-15b	JKEM-15b	JKEM-15b	JKEM-15b
Mineral	bt	bt	bt	bt	bt	bt	bt	bt	bt	bt	bt	bt	bt
No.	208	34	82	119	120	121	122	266	267	268	269	270	287
Weight %													
SiO2	36.02	34.94	34.12	36.67	36.82	36.53	35.54	35.59	36.25	35.45	35.89	35.76	33.44
TiO2	5.53	2.84	3.02	2.17	2.25	2.09	3.42	3.49	3.27	3.70	3.49	3.57	3.87
Al2O3	13.67	16.71	17.94	17.22	17.10	17.18	16.21	14.89	15.55	14.86	14.74	14.82	16.94
Cr2O3	0.07	0.08	0.07	0.00	0.00	0.00	0.00	0.04	0.03	0.02	0.00	0.02	0.00
FeO	20.73	16.16	17.66	12.29	12.93	12.50	16.75	18.75	17.67	18.61	18.18	18.76	20.26
MnO	0.08	0.03	0.03	0.01	0.00	0.01	0.03	0.04	0.05	0.03	0.05	0.05	0.00
MgO	10.24	13.17	11.30	16.62	16.39	16.80	13.24	11.25	12.56	11.37	11.96	11.65	9.28
CaO	0.09	0.09	0.16	0.00	0.01	0.01	0.10	0.04	0.02	0.06	0.02	0.01	0.00
Na2O	0.05	0.19	0.26	0.43	0.39	0.41	0.37	0.32	0.32	0.31	0.34	0.30	0.17
K2O	9.68	8.68	9.15	9.28	9.08	8.94	9.14	8.55	9.22	9.15	9.26	9.05	8.88
ZrO2	0.04	0.04	0.02	0.00	0.00	0.00	0.01	0.00	0.05	0.02	0.04	0.00	0.00
Total	96.20	92.93	93.73	94.68	94.95	94.46	94.81	92.95	94.98	93.56	93.97	93.99	92.84
No.	208	34	82	119	120	121	122	266	267	268	269	270	287
Cations, O = 6													
Si	5.518	5.383	5.267	5.434	5.447	5.423	5.394	5.548	5.511	5.511	5.544	5.529	5.282
Ti	0.638	0.330	0.352	0.242	0.251	0.233	0.392	0.409	0.374	0.433	0.405	0.414	0.460
Al	2.468	3.034	3.265	3.010	2.983	3.005	2.900	2.737	2.785	2.724	2.684	2.702	3.155
Cr	0.009	0.009	0.009	0.000	0.000	0.000	0.000	0.004	0.004	0.002	0.000	0.002	0.000
Fe	2.655	2.083	2.281	1.522	1.599	1.551	2.125	2.446	2.246	2.420	2.347	2.424	2.677
Mn	0.011	0.004	0.004	0.002	0.000	0.000	0.004	0.007	0.007	0.004	0.007	0.007	0.000
Mg	2.336	3.023	2.600	3.672	3.615	3.718	2.996	2.614	2.845	2.633	2.754	2.684	2.187
Ca	0.015	0.015	0.026	0.000	0.000	0.000	0.015	0.007	0.002	0.009	0.002	0.002	0.000
Na	0.015	0.057	0.079	0.123	0.112	0.119	0.110	0.097	0.095	0.095	0.101	0.090	0.053
K	1.892	1.707	1.802	1.753	1.714	1.694	1.769	1.701	1.786	1.815	1.826	1.784	1.791
Zr	0.002	0.002	0.002	0.000	0.000	0.000	0.000	0.000	0.004	0.002	0.002	0.000	0.000
Total	15.563	15.649	15.688	15.759	15.721	15.745	15.706	15.569	15.660	15.651	15.675	15.640	15.605

Sample	JKEM-15b	JKEM-15b	JKEM-15b	JKEM-15b	JKEM-10	JKEM-10	JKEM-10	JKEM-10	JKEM-10	JKEM-10	JKEM-10	JKEM-10	JKEM-10
Mineral	bt	bt	bt	bt	bt	bt	bt	bt	bt	bt	bt	bt	bt
No.	288	289	290	291	144	145	146	147	148	192	193	194	195
Weight %													
SiO2	33.52	33.46	33.11	33.51	36.22	36.00	36.12	36.70	35.78	35.82	35.81	36.04	36.02
TiO2	2.92	2.82	2.93	2.93	4.54	4.38	3.37	3.00	4.44	4.23	4.53	4.26	4.39
Al2O3	17.70	17.74	17.69	17.00	14.39	14.32	14.54	14.09	14.48	14.14	14.02	13.99	14.24
Cr2O3	0.00	0.00	0.00	0.00	0.00	0.00	0.00	0.00	0.00	0.07	0.06	0.08	0.09
FeO	19.32	19.39	19.49	19.62	21.67	21.58	19.68	20.51	21.57	20.55	20.79	20.75	20.69
MnO	0.00	0.00	0.00	0.00	0.06	0.03	0.00	0.02	0.03	0.08	0.09	0.10	0.10
MgO	10.05	9.77	9.80	10.19	9.58	9.45	11.25	11.27	9.53	10.37	9.94	10.27	10.09
CaO	0.00	0.00	0.00	0.00	0.00	0.06	0.13	0.15	0.01	0.05	0.06	0.04	0.07
Na2O	0.16	0.15	0.19	0.13	0.07	0.09	0.11	0.07	0.08	0.21	0.19	0.19	0.17
K2O	8.94	8.80	8.63	8.53	9.81	9.38	8.98	8.82	9.60	9.36	9.47	9.44	9.51
ZrO2	0.00	0.00	0.00	0.00	0.00	0.00	0.00	0.00	0.00	0.08	0.06	0.05	0.06
Total	92.61	92.11	91.83	91.91	96.33	95.29	94.17	94.62	95.52	94.95	95.01	95.23	95.42
No.	288	289	290	291	144	145	146	147	148	192	193	194	195
Cations, O = 6													
Si	5.278	5.293	5.260	5.317	5.553	5.570	5.588	5.661	5.531	5.546	5.551	5.568	5.553
Ti	0.345	0.337	0.350	0.350	0.524	0.510	0.392	0.348	0.517	0.493	0.528	0.495	0.508
Al	3.285	3.309	3.313	3.179	2.600	2.611	2.651	2.561	2.638	2.581	2.561	2.548	2.587
Cr	0.000	0.000	0.000	0.000	0.000	0.000	0.000	0.000	0.000	0.009	0.007	0.009	0.011
Fe	2.543	2.565	2.589	2.603	2.779	2.792	2.545	2.644	2.787	2.660	2.695	2.682	2.669
Mn	0.000	0.000	0.000	0.000	0.009	0.004	0.000	0.002	0.004	0.011	0.011	0.013	0.013
Mg	2.358	2.303	2.321	2.411	2.191	2.180	2.594	2.592	2.196	2.394	2.297	2.367	2.319
Ca	0.000	0.000	0.000	0.000	0.000	0.009	0.022	0.024	0.002	0.009	0.011	0.007	0.011
Na	0.048	0.044	0.057	0.037	0.020	0.026	0.033	0.020	0.024	0.062	0.057	0.057	0.051
K	1.795	1.775	1.749	1.727	1.918	1.852	1.771	1.736	1.894	1.848	1.874	1.861	1.870
Zr	0.000	0.000	0.000	0.000	0.000	0.000	0.000	0.000	0.000	0.007	0.004	0.004	0.004
Total	15.653	15.627	15.640	15.627	15.596	15.556	15.596	15.587	15.594	15.618	15.596	15.613	15.598

Sample	JKEM-10	JKEM-10	JKEM-10	JKEM-10
Mineral	bt	bt	bt	bt
No.	196	197	198	199
Weight %				
SiO2	35.86	36.14	36.03	36.45
TiO2	4.76	4.85	4.47	4.36
Al2O3	14.00	14.06	14.24	14.25
Cr2O3	0.09	0.09	0.09	0.08
FeO	21.56	21.51	21.14	21.00
MnO	0.09	0.11	0.09	0.10
MgO	9.57	9.78	10.15	10.39
CaO	0.05	0.04	0.06	0.05
Na2O	0.14	0.17	0.17	0.16
K2O	9.40	9.68	9.40	9.52
ZrO2	0.08	0.05	0.06	0.05
Total	95.61	96.46	95.89	96.41
No.	196	197	198	199
Cations, O = 6				
Si	5.542	5.535	5.535	5.562
Ti	0.554	0.559	0.517	0.499
Al	2.550	2.539	2.578	2.563
Cr	0.011	0.011	0.011	0.009
Fe	2.785	2.757	2.715	2.680
Mn	0.011	0.015	0.011	0.013
Mg	2.204	2.233	2.325	2.361
Ca	0.009	0.007	0.009	0.009
Na	0.044	0.048	0.051	0.048
K	1.852	1.892	1.841	1.852
Zr	0.007	0.004	0.004	0.004
Total	15.569	15.602	15.600	15.602

Sample	JKEM-12	JKEM-12	JKEM-12	JKEM-12	JKEM-12	JKEM-12	JKEM-12	JKEM-12	JKEM-12	JKEM-12	JKEM-12	JKEM-12	JKEM-12
Mineral	grt	grt	grt	grt	grt	grt	grt	grt	grt	grt	grt	grt	grt
No.	135	136	137	138	139	140	141	142	181	185	187	188	205
Weight %													
SiO2	38.63	38.51	38.70	38.79	38.48	38.83	38.61	38.61	38.22	38.60	38.47	38.42	38.43
TiO2	0.10	0.08	0.13	0.10	0.07	0.08	0.10	0.10	0.00	0.03	0.02	0.00	0.02
Al2O3	21.43	21.31	21.41	21.37	21.49	20.93	21.34	21.21	21.35	21.36	21.28	21.14	21.31
Cr2O3	0.08	0.07	0.07	0.05	0.06	0.11	0.10	0.08	0.00	0.00	0.00	0.00	0.00
FeO	28.75	28.53	28.26	29.78	30.20	29.67	30.04	30.18	31.69	28.85	30.38	30.66	30.41
MnO	1.10	1.08	1.11	1.14	1.23	1.33	1.34	1.45	1.51	1.17	1.36	1.49	1.31
MgO	4.06	3.85	4.10	4.23	4.06	3.70	3.78	3.42	3.32	3.60	3.47	3.15	3.68
CaO	6.93	6.76	7.64	6.47	6.02	6.86	6.55	6.47	5.04	7.43	6.08	6.58	6.13
Na2O	0.00	0.01	0.01	0.01	0.00	0.00	0.00	0.00	0.00	0.01	0.01	0.00	0.00
K2O	0.04	0.04	0.03	0.04	0.03	0.03	0.02	0.03	0.02	0.00	0.03	0.01	0.01
ZrO2	0.00	0.00	0.00	0.00	0.00	0.00	0.00	0.00	0.00	0.00	0.00	0.00	0.00
Total	101.11	100.22	101.46	101.98	101.63	101.54	101.87	101.55	101.15	101.05	101.09	101.45	101.28
No.	135	136	137	138	139	140	141	142	181	185	187	188	205
Cations, O = 12													
Si	3.012	3.026	3.007	3.008	3.000	3.030	3.006	3.019	3.011	3.018	3.020	3.016	3.011
Ti	0.006	0.005	0.008	0.006	0.004	0.005	0.006	0.006	0.000	0.001	0.001	0.000	0.001
Al	1.970	1.974	1.961	1.954	1.974	1.926	1.958	1.955	1.982	1.968	1.969	1.956	1.968
Cr	0.005	0.004	0.005	0.002	0.004	0.006	0.006	0.005	0.000	0.000	0.000	0.000	0.000
Fe	1.874	1.876	1.836	1.932	1.969	1.937	1.956	1.974	2.088	1.886	1.994	2.012	1.993
Mn	0.073	0.072	0.073	0.076	0.082	0.088	0.088	0.096	0.101	0.078	0.090	0.098	0.086
Mg	0.472	0.451	0.475	0.488	0.472	0.431	0.439	0.398	0.390	0.420	0.407	0.368	0.430
Ca	0.578	0.570	0.636	0.538	0.503	0.574	0.546	0.541	0.425	0.623	0.511	0.553	0.515
Na	0.000	0.001	0.002	0.001	0.000	0.000	0.000	0.000	0.000	0.001	0.001	0.000	0.000
K	0.004	0.005	0.004	0.004	0.004	0.004	0.002	0.004	0.002	0.000	0.002	0.001	0.001
Zr	0.000	0.000	0.000	0.000	0.000	0.000	0.000	0.000	0.000	0.000	0.000	0.000	0.000
Total	7.994	7.985	8.008	8.010	8.010	7.999	8.008	7.998	7.999	7.997	7.998	8.005	8.006

Sample	JKEM-12	JKEM-12	JKEM-12	JKEM-12	JKEM-12	JKEM-12	JKEM-14a	JKEM-14a	JKEM-14a	JKEM-14a	JKEM-14a	JKEM-14a	JKEM-14a
Mineral	grt	grt	grt	grt	grt	grt	grt	grt	grt	grt	grt	grt	grt
No.	206	207	208	209	210	211	289	292	296	297	298	302	326
Weight %													
SiO2	38.48	38.61	38.36	38.36	38.59	38.30	36.85	36.64	37.22	37.14	37.37	37.47	36.83
TiO2	0.01	0.01	0.02	0.05	0.02	0.00	0.00	0.00	0.00	0.01	0.00	0.00	0.07
Al2O3	21.34	21.36	21.15	21.33	21.17	21.26	20.86	20.49	20.90	20.87	20.92	20.79	21.23
Cr2O3	0.04	0.03	0.05	0.04	0.03	0.00	0.00	0.00	0.00	0.00	0.00	0.01	0.04
FeO	30.36	30.24	30.54	30.79	30.98	31.16	30.68	30.41	29.68	30.10	29.65	29.69	30.23
MnO	1.27	1.29	1.26	1.23	1.33	1.22	1.50	1.34	1.43	1.42	1.47	1.39	1.71
MgO	3.78	3.60	3.62	3.62	3.38	3.66	2.23	2.44	3.18	2.97	3.22	3.19	3.22
CaO	6.05	6.35	6.08	5.92	5.99	5.76	6.56	6.46	6.73	6.63	6.70	6.74	6.32
Na2O	0.00	0.00	0.00	0.00	0.00	0.00	0.00	0.00	0.01	0.03	0.01	0.01	0.00
K2O	0.02	0.02	0.03	0.03	0.01	0.01	0.03	0.01	0.02	0.03	0.03	0.03	0.03
ZrO2	0.00	0.00	0.00	0.00	0.00	0.00	0.00	0.00	0.00	0.00	0.00	0.00	0.00
Total	101.35	101.50	101.10	101.39	101.51	101.37	98.71	97.80	99.18	99.20	99.35	99.30	99.67
No.	206	207	208	209	210	211	289	292	296	297	298	302	326
Cations, O = 6													
Si	3.011	3.016	3.014	3.006	3.023	3.006	2.990	2.998	2.989	2.989	2.994	3.004	2.953
Ti	0.001	0.001	0.001	0.004	0.001	0.000	0.000	0.000	0.000	0.000	0.000	0.000	0.004
Al	1.969	1.967	1.958	1.970	1.955	1.967	1.994	1.976	1.979	1.979	1.976	1.964	2.006
Cr	0.002	0.001	0.002	0.002	0.002	0.000	0.000	0.000	0.000	0.000	0.000	0.000	0.002
Fe	1.987	1.976	2.006	2.018	2.029	2.045	2.082	2.081	1.994	2.026	1.987	1.990	2.027
Mn	0.084	0.085	0.084	0.082	0.088	0.082	0.103	0.094	0.097	0.097	0.100	0.094	0.116
Mg	0.442	0.419	0.425	0.424	0.395	0.428	0.270	0.298	0.380	0.355	0.384	0.382	0.385
Ca	0.506	0.532	0.511	0.497	0.503	0.484	0.570	0.566	0.578	0.571	0.575	0.578	0.542
Na	0.000	0.000	0.000	0.000	0.000	0.000	0.000	0.000	0.001	0.005	0.001	0.001	0.000
K	0.001	0.001	0.002	0.002	0.001	0.000	0.004	0.001	0.002	0.004	0.002	0.002	0.002
Zr	0.000	0.000	0.000	0.000	0.000	0.000	0.000	0.000	0.000	0.000	0.000	0.000	0.000
Total	8.005	7.998	8.005	8.006	7.997	8.012	8.014	8.015	8.023	8.026	8.020	8.017	8.040

Sample	JKEM-14a	JKEM-14a	JKEM-14a	JKEM-14a	JKEM-14a	JKEM-14a	JKEM-14a	JKEM-15a	JKEM-15a	JKEM-15a	JKEM-15a	JKEM-15a	JKEM-15a
Mineral	grt	grt	grt	grt	grt	grt	grt	grt	grt	grt	grt	grt	grt
No.	327	345	346	348	349	350	351	44	45	46	51	52	53
Weight %													
SiO2	37.03	37.20	37.34	37.23	37.40	37.21	37.14	37.34	37.31	37.31	37.15	36.94	37.26
TiO2	0.06	0.02	0.02	0.02	0.00	0.00	0.03	0.03	0.05	0.01	0.04	0.02	0.06
Al2O3	20.88	21.14	20.98	21.08	20.85	21.29	21.07	21.53	21.31	21.50	21.53	21.43	21.44
Cr2O3	0.03	0.02	0.00	0.02	0.00	0.00	0.00	0.04	0.01	0.00	0.00	0.03	0.00
FeO	30.19	27.98	29.47	29.66	29.59	29.68	30.15	29.79	29.53	29.93	29.70	29.79	29.51
MnO	1.70	1.14	1.21	1.22	1.33	1.30	1.41	1.50	1.46	1.60	1.45	1.47	1.46
MgO	2.91	3.98	4.05	3.87	3.64	3.72	2.96	3.85	3.66	3.79	3.90	3.79	3.84
CaO	6.31	7.12	6.23	6.24	6.35	6.24	6.64	6.45	6.28	6.35	6.53	6.50	6.43
Na2O	0.00	0.03	0.03	0.03	0.02	0.00	0.00	0.03	0.00	0.00	0.01	0.01	0.00
K2O	0.02	0.03	0.03	0.03	0.02	0.03	0.05	0.02	0.03	0.03	0.03	0.04	0.04
ZrO2	0.00	0.00	0.00	0.00	0.00	0.00	0.00	0.00	0.01	0.00	0.04	0.00	0.03
Total	99.13	98.67	99.34	99.40	99.21	99.46	99.44	100.58	99.65	100.51	100.37	100.00	100.08
No.	327	345	346	348	349	350	351	44	45	46	51	52	53
Cations, O = 6													
Si	2.984	2.980	2.983	2.976	2.995	2.972	2.980	2.953	2.975	2.956	2.946	2.944	2.958
Ti	0.004	0.001	0.001	0.001	0.000	0.000	0.002	0.002	0.002	0.001	0.002	0.001	0.004
Al	1.984	1.996	1.976	1.986	1.969	2.005	1.993	2.008	2.003	2.008	2.012	2.012	2.008
Cr	0.002	0.001	0.000	0.001	0.000	0.000	0.000	0.002	0.001	0.000	0.000	0.001	0.000
Fe	2.034	1.874	1.968	1.984	1.982	1.982	2.023	1.970	1.968	1.982	1.969	1.985	1.960
Mn	0.116	0.077	0.082	0.083	0.090	0.088	0.096	0.101	0.098	0.107	0.097	0.100	0.098
Mg	0.349	0.475	0.482	0.461	0.434	0.443	0.354	0.455	0.436	0.448	0.461	0.450	0.455
Ca	0.545	0.611	0.533	0.535	0.545	0.534	0.570	0.547	0.536	0.539	0.554	0.554	0.547
Na	0.000	0.005	0.004	0.005	0.004	0.000	0.001	0.005	0.000	0.000	0.001	0.001	0.000
K	0.002	0.002	0.002	0.004	0.002	0.004	0.005	0.002	0.002	0.004	0.004	0.004	0.005
Zr	0.000	0.000	0.000	0.000	0.000	0.000	0.000	0.000	0.000	0.000	0.001	0.000	0.001
Total	8.021	8.024	8.032	8.034	8.022	8.027	8.024	8.046	8.022	8.044	8.050	8.053	8.036

Sample	JKEM-15a	JKEM-15a	JKEM-15a	JKEM-15a	JKEM-15a	JKEM-15a	JKEM-15a	JKEM-15a	JKEM-15a	JKEM-15a	JKEM-15a	JKEM-01	JKEM-01
Mineral	grt	grt	grt	grt	grt	grt	grt	grt	grt	grt	grt	grt	grt
No.	54	55	56	68	96	97	98	99	100	101	102	45	46
Weight %													
SiO2	37.54	37.56	37.42	37.15	37.61	37.27	37.00	37.23	37.24	37.39	37.91	37.15	37.16
TiO2	0.07	0.03	0.07	0.02	0.08	0.08	0.12	0.11	0.09	0.08	0.08	0.06	0.01
Al2O3	21.29	21.26	21.41	21.23	21.05	21.30	21.36	21.09	21.17	21.54	21.43	20.72	20.66
Cr2O3	0.03	0.03	0.02	0.07	0.14	0.10	0.11	0.13	0.11	0.10	0.11	0.06	0.07
FeO	29.58	29.55	28.88	29.54	31.11	30.68	31.14	31.35	31.11	29.83	28.58	30.38	30.82
MnO	1.37	1.36	1.30	1.63	1.49	1.42	1.50	1.54	1.53	1.23	1.15	1.84	1.85
MgO	4.06	4.08	3.94	3.46	3.63	3.90	3.63	3.56	3.66	4.48	4.71	2.58	2.56
CaO	6.40	6.40	7.00	6.59	5.64	5.67	5.58	5.55	5.65	5.97	6.47	6.41	6.34
Na2O	0.00	0.01	0.00	0.00	0.03	0.04	0.04	0.03	0.01	0.03	0.02	0.03	0.01
K2O	0.04	0.03	0.03	0.02	0.06	0.05	0.06	0.06	0.05	0.04	0.04	0.04	0.03
ZrO2	0.01	0.00	0.00	0.03	0.04	0.06	0.02	0.04	0.08	0.03	0.01	0.05	0.02
Total	100.39	100.29	100.06	99.74	100.88	100.58	100.55	100.69	100.69	100.72	100.50	99.31	99.53
No.	54	55	56	68	96	97	98	99	100	101	102	45	46
Cations, O = 6													
Si	2.969	2.972	2.965	2.966	2.977	2.956	2.944	2.960	2.958	2.947	2.977	2.994	2.994
Ti	0.004	0.001	0.004	0.001	0.005	0.005	0.007	0.006	0.005	0.005	0.005	0.004	0.000
Al	1.985	1.984	1.999	1.998	1.964	1.991	2.003	1.976	1.981	2.002	1.984	1.969	1.962
Cr	0.001	0.001	0.001	0.004	0.008	0.006	0.007	0.008	0.007	0.006	0.006	0.004	0.004
Fe	1.957	1.956	1.914	1.973	2.060	2.035	2.071	2.084	2.066	1.966	1.877	2.047	2.076
Mn	0.092	0.091	0.086	0.110	0.100	0.096	0.101	0.104	0.102	0.082	0.077	0.126	0.126
Mg	0.479	0.481	0.466	0.412	0.428	0.461	0.430	0.421	0.433	0.527	0.551	0.311	0.308
Ca	0.542	0.542	0.594	0.563	0.479	0.482	0.475	0.473	0.480	0.504	0.545	0.553	0.547
Na	0.000	0.001	0.001	0.000	0.005	0.006	0.006	0.005	0.002	0.005	0.002	0.005	0.002
K	0.004	0.002	0.002	0.002	0.006	0.006	0.006	0.006	0.005	0.005	0.004	0.004	0.004
Zr	0.000	0.000	0.000	0.001	0.001	0.002	0.001	0.001	0.002	0.001	0.000	0.002	0.001
Total	8.033	8.033	8.033	8.032	8.035	8.046	8.051	8.047	8.042	8.050	8.027	8.020	8.024

Sample	JKEM-01	JKEM-01	JKEM-01	JKEM-01	JKEM-01	JKEM-01	JKEM-01	JKEM-01	JKEM-01	JKEM-01	JKEM-02	JKEM-02	JKEM-02
Mineral	grt	grt	grt	grt	grt	grt	grt	grt	grt	grt	grt	grt	grt
No.	49	75	76	77	78	79	80	81	82	83	201	202	203
Weight %													
SiO2	37.27	37.06	37.26	37.32	37.11	37.27	37.35	37.09	37.13	37.35	37.25	36.98	36.97
TiO2	0.03	0.02	0.06	0.04	0.06	0.00	0.01	0.00	0.00	0.00	0.07	0.10	0.04
Al2O3	20.64	20.75	20.85	20.68	20.65	20.83	20.77	20.70	20.64	20.72	20.88	20.70	20.21
Cr2O3	0.05	0.02	0.04	0.02	0.00	0.00	0.00	0.00	0.00	0.00	0.10	0.12	0.13
FeO	30.64	30.24	30.15	30.41	30.45	30.44	30.17	30.39	30.34	30.49	30.00	30.26	30.37
MnO	1.88	1.67	1.71	1.71	1.68	1.67	1.67	1.69	1.65	1.69	1.84	1.99	1.92
MgO	2.61	2.86	2.83	2.75	2.82	2.81	2.89	2.89	2.68	2.87	3.23	3.08	3.12
CaO	6.47	6.46	6.61	6.52	6.40	6.38	6.44	6.24	6.61	6.42	6.70	6.60	6.58
Na2O	0.04	0.01	0.04	0.00	0.00	0.01	0.02	0.01	0.02	0.02	0.01	0.02	0.00
K2O	0.05	0.06	0.06	0.04	0.04	0.02	0.02	0.06	0.03	0.03	0.04	0.04	0.03
ZrO2	0.02	0.00	0.01	0.00	0.00	0.04	0.00	0.01	0.00	0.01	0.02	0.07	0.00
Total	99.70	99.14	99.64	99.48	99.21	99.46	99.35	99.08	99.08	99.61	100.13	99.95	99.36
No.	49	75	76	77	78	79	80	81	82	83	201	202	203
Cations, O = 6													
Si	2.996	2.989	2.989	3.000	2.993	2.995	3.001	2.994	2.998	2.998	2.974	2.966	2.984
Ti	0.001	0.001	0.004	0.002	0.004	0.000	0.000	0.000	0.000	0.000	0.004	0.006	0.002
Al	1.956	1.973	1.972	1.960	1.963	1.973	1.967	1.969	1.964	1.961	1.964	1.957	1.924
Cr	0.004	0.001	0.002	0.001	0.000	0.000	0.000	0.000	0.000	0.000	0.006	0.008	0.008
Fe	2.060	2.039	2.023	2.045	2.054	2.046	2.028	2.052	2.048	2.047	2.003	2.029	2.051
Mn	0.127	0.114	0.116	0.116	0.115	0.113	0.114	0.115	0.113	0.115	0.125	0.134	0.131
Mg	0.312	0.344	0.338	0.330	0.338	0.336	0.347	0.348	0.323	0.343	0.384	0.368	0.376
Ca	0.557	0.558	0.569	0.562	0.553	0.550	0.554	0.540	0.572	0.552	0.574	0.568	0.570
Na	0.007	0.002	0.006	0.000	0.000	0.001	0.004	0.002	0.002	0.004	0.001	0.002	0.000
K	0.005	0.006	0.006	0.004	0.004	0.002	0.002	0.006	0.002	0.004	0.005	0.004	0.002
Zr	0.001	0.000	0.000	0.000	0.000	0.001	0.000	0.000	0.000	0.000	0.001	0.002	0.000
Total	8.027	8.028	8.026	8.021	8.024	8.018	8.018	8.028	8.024	8.023	8.041	8.046	8.048

Sample	JKEM-02	JKEM-02	JKEM-14b	JKEM-14b	JKEM-14b	JKEM-14b	JKEM-14b	JKEM-14b	JKEM-14b	JKEM-14b	JKEM-14b	JKEM-14b	JKEM-14b
Mineral	grt	grt	grt	grt	grt	grt	grt	grt	grt	grt	grt	grt	grt
No.	204	205	36	37	38	39	40	41	42	96	97	98	99
Weight %													
SiO2	37.21	37.18	37.68	37.33	37.56	37.54	37.08	37.28	37.08	37.93	37.60	37.86	37.96
TiO2	0.07	0.09	0.06	0.09	0.08	0.09	0.08	0.08	0.08	0.11	0.11	0.11	0.11
Al2O3	20.58	20.76	21.57	21.38	21.59	21.42	21.75	21.48	21.16	21.73	21.80	21.75	21.66
Cr2O3	0.13	0.10	0.12	0.11	0.12	0.13	0.10	0.11	0.12	0.00	0.00	0.00	0.00
FeO	30.10	30.12	28.34	28.18	28.18	28.78	28.98	30.34	30.19	23.65	24.09	24.47	23.16
MnO	2.10	2.17	0.98	1.04	0.97	1.05	1.05	1.19	1.14	0.70	0.80	0.80	0.64
MgO	2.82	2.62	5.25	5.15	5.12	5.24	5.30	5.42	5.33	4.84	4.65	4.88	5.10
CaO	6.88	6.82	6.28	6.61	7.06	5.69	5.50	4.24	4.38	11.24	10.80	10.42	11.12
Na2O	0.05	0.01	0.01	0.03	0.00	0.02	0.01	0.03	0.01	0.02	0.02	0.00	0.03
K2O	0.04	0.04	0.04	0.03	0.03	0.03	0.03	0.04	0.03	0.03	0.02	0.03	0.01
ZrO2	0.03	0.00	0.07	0.06	0.03	0.03	0.03	0.03	0.07	0.03	0.04	0.04	0.03
Total	100.00	99.93	100.40	100.00	100.72	100.01	99.91	100.22	99.59	100.27	99.93	100.36	99.81
No.	204	205	36	37	38	39	40	41	42	96	97	98	99
Cations, O = 6													
Si	2.983	2.982	2.957	2.947	2.942	2.960	2.930	2.946	2.951	2.953	2.944	2.951	2.960
Ti	0.005	0.006	0.004	0.005	0.005	0.005	0.005	0.005	0.005	0.006	0.007	0.006	0.007
Al	1.944	1.963	1.996	1.990	1.993	1.991	2.026	2.000	1.985	1.994	2.011	1.998	1.991
Cr	0.008	0.007	0.007	0.007	0.007	0.008	0.006	0.007	0.007	0.000	0.000	0.000	0.000
Fe	2.017	2.021	1.860	1.860	1.846	1.898	1.915	2.005	2.010	1.540	1.577	1.595	1.511
Mn	0.143	0.148	0.065	0.070	0.064	0.071	0.071	0.080	0.077	0.047	0.053	0.053	0.042
Mg	0.337	0.313	0.614	0.606	0.599	0.616	0.624	0.638	0.632	0.562	0.542	0.566	0.593
Ca	0.592	0.586	0.528	0.559	0.593	0.481	0.466	0.359	0.373	0.937	0.905	0.870	0.929
Na	0.007	0.001	0.002	0.004	0.000	0.002	0.001	0.004	0.001	0.004	0.002	0.000	0.004
K	0.004	0.004	0.005	0.002	0.002	0.002	0.002	0.004	0.004	0.002	0.002	0.002	0.001
Zr	0.001	0.000	0.002	0.002	0.001	0.001	0.001	0.001	0.002	0.001	0.001	0.001	0.001
Total	8.042	8.032	8.039	8.051	8.052	8.036	8.050	8.048	8.047	8.046	8.045	8.044	8.039

Sample	JKEM-14b	JKEM-14b	JKEM-14b	JKEM-14b	JKEM-14b	JKEM-14b	JKEM-14b	JKEM-14b	JKEM-14b	JKEM-14b	JKEM-15b	JKEM-15b	JKEM-15b
Mineral	grt	grt	grt	grt	grt	grt	grt	grt	grt	grt	grt	grt	grt
No.	100	101	102	103	104	105	106	107	108	109	228	229	230
Weight %													
SiO2	37.66	37.56	37.87	37.65	37.31	37.49	37.36	37.41	37.32	37.16	37.83	37.79	37.56
TiO2	0.11	0.12	0.08	0.07	0.09	0.08	0.04	0.05	0.08	0.10	0.08	0.09	0.06
Al2O3	21.50	21.40	21.55	21.41	21.44	21.75	21.43	21.18	21.46	21.31	21.24	21.05	20.92
Cr2O3	0.00	0.00	0.00	0.00	0.00	0.00	0.00	0.00	0.00	0.00	0.08	0.09	0.08
FeO	23.91	24.85	26.17	26.37	25.52	26.16	28.32	28.12	27.03	27.90	27.63	27.36	28.44
MnO	0.82	1.07	1.06	1.11	1.01	1.09	1.16	1.31	1.10	1.18	0.93	0.74	0.91
MgO	4.62	4.07	4.15	4.40	4.12	4.48	4.60	4.20	4.68	4.33	5.20	5.03	5.21
CaO	10.85	10.38	9.39	8.97	9.68	8.99	6.95	7.22	7.88	7.45	6.67	7.40	6.21
Na2O	0.01	0.01	0.04	0.00	0.02	0.01	0.01	0.01	0.02	0.01	0.00	0.02	0.02
K2O	0.03	0.02	0.01	0.04	0.02	0.03	0.03	0.03	0.02	0.02	0.02	0.04	0.05
ZrO2	0.03	0.02	0.04	0.02	0.02	0.03	0.03	0.02	0.03	0.05	0.00	0.03	0.01
Total	99.55	99.50	100.36	100.02	99.22	100.11	99.93	99.54	99.63	99.51	99.67	99.64	99.48
No.	100	101	102	103	104	105	106	107	108	109	228	229	230
Cations, O = 6													
Si	2.958	2.964	2.969	2.963	2.957	2.945	2.956	2.974	2.952	2.953	2.982	2.983	2.978
Ti	0.006	0.007	0.005	0.005	0.006	0.005	0.002	0.002	0.005	0.006	0.005	0.005	0.004
Al	1.991	1.991	1.991	1.986	2.003	2.015	1.998	1.984	2.000	1.996	1.974	1.958	1.956
Cr	0.000	0.000	0.000	0.000	0.000	0.000	0.000	0.000	0.000	0.000	0.005	0.006	0.005
Fe	1.571	1.640	1.716	1.735	1.691	1.718	1.873	1.868	1.788	1.854	1.822	1.806	1.886
Mn	0.054	0.071	0.071	0.074	0.067	0.072	0.078	0.088	0.073	0.079	0.062	0.049	0.061
Mg	0.541	0.479	0.485	0.516	0.486	0.524	0.542	0.497	0.552	0.512	0.611	0.592	0.617
Ca	0.913	0.878	0.788	0.756	0.822	0.757	0.589	0.616	0.668	0.635	0.563	0.626	0.527
Na	0.002	0.001	0.005	0.000	0.002	0.001	0.001	0.001	0.002	0.001	0.000	0.002	0.002
K	0.004	0.002	0.001	0.004	0.002	0.004	0.004	0.002	0.002	0.002	0.002	0.004	0.005
Zr	0.001	0.001	0.001	0.001	0.001	0.001	0.001	0.001	0.001	0.002	0.000	0.001	0.000
Total	8.042	8.034	8.033	8.040	8.038	8.044	8.044	7.997	8.045	8.042	8.027	8.034	8.041

Sample	JKEM-15b	JKEM-15b	JKEM-15b	JKEM-15b	JKEM-15b	JKEM-15b	JKEM-15b	JKEM-15b	JKEM-15b	JKEM-15b	JKEM-15b	JKEM-10	JKEM-10
Mineral	grt	grt	grt	grt	grt	grt	grt	grt	grt	grt	grt	grt	grt
No.	231	232	271	272	273	274	275	276	277	278	279	137	138
Weight %													
SiO2	37.48	37.53	36.99	36.61	37.35	37.15	37.29	37.13	36.89	37.02	37.16	37.35	37.21
TiO2	0.06	0.08	0.00	0.03	0.00	0.02	0.00	0.02	0.00	0.04	0.01	0.04	0.03
Al2O3	20.87	20.72	21.00	20.70	21.06	21.00	21.01	20.96	20.90	20.77	20.57	20.73	20.86
Cr2O3	0.12	0.14	0.00	0.01	0.03	0.01	0.01	0.04	0.01	0.04	0.00	0.03	0.04
FeO	27.75	28.90	25.07	29.45	24.87	26.83	25.60	25.16	27.81	27.71	28.73	29.65	29.30
MnO	0.84	1.01	0.50	1.12	0.70	0.87	0.73	0.59	0.97	1.00	1.08	1.70	1.62
MgO	5.20	5.00	3.67	4.07	4.25	4.41	4.20	3.82	4.21	4.60	4.66	3.66	3.84
CaO	6.28	5.85	10.71	5.65	10.16	7.88	9.55	10.54	7.40	6.98	6.41	6.10	6.12
Na2O	0.03	0.03	0.00	0.00	0.00	0.00	0.00	0.00	0.00	0.00	0.00	0.00	0.00
K2O	0.04	0.04	0.03	0.04	0.02	0.02	0.03	0.03	0.03	0.03	0.04	0.04	0.04
ZrO2	0.01	0.00	0.03	0.00	0.02	0.00	0.05	0.00	0.00	0.00	0.02	0.00	0.00
Total	98.67	99.29	98.01	97.68	98.45	98.19	98.46	98.29	98.22	98.18	98.66	99.30	99.05
No.	231	232	271	272	273	274	275	276	277	278	279	137	138
Cations, O = 6													
Si	2.987	2.987	2.969	2.977	2.976	2.978	2.977	2.971	2.970	2.976	2.983	2.994	2.986
Ti	0.004	0.005	0.000	0.001	0.000	0.001	0.000	0.001	0.000	0.002	0.000	0.002	0.001
Al	1.961	1.943	1.986	1.984	1.978	1.985	1.978	1.978	1.984	1.969	1.946	1.958	1.973
Cr	0.007	0.008	0.000	0.001	0.002	0.001	0.000	0.002	0.000	0.002	0.000	0.002	0.002
Fe	1.849	1.924	1.684	2.003	1.657	1.799	1.710	1.684	1.872	1.864	1.928	1.987	1.966
Mn	0.056	0.068	0.034	0.078	0.047	0.059	0.049	0.040	0.066	0.068	0.073	0.115	0.110
Mg	0.618	0.593	0.439	0.493	0.504	0.528	0.499	0.456	0.505	0.552	0.558	0.438	0.460
Ca	0.536	0.499	0.922	0.492	0.868	0.677	0.817	0.904	0.638	0.601	0.551	0.523	0.526
Na	0.005	0.004	0.001	0.000	0.000	0.000	0.000	0.000	0.000	0.000	0.000	0.000	0.000
K	0.004	0.005	0.004	0.004	0.001	0.002	0.004	0.004	0.004	0.004	0.004	0.004	0.004
Zr	0.000	0.000	0.001	0.000	0.001	0.000	0.001	0.000	0.000	0.000	0.000	0.000	0.000
Total	8.027	8.036	8.039	8.033	8.034	8.032	8.035	8.040	8.040	8.040	8.045	8.024	8.027

Sample	JKEM-10	JKEM-10	JKEM-10	JKEM-10
Mineral	grt	grt	grt	grt
No.	139	140	141	143
Weight %				
SiO2	37.42	37.37	37.60	37.58
TiO2	0.01	0.00	0.00	0.00
Al2O3	20.88	20.87	20.81	20.82
Cr2O3	0.04	0.03	0.00	0.00
FeO	29.63	29.36	29.79	29.56
MnO	1.87	1.72	1.45	1.45
MgO	3.36	3.61	4.07	3.78
CaO	6.23	6.20	5.95	6.03
Na2O	0.01	0.02	0.01	0.02
K2O	0.03	0.02	0.02	0.02
ZrO2	0.00	0.00	0.00	0.00
Total	99.48	99.18	99.69	99.25
No.	139	140	141	143
Cations, O = 6				
Si	2.996	2.995	2.996	3.006
Ti	0.000	0.000	0.000	0.000
Al	1.970	1.972	1.954	1.962
Cr	0.002	0.001	0.000	0.000
Fe	1.984	1.968	1.985	1.978
Mn	0.127	0.116	0.097	0.098
Mg	0.401	0.431	0.484	0.450
Ca	0.534	0.532	0.509	0.516
Na	0.001	0.004	0.001	0.002
K	0.004	0.002	0.002	0.002
Zr	0.000	0.000	0.000	0.000
Total	8.020	8.022	8.029	8.015

Sample	JKEM-12	JKEM-12	JKEM-12	JKEM-12	JKEM-12	JKEM-12	JKEM-12	JKEM-12	JKEM-12	JKEM-12	JKEM-12	JKEM-12	JKEM-12
Mineral	plag	plag	plag	plag	plag	plag	plag	plag	plag	plag	plag	plag	plag
No.	132	133	134	143	144	184	192	193	245	246	247	248	249
Weight %													
SiO2	57.80	57.74	57.06	63.96	63.08	57.98	63.32	63.22	58.10	59.08	59.00	59.18	58.84
TiO2	0.01	0.00	0.00	0.00	0.02	0.00	0.00	0.00	0.00	0.00	0.00	0.00	0.00
Al2O3	26.57	26.29	27.17	22.76	22.86	26.23	22.83	22.68	26.11	25.43	25.43	25.55	25.65
Cr2O3	0.00	0.00	0.00	0.00	0.00	0.00	0.00	0.00	0.00	0.00	0.00	0.00	0.00
FeO	0.20	0.03	0.06	0.76	0.72	0.07	0.77	0.54	0.00	0.05	0.07	0.00	0.00
MnO	0.01	0.02	0.01	0.03	0.03	0.00	0.00	0.00	0.00	0.00	0.00	0.00	0.00
MgO	0.00	0.00	0.00	0.00	0.00	0.00	0.00	0.00	0.00	0.00	0.00	0.00	0.00
CaO	8.67	8.37	9.32	3.90	4.31	8.09	4.13	4.09	8.21	7.28	7.52	7.29	7.56
Na2O	6.69	6.69	6.21	9.44	9.31	6.71	9.24	9.14	6.81	7.29	7.24	7.32	7.14
K2O	0.16	0.17	0.11	0.21	0.12	0.13	0.26	0.21	0.15	0.17	0.16	0.17	0.17
ZrO2	0.00	0.00	0.00	0.00	0.00	0.00	0.00	0.00	0.00	0.00	0.00	0.00	0.00
Total	100.12	99.32	99.93	101.07	100.45	99.21	100.55	99.88	99.38	99.30	99.41	99.51	99.37
No.	132	133	134	143	144	184	192	193	245	246	247	248	249
Cations, O = 8													
Si	2.588	2.602	2.560	2.807	2.789	2.611	2.796	2.804	2.613	2.654	2.649	2.651	2.642
Ti	0.000	0.000	0.000	0.000	0.001	0.000	0.000	0.000	0.000	0.000	0.000	0.000	0.000
Al	1.402	1.396	1.437	1.178	1.191	1.392	1.188	1.186	1.385	1.346	1.346	1.350	1.358
Cr	0.000	0.000	0.000	0.000	0.000	0.000	0.000	0.000	0.000	0.000	0.000	0.000	0.000
Fe	0.008	0.002	0.002	0.028	0.026	0.002	0.028	0.020	0.000	0.002	0.002	0.000	0.000
Mn	0.000	0.001	0.000	0.001	0.002	0.000	0.000	0.000	0.000	0.000	0.000	0.000	0.000
Mg	0.000	0.000	0.000	0.000	0.000	0.000	0.000	0.000	0.000	0.000	0.000	0.000	0.000
Ca	0.416	0.404	0.448	0.183	0.204	0.390	0.195	0.194	0.396	0.350	0.362	0.350	0.364
Na	0.581	0.585	0.540	0.803	0.798	0.586	0.791	0.786	0.594	0.635	0.630	0.635	0.622
K	0.009	0.010	0.006	0.012	0.006	0.008	0.015	0.012	0.009	0.010	0.009	0.010	0.010
Zr	0.000	0.000	0.000	0.000	0.000	0.000	0.000	0.000	0.000	0.000	0.000	0.000	0.000
Total	5.005	4.998	4.994	5.013	5.018	4.990	5.014	5.002	4.998	4.998	4.998	4.996	4.995

Sample	JKEM-14a	JKEM-14a	JKEM-14a	JKEM-14a	JKEM-14a	JKEM-14a	JKEM-14a	JKEM-14a	JKEM-14a	JKEM-14a	JKEM-14a	JKEM-14a	JKEM-14a
Mineral	plag	plag	plag	plag	plag	plag	plag	plag	plag	plag	plag	plag	plag
No.	295	299	300	301	303	304	320	323	325	335	336	337	338
Weight %													
SiO2	64.40	65.58	65.54	64.91	58.91	57.85	66.52	66.70	62.71	61.36	58.75	59.64	59.69
TiO2	0.00	0.00	0.00	0.00	0.00	0.00	0.00	0.00	0.00	0.00	0.00	0.00	0.00
Al2O3	21.94	22.19	22.42	22.67	26.76	27.60	21.23	21.36	23.66	24.64	26.74	26.15	26.29
Cr2O3	0.00	0.00	0.00	0.00	0.00	0.00	0.00	0.00	0.00	0.00	0.00	0.00	0.00
FeO	1.03	0.46	0.56	0.46	0.14	0.06	0.04	0.00	0.03	0.00	0.00	0.00	0.00
MnO	0.00	0.00	0.00	0.00	0.00	0.00	0.00	0.00	0.00	0.00	0.00	0.00	0.00
MgO	0.26	0.00	0.00	0.00	0.00	0.00	0.00	0.00	0.00	0.00	0.00	0.00	0.00
CaO	3.06	3.28	3.32	3.79	8.59	9.26	1.68	1.88	4.72	5.86	8.02	7.29	7.75
Na2O	9.42	9.74	9.86	9.41	6.76	6.34	10.71	10.52	8.72	8.16	6.91	7.18	7.16
K2O	0.16	0.19	0.16	0.29	0.18	0.18	0.14	0.17	0.28	0.25	0.18	0.24	0.25
ZrO2	0.00	0.00	0.00	0.00	0.00	0.00	0.00	0.00	0.00	0.00	0.00	0.00	0.00
Total	100.26	101.45	101.85	101.53	101.34	101.30	100.32	100.62	100.12	100.27	100.60	100.51	101.15
No.	295	299	300	301	303	304	320	323	325	335	336	337	338
Cations, O = 6													
Si	2.841	2.854	2.843	2.827	2.602	2.561	2.910	2.908	2.772	2.718	2.608	2.644	2.634
Ti	0.000	0.000	0.000	0.000	0.000	0.000	0.000	0.000	0.000	0.000	0.000	0.000	0.000
Al	1.141	1.138	1.146	1.164	1.394	1.440	1.094	1.098	1.233	1.286	1.399	1.366	1.367
Cr	0.000	0.000	0.000	0.000	0.000	0.000	0.000	0.000	0.000	0.000	0.000	0.000	0.000
Fe	0.038	0.017	0.020	0.017	0.006	0.002	0.002	0.000	0.001	0.000	0.000	0.000	0.000
Mn	0.000	0.000	0.000	0.000	0.000	0.000	0.000	0.000	0.000	0.000	0.000	0.000	0.000
Mg	0.018	0.000	0.000	0.000	0.000	0.000	0.000	0.000	0.000	0.000	0.000	0.000	0.000
Ca	0.145	0.153	0.154	0.177	0.406	0.439	0.079	0.088	0.223	0.278	0.382	0.346	0.366
Na	0.806	0.822	0.830	0.794	0.579	0.545	0.908	0.890	0.747	0.701	0.595	0.618	0.613
K	0.009	0.010	0.009	0.016	0.010	0.010	0.008	0.009	0.016	0.014	0.010	0.014	0.014
Zr	0.000	0.000	0.000	0.000	0.000	0.000	0.000	0.000	0.000	0.000	0.000	0.000	0.000
Total	4.997	4.994	5.002	4.996	4.998	4.998	5.002	4.993	4.993	4.998	4.995	4.988	4.995

Sample	JKEM-14a	JKEM-14a	JKEM-14a	JKEM-14a	JKEM-14a	JKEM-14a	JKEM-15a	JKEM-15a	JKEM-15a	JKEM-15a	JKEM-15a	JKEM-15a	JKEM-15a
Mineral	plag	plag	plag	plag	plag	plag	plag	plag	plag	plag	plag	plag	plag
No.	339	340	341	347	352	353	47	48	49	50	61	62	63
Weight %													
SiO2	58.04	58.70	64.59	63.57	64.86	64.71	63.14	63.72	64.85	63.84	62.87	61.38	62.67
TiO2	0.00	0.00	0.00	0.00	0.00	0.00	0.00	0.00	0.00	0.00	0.00	0.00	0.00
Al2O3	27.07	26.97	22.46	23.53	22.80	22.37	23.37	22.78	22.50	22.66	23.59	22.14	23.81
Cr2O3	0.00	0.00	0.00	0.00	0.00	0.00	0.00	0.00	0.00	0.00	0.00	0.00	0.00
FeO	0.00	0.00	0.00	0.39	0.73	0.65	0.52	0.25	0.40	0.25	0.52	2.33	0.63
MnO	0.00	0.00	0.00	0.00	0.00	0.00	0.00	0.00	0.00	0.00	0.00	0.01	0.01
MgO	0.00	0.00	0.00	0.00	0.00	0.00	0.00	0.00	0.00	0.00	0.00	0.82	0.00
CaO	8.66	8.46	3.26	4.55	3.59	3.47	4.61	4.12	3.39	3.90	4.72	4.59	5.00
Na2O	6.53	6.72	9.50	8.73	9.43	9.34	8.96	9.38	9.72	9.47	8.93	8.17	8.81
K2O	0.19	0.18	0.38	0.42	0.42	0.44	0.17	0.15	0.19	0.13	0.15	0.15	0.14
ZrO2	0.00	0.00	0.00	0.00	0.00	0.00	0.00	0.00	0.00	0.00	0.00	0.00	0.00
Total	100.49	101.02	100.19	101.18	101.82	100.97	100.77	100.40	101.05	100.24	100.77	99.59	101.07
No.	339	340	341	347	352	353	47	48	49	50	61	62	63
Cations, O = 6													
Si	2.584	2.598	2.842	2.784	2.822	2.836	2.779	2.808	2.835	2.815	2.768	2.758	2.755
Ti	0.000	0.000	0.000	0.000	0.000	0.000	0.000	0.000	0.000	0.000	0.000	0.000	0.000
Al	1.421	1.407	1.165	1.214	1.169	1.155	1.212	1.183	1.159	1.178	1.225	1.173	1.234
Cr	0.000	0.000	0.000	0.000	0.000	0.000	0.000	0.000	0.000	0.000	0.000	0.000	0.000
Fe	0.000	0.000	0.000	0.014	0.026	0.024	0.019	0.009	0.014	0.009	0.019	0.087	0.023
Mn	0.000	0.000	0.000	0.000	0.000	0.000	0.000	0.000	0.000	0.000	0.000	0.001	0.000
Mg	0.000	0.000	0.000	0.000	0.000	0.000	0.000	0.000	0.000	0.000	0.000	0.055	0.000
Ca	0.413	0.401	0.154	0.214	0.167	0.163	0.218	0.194	0.159	0.185	0.222	0.221	0.235
Na	0.564	0.576	0.810	0.742	0.796	0.794	0.765	0.802	0.824	0.810	0.762	0.712	0.751
K	0.010	0.010	0.021	0.023	0.023	0.025	0.010	0.009	0.010	0.007	0.008	0.009	0.008
Zr	0.000	0.000	0.000	0.000	0.000	0.000	0.000	0.000	0.000	0.000	0.000	0.000	0.000
Total	4.993	4.992	4.992	4.992	5.004	4.998	5.002	5.006	5.002	5.004	5.005	5.017	5.008

Sample	JKEM-15a	JKEM-15a	JKEM-15a	JKEM-15a	JKEM-15a	JKEM-15a	JKEM-15a	JKEM-15a	JKEM-15a	JKEM-15a	JKEM-15a	JKEM-15a	JKEM-15a
Mineral	plag	plag	plag	plag	plag	plag	plag	plag	plag	plag	plag	plag	plag
No.	64	65	89	90	91	92	93	103	104	105	120	121	122
Weight %													
SiO2	61.24	59.65	64.04	64.10	64.17	63.76	63.33	58.62	59.40	58.44	61.64	56.91	58.14
TiO2	0.00	0.00	0.00	0.00	0.00	0.00	0.00	0.00	0.00	0.04	0.00	0.00	0.00
Al2O3	24.42	25.60	22.93	22.74	22.42	23.03	22.96	26.22	25.51	25.97	24.39	27.45	26.60
Cr2O3	0.00	0.00	0.00	0.00	0.00	0.00	0.00	0.00	0.01	0.00	0.00	0.00	0.00
FeO	0.32	0.30	0.40	0.44	0.24	0.45	0.71	0.11	0.10	0.06	0.16	0.01	0.03
MnO	0.00	0.00	0.00	0.00	0.00	0.00	0.03	0.00	0.00	0.02	0.00	0.00	0.00
MgO	0.00	0.00	0.00	0.06	0.00	0.00	0.00	0.00	0.00	0.00	0.01	0.00	0.02
CaO	5.88	7.30	4.07	3.67	3.54	4.07	4.29	8.11	7.52	8.23	5.78	9.45	8.37
Na2O	8.25	7.41	9.31	9.31	9.74	9.38	9.22	7.00	7.38	7.06	8.26	6.14	6.88
K2O	0.15	0.11	0.05	0.10	0.07	0.05	0.13	0.12	0.12	0.12	0.12	0.08	0.11
ZrO2	0.00	0.00	0.00	0.00	0.00	0.00	0.00	0.00	0.05	0.01	0.00	0.00	0.01
Total	100.27	100.38	100.80	100.44	100.18	100.73	100.67	100.18	100.10	99.95	100.36	100.04	100.15
No.	64	65	89	90	91	92	93	103	104	105	120	121	122
Cations, O = 6													
Si	2.717	2.653	2.809	2.819	2.829	2.802	2.791	2.617	2.650	2.617	2.727	2.550	2.598
Ti	0.000	0.000	0.000	0.000	0.000	0.000	0.000	0.000	0.000	0.001	0.000	0.000	0.000
Al	1.277	1.342	1.186	1.179	1.165	1.193	1.193	1.379	1.342	1.370	1.272	1.450	1.401
Cr	0.000	0.000	0.000	0.000	0.000	0.000	0.000	0.000	0.001	0.000	0.000	0.000	0.000
Fe	0.012	0.011	0.014	0.016	0.009	0.017	0.026	0.004	0.004	0.002	0.006	0.001	0.001
Mn	0.000	0.000	0.000	0.000	0.000	0.000	0.001	0.000	0.000	0.001	0.000	0.000	0.000
Mg	0.000	0.000	0.000	0.004	0.000	0.000	0.000	0.000	0.000	0.000	0.001	0.000	0.001
Ca	0.279	0.348	0.191	0.173	0.167	0.191	0.202	0.388	0.359	0.395	0.274	0.454	0.401
Na	0.710	0.639	0.792	0.794	0.833	0.799	0.788	0.606	0.638	0.613	0.708	0.534	0.596
K	0.009	0.006	0.002	0.006	0.004	0.002	0.007	0.007	0.007	0.007	0.007	0.005	0.006
Zr	0.000	0.000	0.000	0.000	0.000	0.000	0.000	0.000	0.001	0.000	0.000	0.000	0.000
Total	5.005	4.999	4.995	4.990	5.007	5.004	5.010	5.002	5.002	5.006	4.996	4.994	5.004

Sample	JKEM-15a	JKEM-15a	JKEM-02	JKEM-02	JKEM-02	JKEM-02	JKEM-02	JKEM-02	JKEM-02	JKEM-02	JKEM-02	JKEM-02	JKEM-02
Mineral	plag	plag	plag	plag	plag	plag	plag	plag	plag	plag	plag	plag	plag
No.	123	124	164	165	166	172	173	192	193	194	195	196	197
Weight %													
SiO2	58.57	62.87	65.20	63.97	65.54	64.80	64.12	66.44	65.18	60.02	65.21	64.74	64.66
TiO2	0.00	0.00	0.00	0.00	0.00	0.00	0.00	0.01	0.00	0.55	0.00	0.00	0.00
Al2O3	26.65	23.60	21.27	21.71	21.07	21.93	21.76	21.01	21.47	24.38	22.64	22.52	22.36
Cr2O3	0.00	0.00	0.00	0.00	0.00	0.00	0.00	0.00	0.00	0.00	0.00	0.00	0.00
FeO	0.06	0.29	0.06	0.32	0.00	0.11	0.22	0.07	0.06	0.63	0.53	0.46	0.65
MnO	0.00	0.00	0.00	0.00	0.00	0.00	0.00	0.02	0.01	0.03	0.02	0.05	0.05
MgO	0.01	0.02	0.00	0.05	0.00	0.00	0.00	0.00	0.00	0.01	0.00	0.00	0.00
CaO	8.38	4.85	2.36	2.68	2.13	2.77	2.95	1.51	2.40	6.03	3.27	3.12	3.18
Na2O	6.93	8.83	10.09	9.28	9.91	9.72	9.66	9.86	9.88	7.60	9.74	9.59	9.47
K2O	0.13	0.20	0.23	0.65	0.46	0.20	0.24	1.11	0.57	0.33	0.42	0.41	0.58
ZrO2	0.01	0.02	0.00	0.00	0.00	0.00	0.00	0.00	0.03	0.02	0.01	0.00	0.00
Total	100.73	100.67	99.21	98.65	99.10	99.53	98.94	100.02	99.61	99.61	101.85	100.88	100.94
No.	123	124	164	165	166	172	173	192	193	194	195	196	197
Cations, O = 6													
Si	2.602	2.769	2.890	2.860	2.905	2.864	2.857	2.921	2.882	2.688	2.834	2.836	2.836
Ti	0.000	0.000	0.000	0.000	0.000	0.000	0.000	0.000	0.000	0.018	0.000	0.000	0.000
Al	1.395	1.225	1.111	1.144	1.101	1.142	1.142	1.089	1.119	1.287	1.159	1.162	1.156
Cr	0.000	0.000	0.000	0.000	0.000	0.000	0.000	0.000	0.000	0.000	0.000	0.000	0.000
Fe	0.002	0.010	0.002	0.012	0.000	0.004	0.008	0.002	0.002	0.024	0.019	0.017	0.024
Mn	0.000	0.000	0.000	0.000	0.000	0.000	0.000	0.001	0.001	0.001	0.001	0.002	0.002
Mg	0.001	0.001	0.000	0.004	0.000	0.000	0.000	0.000	0.000	0.001	0.000	0.000	0.000
Ca	0.399	0.229	0.112	0.128	0.101	0.131	0.141	0.071	0.114	0.290	0.152	0.146	0.150
Na	0.597	0.754	0.866	0.805	0.851	0.833	0.834	0.841	0.847	0.660	0.820	0.814	0.805
K	0.007	0.011	0.014	0.037	0.026	0.011	0.014	0.062	0.032	0.019	0.023	0.023	0.032
Zr	0.000	0.001	0.000	0.000	0.000	0.000	0.000	0.000	0.001	0.000	0.000	0.000	0.000
Total	5.004	5.001	4.996	4.990	4.984	4.986	4.996	4.987	4.998	4.988	5.008	5.002	5.005

Sample	JKEM-02	JKEM-02	JKEM-02	JKEM-02	JKEM-14b	JKEM-14b	JKEM-14b	JKEM-14b	JKEM-14b	JKEM-14b	JKEM-14b	JKEM-14b
Mineral	plag	plag	plag	plag	plag	plag	plag	plag	plag	plag	plag	plag
No.	198	199	200	228	28	29	30	31	32	44	45	46	53
Weight %													
SiO2	64.78	65.43	65.32	65.26	59.11	59.35	62.13	60.31	59.24	64.01	63.65	62.93	63.74
TiO2	0.01	0.00	0.00	0.00	0.00	0.01	0.01	0.00	0.00	0.00	0.00	0.00	0.00
Al2O3	22.24	21.67	21.88	21.90	25.56	25.65	23.71	24.86	25.04	22.34	22.65	23.18	22.61
Cr2O3	0.00	0.00	0.00	0.00	0.00	0.01	0.00	0.01	0.00	0.00	0.01	0.00	0.00
FeO	0.33	0.23	0.22	0.10	0.15	0.02	0.09	0.04	0.13	0.56	0.50	0.73	0.18
MnO	0.00	0.03	0.00	0.00	0.00	0.00	0.00	0.02	0.00	0.02	0.00	0.01	0.00
MgO	0.00	0.00	0.00	0.00	0.00	0.00	0.00	0.00	0.01	0.00	0.00	0.01	0.00
CaO	3.14	2.58	2.82	2.81	7.05	7.27	5.04	6.39	6.79	3.35	3.74	4.20	3.58
Na2O	9.38	9.98	9.84	9.94	7.62	7.46	8.82	8.09	7.71	9.85	9.58	9.40	9.64
K2O	0.55	0.38	0.36	0.28	0.09	0.08	0.11	0.10	0.08	0.18	0.12	0.13	0.10
ZrO2	0.00	0.00	0.00	0.00	0.00	0.00	0.03	0.00	0.00	0.00	0.00	0.00	0.00
Total	100.42	100.29	100.43	100.29	99.58	99.85	99.94	99.83	98.99	100.32	100.26	100.59	99.85
No.	198	199	200	228	28	29	30	31	32	44	45	46	53
Cations, O = 6													
Si	2.848	2.875	2.866	2.866	2.649	2.650	2.757	2.690	2.667	2.825	2.810	2.778	2.819
Ti	0.000	0.000	0.000	0.000	0.000	0.000	0.000	0.000	0.000	0.000	0.000	0.000	0.000
Al	1.153	1.122	1.132	1.134	1.350	1.350	1.240	1.306	1.329	1.162	1.179	1.206	1.178
Cr	0.000	0.000	0.000	0.000	0.000	0.001	0.000	0.000	0.000	0.000	0.001	0.000	0.000
Fe	0.012	0.008	0.008	0.003	0.006	0.001	0.003	0.002	0.005	0.021	0.018	0.027	0.006
Mn	0.000	0.001	0.000	0.000	0.000	0.000	0.000	0.001	0.000	0.001	0.000	0.001	0.000
Mg	0.000	0.000	0.000	0.000	0.000	0.000	0.000	0.000	0.000	0.000	0.000	0.001	0.000
Ca	0.148	0.122	0.133	0.132	0.338	0.348	0.240	0.306	0.328	0.158	0.177	0.198	0.170
Na	0.799	0.850	0.837	0.846	0.662	0.646	0.759	0.699	0.673	0.843	0.821	0.805	0.827
K	0.030	0.021	0.020	0.016	0.005	0.004	0.006	0.006	0.005	0.010	0.006	0.007	0.006
Zr	0.000	0.000	0.000	0.000	0.000	0.000	0.001	0.000	0.000	0.000	0.000	0.000	0.000
Total	4.991	4.999	4.996	4.998	5.010	5.000	5.007	5.009	5.007	5.022	5.014	5.025	5.007

Sample	JKEM-14b	JKEM-14b	JKEM-14b	JKEM-14b	JKEM-14b	JKEM-14b	JKEM-14b	JKEM-14b	JKEM-14b	JKEM-14b	JKEM-14b	JKEM-15b	JKEM-15b
Mineral	plag	plag	plag	plag	plag	plag	plag	plag	plag	plag	plag	plag	plag
No.	54	55	56	77	78	79	80	81	86	87	88	215	216
Weight %													
SiO2	64.07	63.90	62.59	62.42	58.53	58.38	55.75	61.63	61.39	59.00	61.38	65.55	66.84
TiO2	0.00	0.00	0.00	0.00	0.00	0.00	0.00	0.00	0.00	0.00	0.00	0.00	0.00
Al2O3	22.50	21.82	22.88	23.40	26.24	26.39	28.22	24.29	24.92	25.18	24.54	21.54	20.89
Cr2O3	0.00	0.00	0.00	0.00	0.00	0.00	0.00	0.00	0.00	0.00	0.00	0.00	0.00
FeO	0.15	0.73	0.94	0.13	0.01	0.02	0.02	0.27	0.08	0.54	0.10	0.05	0.05
MnO	0.00	0.00	0.00	0.00	0.00	0.00	0.00	0.00	0.00	0.00	0.00	0.00	0.00
MgO	0.00	0.19	0.30	0.00	0.00	0.00	0.00	0.00	0.00	0.17	0.01	0.00	0.00
CaO	3.36	2.99	4.18	4.71	7.88	8.07	10.08	5.64	5.92	7.26	5.73	2.63	1.95
Na2O	9.76	9.74	8.83	8.98	7.14	7.11	5.97	8.59	8.41	7.40	8.37	10.15	10.55
K2O	0.13	0.08	0.16	0.17	0.12	0.10	0.07	0.12	0.15	0.13	0.16	0.24	0.21
ZrO2	0.00	0.03	0.03	0.00	0.00	0.01	0.01	0.00	0.00	0.00	0.00	0.00	0.00
Total	99.97	99.47	99.91	99.81	99.92	100.06	100.13	100.53	100.88	99.67	100.29	100.16	100.48
No.	54	55	56	77	78	79	80	81	86	87	88	215	216
Cations, O = 6													
Si	2.829	2.840	2.782	2.771	2.618	2.609	2.505	2.726	2.706	2.648	2.719	2.881	2.921
Ti	0.000	0.000	0.000	0.000	0.000	0.000	0.000	0.000	0.000	0.000	0.000	0.000	0.000
Al	1.171	1.143	1.198	1.225	1.383	1.390	1.494	1.266	1.294	1.332	1.282	1.116	1.076
Cr	0.000	0.000	0.000	0.000	0.000	0.000	0.000	0.000	0.000	0.000	0.000	0.000	0.000
Fe	0.006	0.027	0.035	0.005	0.001	0.001	0.001	0.010	0.003	0.020	0.004	0.002	0.002
Mn	0.000	0.000	0.000	0.000	0.000	0.000	0.000	0.000	0.000	0.000	0.000	0.000	0.000
Mg	0.000	0.013	0.020	0.000	0.000	0.000	0.000	0.000	0.000	0.011	0.001	0.000	0.000
Ca	0.159	0.142	0.199	0.224	0.378	0.386	0.486	0.267	0.280	0.349	0.272	0.124	0.091
Na	0.836	0.840	0.761	0.773	0.619	0.616	0.520	0.737	0.718	0.644	0.719	0.865	0.894
K	0.007	0.004	0.009	0.010	0.006	0.006	0.004	0.007	0.009	0.007	0.009	0.014	0.012
Zr	0.000	0.001	0.001	0.000	0.000	0.000	0.000	0.000	0.000	0.000	0.000	0.000	0.000
Total	5.008	5.010	5.005	5.007	5.006	5.008	5.010	5.014	5.011	5.012	5.006	5.002	4.995

Sample	JKEM-15b	JKEM-15b	JKEM-15b	JKEM-15b	JKEM-15b	JKEM-15b	JKEM-15b	JKEM-15b	JKEM-15b	JKEM-15b	JKEM-15b	JKEM-15b	JKEM-15b
Mineral	plag	plag	plag	plag	plag	plag	plag	plag	plag	plag	plag	plag	plag
No.	217	218	219	220	221	222	223	224	225	226	227	257	258
Weight %													
SiO2	65.45	64.14	65.10	64.63	64.65	64.26	64.38	64.30	64.16	63.82	65.16	62.53	63.31
TiO2	0.00	0.00	0.00	0.00	0.00	0.00	0.00	0.00	0.00	0.00	0.01	0.00	0.00
Al2O3	21.35	22.32	21.69	22.17	21.98	22.27	21.69	22.24	22.47	22.32	21.72	22.45	22.12
Cr2O3	0.00	0.00	0.00	0.00	0.00	0.00	0.00	0.00	0.00	0.00	0.00	0.00	0.00
FeO	0.15	0.30	0.20	0.10	0.23	0.52	0.19	0.28	0.40	0.47	0.31	0.11	0.13
MnO	0.00	0.00	0.00	0.01	0.00	0.00	0.00	0.00	0.00	0.00	0.00	0.00	0.00
MgO	0.00	0.00	0.00	0.00	0.00	0.00	0.00	0.00	0.00	0.00	0.00	0.05	0.00
CaO	2.50	3.75	3.07	3.49	3.47	3.79	3.14	3.59	3.95	3.80	3.02	4.29	3.78
Na2O	10.19	9.63	10.00	9.70	9.67	9.53	9.83	9.65	9.41	9.61	9.96	9.25	9.43
K2O	0.24	0.20	0.23	0.23	0.17	0.21	0.20	0.25	0.21	0.19	0.20	0.15	0.17
ZrO2	0.00	0.00	0.00	0.00	0.00	0.00	0.00	0.00	0.00	0.00	0.00	0.00	0.00
Total	99.88	100.34	100.28	100.33	100.18	100.58	99.42	100.31	100.60	100.21	100.38	98.83	98.94
No.	217	218	219	220	221	222	223	224	225	226	227	257	258
Cations, O = 6													
Si	2.885	2.827	2.864	2.843	2.849	2.829	2.857	2.834	2.822	2.821	2.864	2.801	2.827
Ti	0.000	0.000	0.000	0.000	0.000	0.000	0.000	0.000	0.000	0.000	0.000	0.000	0.000
Al	1.110	1.160	1.125	1.150	1.142	1.155	1.134	1.155	1.165	1.163	1.126	1.186	1.164
Cr	0.000	0.000	0.000	0.000	0.000	0.000	0.000	0.000	0.000	0.000	0.000	0.000	0.000
Fe	0.006	0.011	0.007	0.004	0.009	0.019	0.007	0.010	0.014	0.018	0.011	0.004	0.005
Mn	0.000	0.000	0.000	0.001	0.000	0.000	0.000	0.000	0.000	0.000	0.000	0.000	0.000
Mg	0.000	0.000	0.000	0.000	0.000	0.000	0.000	0.000	0.000	0.000	0.000	0.003	0.000
Ca	0.118	0.177	0.145	0.164	0.164	0.179	0.149	0.170	0.186	0.180	0.142	0.206	0.181
Na	0.871	0.823	0.853	0.827	0.826	0.813	0.846	0.825	0.802	0.823	0.849	0.803	0.817
K	0.014	0.011	0.013	0.013	0.010	0.012	0.011	0.014	0.012	0.010	0.011	0.009	0.010
Zr	0.000	0.000	0.000	0.000	0.000	0.000	0.000	0.000	0.000	0.000	0.000	0.000	0.000
Total	5.004	5.010	5.006	5.002	4.999	5.007	5.004	5.008	5.002	5.016	5.004	5.012	5.003

Sample	JKEM-15b	JKEM-15b	JKEM-15b	JKEM-15b	JKEM-15b	JKEM-15b	JKEM-15b	JKEM-10	JKEM-10	JKEM-10	JKEM-10	JKEM-10	JKEM-10
Mineral	plag	plag	plag	plag	plag	plag	plag	plag	plag	plag	plag	plag	plag
No.	259	260	261	262	263	264	265	103	104	127	128	129	130
Weight %													
SiO2	64.40	65.14	63.24	62.29	63.21	62.30	63.02	63.43	63.86	63.70	63.83	63.96	64.32
TiO2	0.00	0.00	0.00	0.00	0.00	0.00	0.00	0.00	0.00	0.00	0.00	0.00	0.00
Al2O3	21.14	21.03	22.13	22.57	22.39	23.07	21.89	22.90	22.90	22.99	22.83	22.62	22.64
Cr2O3	0.00	0.00	0.00	0.00	0.00	0.00	0.00	0.00	0.00	0.00	0.00	0.00	0.00
FeO	0.06	0.11	0.01	0.24	0.25	0.35	0.28	0.11	0.05	0.16	0.15	0.14	0.16
MnO	0.00	0.00	0.00	0.00	0.00	0.00	0.00	0.00	0.00	0.00	0.00	0.00	0.00
MgO	0.00	0.00	0.00	0.00	0.00	0.00	0.00	0.00	0.00	0.00	0.00	0.00	0.00
CaO	2.85	2.38	3.89	4.58	4.14	4.55	3.82	4.29	4.13	4.24	4.02	3.86	3.90
Na2O	9.96	10.21	9.37	9.04	9.38	9.05	9.45	8.99	9.22	9.21	9.16	9.22	9.28
K2O	0.13	0.14	0.15	0.06	0.08	0.16	0.09	0.35	0.25	0.33	0.39	0.34	0.40
ZrO2	0.00	0.00	0.00	0.00	0.00	0.00	0.00	0.00	0.00	0.00	0.00	0.00	0.00
Total	98.54	99.00	98.79	98.77	99.45	99.48	98.56	100.06	100.40	100.63	100.37	100.14	100.70
No.	259	260	261	262	263	264	265	103	104	127	128	129	130
Cations, O = 6													
Si	2.878	2.894	2.827	2.794	2.813	2.778	2.828	2.804	2.810	2.802	2.812	2.822	2.824
Ti	0.000	0.000	0.000	0.000	0.000	0.000	0.000	0.000	0.000	0.000	0.000	0.000	0.000
Al	1.114	1.101	1.166	1.193	1.174	1.213	1.158	1.194	1.188	1.192	1.186	1.176	1.171
Cr	0.000	0.000	0.000	0.000	0.000	0.000	0.000	0.000	0.000	0.000	0.000	0.000	0.000
Fe	0.002	0.004	0.000	0.009	0.010	0.013	0.010	0.004	0.002	0.006	0.006	0.006	0.006
Mn	0.000	0.000	0.000	0.000	0.000	0.000	0.000	0.000	0.000	0.000	0.000	0.000	0.000
Mg	0.000	0.000	0.000	0.000	0.000	0.000	0.000	0.000	0.000	0.000	0.000	0.000	0.000
Ca	0.137	0.114	0.186	0.220	0.198	0.218	0.184	0.203	0.194	0.200	0.190	0.182	0.183
Na	0.863	0.879	0.812	0.786	0.809	0.782	0.822	0.770	0.786	0.786	0.782	0.789	0.790
K	0.007	0.008	0.009	0.003	0.005	0.009	0.005	0.019	0.014	0.018	0.022	0.019	0.022
Zr	0.000	0.000	0.000	0.000	0.000	0.000	0.000	0.000	0.000	0.000	0.000	0.000	0.000
Total	5.002	5.000	5.002	5.005	5.009	5.013	5.008	4.995	4.995	5.005	4.998	4.994	4.996

Sample	JKEM-10	JKEM-10	JKEM-10	JKEM-10	JKEM-10	JKEM-10	JKEM-10	JKEM-10	JKEM-10	JKEM-10	JKEM-10	JKEM-10	JKEM-10
Mineral	plag	plag	plag	plag	plag	plag	plag	plag	plag	plag	plag	plag	plag
No.	131	132	149	150	151	153	154	155	183	184	185	186	187
Weight %													
SiO2	63.79	63.51	63.24	63.74	63.76	63.40	63.91	63.12	63.73	63.82	63.92	64.07	63.60
TiO2	0.00	0.00	0.00	0.00	0.00	0.00	0.00	0.00	0.00	0.00	0.00	0.00	0.00
Al2O3	22.90	22.84	23.23	23.03	23.27	23.54	22.96	23.35	22.96	22.80	23.06	22.66	23.20
Cr2O3	0.00	0.00	0.00	0.00	0.00	0.00	0.00	0.00	0.00	0.00	0.00	0.00	0.00
FeO	0.14	0.34	0.00	0.02	0.12	0.06	0.00	0.08	0.15	0.09	0.12	0.06	0.16
MnO	0.00	0.00	0.00	0.00	0.00	0.00	0.00	0.00	0.00	0.00	0.00	0.00	0.01
MgO	0.00	0.01	0.00	0.00	0.00	0.00	0.00	0.00	0.00	0.00	0.00	0.00	0.00
CaO	4.23	4.23	4.73	4.20	4.42	4.89	4.07	4.67	4.00	3.99	4.19	3.81	4.46
Na2O	9.04	9.09	8.98	9.18	9.19	8.83	9.15	9.02	9.28	9.28	9.21	9.37	9.22
K2O	0.48	0.34	0.31	0.37	0.32	0.29	0.34	0.35	0.41	0.36	0.34	0.42	0.33
ZrO2	0.00	0.00	0.00	0.00	0.00	0.00	0.00	0.00	0.00	0.00	0.00	0.09	0.00
Total	100.58	100.36	100.48	100.53	101.09	101.01	100.43	100.59	100.52	100.33	100.83	100.48	100.98
No.	131	132	149	150	151	153	154	155	183	184	185	186	187
Cations, O = 6													
Si	2.807	2.803	2.787	2.804	2.793	2.780	2.811	2.781	2.806	2.813	2.805	2.820	2.791
Ti	0.000	0.000	0.000	0.000	0.000	0.000	0.000	0.000	0.000	0.000	0.000	0.000	0.000
Al	1.188	1.188	1.207	1.194	1.202	1.217	1.190	1.213	1.191	1.184	1.192	1.175	1.200
Cr	0.000	0.000	0.000	0.000	0.000	0.000	0.000	0.000	0.000	0.000	0.000	0.000	0.000
Fe	0.006	0.013	0.000	0.001	0.004	0.002	0.000	0.003	0.006	0.003	0.004	0.002	0.006
Mn	0.000	0.000	0.000	0.000	0.000	0.000	0.000	0.000	0.000	0.000	0.000	0.000	0.000
Mg	0.000	0.001	0.000	0.000	0.000	0.000	0.000	0.000	0.000	0.000	0.000	0.000	0.000
Ca	0.199	0.200	0.223	0.198	0.207	0.230	0.192	0.221	0.189	0.189	0.197	0.180	0.210
Na	0.771	0.778	0.767	0.783	0.781	0.750	0.780	0.770	0.792	0.793	0.783	0.800	0.785
K	0.026	0.019	0.018	0.021	0.018	0.016	0.019	0.019	0.023	0.020	0.019	0.024	0.018
Zr	0.000	0.000	0.000	0.000	0.000	0.000	0.000	0.000	0.000	0.000	0.000	0.002	0.000
Total	4.998	5.002	5.002	5.002	5.005	4.995	4.993	5.008	5.007	5.002	5.001	5.004	5.010

Sample	JKEM-10	JKEM-10	JKEM-10	JKEM-10	JKEM-10	JKEM-10	JKEM-10
Mineral	plag	plag	plag	plag	plag	plag	plag
No.	188	206	207	208	209	210	211
Weight %							
SiO2	63.94	63.19	62.49	63.29	63.15	63.22	62.46
TiO2	0.00	0.02	0.00	0.00	0.02	0.00	0.00
Al2O3	22.95	23.34	22.56	23.19	23.05	22.53	23.28
Cr2O3	0.00	0.00	0.00	0.00	0.00	0.00	0.01
FeO	0.12	0.24	0.93	0.32	0.18	0.37	0.24
MnO	0.02	0.00	0.01	0.00	0.00	0.00	0.00
MgO	0.00	0.00	0.35	0.05	0.00	0.09	0.06
CaO	4.05	4.70	4.47	4.62	4.55	4.32	4.95
Na2O	9.31	8.95	8.76	9.04	8.92	9.04	8.77
K2O	0.41	0.28	0.28	0.20	0.24	0.20	0.26
ZrO2	0.04	0.00	0.00	0.00	0.00	0.00	0.00
Total	100.84	100.73	99.83	100.71	100.10	99.77	100.01
No.	188	206	207	208	209	210	211
Cations, O = 6							
Si	2.807	2.781	2.783	2.786	2.793	2.806	2.770
Ti	0.000	0.001	0.000	0.000	0.001	0.000	0.000
Al	1.187	1.210	1.184	1.203	1.202	1.178	1.217
Cr	0.000	0.000	0.000	0.000	0.000	0.000	0.001
Fe	0.004	0.009	0.034	0.012	0.006	0.014	0.009
Mn	0.001	0.000	0.000	0.000	0.000	0.000	0.000
Mg	0.000	0.000	0.023	0.003	0.000	0.006	0.004
Ca	0.190	0.222	0.214	0.218	0.216	0.206	0.235
Na	0.793	0.764	0.757	0.772	0.765	0.778	0.754
K	0.023	0.016	0.016	0.011	0.014	0.011	0.014
Zr	0.001	0.000	0.000	0.000	0.000	0.000	0.000
Total	5.007	5.002	5.012	5.005	4.997	4.999	5.006

Sample	JKEM-12	JKEM-12	JKEM-12	JKEM-12	JKEM-14a	JKEM-14a	JKEM-15a	JKEM-15a	JKEM-15a	JKEM-15a	JKEM-15a	JKEM-02	JKEM-02
Mineral	ilm	ilm	ilm	ilm	ilm	ilm	ilm	ilm	ilm	ilm	ilm	ilm	ilm
No.	165	170	177	182	375	377	73	74	75	76	95	179	187
Weight %													
SiO2	0.04	0.03	0.01	0.00	0.12	0.09	0.00	0.00	0.00	0.00	0.19	0.04	0.06
TiO2	51.05	51.23	51.77	50.65	51.80	51.30	50.73	50.88	50.67	51.40	51.00	50.76	51.53
Al2O3	0.02	0.03	0.01	0.03	0.02	0.04	0.00	0.02	0.01	0.00	0.00	0.00	0.00
Cr2O3	0.02	0.02	0.02	0.00	0.15	0.12	0.00	0.02	0.05	0.01	0.24	0.00	0.01
FeO	47.15	47.45	47.28	47.74	47.30	47.58	48.79	48.84	48.92	49.57	48.31	47.31	46.66
MnO	0.43	0.39	0.36	0.36	0.46	0.43	0.31	0.32	0.31	0.31	0.44	0.67	0.69
MgO	0.45	0.38	0.40	0.43	0.50	0.50	0.50	0.51	0.47	0.48	0.24	0.35	0.39
CaO	0.02	0.02	0.01	0.01	0.04	0.03	0.00	0.00	0.00	0.00	0.41	0.12	0.00
Na2O	0.02	0.00	0.01	0.00	0.04	0.05	0.03	0.02	0.02	0.01	0.03	0.01	0.00
K2O	0.02	0.05	0.04	0.03	0.05	0.05	0.01	0.03	0.01	0.02	0.09	0.03	0.02
ZrO2	0.00	0.00	0.00	0.00	0.00	0.00	0.00	0.00	0.00	0.00	0.10	0.02	0.01
Total	99.21	99.61	99.92	99.25	100.48	100.19	100.37	100.64	100.44	101.80	101.05	99.30	99.38
No.	165	170	177	182	375	377	73	74	75	76	95	179	187
Cations, O = 3													
Si	0.001	0.001	0.000	0.000	0.003	0.002	0.000	0.000	0.000	0.000	0.005	0.001	0.002
Ti	0.981	0.981	0.986	0.976	0.981	0.976	0.969	0.969	0.968	0.968	0.966	0.977	0.986
Al	0.001	0.001	0.000	0.001	0.001	0.001	0.000	0.001	0.000	0.000	0.000	0.000	0.000
Cr	0.000	0.001	0.000	0.000	0.003	0.002	0.000	0.000	0.001	0.000	0.005	0.000	0.000
Fe	1.007	1.010	1.002	1.023	0.996	1.007	1.036	1.034	1.039	1.038	1.017	1.013	0.993
Mn	0.009	0.008	0.008	0.008	0.010	0.009	0.007	0.007	0.007	0.007	0.010	0.014	0.015
Mg	0.017	0.014	0.015	0.017	0.019	0.019	0.019	0.019	0.018	0.018	0.009	0.014	0.015
Ca	0.001	0.001	0.000	0.000	0.001	0.001	0.000	0.000	0.000	0.000	0.011	0.003	0.000
Na	0.001	0.000	0.000	0.000	0.002	0.002	0.002	0.001	0.001	0.000	0.002	0.000	0.000
K	0.001	0.002	0.001	0.001	0.002	0.002	0.001	0.001	0.001	0.001	0.003	0.001	0.001
Zr	0.000	0.000	0.000	0.000	0.000	0.000	0.000	0.000	0.000	0.000	0.001	0.000	0.000
Total	2.019	2.019	2.014	2.025	2.016	2.022	2.033	2.032	2.033	2.032	2.028	2.022	2.012

Sample	JKEM-02	JKEM-14b	JKEM-14b	JKEM-14b	JKEM-14b	JKEM-14b	JKEM-15b	JKEM-15b	JKEM-10	JKEM-10
Mineral	ilm	ilm	ilm	ilm	ilm	ilm	ilm	ilm	ilm	ilm
No.	217	72	123	124	125	126	285	286	190	191
Weight %										
SiO2	0.11	0.17	0.10	0.08	0.09	0.10	0.08	0.03	0.14	0.14
TiO2	51.32	48.18	47.67	47.72	46.81	48.19	45.76	45.88	50.16	49.97
Al2O3	0.03	0.03	0.03	0.02	0.04	0.03	0.03	0.05	0.00	0.00
Cr2O3	0.18	0.17	0.00	0.00	0.00	0.00	0.21	0.00	0.22	0.22
FeO	47.87	48.06	47.09	47.43	47.60	47.24	48.34	47.80	47.81	47.47
MnO	0.62	0.35	0.38	0.41	0.38	0.42	0.38	0.29	0.63	0.62
MgO	0.34	0.65	0.88	0.85	0.82	0.87	0.55	0.55	0.30	0.27
CaO	0.03	0.08	0.04	0.04	0.04	0.05	0.04	0.00	0.07	0.09
Na2O	0.00	0.02	0.00	0.00	0.00	0.00	0.00	0.00	0.02	0.02
K2O	0.03	0.07	0.04	0.05	0.04	0.05	0.06	0.02	0.09	0.08
ZrO2	0.07	0.08	0.00	0.00	0.01	0.01	0.08	0.03	0.04	0.11
Total	100.61	97.86	96.21	96.61	95.84	96.95	95.53	94.64	99.47	98.99
No.	217	72	123	124	125	126	285	286	190	191
Cations, O = 6										
Si	0.003	0.005	0.003	0.002	0.002	0.003	0.002	0.001	0.004	0.004
Ti	0.974	0.947	0.952	0.950	0.942	0.954	0.930	0.939	0.966	0.967
Al	0.001	0.001	0.001	0.001	0.001	0.001	0.001	0.002	0.000	0.000
Cr	0.004	0.004	0.000	0.000	0.000	0.000	0.005	0.000	0.005	0.005
Fe	1.010	1.051	1.046	1.050	1.065	1.040	1.092	1.088	1.024	1.022
Mn	0.013	0.008	0.008	0.009	0.009	0.009	0.009	0.007	0.014	0.014
Mg	0.013	0.025	0.035	0.034	0.033	0.034	0.022	0.022	0.011	0.010
Ca	0.001	0.002	0.001	0.001	0.001	0.001	0.001	0.000	0.002	0.002
Na	0.000	0.001	0.000	0.000	0.000	0.000	0.000	0.000	0.001	0.001
K	0.001	0.002	0.002	0.002	0.001	0.002	0.002	0.001	0.003	0.003
Zr	0.001	0.001	0.000	0.000	0.000	0.000	0.001	0.000	0.001	0.001
Total	2.021	2.047	2.046	2.049	2.055	2.044	2.066	2.059	2.030	2.028

Sample	JKEM-12	JKEM-12	JKEM-12	JKEM-14a	JKEM-14a	JKEM-01	JKEM-01	JKEM-01	JKEM-01	JKEM-02	JKEM-02	JKEM-14b	JKEM-14b
Mineral	mt	mt	mt	mt	mt	mt	mt	mt	mt	mt	mt	mt	mt
No.	168	178	183	378	376	50	51	52	53	188	180	127	128
Weight %													
SiO2	0.09	0.06	0.09	0.18	0.20	0.15	0.23	0.17	0.16	0.14	0.13	0.15	0.17
TiO2	0.38	0.40	0.46	1.44	1.71	14.02	0.89	5.46	1.37	1.23	0.75	0.88	1.13
Al2O3	0.50	0.66	0.60	1.01	0.87	1.03	0.44	0.91	0.66	0.68	0.62	0.92	1.44
Cr2O3	0.27	0.45	0.52	0.27	0.33	0.28	0.29	0.27	0.27	0.17	0.22	0.00	0.00
FeO	89.45	89.21	89.78	89.77	89.50	77.94	90.14	87.58	90.12	90.41	89.96	86.46	85.70
MnO	0.07	0.09	0.09	0.16	0.16	0.35	0.16	0.20	0.15	0.07	0.06	0.12	0.12
MgO	0.02	0.02	0.02	0.06	0.05	0.07	0.00	0.02	0.00	0.01	0.01	0.16	0.24
CaO	0.06	0.05	0.02	0.06	0.09	0.08	0.13	0.07	0.06	0.00	0.04	0.06	0.06
Na2O	0.00	0.00	0.00	0.06	0.06	0.06	0.03	0.02	0.00	0.03	0.00	0.02	0.01
K2O	0.05	0.03	0.04	0.06	0.05	0.05	0.06	0.06	0.07	0.03	0.02	0.06	0.06
ZrO2	0.00	0.00	0.00	0.00	0.00	0.11	0.10	0.04	0.08	0.00	0.09	0.00	0.03
Total	90.88	90.95	91.61	93.06	93.03	94.13	92.46	94.81	92.94	92.77	91.90	88.82	88.96
No.	168	178	183	378	376	50	51	52	53	188	180	127	128
Cations, O = 4													
Si	0.004	0.003	0.004	0.009	0.010	0.006	0.012	0.008	0.008	0.007	0.007	0.008	0.009
Ti	0.015	0.016	0.018	0.054	0.064	0.472	0.034	0.195	0.052	0.047	0.029	0.035	0.044
Al	0.030	0.040	0.036	0.059	0.052	0.054	0.026	0.051	0.039	0.041	0.037	0.057	0.088
Cr	0.011	0.018	0.021	0.010	0.013	0.010	0.012	0.010	0.011	0.007	0.009	0.000	0.000
Fe	3.890	3.866	3.862	3.750	3.735	2.917	3.830	3.483	3.790	3.815	3.849	3.806	3.730
Mn	0.003	0.004	0.004	0.007	0.007	0.013	0.007	0.008	0.006	0.003	0.002	0.006	0.005
Mg	0.001	0.001	0.002	0.004	0.004	0.005	0.000	0.002	0.000	0.000	0.001	0.012	0.018
Ca	0.003	0.002	0.001	0.003	0.005	0.004	0.007	0.004	0.003	0.000	0.002	0.003	0.004
Na	0.000	0.000	0.000	0.006	0.006	0.005	0.003	0.002	0.000	0.003	0.000	0.002	0.001
K	0.004	0.002	0.003	0.004	0.004	0.003	0.004	0.004	0.004	0.002	0.002	0.004	0.004
Zr	0.000	0.000	0.000	0.000	0.000	0.002	0.002	0.001	0.002	0.000	0.002	0.000	0.001
Total	3.962	3.953	3.951	3.906	3.899	3.491	3.937	3.768	3.916	3.926	3.941	3.932	3.905

Sample	JKEM-14b	JKEM-14b
Mineral	mt	mt
No.	129	130
Weight %		
SiO2	0.13	0.13
TiO2	0.68	0.77
Al2O3	0.61	0.62
Cr2O3	0.00	0.00
FeO	87.03	87.01
MnO	0.12	0.12
MgO	0.10	0.09
CaO	0.07	0.05
Na2O	0.01	0.02
K2O	0.06	0.06
ZrO2	0.02	0.01
Total	88.81	88.87
No.	129	130
Cations, O = 6		
Si	0.007	0.007
Ti	0.027	0.030
Al	0.038	0.039
Cr	0.000	0.000
Fe	3.856	3.848
Mn	0.005	0.005
Mg	0.008	0.007
Ca	0.004	0.003
Na	0.000	0.002
K	0.004	0.004
Zr	0.000	0.000
Total	3.950	3.946

Sample	JKEM-15a	JKEM-15a	JKEM-15a	JKEM-15a	JKEM-14a	JKEM-02	JKEM-10	JKEM-10	JKEM-10
Mineral	cal	cal	cal	cal	cal	cal	cal	cal	cal
No.	29	111	116	119	316	162	121	136	142
Weight %									
SiO2	0.47	0.22	0.81	2.01	0.02	0.00	0.16	0.03	0.22
TiO2	0.00	0.00	0.00	0.02	0.00	0.00	0.02	0.00	0.00
Al2O3	0.00	0.00	0.02	0.26	0.00	0.00	0.00	0.00	0.04
Cr2O3	0.00	0.00	0.00	0.00	0.00	0.00	0.01	0.00	0.00
FeO	0.66	1.05	1.13	4.11	1.09	3.63	0.34	2.59	0.92
MnO	0.58	0.56	0.61	0.38	0.81	0.33	0.06	0.40	0.04
MgO	0.11	0.15	0.20	0.95	0.23	1.17	0.00	0.94	0.02
CaO	59.78	56.85	55.97	53.60	53.29	54.56	54.82	58.72	54.72
Na2O	0.08	0.03	0.03	0.05	0.00	0.00	0.06	0.00	0.14
K2O	0.09	0.01	0.02	0.04	0.17	0.00	0.03	0.02	0.02
ZrO2	0.02	0.02	0.02	0.01	55.60	0.00	0.14	0.00	0.13
Total	61.79	58.90	58.81	61.44	Area2 Prir	59.69	55.65	62.70	56.24
No.	29	111	116	119	316	162	121	136	142
Cations, O = 3									
Si	0.021	0.011	0.038	0.090	0.001	0.000	0.008	0.001	0.011
Ti	0.000	0.000	0.000	0.001	0.000	0.000	0.001	0.000	0.000
Al	0.000	0.000	0.001	0.014	0.000	0.000	0.000	0.000	0.003
Cr	0.000	0.000	0.000	0.000	0.000	0.000	0.000	0.000	0.000
Fe	0.025	0.042	0.045	0.154	0.046	0.143	0.014	0.097	0.038
Mn	0.022	0.023	0.024	0.014	0.035	0.013	0.003	0.015	0.002
Mg	0.008	0.011	0.014	0.063	0.018	0.083	0.000	0.063	0.002
Ca	2.896	2.901	2.835	2.564	2.894	2.761	2.954	2.822	2.920
Na	0.007	0.003	0.003	0.004	0.000	0.000	0.006	0.000	0.013
K	0.005	0.001	0.001	0.002	0.011	0.000	0.002	0.001	0.001
Zr	0.000	0.001	0.001	0.000	0.000	0.000	0.004	0.000	0.003
Total	2.984	2.991	2.963	2.906	3.005	3.000	2.992	3.000	2.992

Sample	JKEM-12	JKEM-14b	JKEM-14b	JKEM-15b	JKEM-15b	JKEM-15b	JKEM-15b	JKEM-15b
Mineral	sp	sp	sp	sp	sp	sp	sp	sp
No.	243	33	35	292	293	294	295	296
Weight %								
SiO2	0.04	0.03	0.04	0.00	0.00	0.00	0.00	0.00
TiO2	0.05	0.08	0.09	0.00	0.00	0.00	0.00	0.00
Al2O3	55.23	57.19	57.90	55.88	55.26	56.06	55.31	55.51
Cr2O3	0.05	0.11	0.11	0.00	0.00	0.00	0.00	0.00
FeO	40.12	34.26	33.43	38.26	38.41	37.85	38.06	38.47
MnO	0.15	0.13	0.12	0.05	0.04	0.07	0.02	0.05
MgO	3.51	4.07	4.80	3.32	3.62	3.33	3.76	3.45
CaO	0.09	0.11	0.11	0.00	0.00	0.00	0.00	0.02
Na2O	0.01	0.21	0.20	0.08	0.13	0.10	0.09	0.11
K2O	0.03	0.02	0.04	0.02	0.00	0.00	0.00	0.00
ZrO2	0.00	0.02	0.07	0.00	0.00	0.00	0.00	0.00
Total	99.29	96.23	96.90	97.61	97.46	97.40	97.25	97.60
No.	243	33	35	292	293	294	295	296
Cations, O = 4								
Si	0.001	0.001	0.001	0.000	0.000	0.000	0.000	0.000
Ti	0.001	0.002	0.002	0.000	0.000	0.000	0.000	0.000
Al	1.902	1.974	1.974	1.939	1.924	1.945	1.927	1.930
Cr	0.001	0.002	0.002	0.000	0.000	0.000	0.000	0.000
Fe	0.980	0.839	0.808	0.942	0.949	0.932	0.941	0.949
Mn	0.004	0.003	0.003	0.001	0.001	0.002	0.000	0.001
Mg	0.153	0.178	0.207	0.146	0.160	0.146	0.166	0.152
Ca	0.003	0.004	0.004	0.000	0.000	0.000	0.000	0.001
Na	0.001	0.012	0.011	0.005	0.007	0.006	0.005	0.006
K	0.001	0.001	0.001	0.001	0.000	0.000	0.000	0.000
Zr		0.000	0.001	0.000	0.000	0.000	0.000	0.000
Total	3.048	3.015	3.014	3.034	3.041	3.030	3.039	3.038

Sample	JKEM-15a	JKEM-15a	JKEM-10	JKEM-10	JKEM-10	JKEM-10	JKEM-10
Mineral	qtz	qtz	qtz	qtz	qtz	qtz	qtz
No.	26	112	159	133	134	135	152
Weight %							
SiO2	96.38	95.05	99.71	99.88	100.00	100.46	100.56
TiO2	0.00	0.00	0.00	0.00	0.00	0.00	0.00
Al2O3	0.27	0.42	0.01	0.00	0.01	0.02	0.00
Cr2O3	0.00	0.00	0.00	0.00	0.00	0.00	0.00
FeO	1.02	1.67	0.06	0.17	0.32	0.33	0.05
MnO	0.00	0.00	0.00	0.00	0.00	0.00	0.00
MgO	0.44	1.20	0.00	0.00	0.00	0.00	0.00
CaO	0.05	0.04	0.00	0.00	0.02	0.02	0.00
Na2O	0.04	0.06	0.00	0.00	0.00	0.00	0.00
K2O	0.04	0.03	0.00	0.02	0.02	0.03	0.00
ZrO2	0.00	0.01	0.00	0.00	0.00	0.00	0.00
Total	98.23	98.46	99.79	100.07	100.37	100.85	100.61
No.	26	112	159	133	134	135	152
Cations, O = 2							
Si	0.989	0.979	1.000	0.999	0.998	0.998	1.000
Ti	0.000	0.000	0.000	0.000	0.000	0.000	0.000
Al	0.003	0.005	0.000	0.000	0.000	0.000	0.000
Cr	0.000	0.000	0.000	0.000	0.000	0.000	0.000
Fe	0.009	0.014	0.001	0.001	0.003	0.003	0.000
Mn	0.000	0.000	0.000	0.000	0.000	0.000	0.000
Mg	0.007	0.018	0.000	0.000	0.000	0.000	0.000
Ca	0.001	0.000	0.000	0.000	0.000	0.000	0.000
Na	0.001	0.001	0.000	0.000	0.000	0.000	0.000
K	0.001	0.000	0.000	0.000	0.000	0.000	0.000
Zr	0.000	0.000	0.000	0.000	0.000	0.000	0.000
Total	1.010	1.019	1.000	1.001	1.002	1.002	1.000

Sample	JKEM-14a	JKEM-14a	JKEM-15a	JKEM-02	JKEM-02	JKEM-02	JKEM-10
Mineral	zrc (inf)	zrc (inf)	zrc	zrc	zrc	zrc	zrc
No.	277	278	130	159	160	161	189
Weight %							
SiO2	34.15	34.50	34.12	33.57	33.35	32.02	34.30
TiO2	0.00	0.00	0.25	0.00	0.00	0.00	0.44
Al2O3	0.00	0.00	0.13	0.00	0.02	0.02	0.07
Cr2O3	0.00	0.00	0.35	0.00	0.02	0.00	0.39
FeO	0.00	0.34	0.64	0.04	0.15	0.18	0.81
MnO	0.00	0.00	0.15	0.00	0.00	0.02	0.17
MgO	0.00	0.09	0.10	0.00	0.03	0.06	0.07
CaO	0.00	0.00	0.10	0.00	0.04	0.02	0.11
Na2O	0.00	0.00	0.14	0.00	0.00	0.01	0.12
K2O	0.01	0.02	0.06	0.03	0.02	0.02	0.10
ZrO2	0.00	0.00	64.87	65.53	64.92	67.43	65.61
Total	34.16	34.95	100.90	99.17	98.54	99.77	102.17
No.	277	278	130	159	160	161	189
Cations, O = 4							
Si	2.000	1.988	1.021	1.024	1.024	0.984	1.016
Ti	0.000	0.000	0.006	0.000	0.000	0.000	0.010
Al	0.000	0.000	0.005	0.000	0.001	0.001	0.002
Cr	0.000	0.000	0.008	0.000	0.000	0.000	0.009
Fe	0.000	0.016	0.016	0.001	0.004	0.005	0.020
Mn	0.000	0.000	0.004	0.000	0.000	0.000	0.004
Mg	0.000	0.008	0.004	0.000	0.001	0.003	0.003
Ca	0.000	0.000	0.003	0.000	0.001	0.000	0.004
Na	0.000	0.000	0.008	0.000	0.000	0.000	0.007
K	0.000	0.001	0.002	0.001	0.001	0.001	0.004
Zr	0.000	0.000	0.947	0.975	0.972	1.011	0.948
Total	2.001	2.013	2.025	2.001	2.004	2.006	2.027

Sample	JKEM-14a
Mineral	bdd (inf)
No.	276
Weight %	
SiO2	0.01
TiO2	0.24
Al2O3	0.00
Cr2O3	0.00
FeO	0.15
MnO	0.01
MgO	0.03
CaO	0.00
Na2O	0.01
K2O	0.03
ZrO2	0.00
Total	0.47
No.	276
Cations, O = 2	
Si	0.018
Ti	0.633
Al	0.000
Cr	0.000
Fe	0.421
Mn	0.015
Mg	0.166
Ca	0.000
Na	0.070
K	0.123
Zr	0.000
Total	1.446

Sample	JKEM-15a	JKEM-02	JKEM-02	JKEM-02	JKEM-02	JKEM-14b
Mineral	pyrr (inf)	pyrr (inf)	pyrr (inf)	pyrr (inf)	pyrr (inf)	pyrr (inf)
No.	132	177	178	182	186	131
Weight %						
SiO2	0.02	0.00	0.00	0.15	0.12	0.19
TiO2	0.00	0.00	0.00	0.00	0.03	0.17
Al2O3	0.04	0.00	0.00	0.05	0.04	0.05
Cr2O3	0.00	0.00	0.00	0.13	0.13	0.00
FeO	76.94	76.70	76.92	76.70	76.71	75.36
MnO	0.00	0.00	0.01	0.04	0.04	0.11
MgO	0.02	0.00	0.00	0.06	0.05	0.10
CaO	0.00	0.04	0.00	0.09	0.02	0.09
Na2O	0.00	0.00	0.00	0.04	0.06	0.08
K2O	0.03	0.03	0.03	0.04	0.04	0.07
ZrO2	0.02	0.00	0.00	0.06	0.06	0.03
Total	77.07	76.76	76.96	77.36	77.28	76.23
No.	132	177	178	182	186	131
Cations, O = 1						
Si	0.000	0.000	0.000	0.002	0.002	0.003
Ti	0.000	0.000	0.000	0.000	0.000	0.002
Al	0.001	0.000	0.000	0.001	0.001	0.001
Cr	0.000	0.000	0.000	0.002	0.002	0.000
Fe	0.997	0.999	1.000	0.987	0.988	0.982
Mn	0.000	0.000	0.000	0.001	0.001	0.001
Mg	0.000	0.000	0.000	0.001	0.001	0.002
Ca	0.000	0.001	0.000	0.002	0.000	0.001
Na	0.000	0.000	0.000	0.001	0.002	0.002
K	0.001	0.001	0.001	0.001	0.001	0.001
Zr	0.000	0.000	0.000	0.001	0.000	0.000
Total	1.000	1.000	1.000	0.997	0.997	0.996

Sample	JKEM-14a	JKEM-14a	JKEM-14a
Mineral	k-fsp	k-fsp	k-fsp
No.	321	322	324
Weight %			
SiO2	64.27	65.07	64.42
TiO2	0.02	0.01	0.15
Al2O3	18.06	18.60	18.56
Cr2O3	0.00	0.00	0.00
FeO	0.90	0.01	0.17
MnO	0.00	0.00	0.00
MgO	0.64	0.00	0.00
CaO	0.03	0.00	0.00
Na2O	0.90	1.32	1.15
K2O	13.96	14.34	14.74
ZrO2	0.00	0.00	0.00
Total	98.78	99.35	99.19
No.	321	322	324
Cations, O = 8			
Si	2.989	3.001	2.987
Ti	0.001	0.000	0.005
Al	0.990	1.011	1.014
Cr	0.000	0.000	0.000
Fe	0.035	0.001	0.006
Mn	0.000	0.000	0.000
Mg	0.045	0.000	0.000
Ca	0.002	0.000	0.000
Na	0.081	0.118	0.103
K	0.828	0.843	0.872
Zr	0.000	0.000	0.000
Total	4.971	4.975	4.988

Sample	JKEM-12	JKEM-15a	JKEM-15a	JKEM-15a	JKEM-15a	JKEM-02	JKEM-02	JKEM-02	JKEM-15b	JKEM-15b
Mineral	unk	unk	unk	unk	unk	unk	unk	unk	unk	unk
No.	175	131	133	134	135	226	163	218	255	256
Weight %										
SiO2	47.60	0.02	1.49	0.00	0.04	43.77	43.12	1.37	45.12	46.08
TiO2	0.00	0.01	0.00	0.05	0.04	0.10	0.00	0.82	0.03	0.00
Al2O3	0.62	0.03	0.13	0.00	0.02	4.31	4.67	0.49	4.55	4.42
Cr2O3	0.00	0.00	0.00	0.00	0.00	0.00	0.00	1.41	0.01	0.03
FeO	29.83	41.59	56.75	41.45	41.64	29.07	27.53	1.07	22.65	24.43
MnO	0.38	0.02	0.00	0.00	0.02	0.20	0.16	0.67	0.24	0.31
MgO	14.93	0.00	0.10	0.01	0.00	8.57	8.25	0.32	11.53	11.34
CaO	4.16	0.01	0.00	0.00	0.02	2.03	2.51	0.36	1.49	1.62
Na2O	0.00	0.00	0.00	0.00	0.00	0.06	0.00	0.30	0.34	0.18
K2O	0.00	0.06	0.04	0.04	0.04	0.44	0.47	0.15	0.44	0.41
ZrO2	0.00	0.00	0.07	0.09	0.03	0.03	0.00	0.24	0.00	0.00
Total	97.51	41.73	58.58	41.64	41.84	88.58	86.70	7.19	86.39	88.82
No.	175	131	133	134	135	226	163	218	255	256
Cations, O = 1										
Si	0.321	0.001	0.029	0.000	0.001	0.324	0.324	0.145	0.330	0.330
Ti	0.000	0.000	0.000	0.001	0.001	0.001	0.000	0.065	0.000	0.000
Al	0.005	0.001	0.003	0.000	0.001	0.038	0.041	0.061	0.039	0.037
Cr	0.000	0.000	0.000	0.000	0.000	0.000	0.000	0.118	0.000	0.000
Fe	0.168	0.995	0.932	0.994	0.993	0.180	0.173	0.095	0.138	0.146
Mn	0.002	0.001	0.000	0.000	0.001	0.001	0.001	0.060	0.002	0.002
Mg	0.150	0.000	0.003	0.000	0.000	0.095	0.093	0.051	0.126	0.121
Ca	0.030	0.000	0.000	0.000	0.001	0.016	0.020	0.041	0.012	0.012
Na	0.000	0.000	0.000	0.000	0.000	0.001	0.000	0.061	0.005	0.003
K	0.000	0.002	0.001	0.002	0.001	0.004	0.005	0.021	0.004	0.004
Zr		0.000	0.001	0.001	0.000	0.000	0.000	0.012	0.000	0.000
Total	0.677	1.000	0.969	0.999	0.998	0.659	0.657	0.729	0.655	0.655

Sample	JKEM-01	JKEM-01	JKEM-01	JKEM-01	JKEM-01	JKEM-01	JKEM-01	JKEM-01	JKEM-01	JKEM-01	JKEM-01	JKEM-01	JKEM-01
Mineral	idd	idd	idd	idd	idd	idd	idd	idd	idd	idd	idd	idd	idd
No.	13	14	15	16	17	18	19	20	21	22	23	24	25
Weight %													
SiO2	57.01	53.12	54.79	52.28	54.52	52.04	54.52	50.40	55.27	53.04	57.32	52.59	55.40
TiO2	0.03	0.03	0.04	0.07	0.05	0.04	0.03	0.06	0.07	0.02	0.05	0.03	0.07
Al2O3	0.04	0.03	0.03	0.02	0.04	0.04	0.02	0.03	0.03	0.00	0.01	0.01	0.03
Cr2O3	0.04	0.07	0.04	0.05	0.04	0.03	0.04	0.05	0.06	0.04	0.02	0.04	0.03
FeO	29.67	32.22	30.86	33.38	31.23	33.24	30.99	34.41	30.04	32.49	28.69	32.40	30.35
MnO	0.36	0.31	0.42	0.37	0.45	0.41	0.37	0.37	0.41	0.38	0.34	0.34	0.43
MgO	2.66	2.45	2.70	2.49	2.84	2.56	2.77	2.41	2.53	2.42	2.58	2.52	2.85
CaO	1.50	1.68	1.52	1.50	1.56	1.53	1.50	1.50	1.72	1.45	1.43	1.44	1.47
Na2O	0.01	0.03	0.04	0.01	0.01	0.03	0.05	0.02	0.03	0.03	0.02	0.02	0.03
K2O	0.13	0.19	0.19	0.21	0.10	0.13	0.16	0.22	0.19	0.21	0.14	0.20	0.20
ZrO2	0.00	0.02	0.01	0.03	0.00	0.02	0.02	0.04	0.00	0.00	0.00	0.00	0.00
Total	91.45	90.14	90.63	90.40	90.83	90.06	90.47	89.50	90.32	90.08	90.58	89.59	90.84
No.	13	14	15	16	17	18	19	20	21	22	23	24	25
Cations, O = 1													
Si	0.393	0.382	0.387	0.378	0.385	0.377	0.386	0.372	0.389	0.382	0.397	0.381	0.388
Ti	0.000	0.000	0.000	0.000	0.000	0.000	0.000	0.000	0.000	0.000	0.000	0.000	0.000
Al	0.000	0.000	0.000	0.000	0.000	0.000	0.000	0.000	0.000	0.000	0.000	0.000	0.000
Cr	0.000	0.000	0.000	0.000	0.000	0.000	0.000	0.000	0.000	0.000	0.000	0.000	0.000
Fe	0.171	0.194	0.182	0.202	0.184	0.202	0.183	0.212	0.177	0.196	0.166	0.196	0.178
Mn	0.002	0.002	0.003	0.002	0.003	0.003	0.002	0.002	0.002	0.002	0.002	0.002	0.003
Mg	0.027	0.026	0.028	0.027	0.030	0.028	0.029	0.027	0.027	0.026	0.027	0.027	0.030
Ca	0.011	0.013	0.012	0.012	0.012	0.012	0.011	0.012	0.013	0.011	0.011	0.011	0.011
Na	0.000	0.000	0.001	0.000	0.000	0.000	0.001	0.000	0.000	0.000	0.000	0.000	0.000
K	0.001	0.002	0.002	0.002	0.001	0.001	0.001	0.002	0.002	0.002	0.001	0.002	0.002
Zr	0.000	0.000	0.000	0.000	0.000	0.000	0.000	0.000	0.000	0.000	0.000	0.000	0.000
Total	0.607	0.619	0.614	0.623	0.615	0.623	0.615	0.628	0.611	0.619	0.604	0.620	0.612

Sample	JKEM-01	JKEM-01	JKEM-01	JKEM-01	JKEM-01	JKEM-01	JKEM-01	JKEM-01
Mineral	idd	idd	idd	idd	idd	idd	idd	idd
No.	26	27	28	29	30	31	32	33
Weight %								
SiO2	52.64	55.17	52.97	51.22	54.47	45.74	49.81	46.31
TiO2	0.08	0.00	0.00	0.00	0.00	0.02	0.01	0.00
Al2O3	0.02	0.02	0.05	0.06	0.00	0.08	0.06	0.08
Cr2O3	0.09	0.00	0.00	0.03	0.00	0.00	0.03	0.03
FeO	33.61	30.29	33.13	33.97	29.44	36.34	33.75	36.38
MnO	0.38	0.36	0.37	0.41	0.51	0.35	0.45	0.39
MgO	2.74	2.51	2.57	2.74	2.57	2.95	2.38	3.75
CaO	1.51	1.53	1.53	1.50	1.57	1.20	1.80	0.97
Na2O	0.04	0.03	0.03	0.04	0.00	0.01	0.00	0.07
K2O	0.21	0.21	0.21	0.17	0.20	0.17	0.16	0.40
ZrO2	0.01	0.00	0.00	0.07	0.02	0.00	0.01	0.04
Total	91.30	90.12	90.86	90.21	88.78	86.88	88.45	88.41
No.	26	27	28	29	30	31	32	33
Cations, O = 6								
Si	0.377	0.390	0.379	0.373	0.390	0.357	0.372	0.355
Ti	0.000	0.000	0.000	0.000	0.000	0.000	0.000	0.000
Al	0.000	0.000	0.000	0.001	0.000	0.001	0.001	0.001
Cr	0.001	0.000	0.000	0.000	0.000	0.000	0.000	0.000
Fe	0.201	0.179	0.198	0.207	0.176	0.237	0.211	0.233
Mn	0.002	0.002	0.002	0.003	0.003	0.002	0.003	0.003
Mg	0.029	0.026	0.027	0.030	0.027	0.034	0.027	0.043
Ca	0.012	0.012	0.012	0.012	0.012	0.010	0.014	0.008
Na	0.001	0.000	0.000	0.001	0.000	0.000	0.000	0.001
K	0.002	0.002	0.002	0.002	0.002	0.002	0.002	0.004
Zr	0.000	0.000	0.000	0.000	0.000	0.000	0.000	0.000
Total	0.624	0.612	0.622	0.627	0.611	0.644	0.628	0.647

Appendix B: Locations of EMP analyses

Analysis legend:

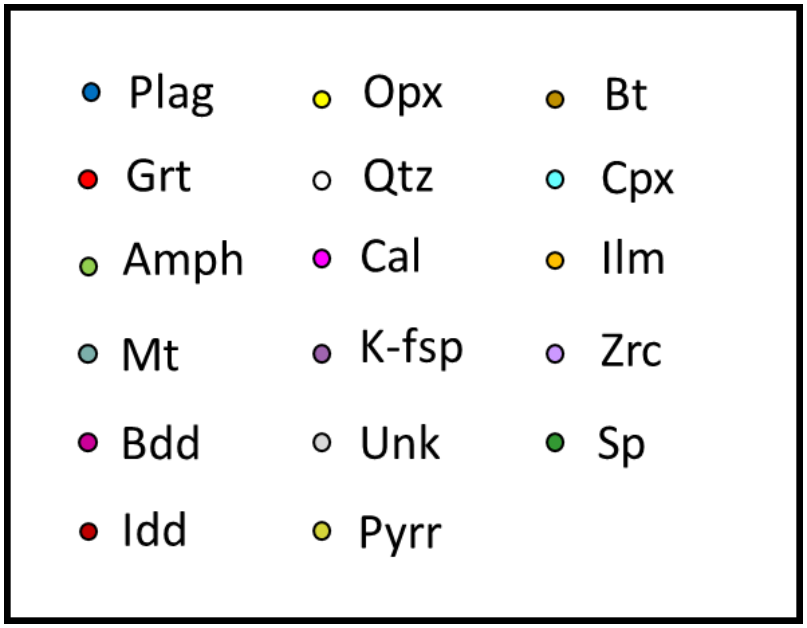

JKEM-12

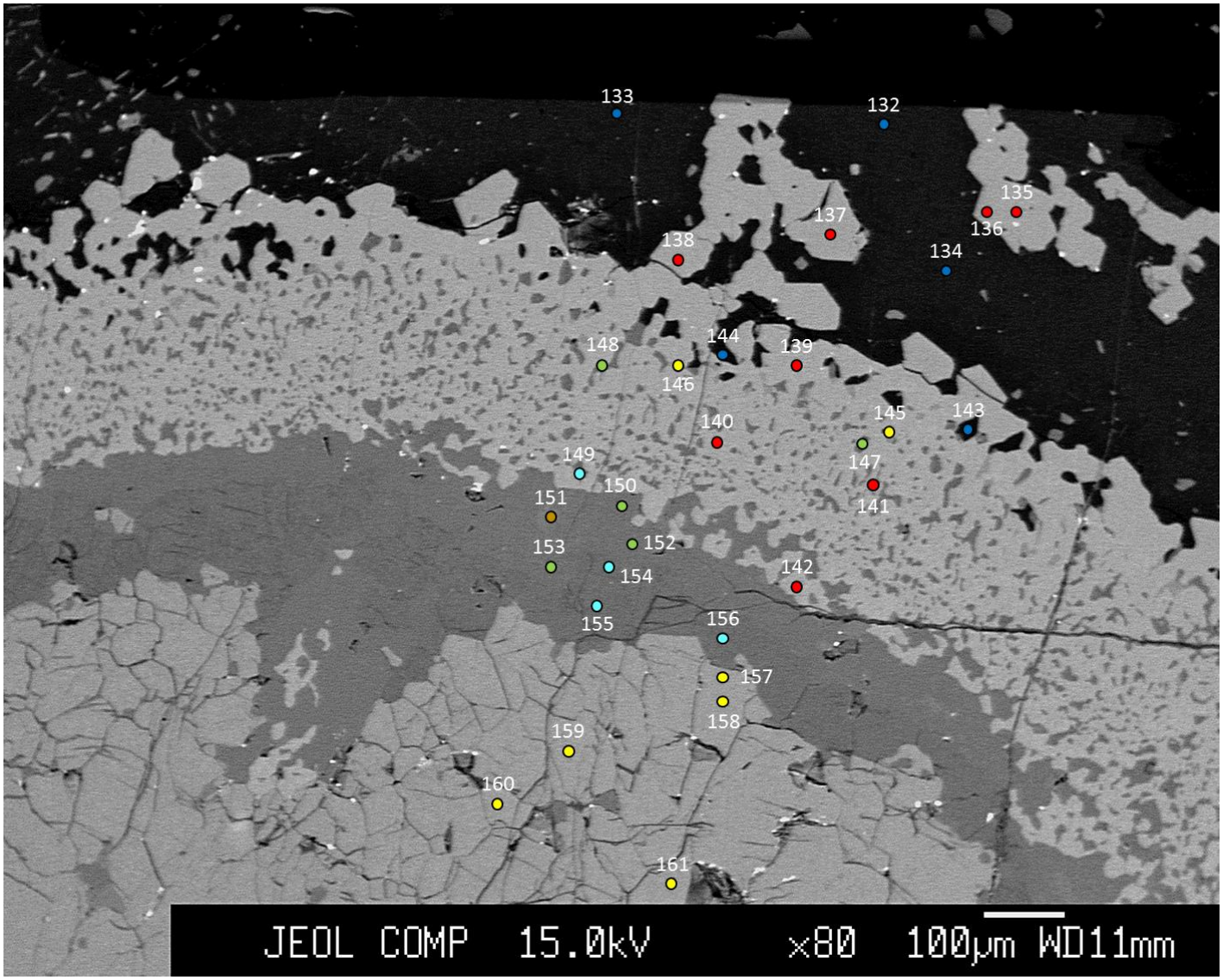
133
132
135
136
137
138
134
148
144
139
146
140
145
143
149
147
150
151
141
153
152
154
142
155
156
157
158
159
160
161
JEOL COMP 15.0kV ×80 100μm WD11mm

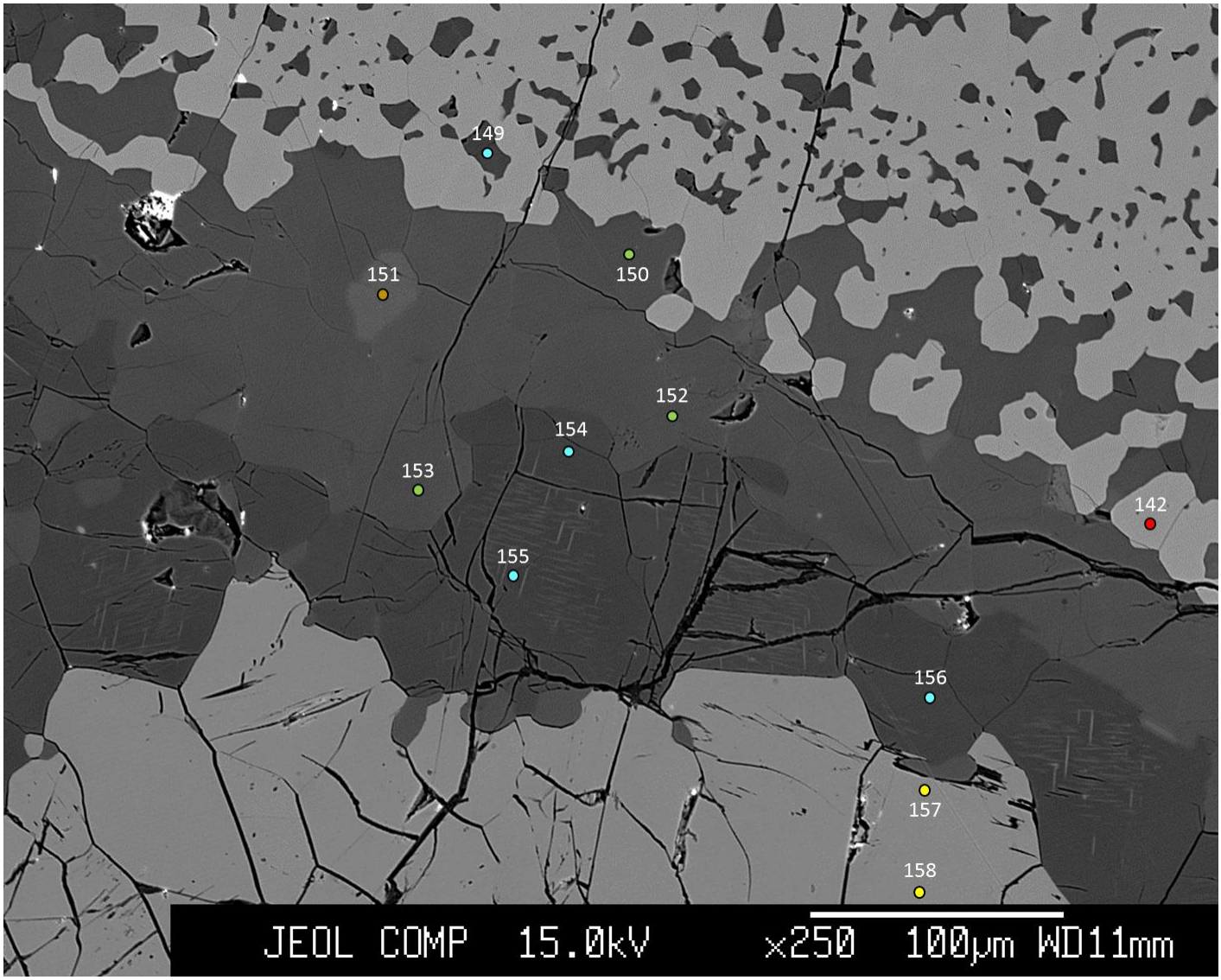
149
151
150
152
154
153
142
155
156
157
158
JEOL COMP 15.0kV x250 100µm WD11mm

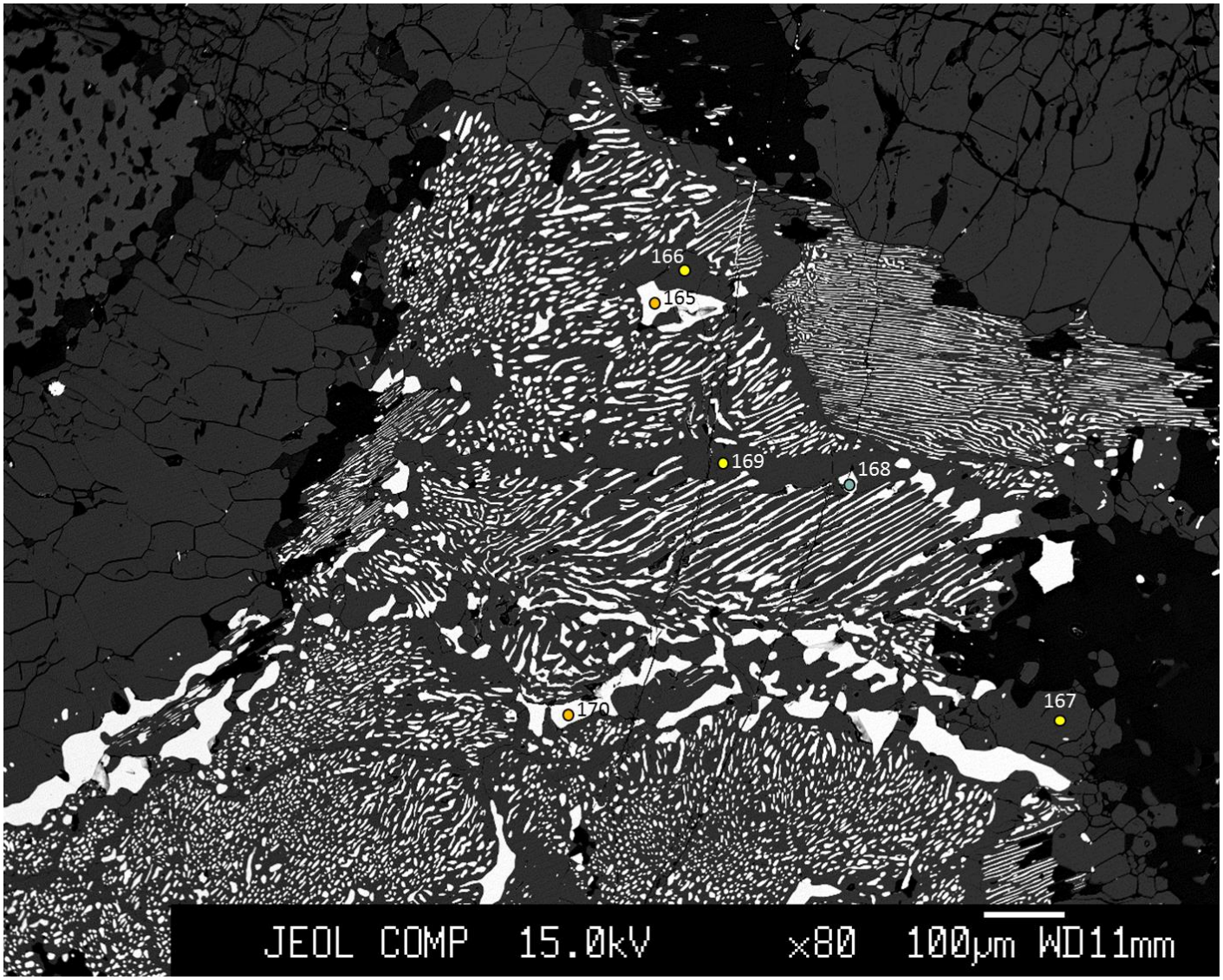
166
165
169
168
170
167
JEOL COMP 15.0kV ×80 100µm WD11mm

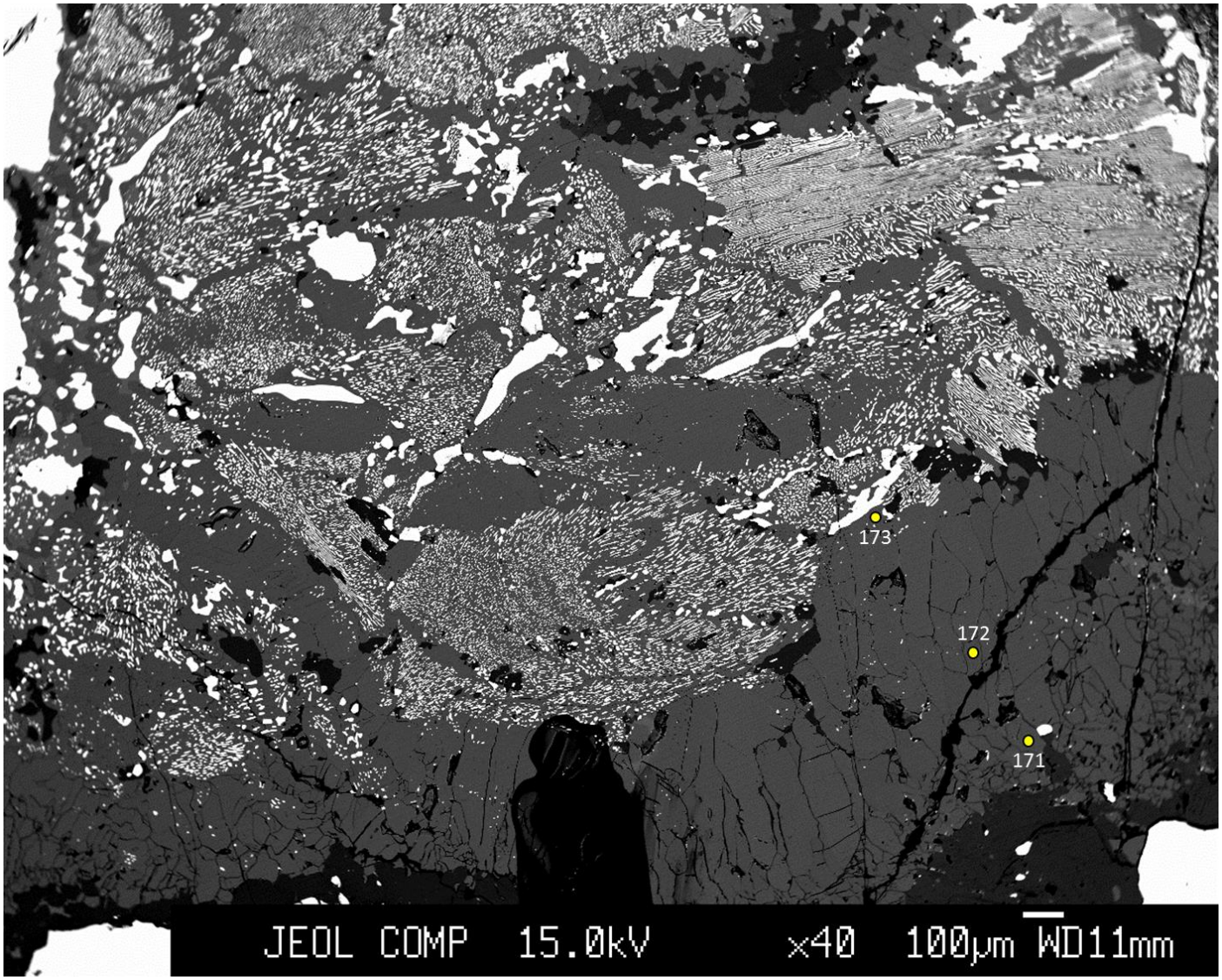
173
172
171
JEOL COMP 15.0kV x40 100µm WD11mm

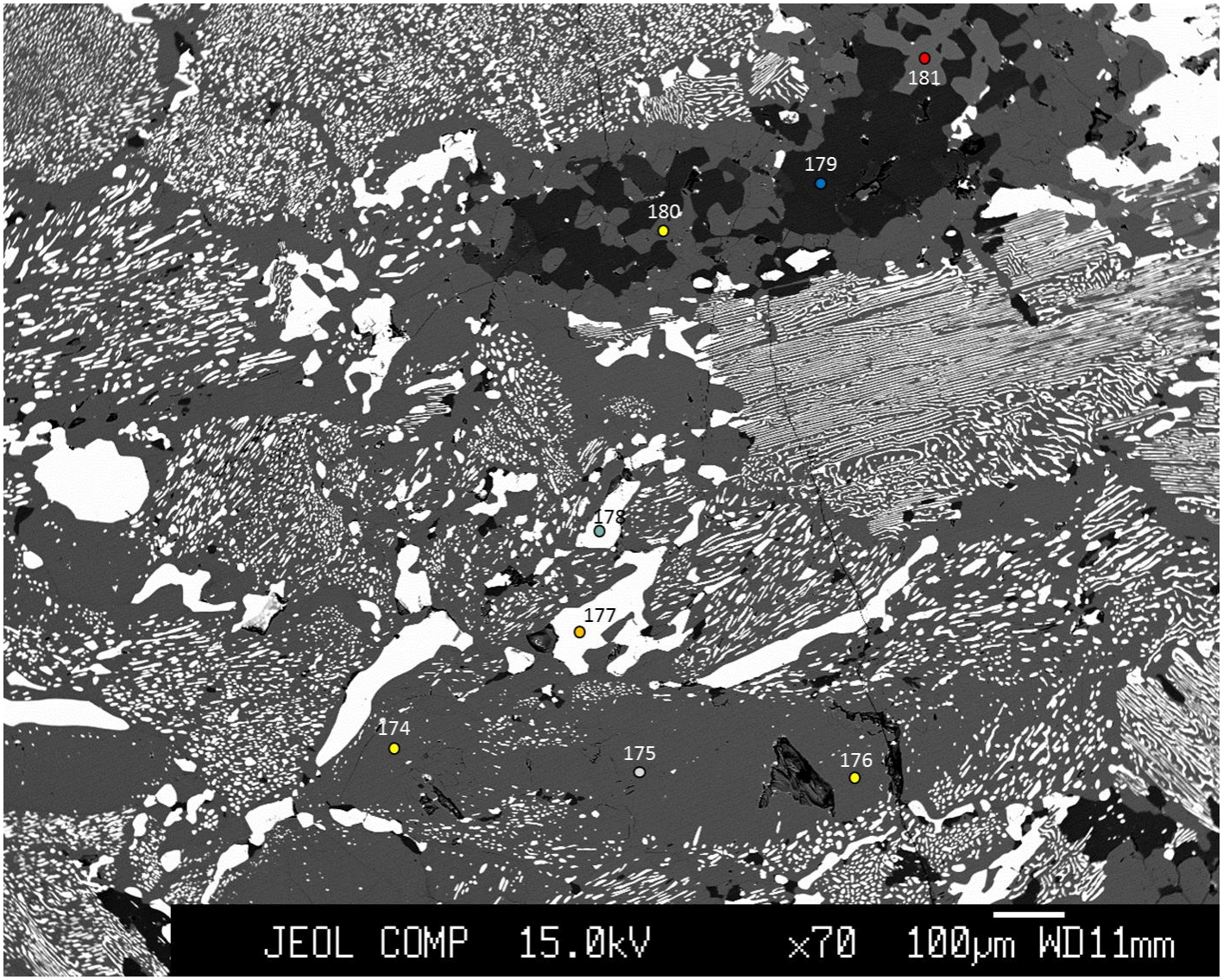
181
179
180
178
177
174
175
176
JEOL COMP 15.0kV ×70 100μm WD11mm

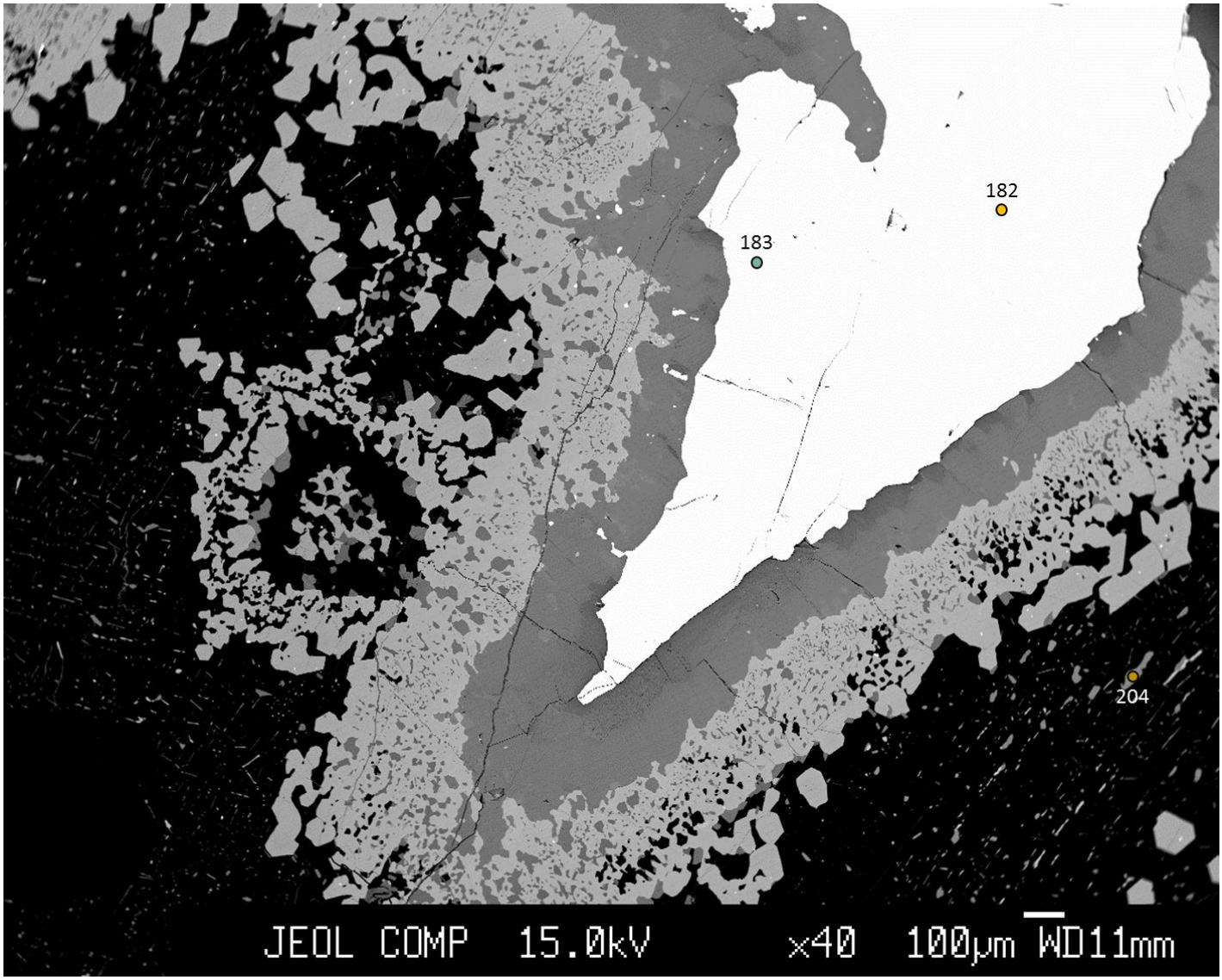
182
183
204
JEOL COMP 15.0kV x40 100µm WD11mm

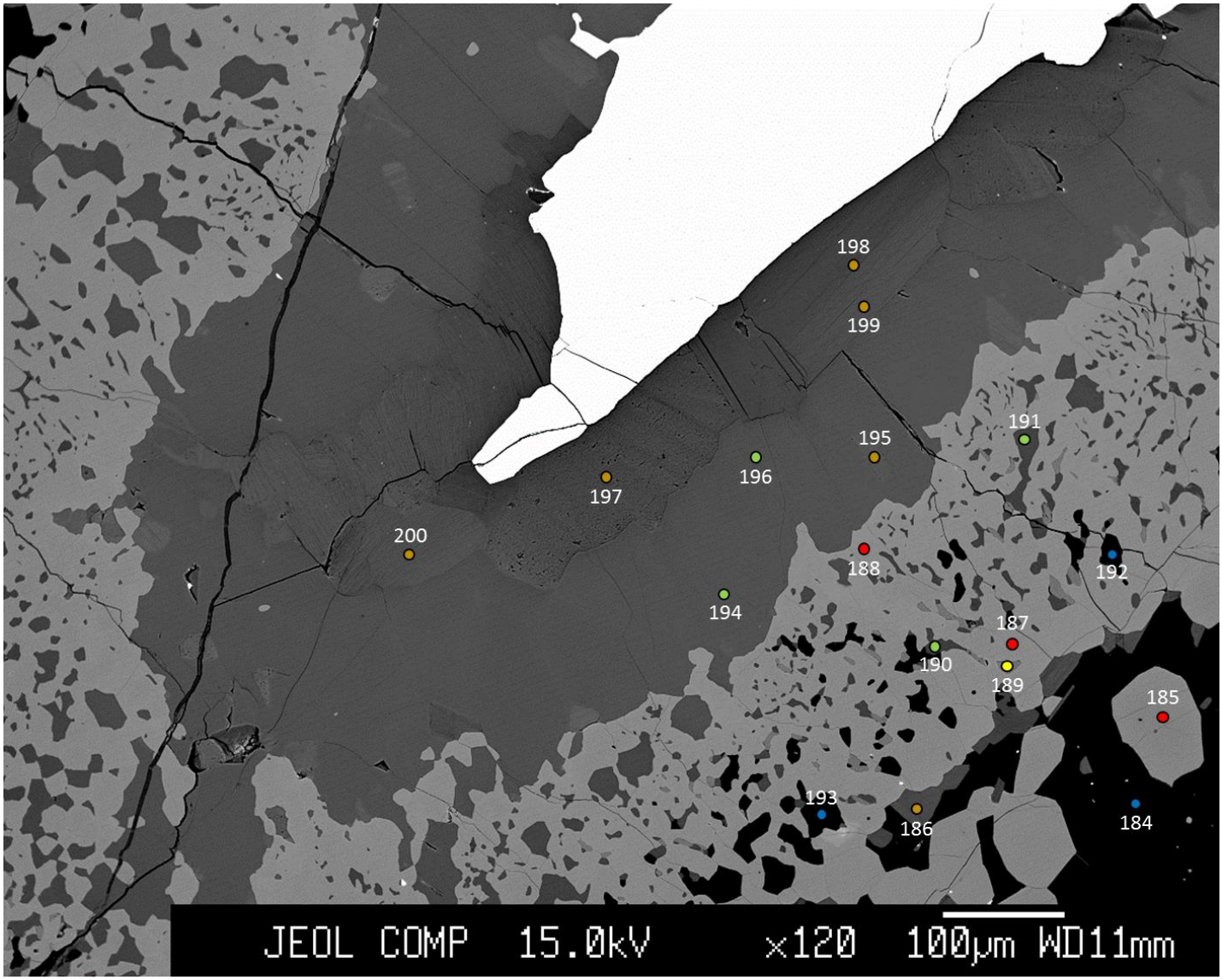
198
199
191
195
196
197
200
188
192
194
187
190
189
185
193
186
184
JEOL COMP 15.0kV ×120 100µm WD11mm

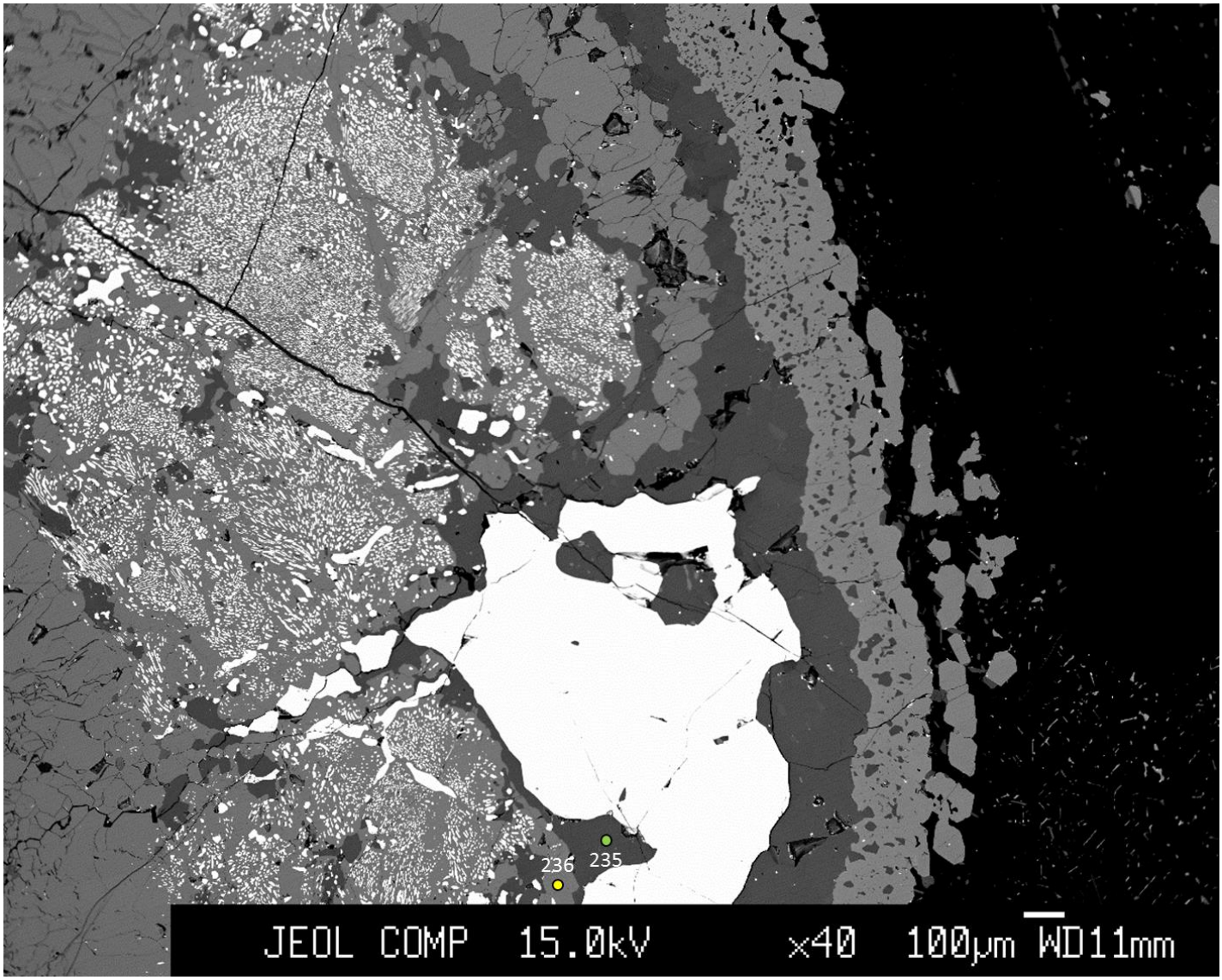
236
235
JEOL COMP 15.0kV x40 100µm WD11mm

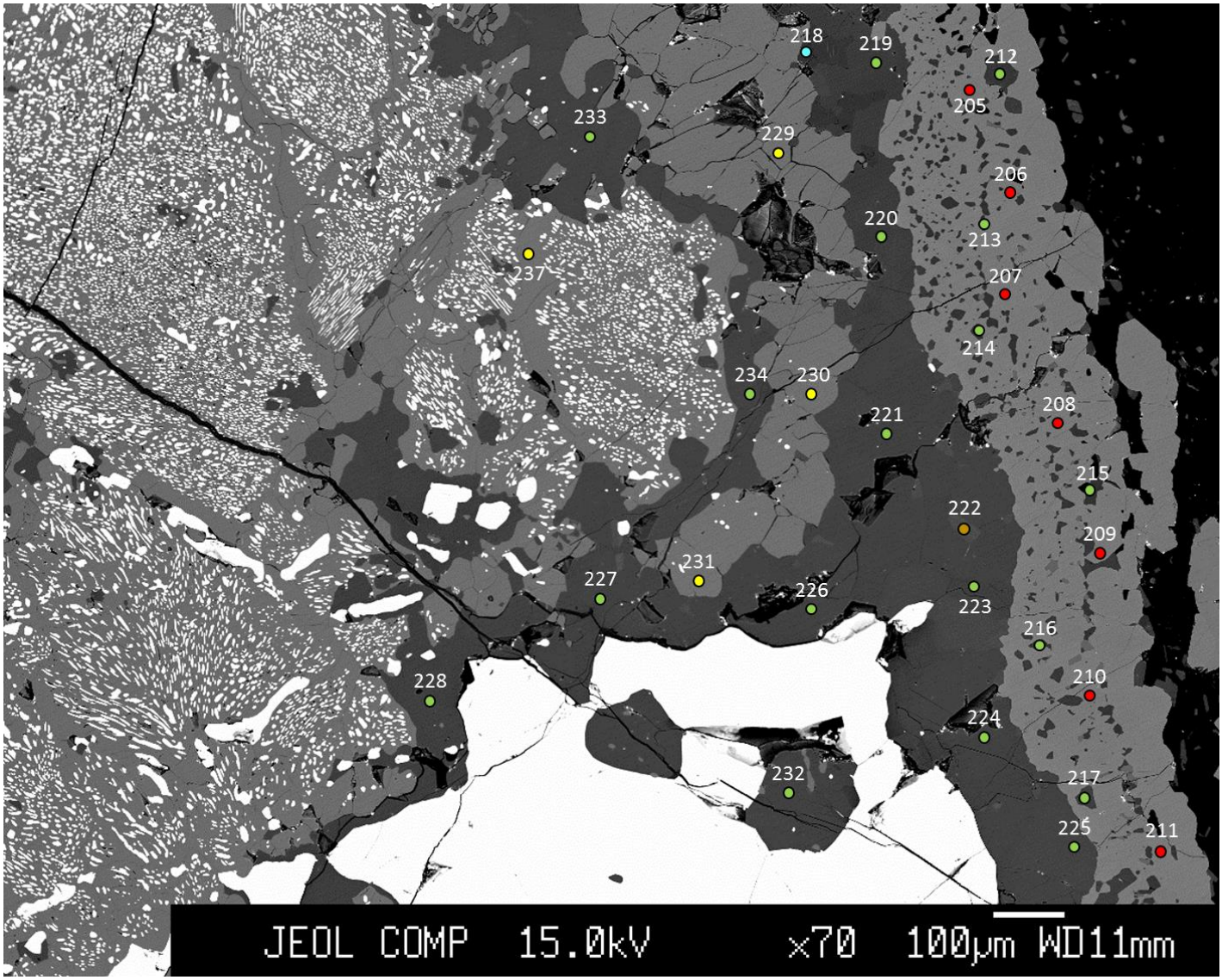
218
219
212
205
233
229
206
220
213
237
207
214
234
230
208
221
215
222
209
231
227
226
223
216
228
210
224
232
217
225
211
JEOL COMP 15.0kV ×70 100µm WD11mm

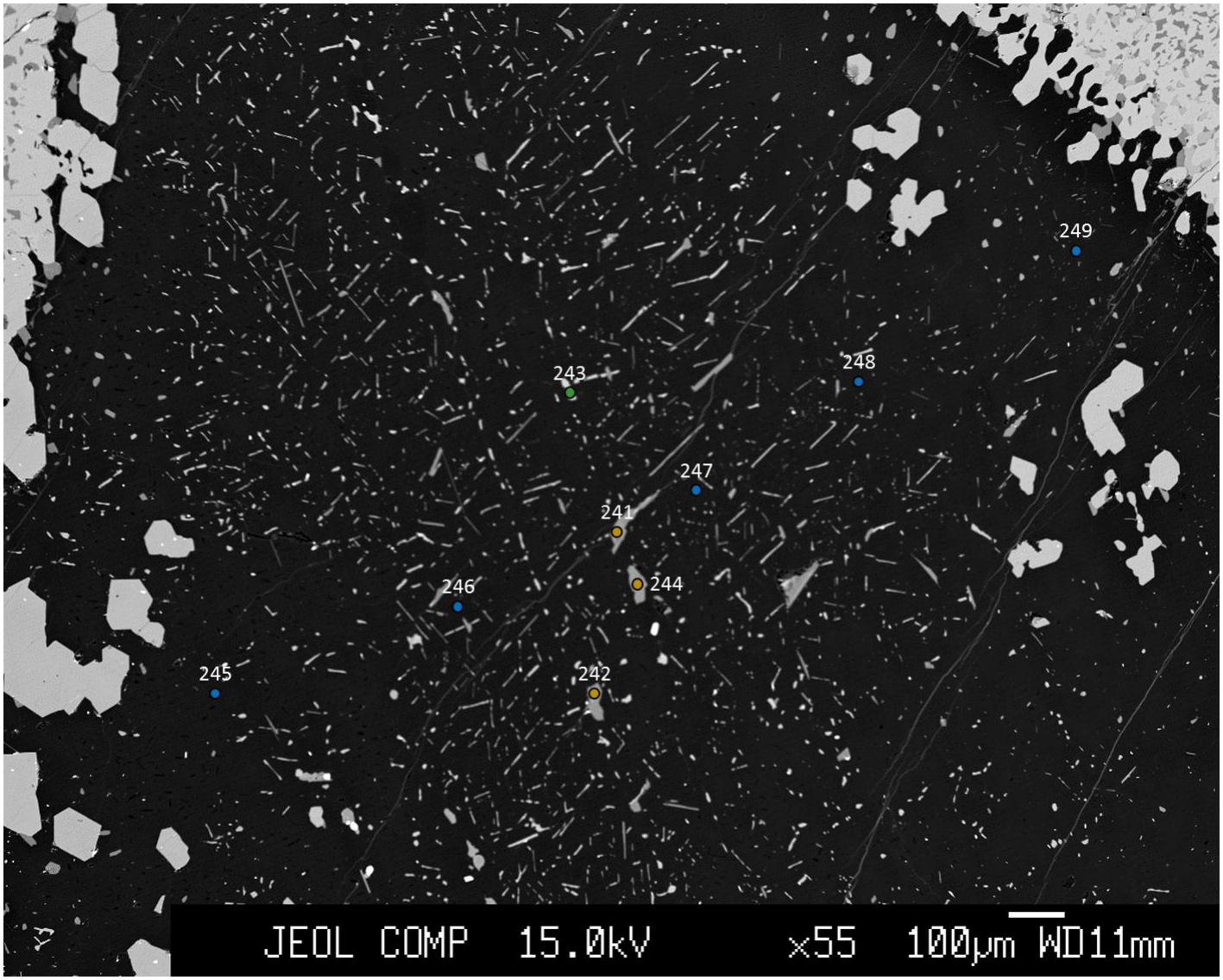
249
248
243
247
241
246
244
245
242
JEOL COMP 15.0kV ×55 100µm WD11mm

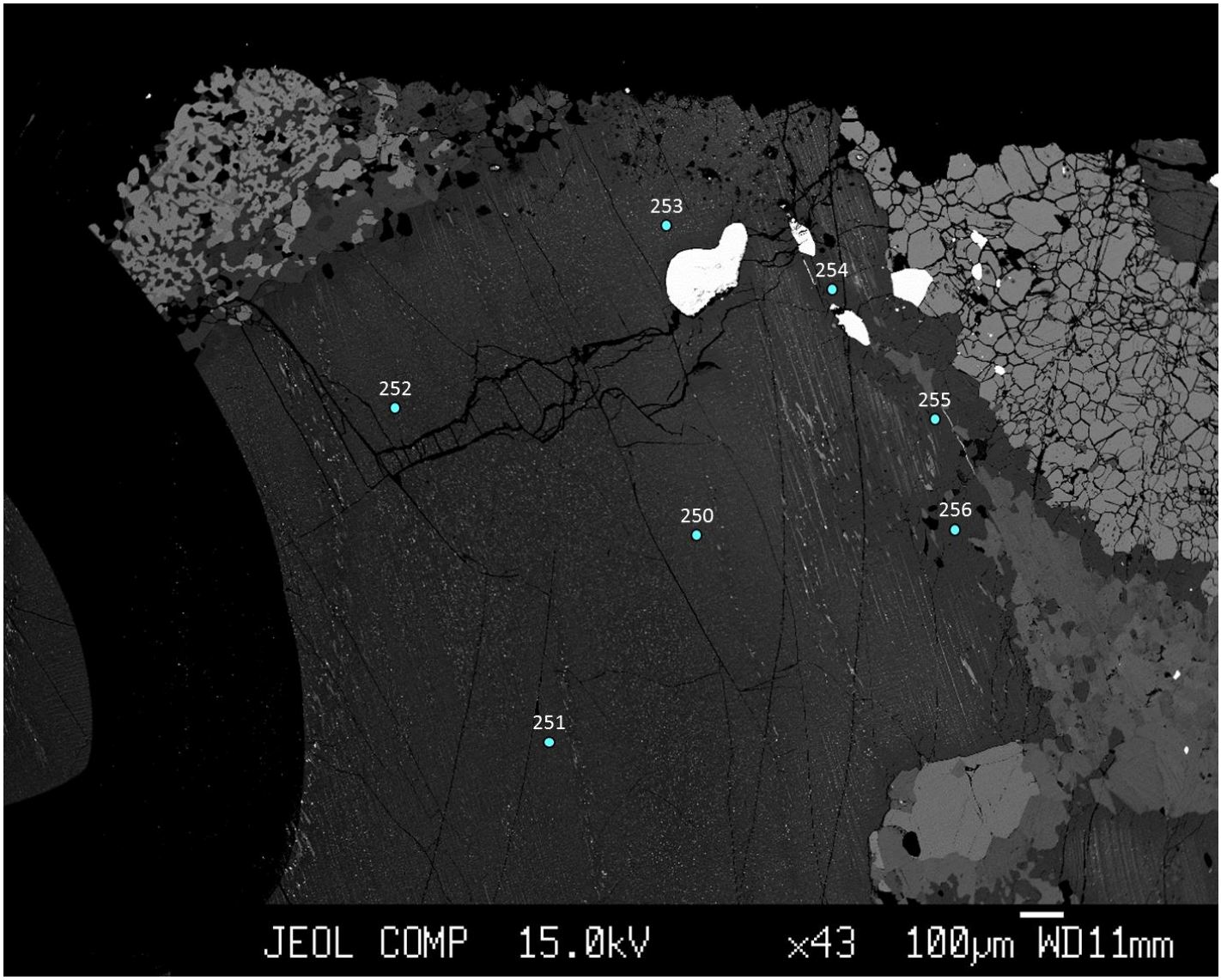
253
254
252
255
250
256
251
JEOL COMP 15.0kV x43 100µm WD11mm

JKEM-14a

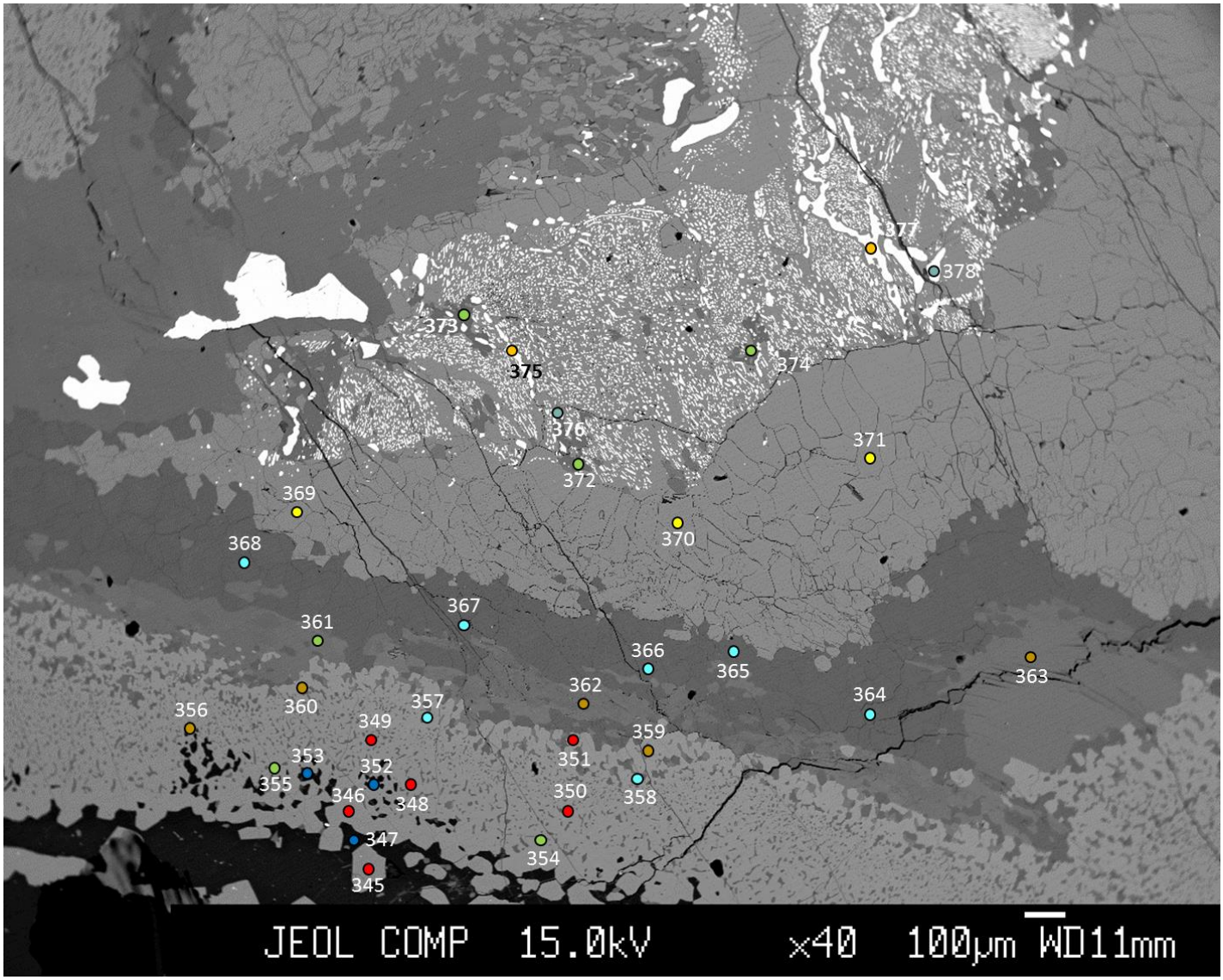
377
378
373
375
374
376
371
372
369
370
368
367
361
366
365
363
362
364
356
360
357
349
359
353
351
352
355
346
348
350
358
347
354
345
JEOL COMP 15.0kV x40 100µm WD11mm

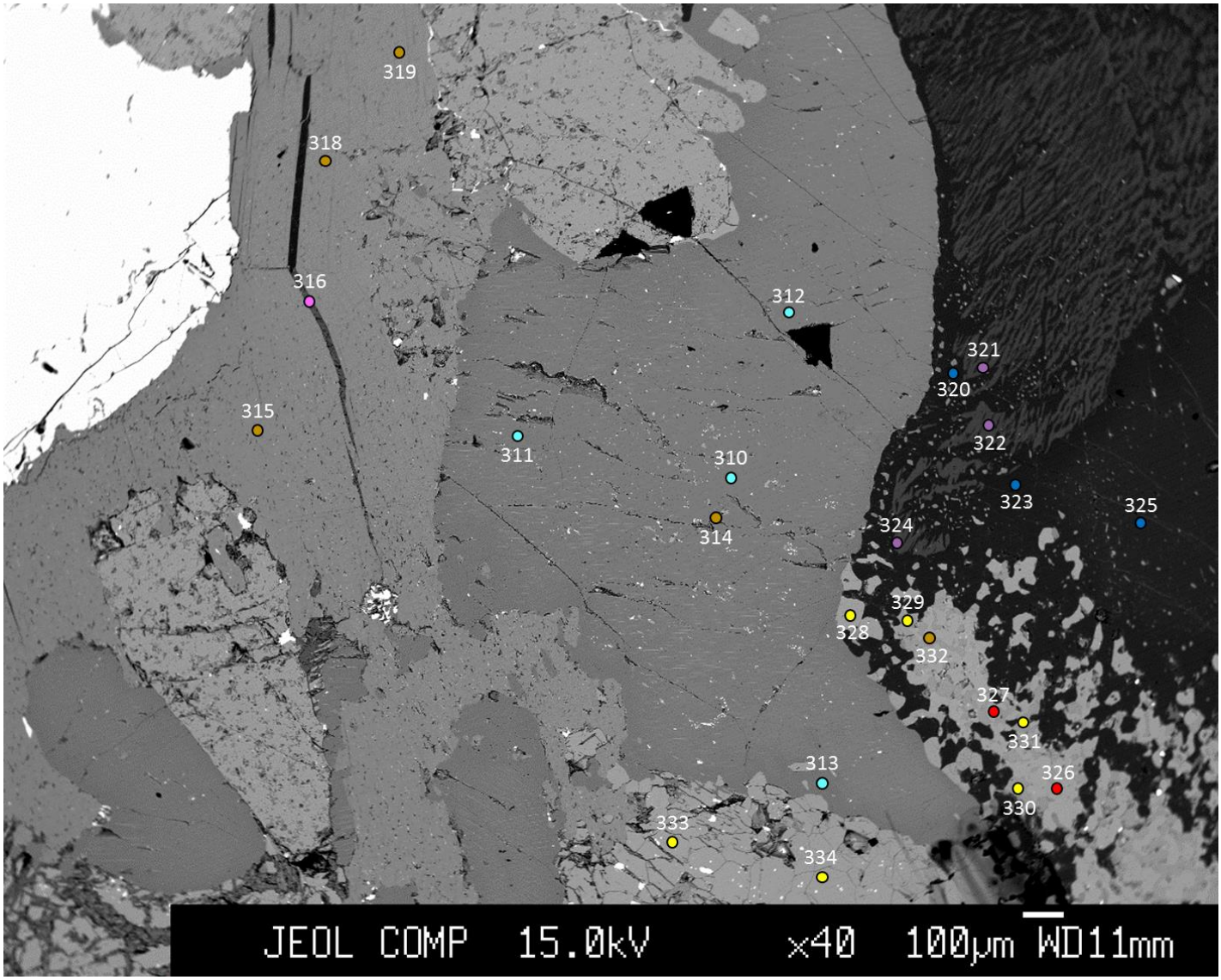
319
318
316
312
321
320
315
322
311
310
323
325
324
314
329
328
332
327
331
313
326
330
333
334
JEOL COMP 15.0kV x40 100µm WD11mm

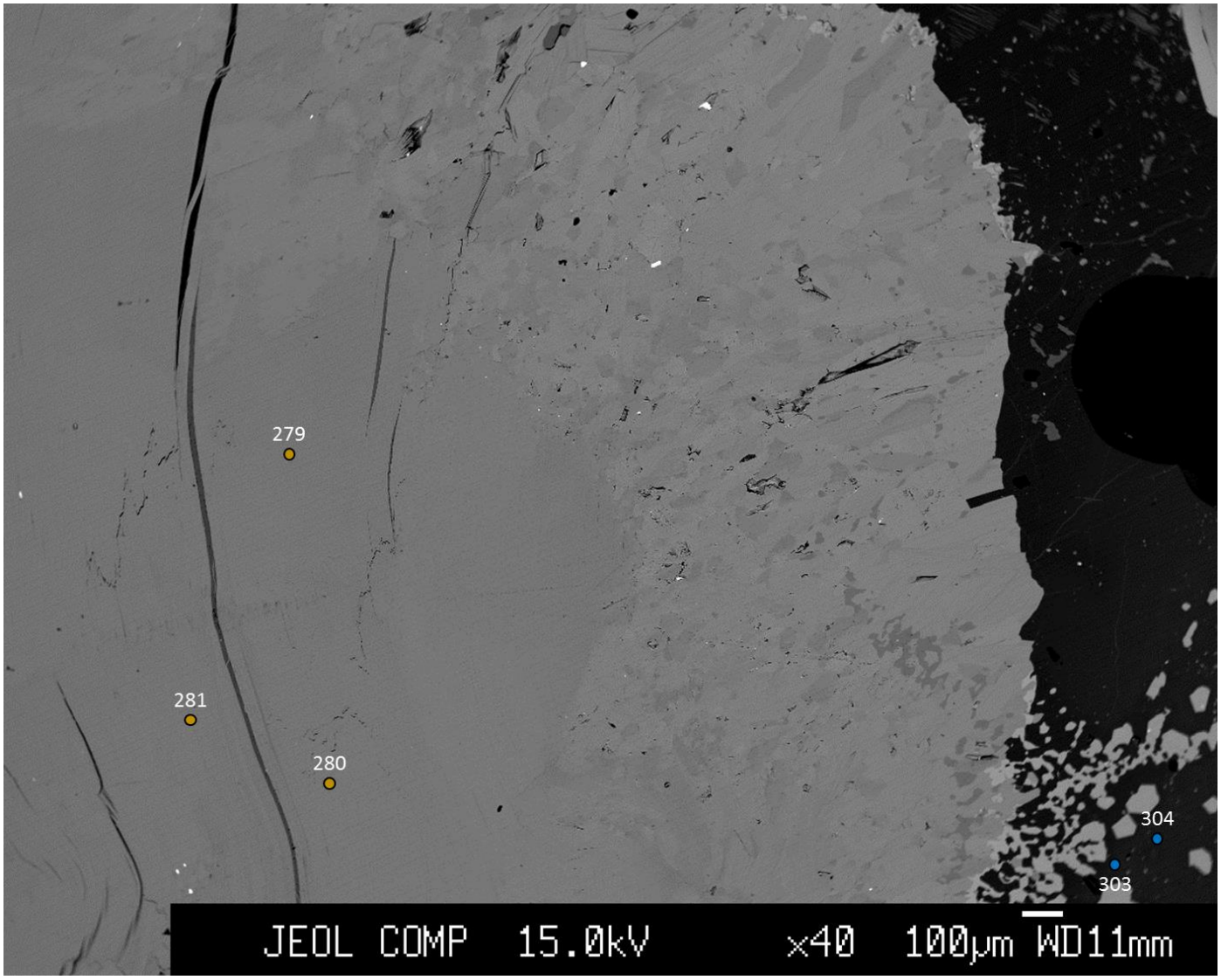
279
281
280
304
303
JEOL COMP 15.0kV x40 100µm WD11mm

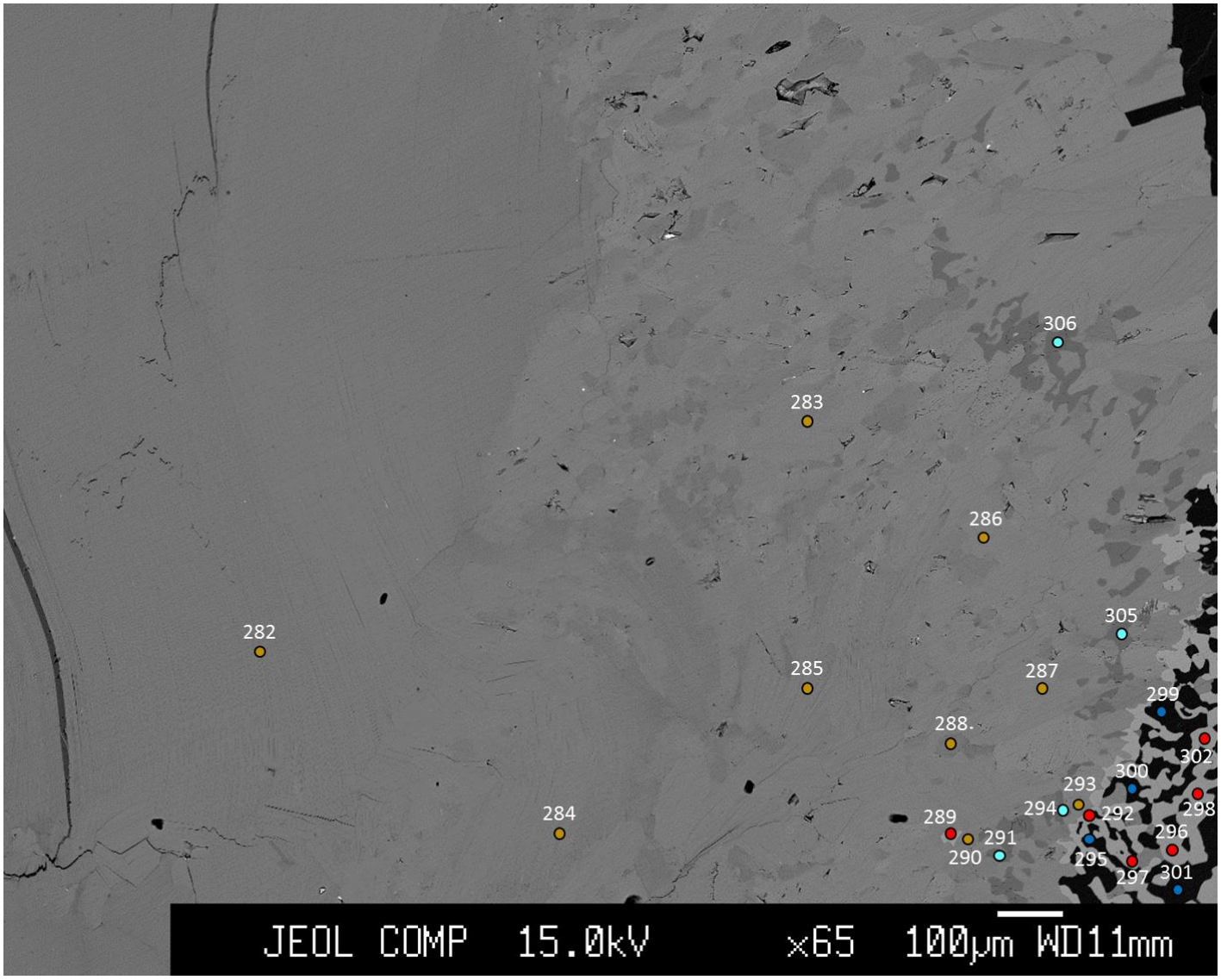
306
283
286
282
305
285
287
299
288.
302
300
293
284
294
298
289
292
296
291
290
295
297
301
JEOL COMP 15.0kV ×65 100µm WD11mm

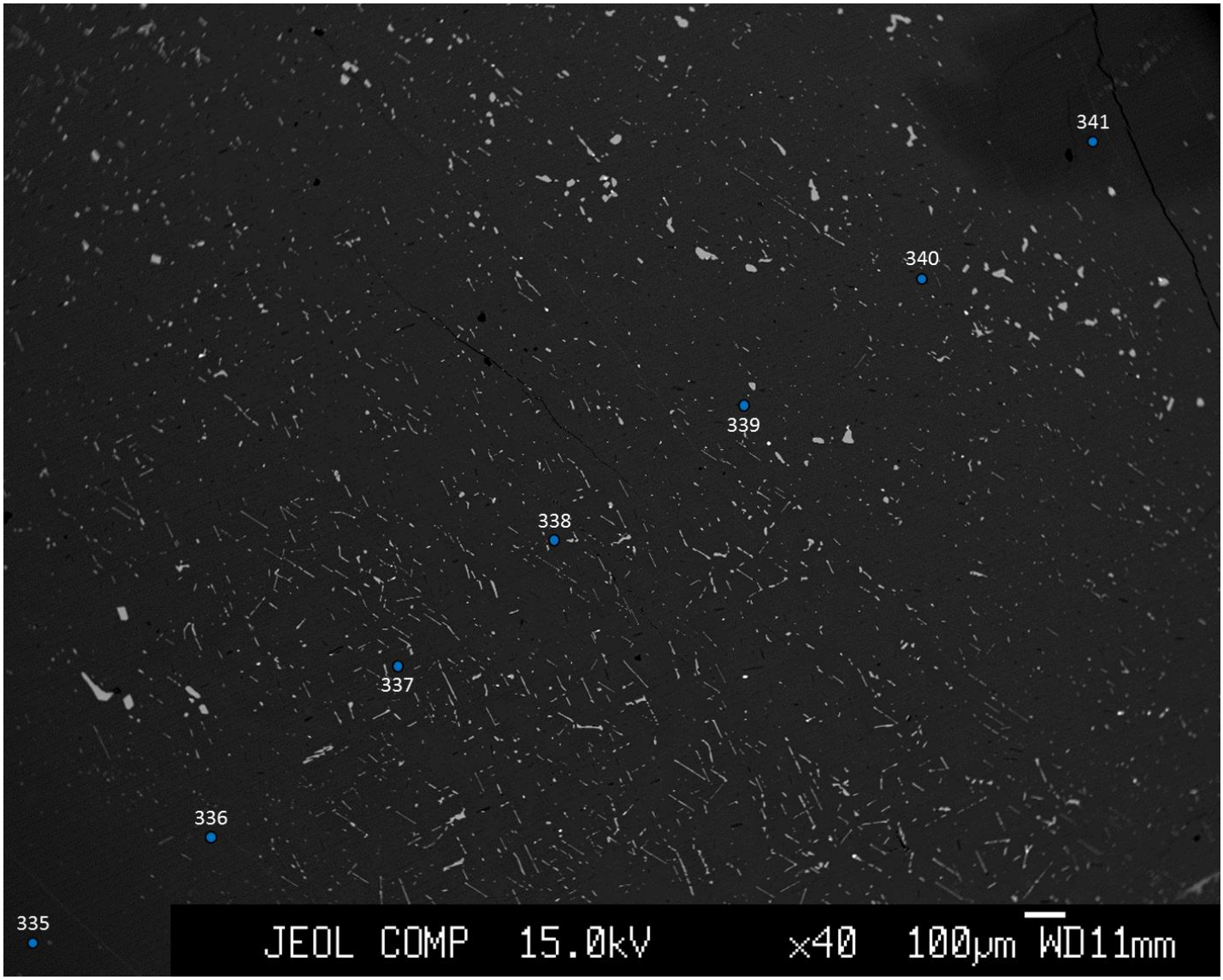
341
340
339
338
337
336
335
JEOL COMP 15.0kV x40 100µm WD11mm

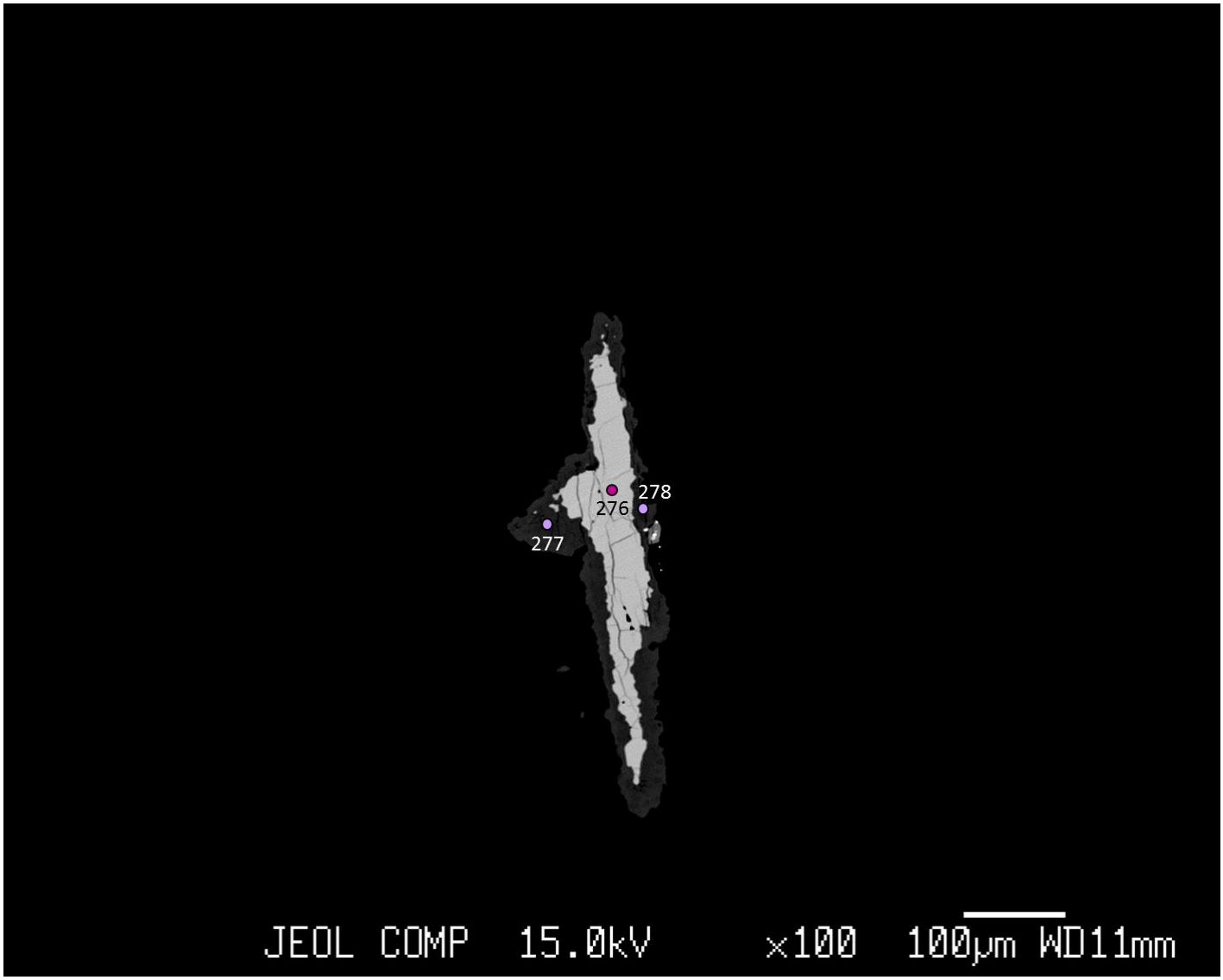
278
276
277
JEOL COMP 15.0kV ×100 100μm WD11mm

JKEM-15a

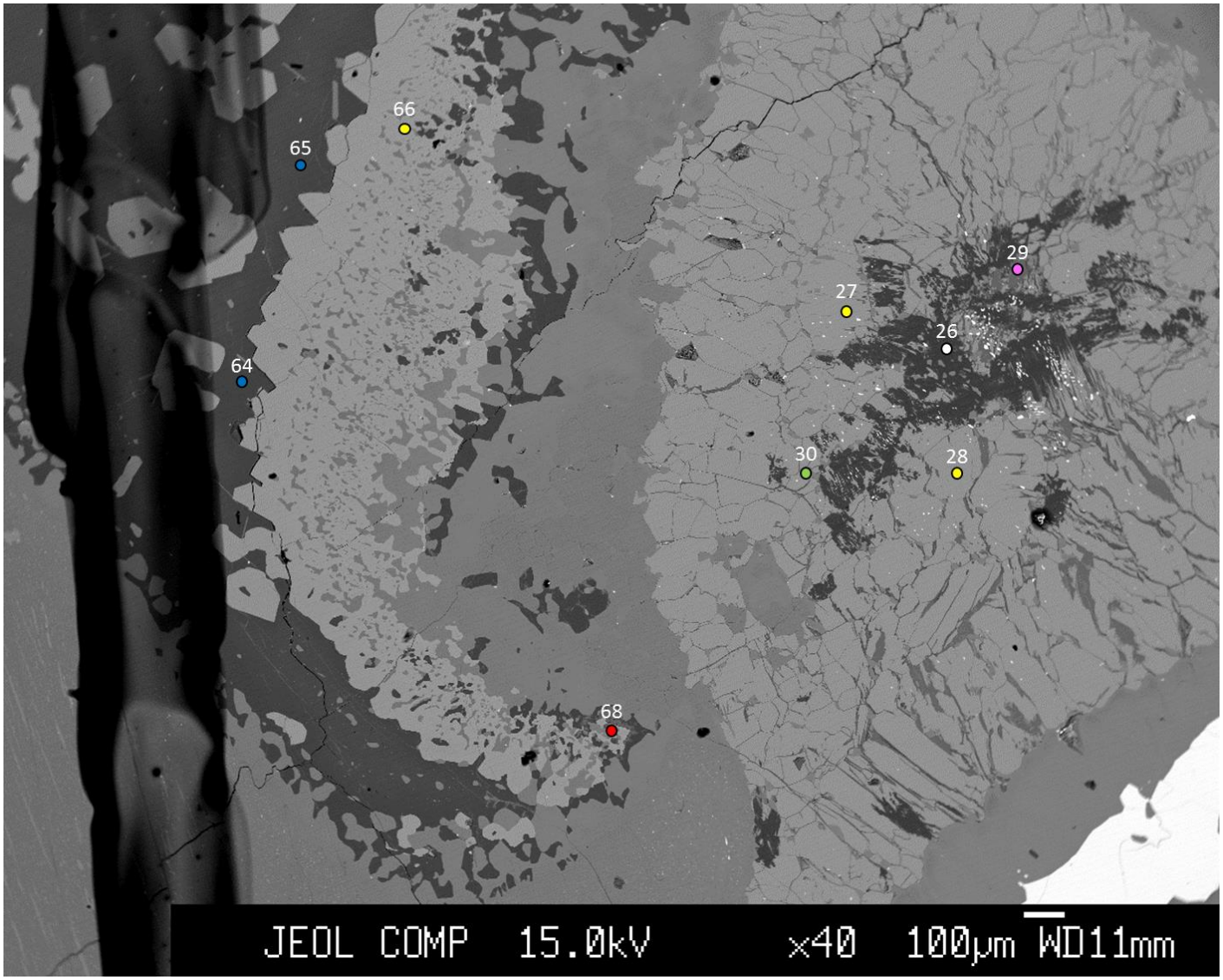

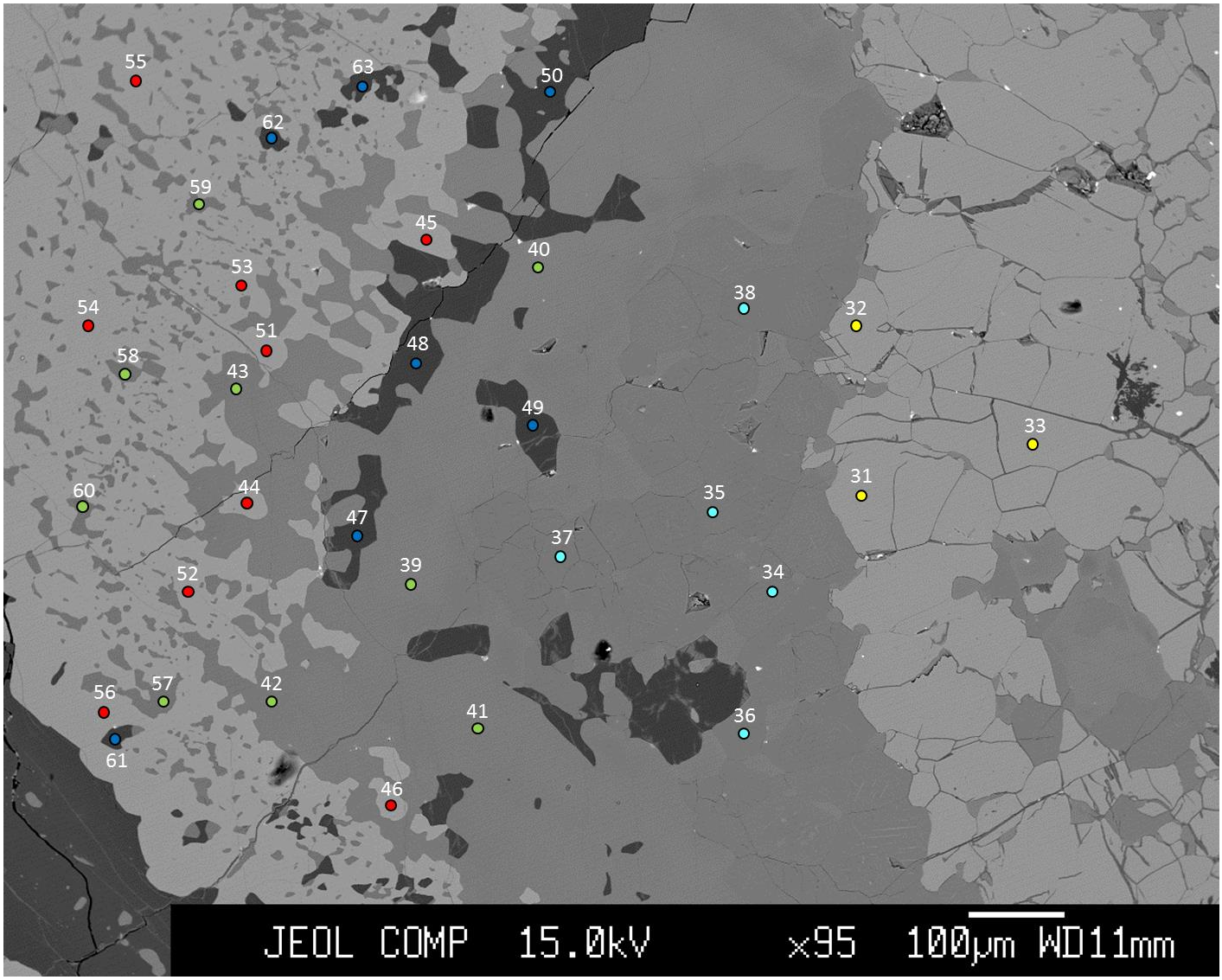
55
63
50
62
59
45
40
53
38
32
54
51
48
58
43
49
33
31
60
44
35
47
37
39
34
52
56
57
42
41
36
61
46
JEOL COMP 15.0kV x95 100µm WD11mm

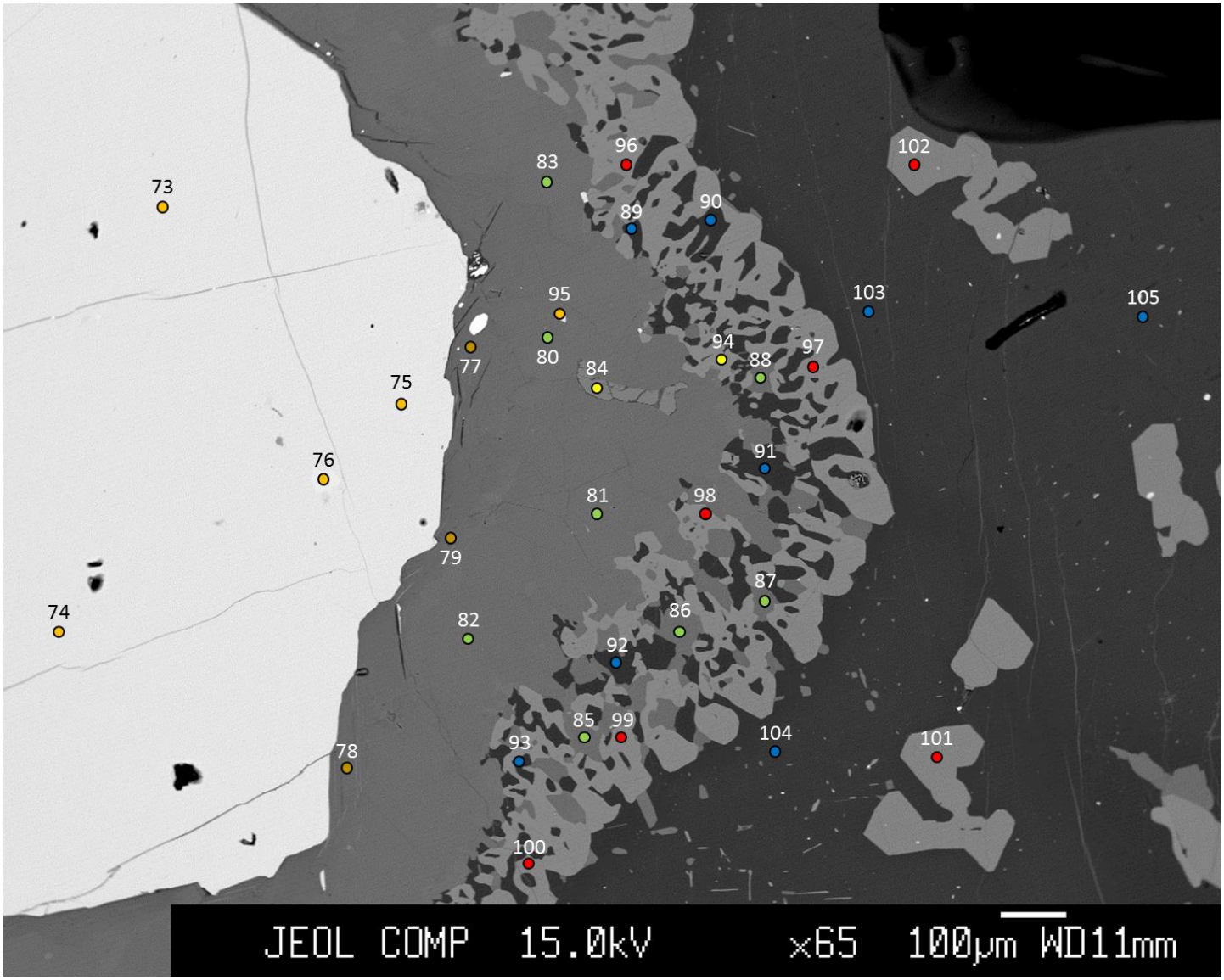
73
74
75
76
77
78
79
80
82
83
84
85
86
87
88
89
90
91
92
93
94
95
96
97
98
99
100
101
102
103
104
105
JEOL COMP 15.0kV ×65 100µm WD11mm

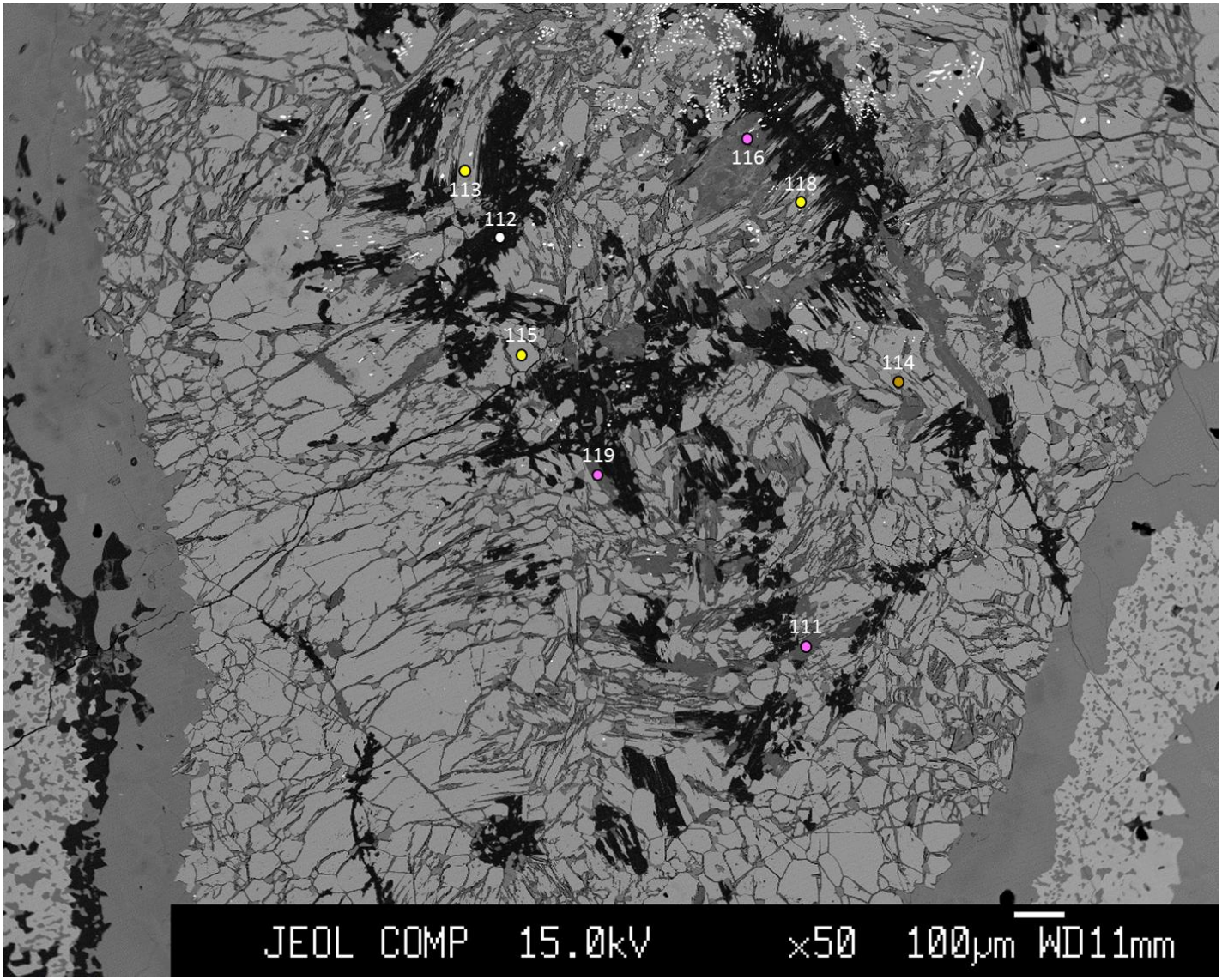
116
113
118
112
115
114
119
111
JEOL COMP 15.0kV x50 100µm WD11mm

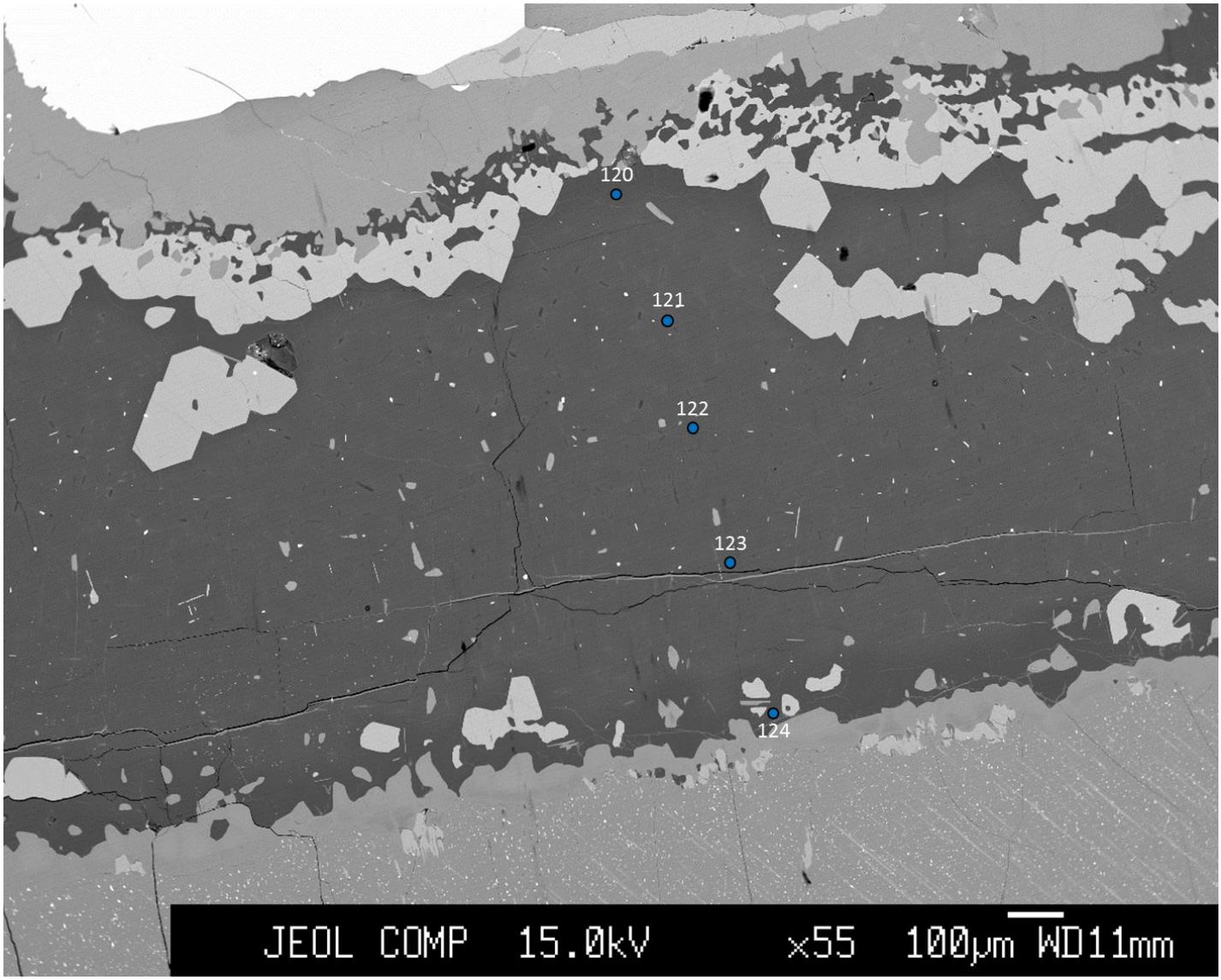
120
121
122
123
124
JEOL COMP 15.0kV x55 100µm WD11mm

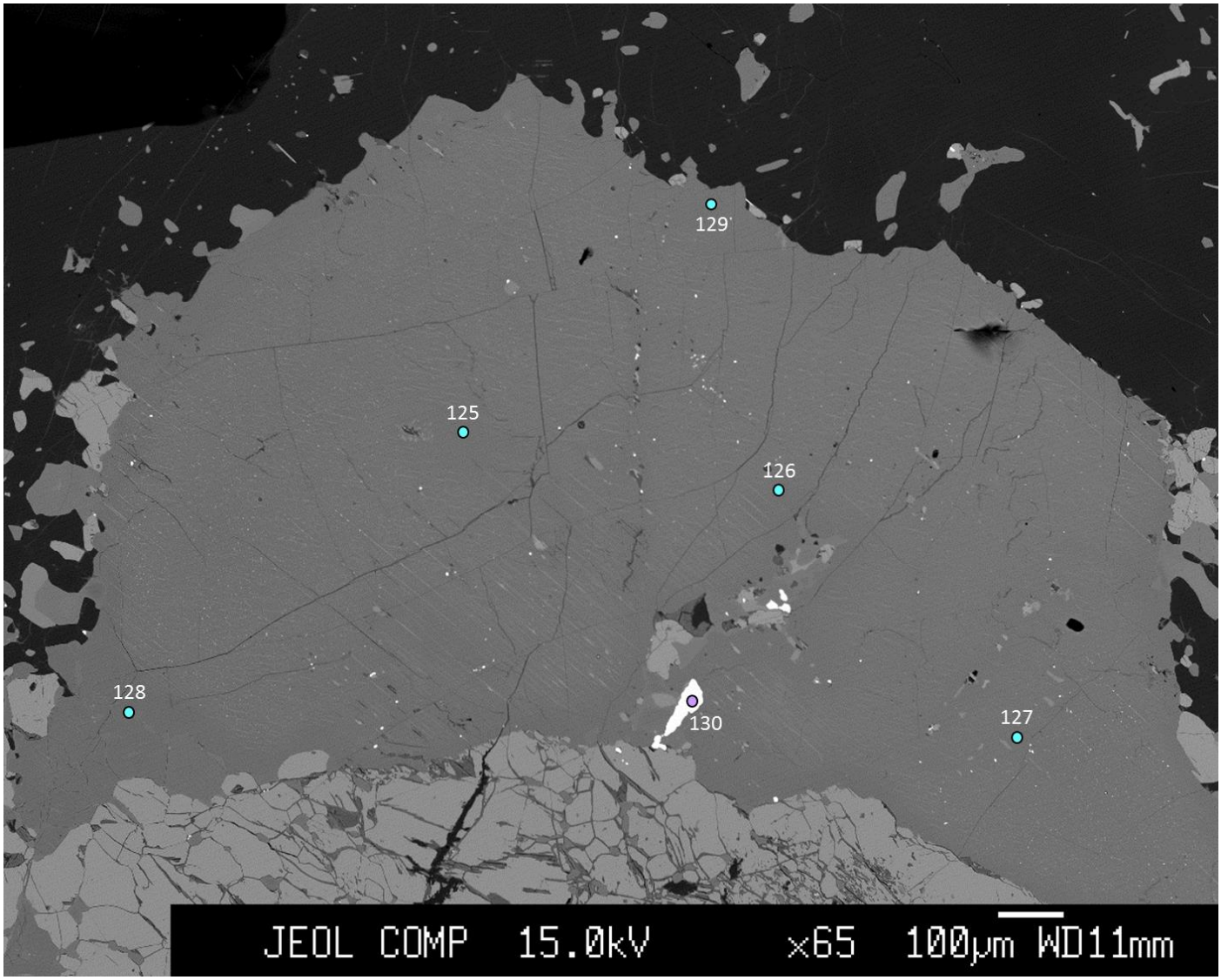
129
125
126
128
130
127
JEOL COMP 15.0kV x65 100µm WD11mm

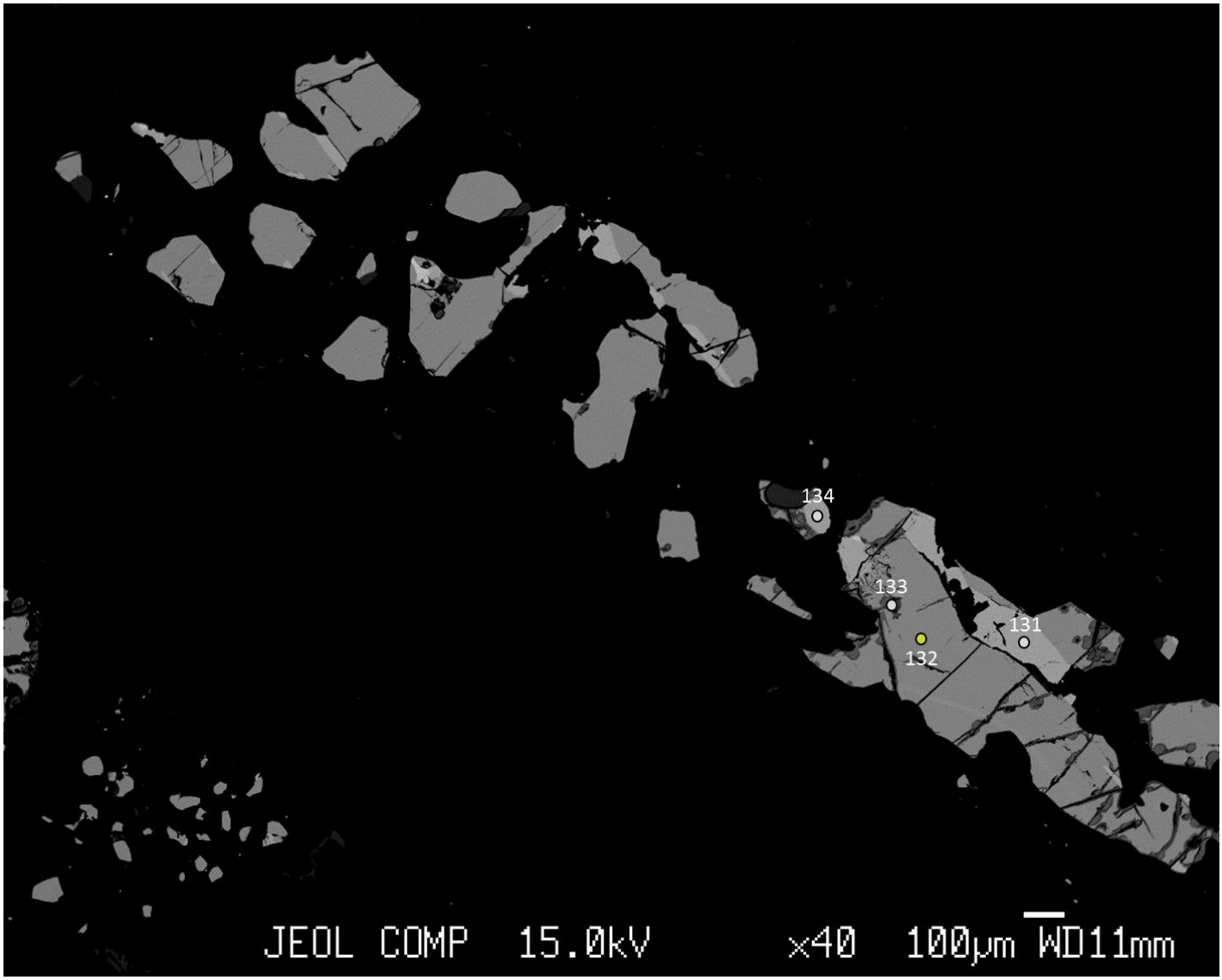
134
133
131
132
JEOL COMP 15.0kV x40 100µm WD11mm

JKEM-01

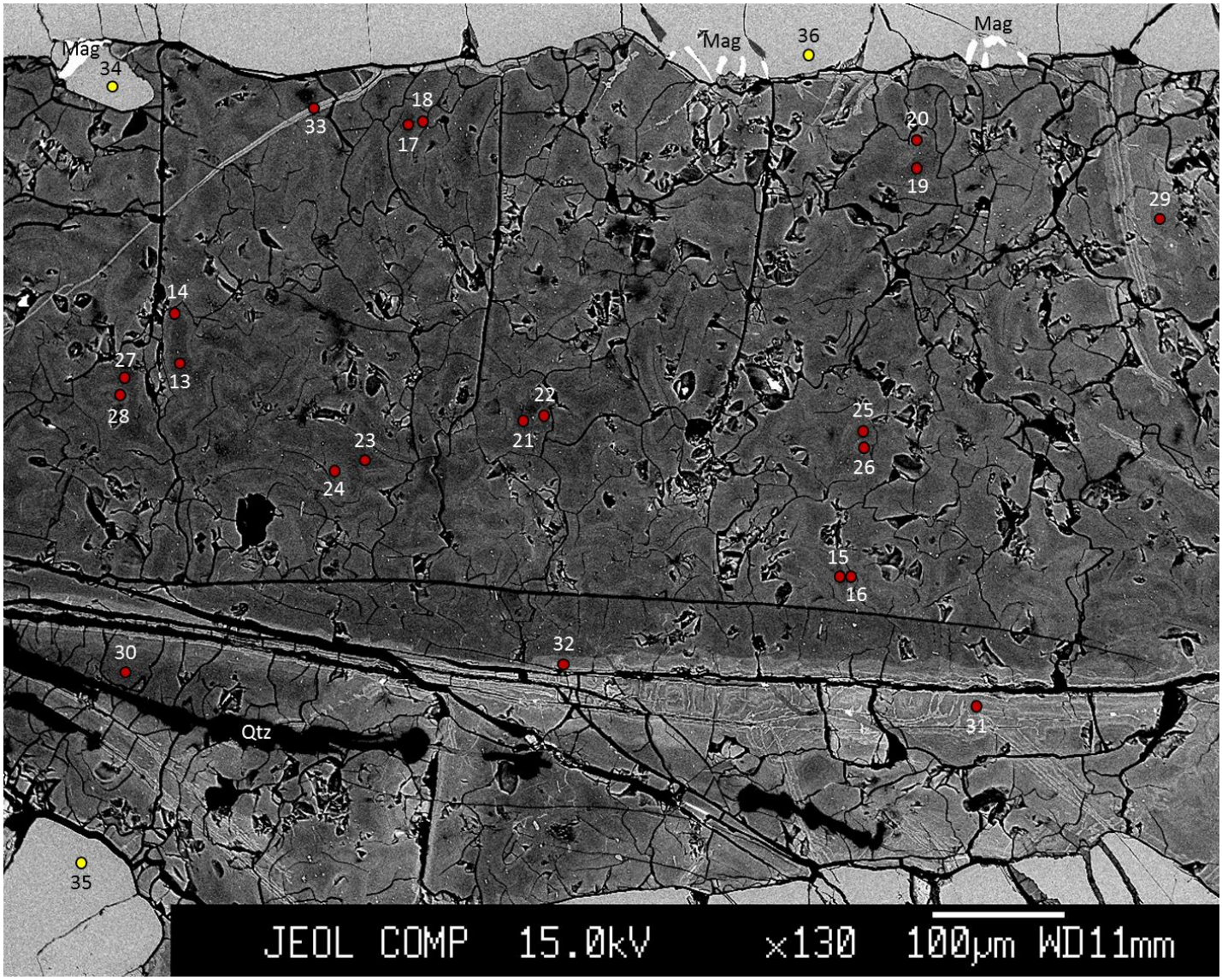
Mag
34
Mag
36
Mag
33
18
17
20
19
29
14
27
13
28
22
21
25
26
23
24
15
16
30
32
31
Qtz
35
JEOL COMP 15.0kV ×130 100µm WD11mm

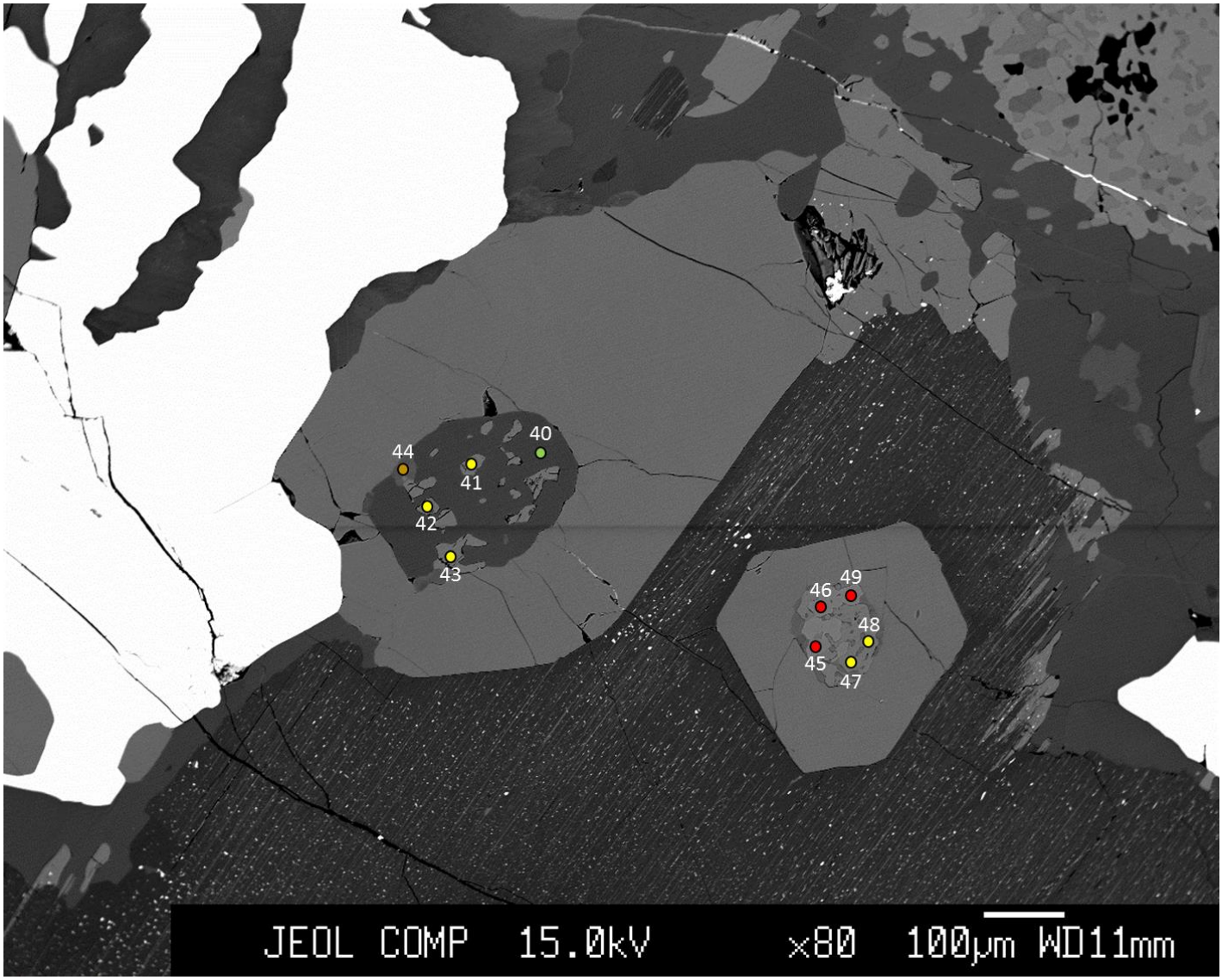
40
44
41
42
43
46
49
48
45
47
JEOL COMP 15.0kV ×80 100μm WD11mm

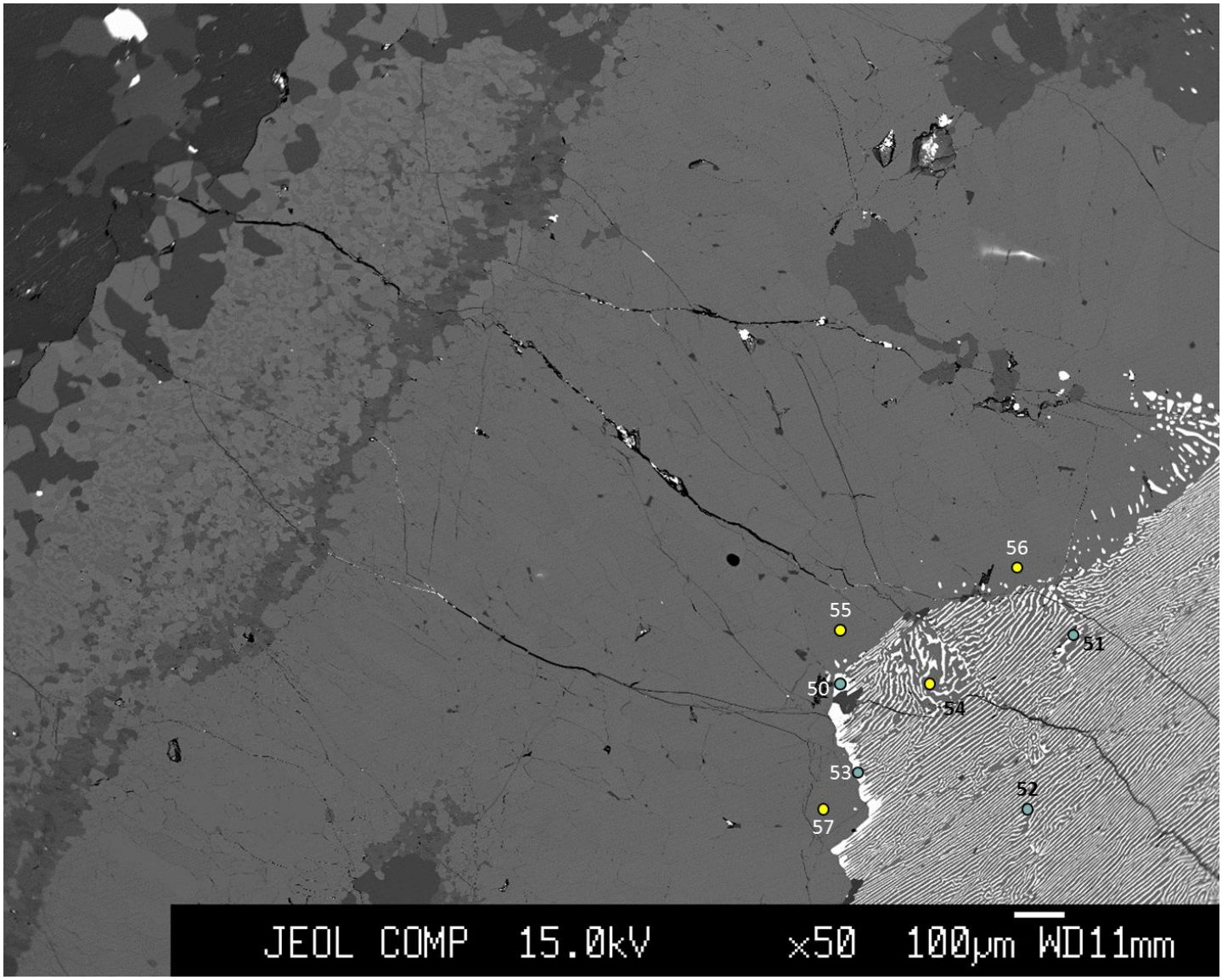
56
55
51
50
54
53
52
57
JEOL COMP 15.0kV ×50 100µm WD11mm

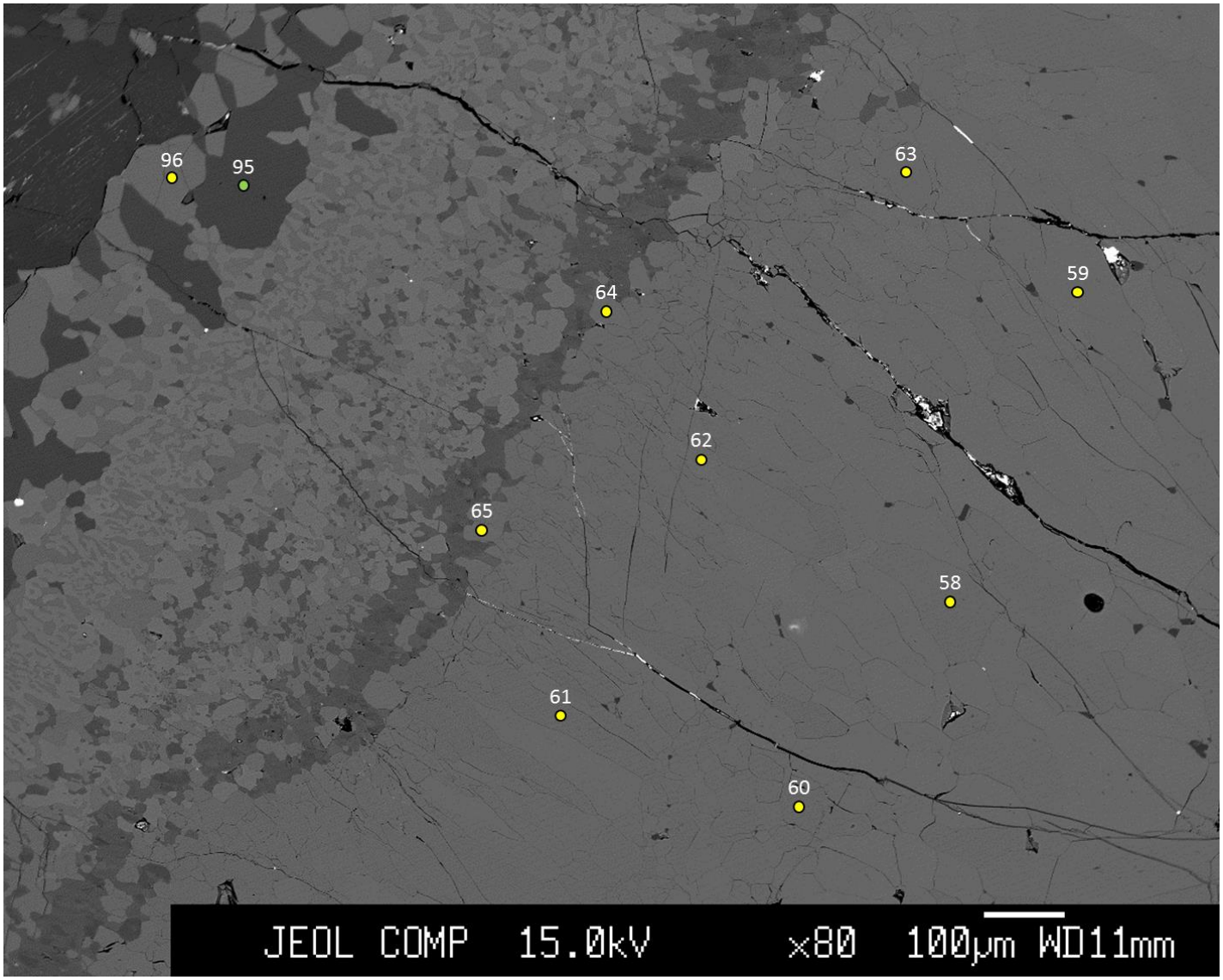
96
95
63
59
64
62
65
58
61
60
JEOL COMP 15.0kV ×80 100µm WD11mm

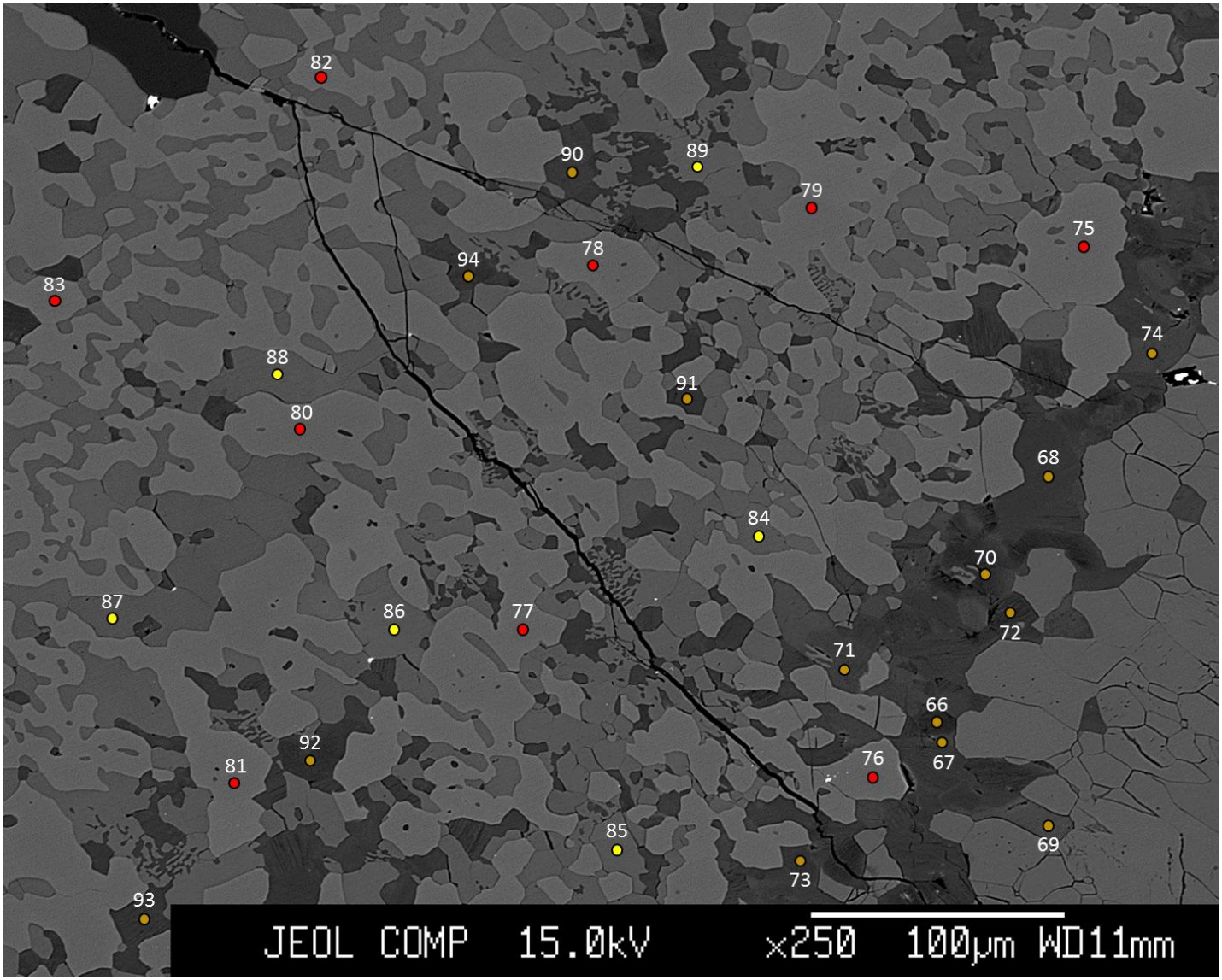
82
90
89
79
75
78
94
83
74
88
91
80
68
84
70
87
86
77
72
71
66
92
81
76
67
85
69
73
93
JEOL COMP 15.0kV ×250 100µm WD11mm

JKEM-02

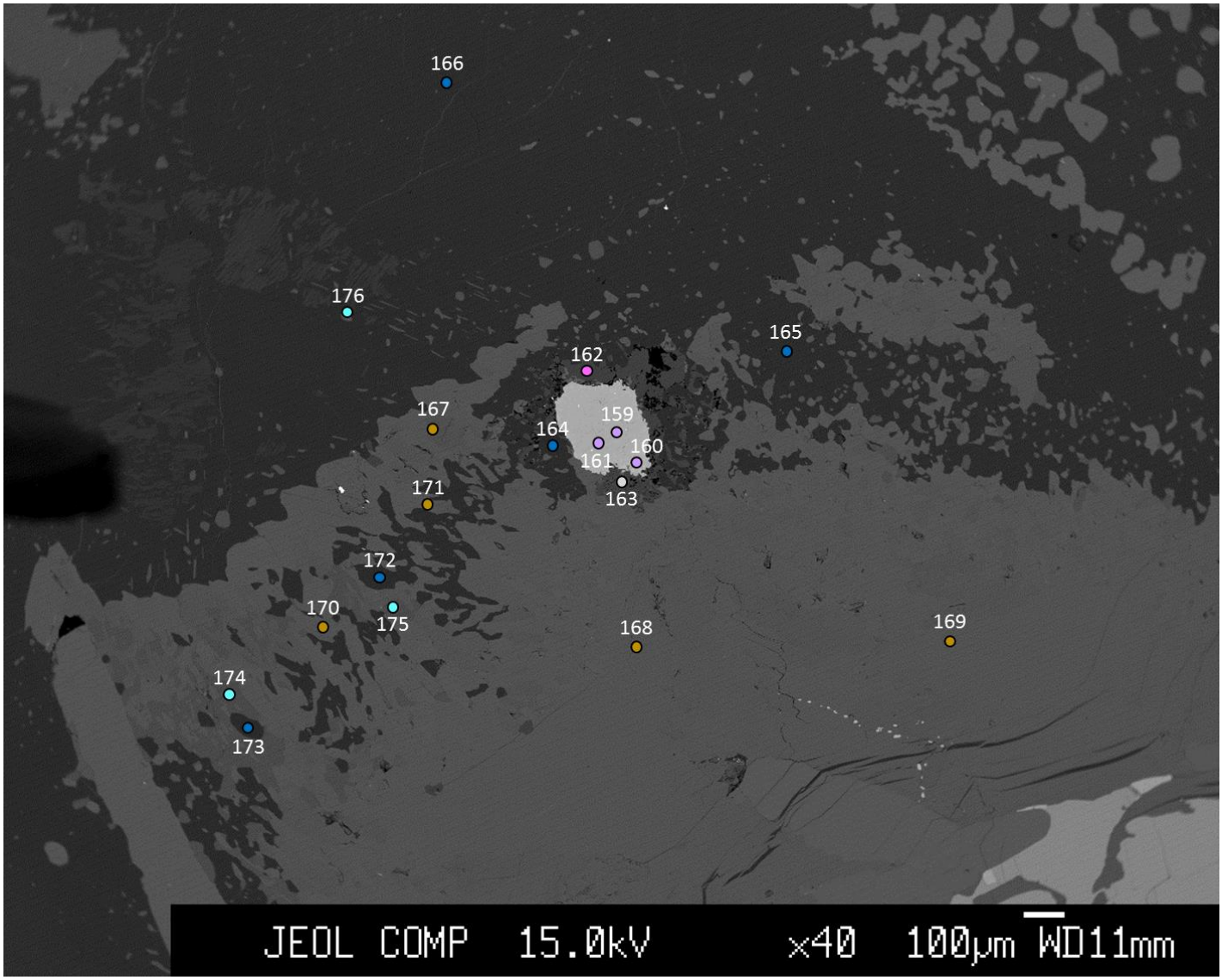
166
176
165
162
167
159
164
160
161
171
163
172
170
175
168
169
174
173
JEOL COMP 15.0kV x40 100μm WD11mm

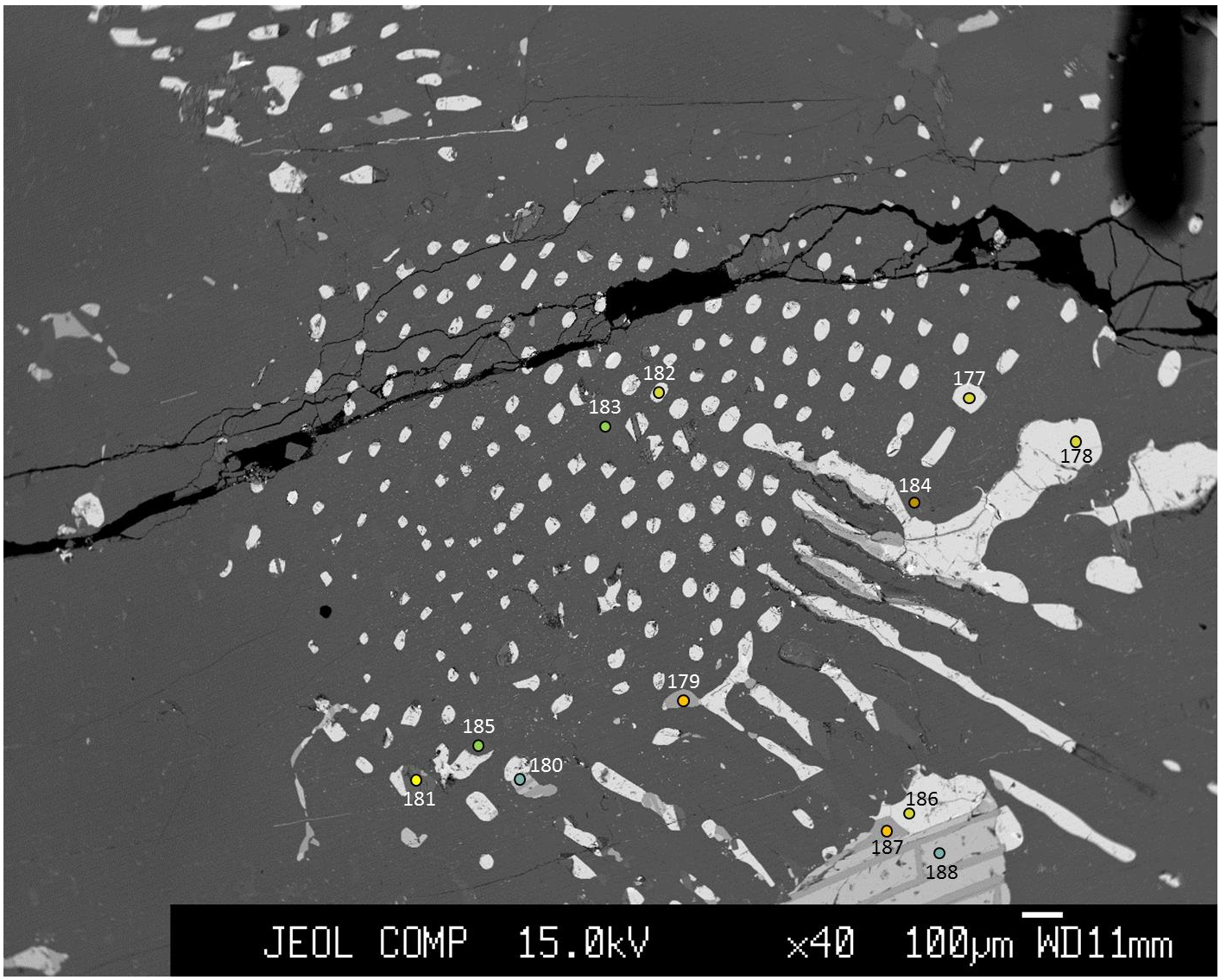
182
177
183
178
184
179
185
180
181
186
187
188
JEOL COMP 15.0kV x40 100µm WD11mm

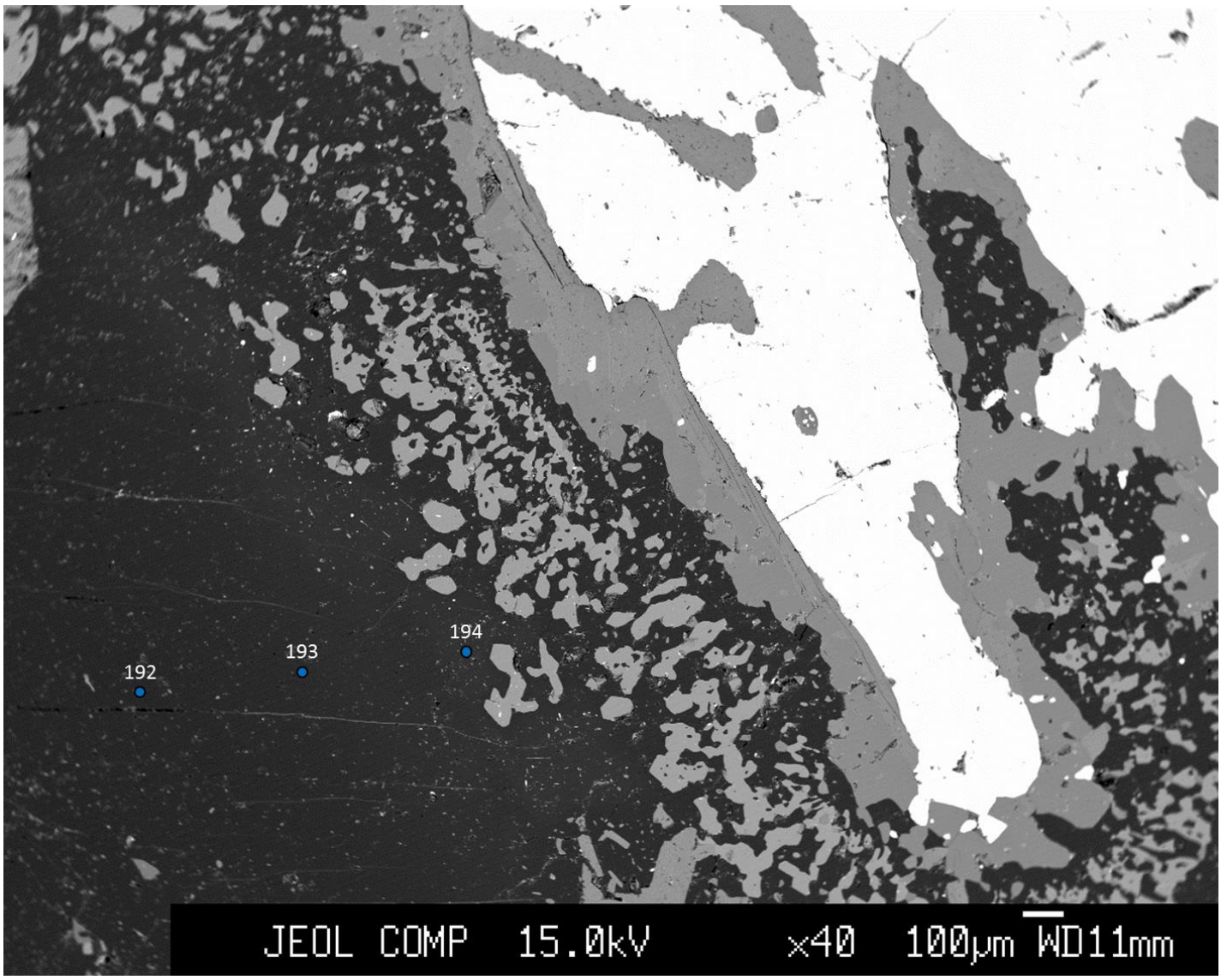
192
193
194
JEOL COMP 15.0kV x40 100µm WD11mm

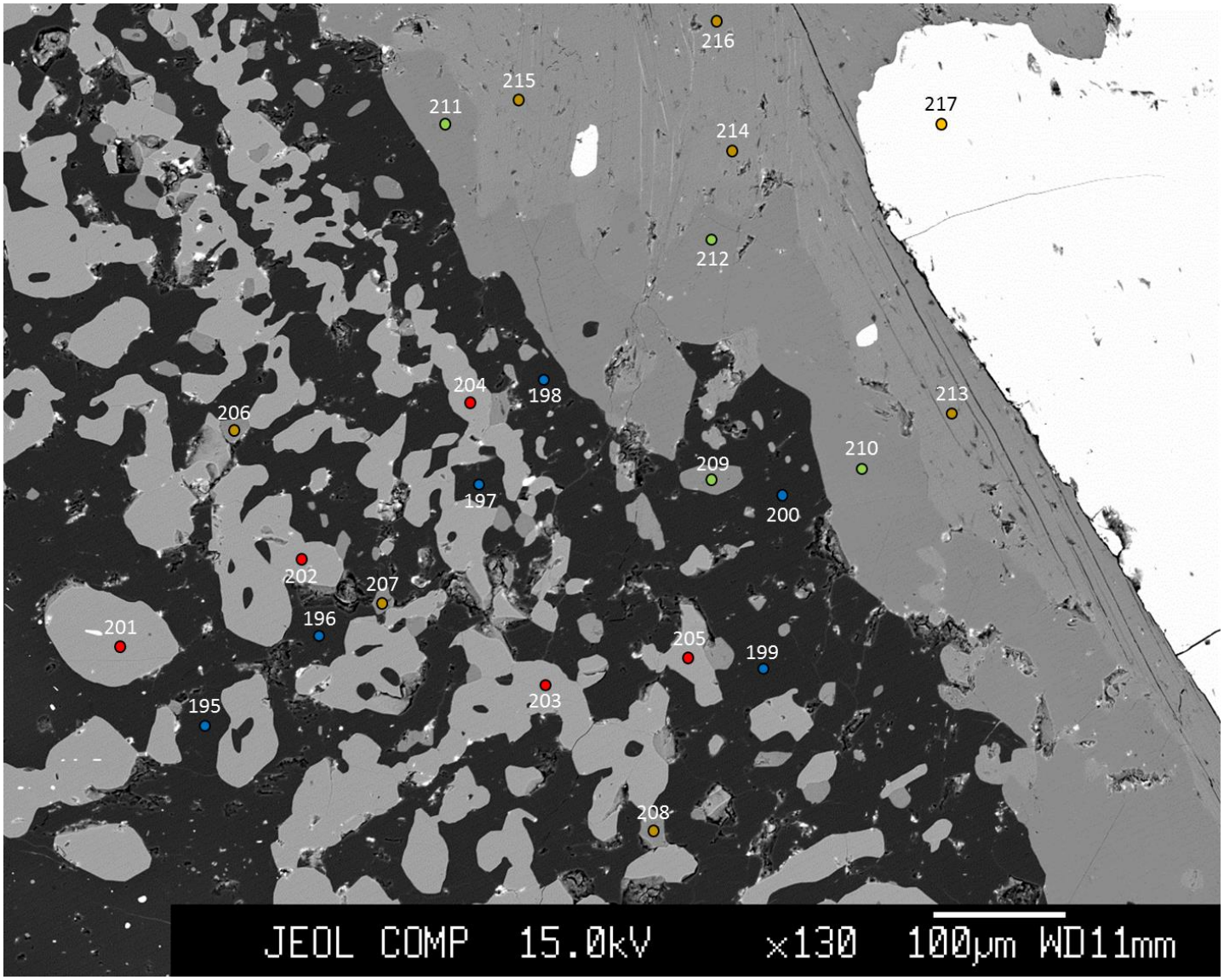
216
215
211
217
214
212
204
198
213
206
210
209
197
200
202
207
196
201
205
199
203
195
208
JEOL COMP 15.0kV ×130 100µm WD11mm

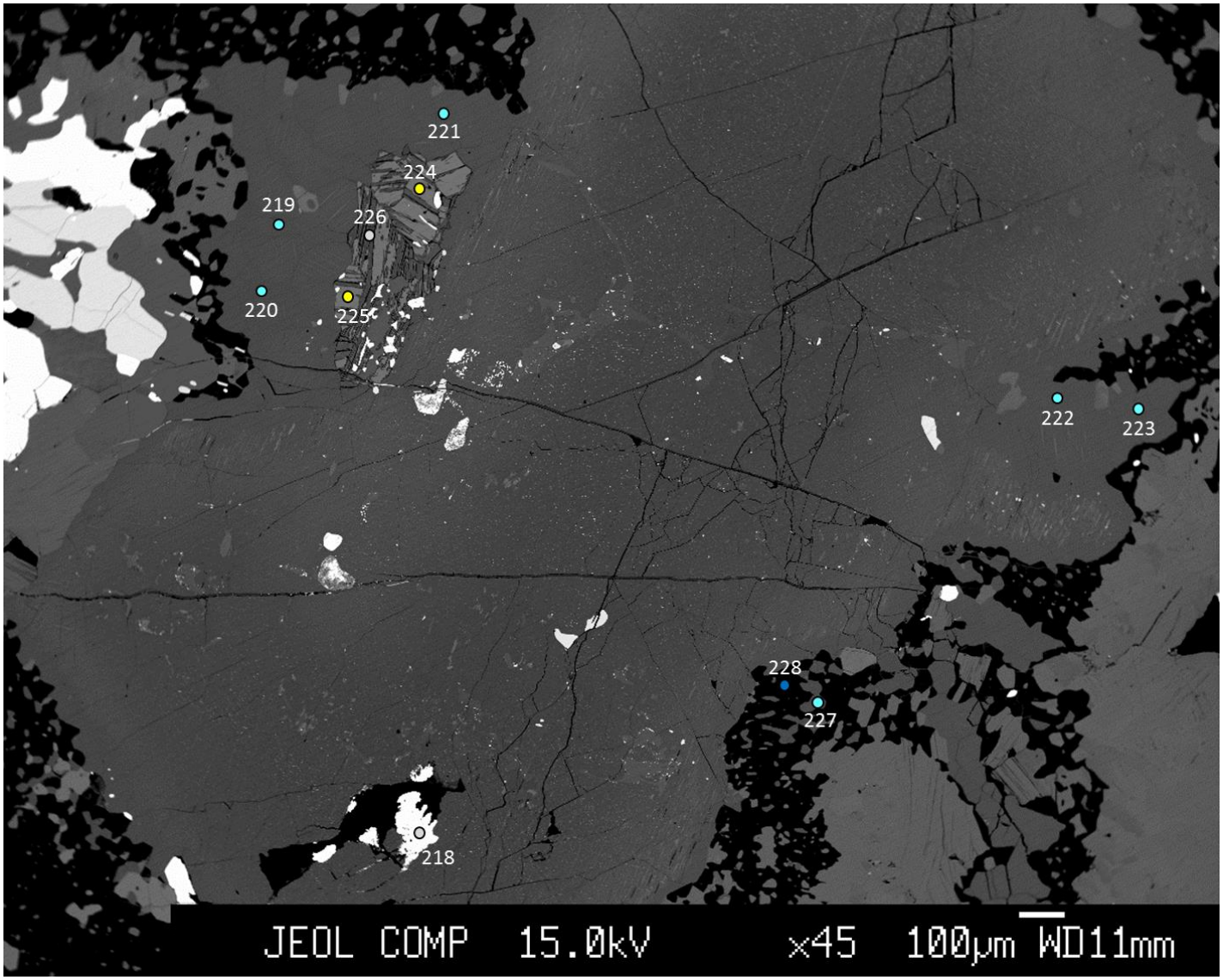
221
224
219
226
220
225
222
223
228
227
218
JEOL COMP 15.0kV x45 100µm WD11mm

JKEM-14b

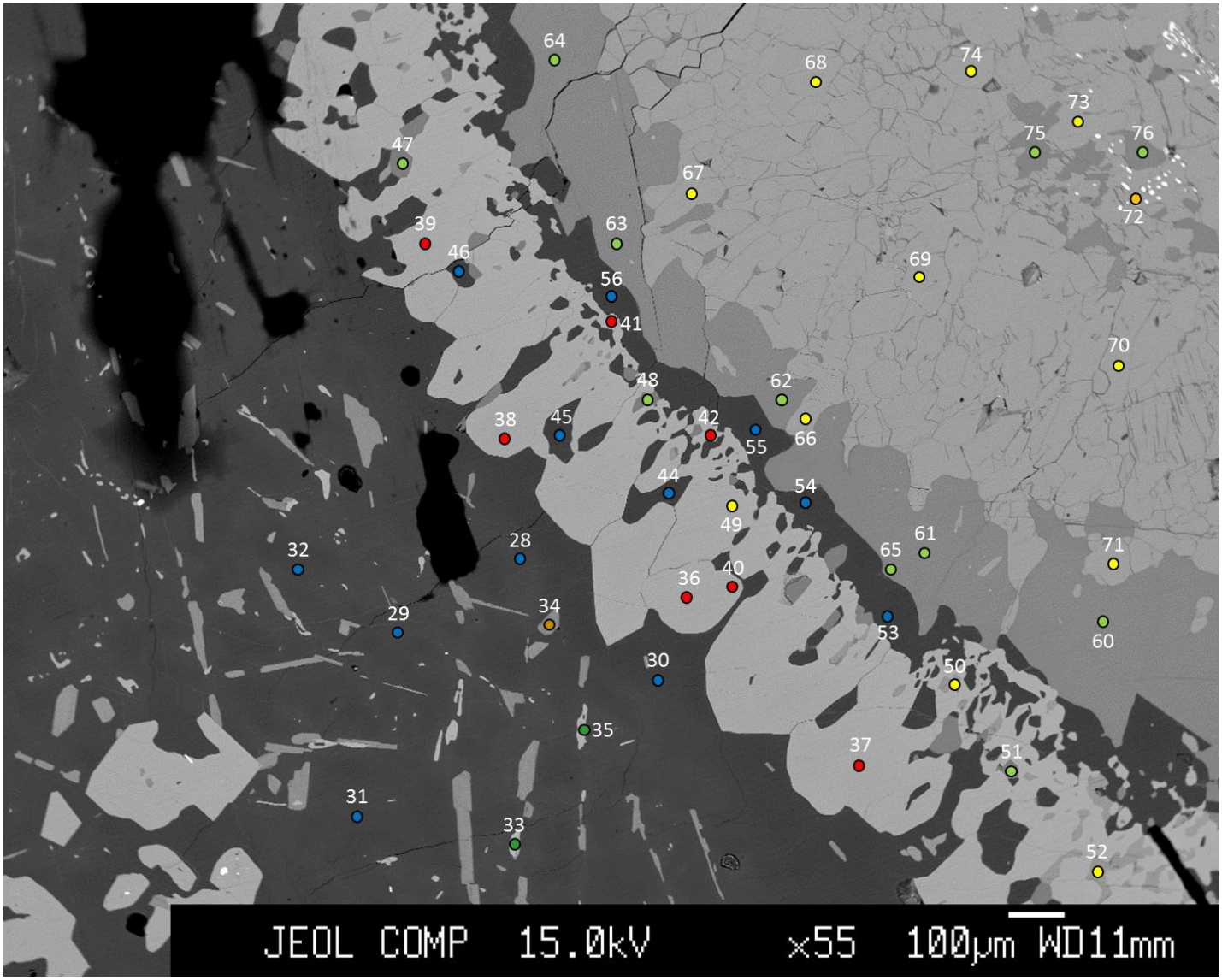
64
68
74
73
75
76
47
67
72
39
63
46
69
56
41
70
48
62
38
45
42
66
55
44
54
49
61
28
65
71
32
40
36
34
29
53
60
30
50
35
37
51
31
33
52
JEOL COMP 15.0kV ×55 100µm WD11mm

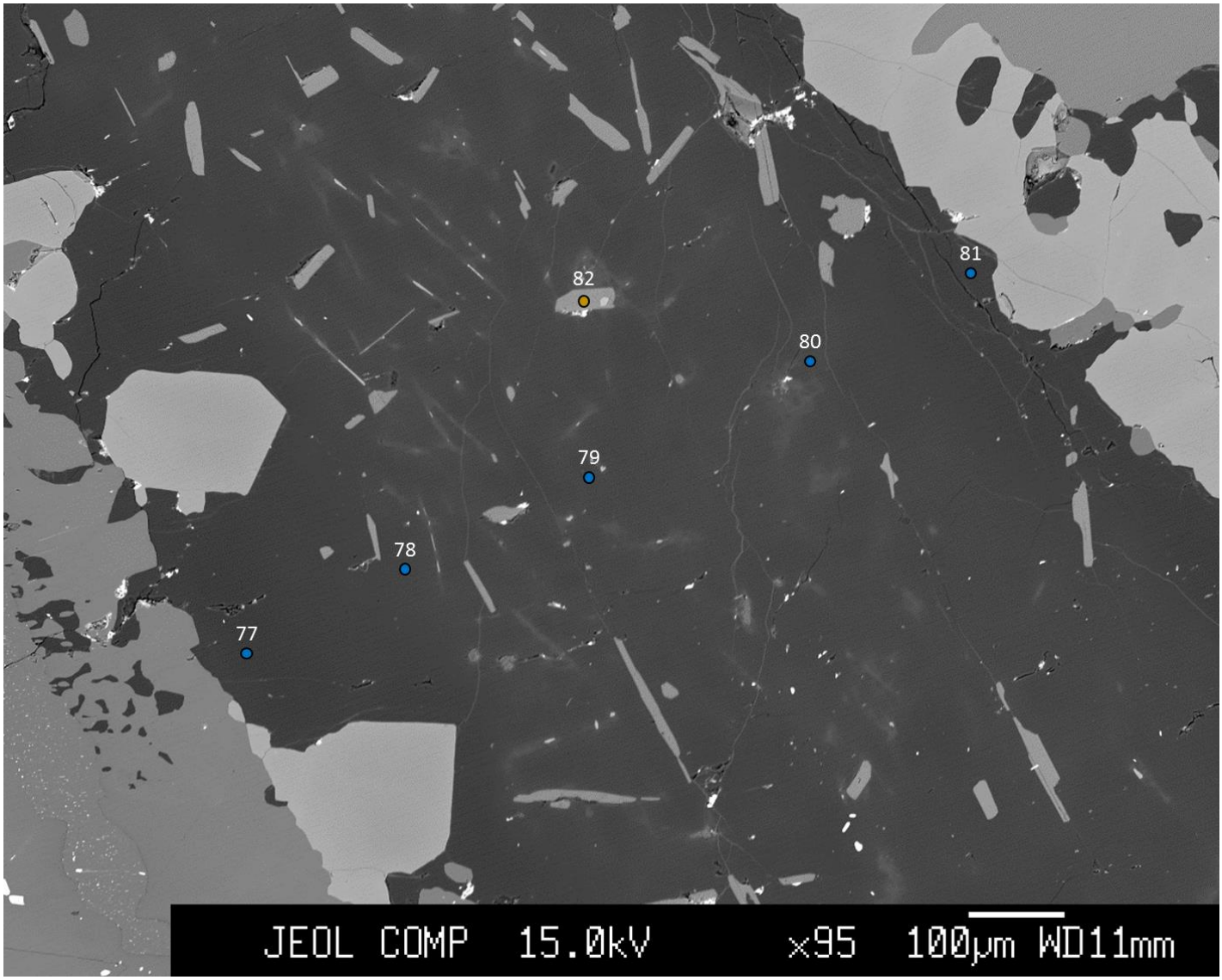
81
82
80
79
78
77
JEOL COMP 15.0kV ×95 100µm WD11mm

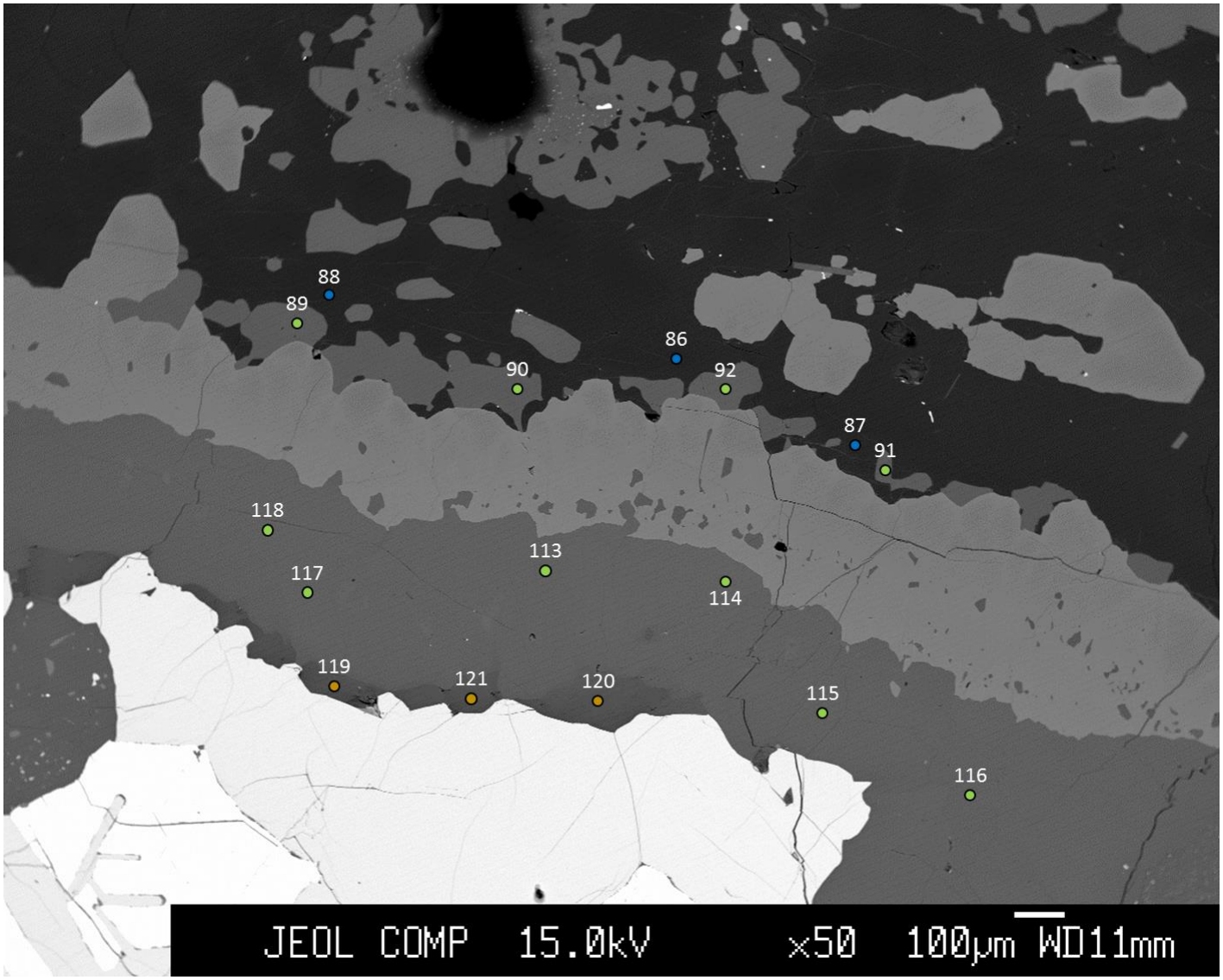
88
89
86
90
92
87
91
118
113
117
114
119
121
120
115
116
JEOL COMP 15.0kV ×50 100µm WD11mm

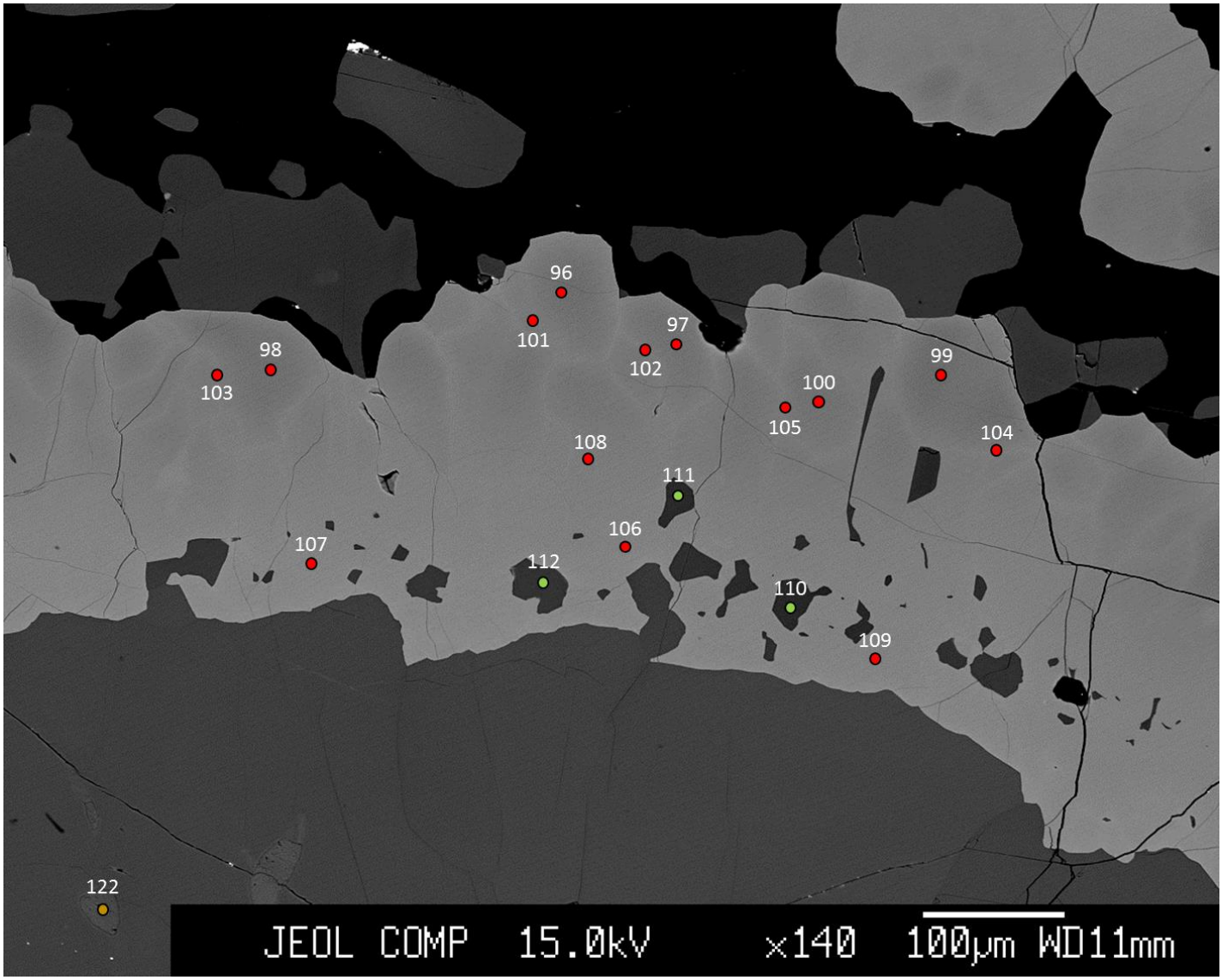
96
101
97
98
102
99
103
100
105
104
108
111
106
107
112
110
109
122
JEOL COMP 15.0kV ×140 100µm WD11mm

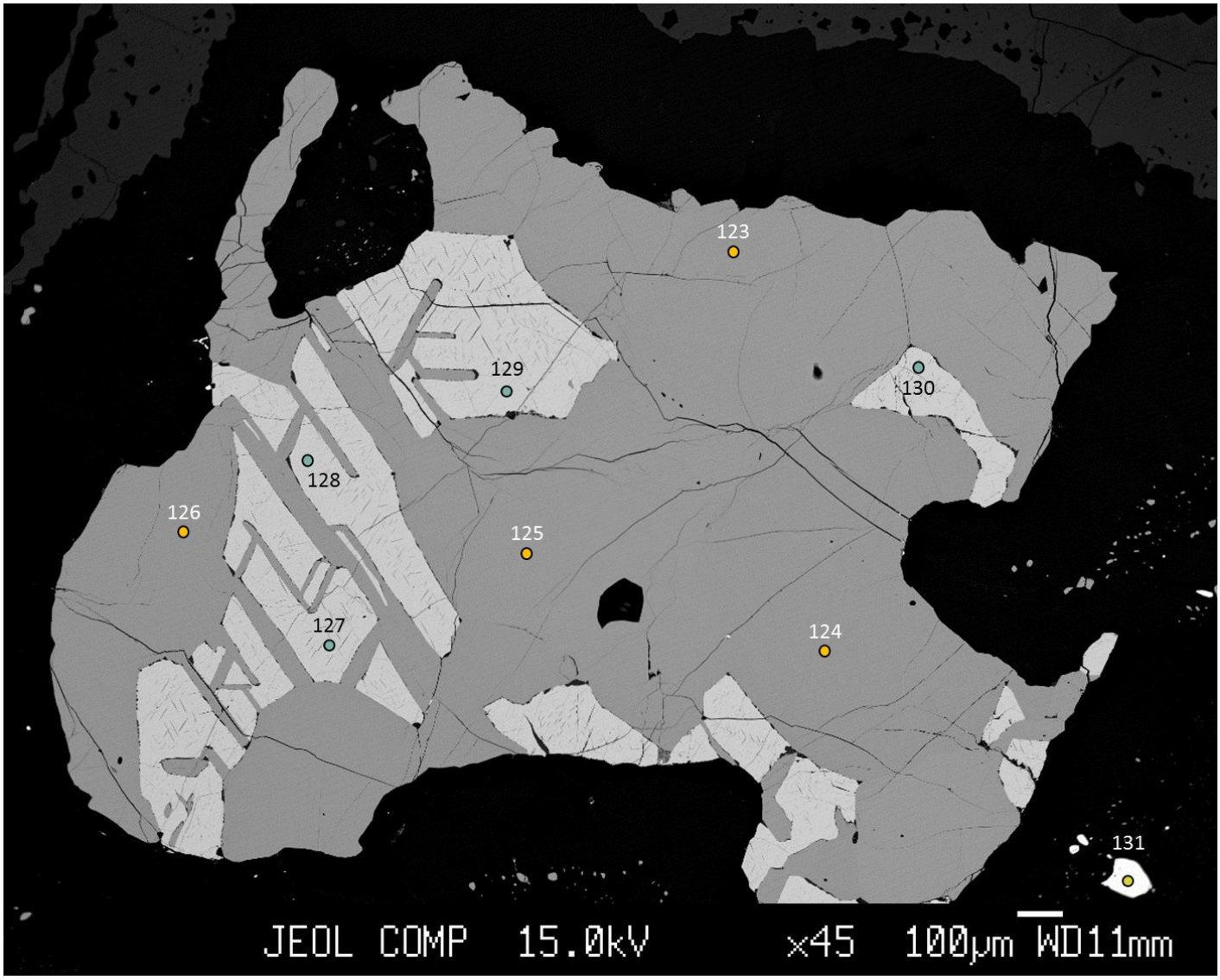
123
129
130
128
126
125
127
124
131
JEOL COMP 15.0kV x45 100µm WD11mm

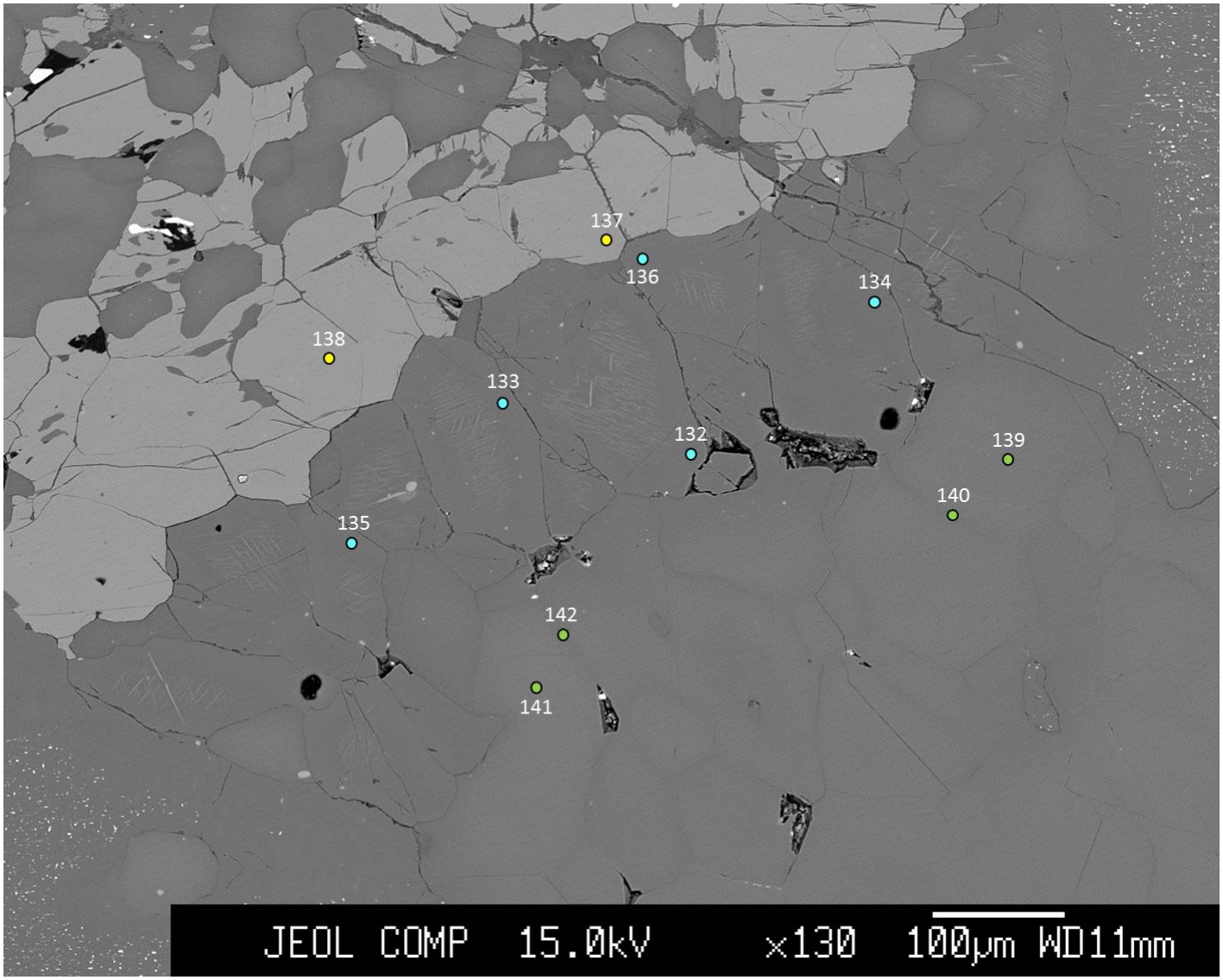
137
136
134
138
133
132
139
140
135
142
141
JEOL COMP 15.0kV ×130 100µm WD11mm

JKEM-15b

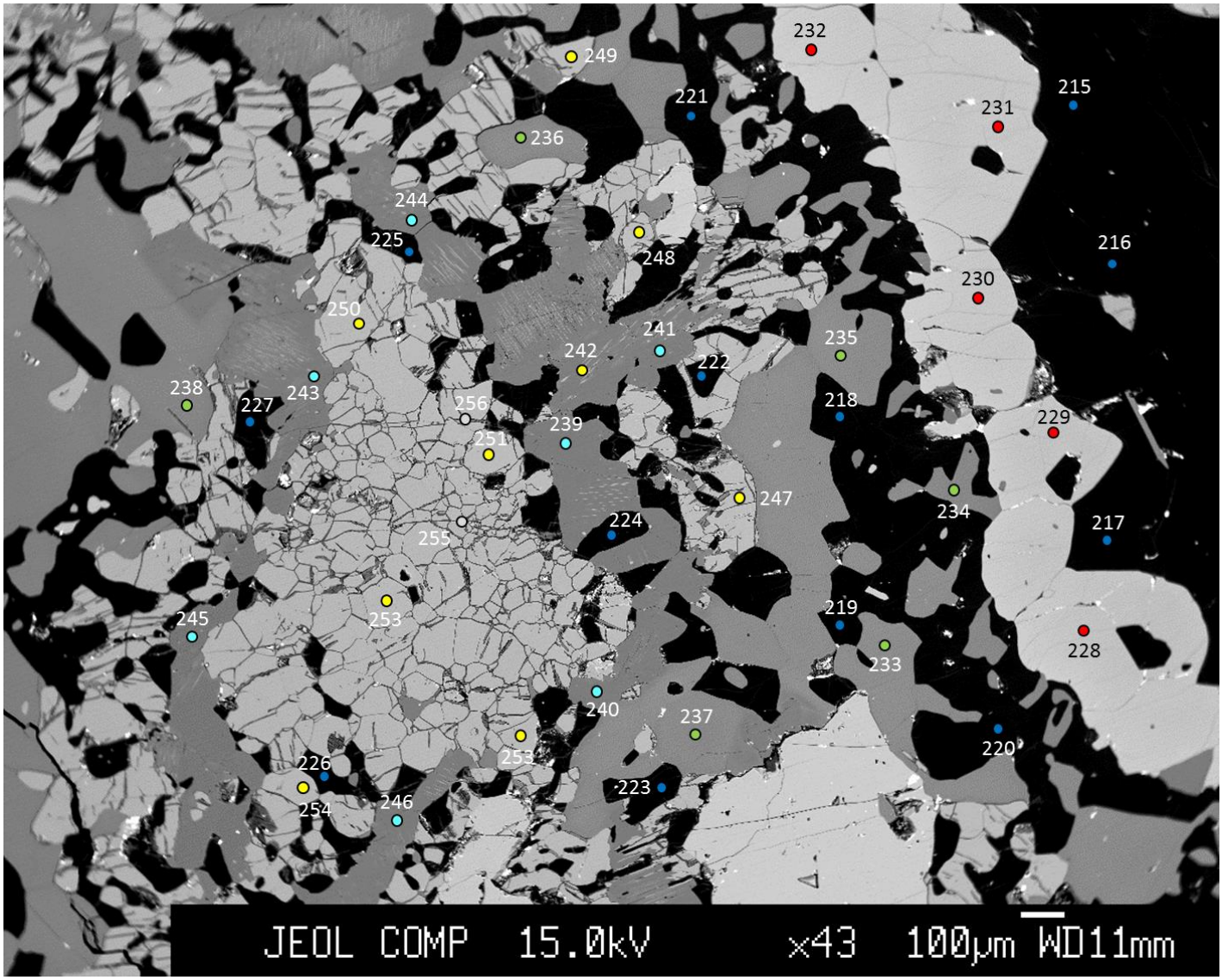
232
249
221
215
231
236
244
225
248
216
230
250
241
235
242
222
238
243
227
256
218
239
229
251
247
234
224
217
255
245
253
219
228
233
240
237
253
220
226
223
254
246
JEOL COMP 15.0kV x43 100µm WD11mm

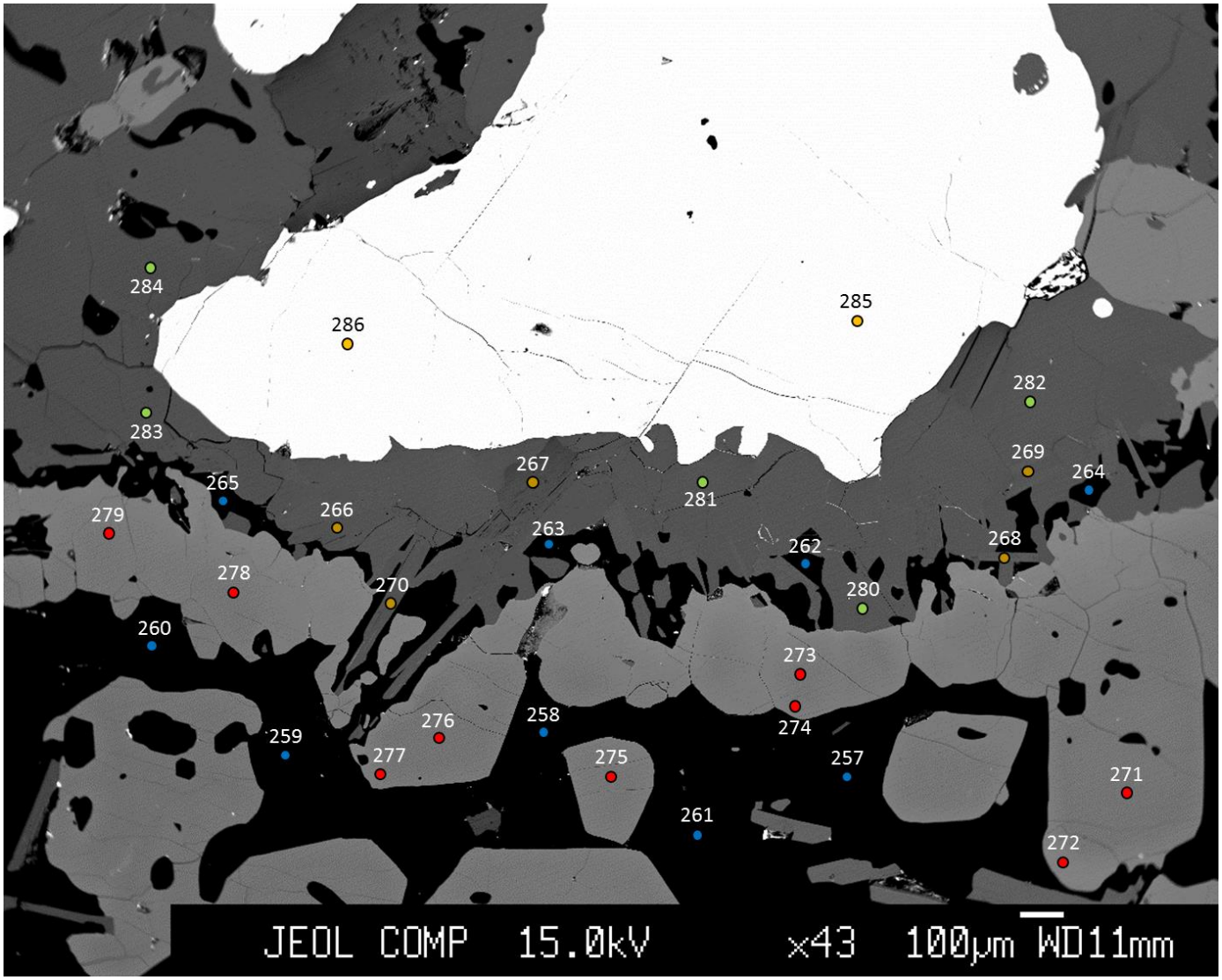
284
286
285
282
283
269
267
264
265
281
279
266
263
262
268
278
270
280
260
273
276
258
259
274
277
275
257
271
261
272
JEOL COMP 15.0kV x43 100µm WD11mm

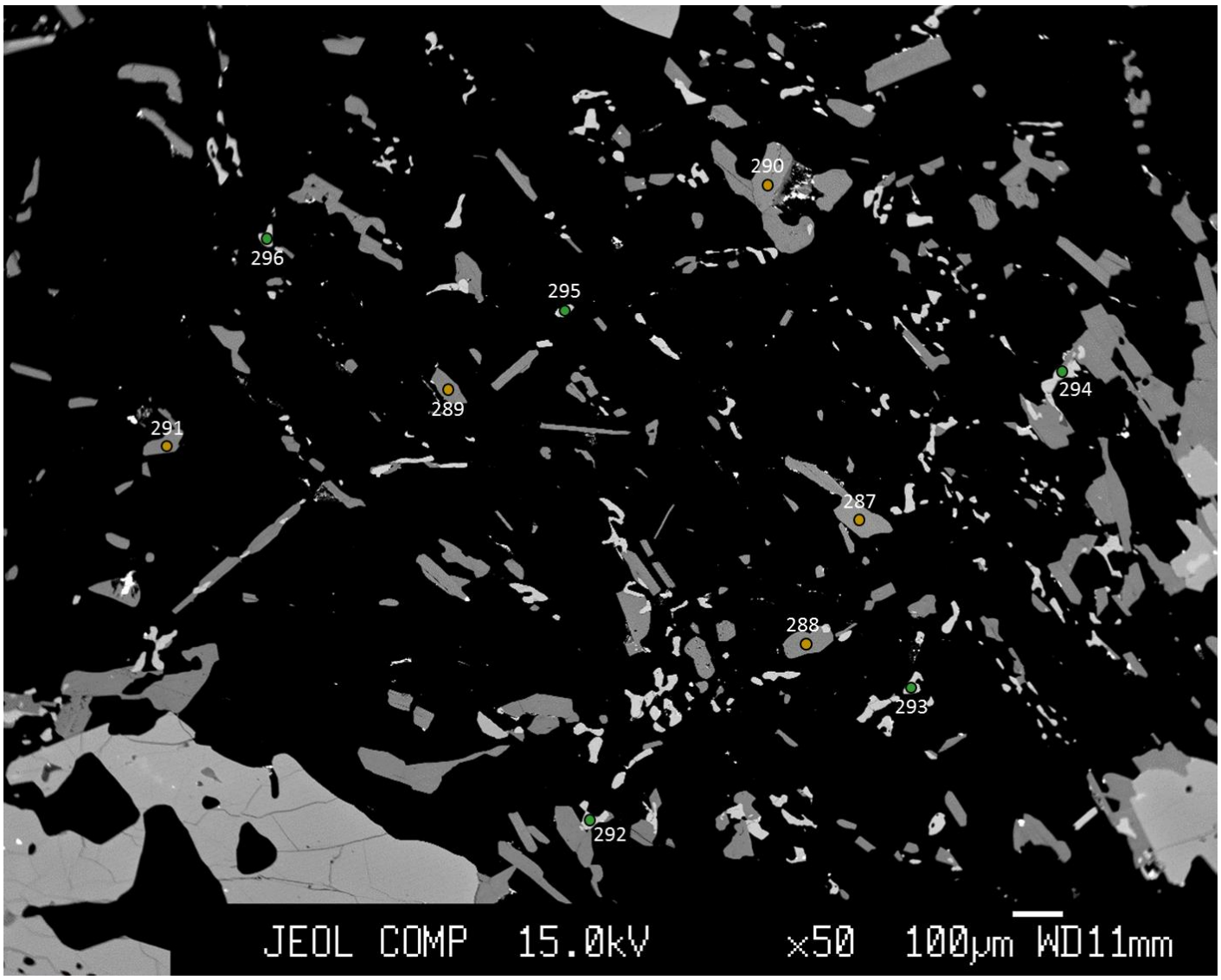
290
296
295
294
289
291
287
288
293
292
JEOL COMP 15.0kV ×50 100µm WD11mm

JKEM-10

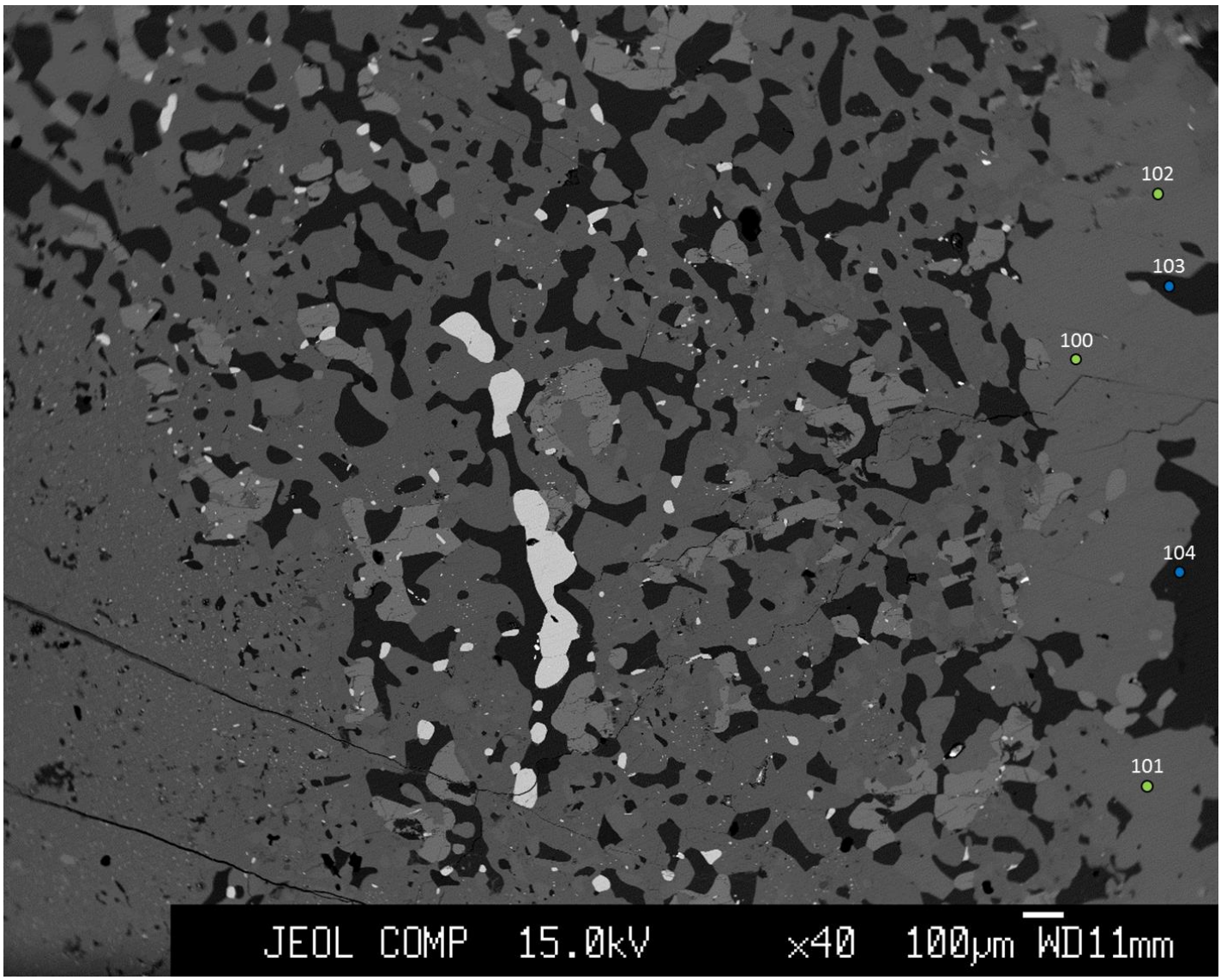

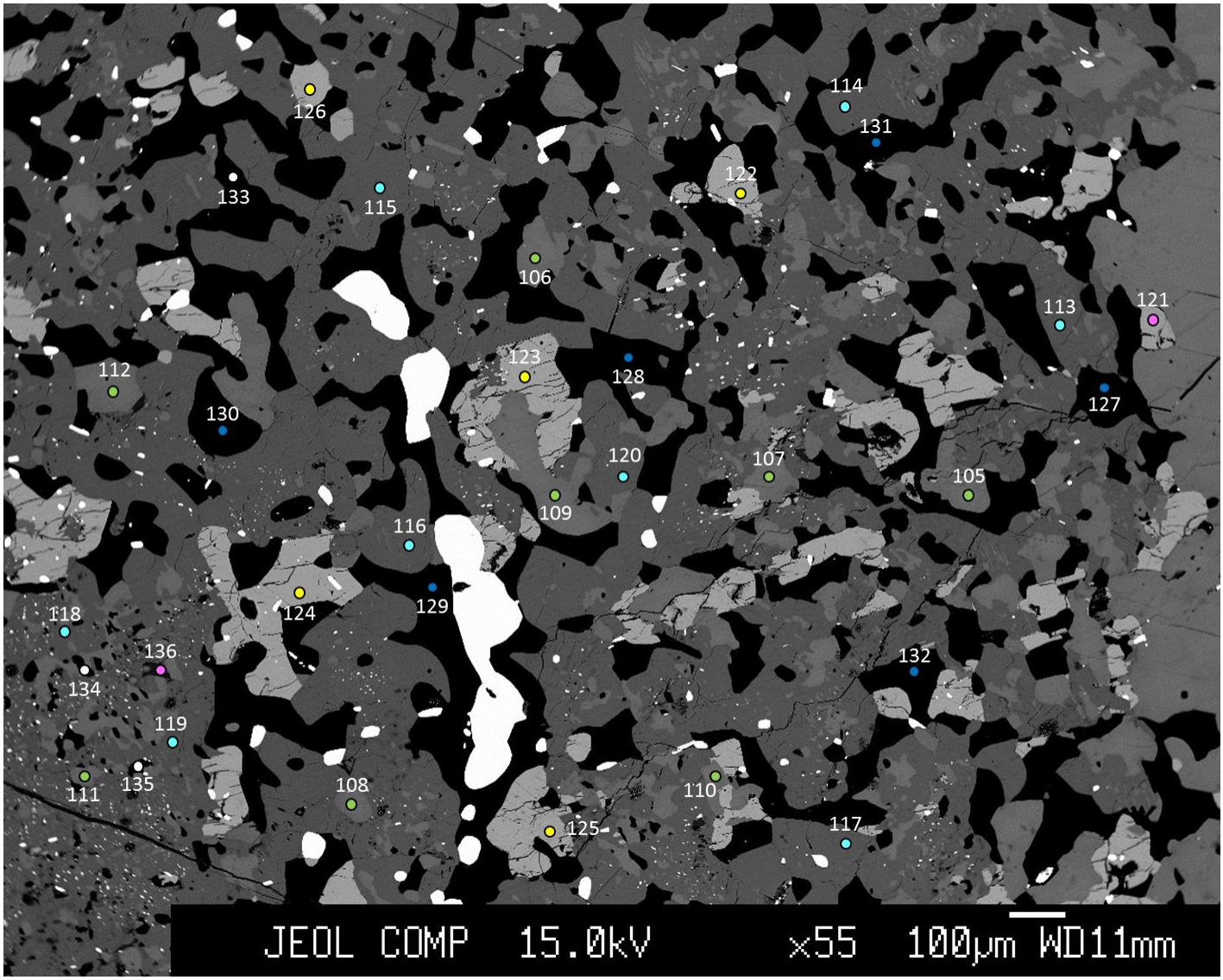
126
114
131
133
115
122
106
113
121
112
123
128
127
130
120
107
105
109
116
124
129
118
136
132
134
119
111
135
108
110
125
117
JEOL COMP 15.0kV ×55 100µm WD11mm

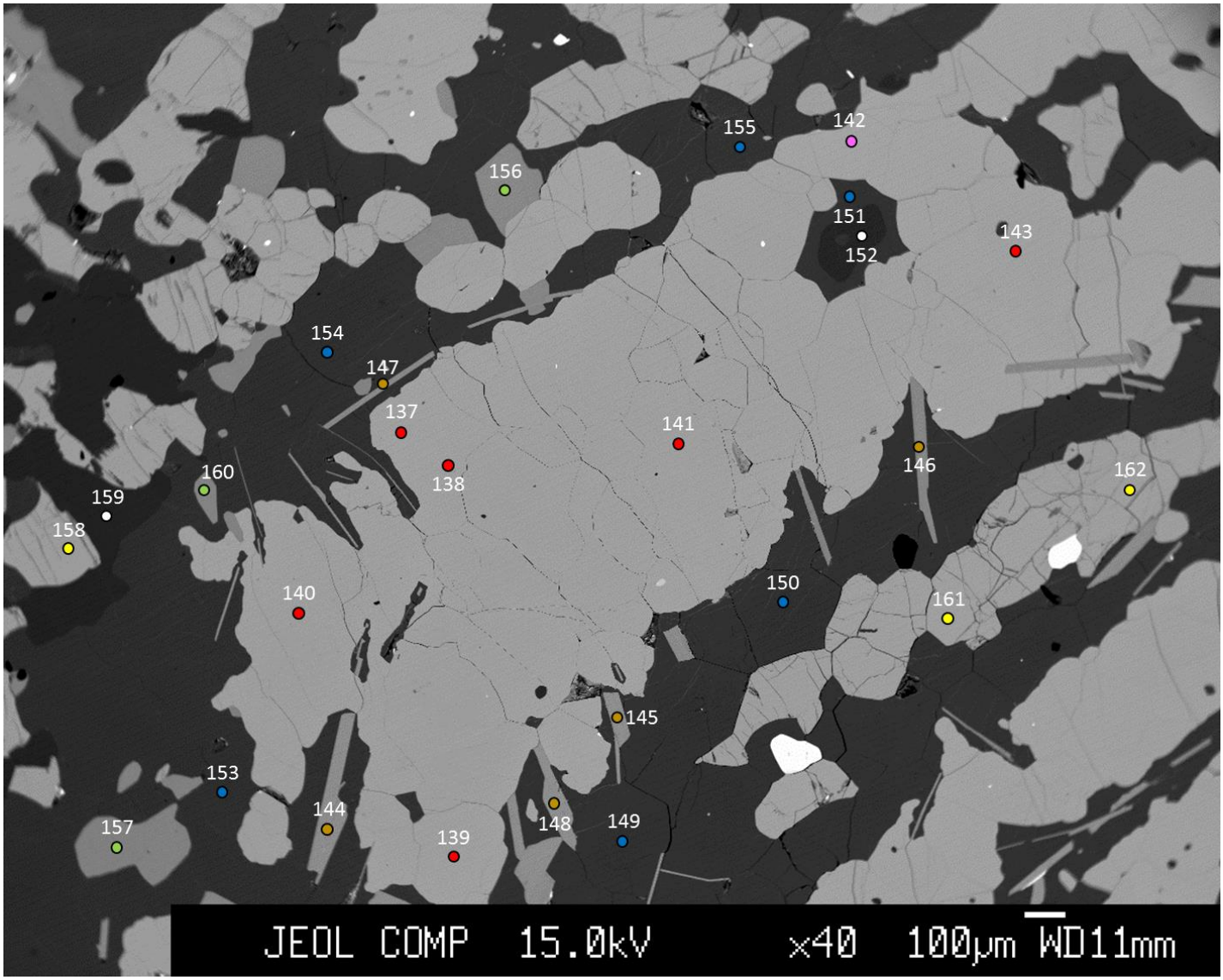
155
142
156
151
152
143
154
147
137
141
160
138
146
162
159
158
140
150
161
145
153
144
148
149
157
139
JEOL COMP 15.0kV x40 100µm WD11mm

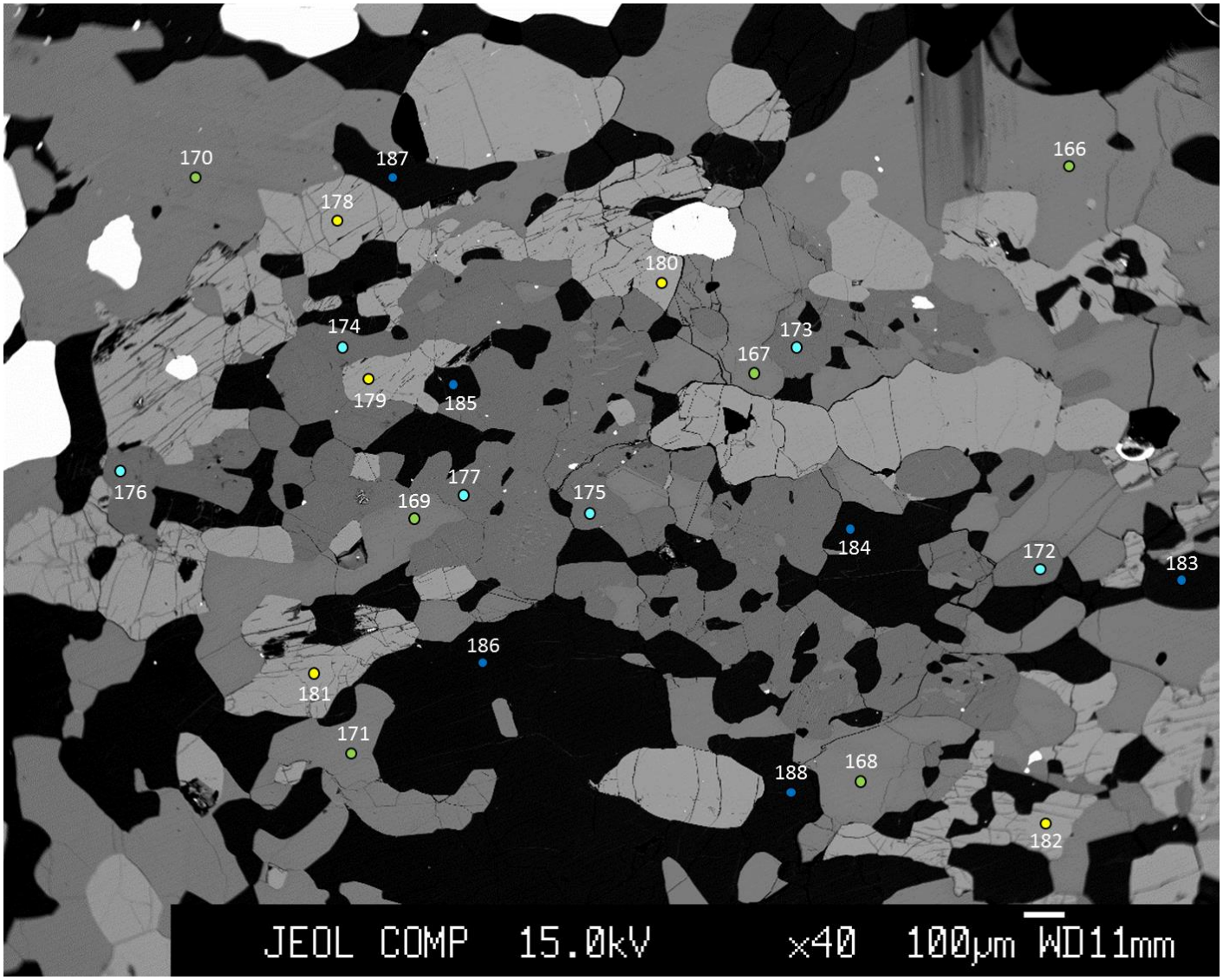
170
187
178
166
180
174
173
167
179
185
176
177
169
175
184
172
183
186
181
171
188
168
182
JEOL COMP 15.0kV ×40 100µm WD11mm

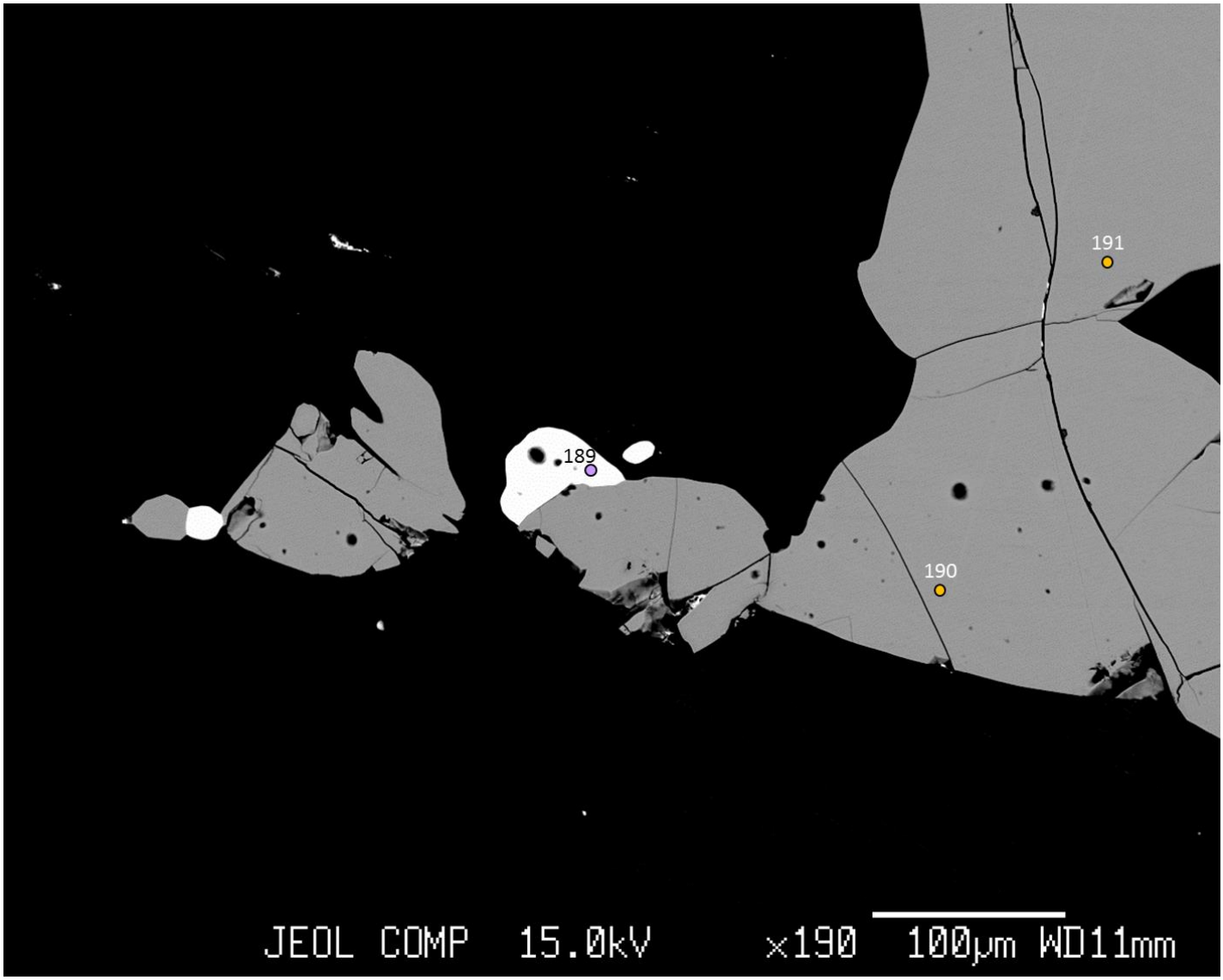
191
189
190
JEOL COMP 15.0kV ×190 100µm WD11mm

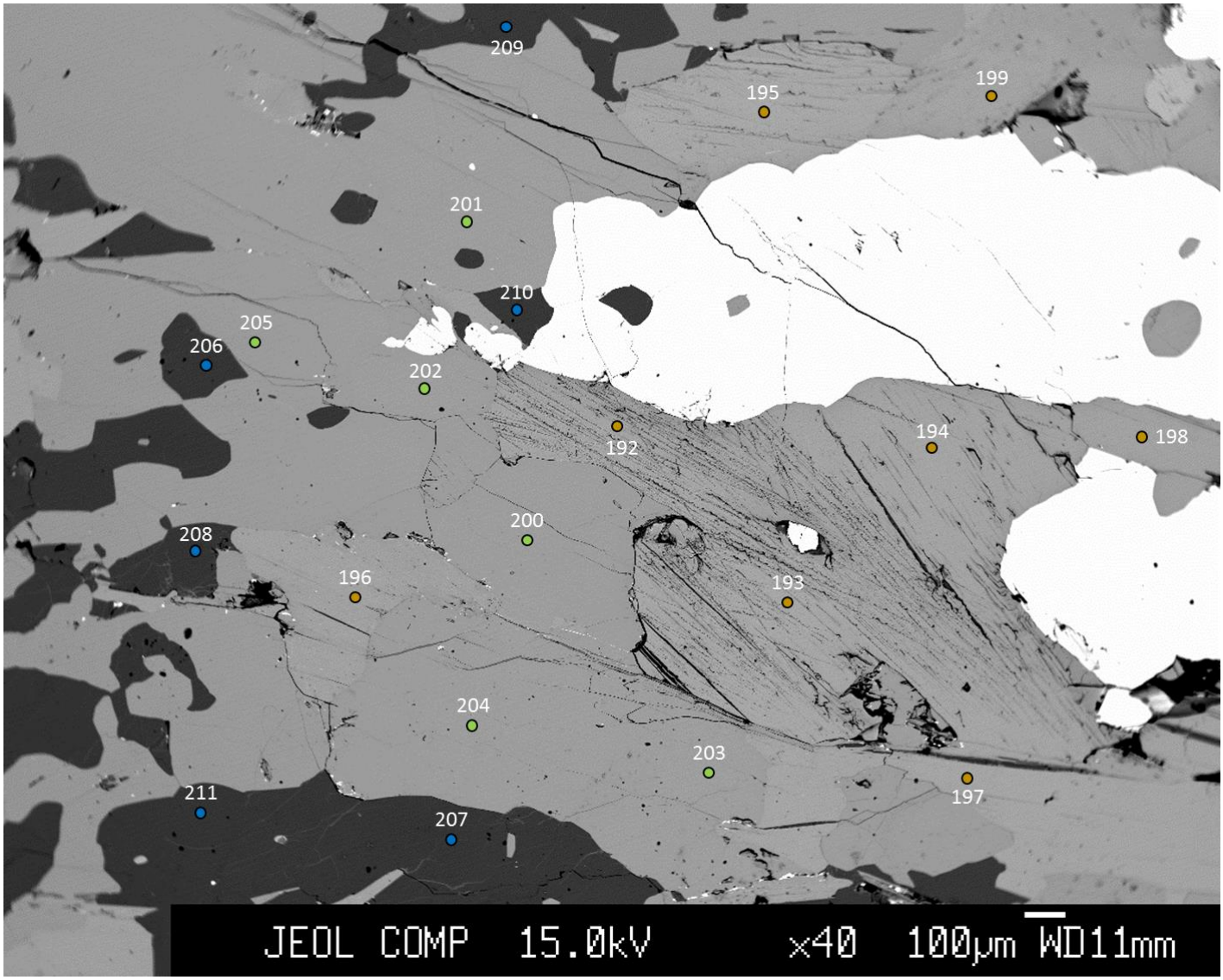
209
195
199
201
210
205
206
202
192
194
198
200
208
196
193
204
203
211
207
197
JEOL COMP 15.0kV x40 100µm WD11mm